Permian-Triassic Rifting Stage

3

José López-Gómez, Jacinto Alonso-Azcárate, Alfredo Arche, José Arribas, José Fernández Barrenechea, Violeta Borruel-Abadía, Sylvie Bourquin, Patricia Cadenas, Julia Cuevas, Raúl De la Horra, José Bienvenido Díez, María José Escudero-Mozo, Gabriela Fernández-Viejo, Belén Galán-Abellán, Carlos Galé, Jorge Gaspar-Escribano, José Gisbert Aguilar, David Gómez-Gras, Antonio Goy, Nicola Gretter, Nemesio Heredia Carballo, Marceliano Lago, Joan Lloret, Javier Luque, Leopoldo Márquez, Ana Márquez-Aliaga, Agustín Martín-Algarra, Javier Martín-Chivelet, Fidel Martín-González, Mariano Marzo, Ramón Mercedes-Martín, Federico Ortí, Alberto Pérez-López, Fernando Pérez-Valera, Juan Alberto Pérez-Valera, Pablo Plasencia, Emilio Ramos, Lidia Rodríguez-Méndez, Ausonio Ronchi, Ramón Salas, David Sánchez-Fernández, Yolanda Sánchez-Moya, Alfonso Sopeña, Ángela Suárez-Rodríguez, José María Tubía, Teresa Ubide, Blas Valero Garcés, Henar Vargas, and César Viseras

Abstract

The Permian-Triassic rifting represents the first of the two Mesozoic rifting stages recorded in the Iberian Peninsula. Its first phases of development started during the Early Permian, and were linked to the beginning of the break-up of Pangea, the large, unique and rheologically unstable supercontinent that mainly resulted from the collision of Gondwana and Laurussia. This chapter analyzes this first rifting stage in Iberia in two separate phases, an initial or tectonic phase, and a later mature phase. This analysis focuses on the main Permian-Triassic basins of the Iberian Peninsula: the Pyrenean, Iberian, Catalan, Ebro and Betic basins, as well as the basins located in the present-day Balearic Islands. In order to achieve a better understanding of the analyses of these basins, a multidisciplinary approach has been carried out by 48 researchers, including

J. López-Gómez (✉) · A. Arche · J. Arribas · J. Fernández Barrenechea · V. Borruel-Abadía · A. Goy · J. Luque · J. Martín-Chivelet · Y. Sánchez-Moya · A. Sopeña
Departamento de Geomateriales, Instituto de Geociencias, IGEO (CSIC-UCM), Universidad Complutense de Madrid, C/Doctor Severo Ochoa 7, 3ª Planta, 28040 Madrid, Spain
e-mail: jlopez@geo.ucm.es

A. Arche
e-mail: aarche@ucm.es

J. Arribas
e-mail: arribas@ucm.es

J. Fernández Barrenechea
e-mail: barrene@ucm.es

V. Borruel-Abadía
e-mail: violeta.borruel@igeo.ucm-csic.es

A. Goy
e-mail: angoy@ucm.es

J. Luque
e-mail: jluque@geo.ucm.es

J. Martín-Chivelet
e-mail: j.m.chivelet@ucm.es

Y. Sánchez-Moya
e-mail: yol@ucm.es

A. Sopeña
e-mail: sopena@ucm.es

J. Alonso-Azcárate
Departamento de Química-Física, Facultad de Ciencias Ambientales y Bioquímica, Universidad de Castilla-La Mancha, Av. Carlos III s/n, 45071 Toledo, Spain
e-mail: Jacinto.Alonso@uclm.es

J. Arribas · J. Fernández Barrenechea · J. Luque
Departamento de Mineralogía y Petrología, Facultad Ciencias Geológicas, Universidad Complutense de Madrid, C/José Antonio Novais 12, 28040 Madrid, Spain

S. Bourquin
UMR 6118 (CNRS/INSU), Géosciences Rennes, Université de Rennes 1, Campus de Beaulieu, 35042 Rennes Cedex, France
e-mail: sylvie.bourquin@univ-rennes1.fr

C. Quesada and J. T. Oliveira (eds.), *The Geology of Iberia: A Geodynamic Approach*, Regional Geology Reviews, https://doi.org/10.1007/978-3-030-11295-0_3

studies of tectonics, sedimentology, magmatism, mineralogy, geochemistry and paleontology.

3.1 Introduction

López-Gómez J

The Permian-Triassic rifting stage represents the first of the two Mesozoic rifting stages in the Iberian Peninsula. Its first phases of development started during the Early Permian, and were linked to the beginning of the break-up of Pangea, the big, unique and rheologically unstable supercontinent that mainly resulted from the collision of Gondwana and Laurussia. This chapter analyzes this first rifting stage in the different basins of Iberia in two separate phases, an initial or tectonic phase, and a later mature phase.

3.1.1 From Initial to Mature Rifting Phase

Gretter N, Arche A, Ronchi A, López-Gómez J and De la Horra R

Towards the end of the Paleozoic era, the southwestern European sector experienced the progressive waning of the Variscan orogenic cycle. The global geodynamic picture was affected by the final stages of Pangea amalgamation, resulting from the collision of Gondwana, Laurussia and several microplates (Pastor Galán et al. 2015 and references therein) (Fig. 3.1a). Rather quickly, a new geodynamic

P. Cadenas · G. Fernández-Viejo
Departamento de Geología, Universidad de Oviedo, Campus de Llamaquique, Jesús Arias de Velasco s/n, 33005 Oviedo, Spain
e-mail: pcadenas@geol.uniovi.es

G. Fernández-Viejo
e-mail: gaby@geol.uniovi.es

J. Cuevas · L. Rodríguez-Méndez · J. M. Tubía
Departamento de Geodinámica, Facultad de Ciencia y Tecnología, Universidad del País Vasco UPV/EHU, Barrio Sarriena s/n, 48940 Leioa (Vizcaya), Spain
e-mail: julia.cuevas@ehu.eus

L. Rodríguez-Méndez
e-mail: lidia.rodriguez@ehu.eus

J. M. Tubía
e-mail: jm.tubia@ehu.eus

R. De la Horra · B. Galán-Abellán · A. Goy · J. Martín-Chivelet · D. Sánchez-Fernández · Y. Sánchez-Moya
Departamento de Geodinámica, Estratigrafía y Paleontología, Facultad de Ciencias Geológicas, Universidad Complutense de Madrid, C/José Antonio Novais 12, 28040 Madrid, Spain
e-mail: rhorraba@ucm.es

B. Galán-Abellán
e-mail: galanabellan@ucm.es

D. Sánchez-Fernández
e-mail: dasafe2004@yahoo.es

J. B. Díez
Departamento de Geociencias Marinas, Universidad de Vigo, Campus Lagoas-Marcosende, 36310 Vigo (Pontevedra), Spain
e-mail: jbdiez@uvigo.es

M. J. Escudero-Mozo
Indra Software Labs, C/Julián Camarillo 16-20, 28037 Madrid, Spain
e-mail: mjescudero@indra.es

C. Galé
h2ï Agua + Innovación, C/Mas de Las Matas 20, 50014 Zaragoza, Spain
e-mail: carlos.gale@gmail.com

J. Gaspar-Escribano
E.T.S.I. Topografía, Geodesia y Cartografía, Universidad Politécnica de Madrid, Madrid, Spain
e-mail: jorge.gaspar@upm.es

J. Gisbert Aguilar · M. Lago
Departamento de Ciencias de La Tierra, Facultad de Ciencias, Universidad de Zaragoza, C/Pedro Cerbuna 12, 50009 Zaragoza, Spain
e-mail: gisbert@unizar.es

M. Lago
e-mail: mlago@unizar.es

D. Gómez-Gras
Departamento de Geología, Facultad de Ciencias, Universidad Autónoma de Barcelona, Barcelona, Spain
e-mail: david.gomez@uab.edu

N. Gretter · J. Lloret · A. Ronchi
Department of Earth and Environmental Sciences, University of Pavia, Via Ferrata 1, 27100 Pavia, Italy
e-mail: nicola.gretter@gmail.com

J. Lloret
e-mail: joan.lloret01@universitadipavia.it

A. Ronchi
e-mail: ausonio.ronchi@unipv.it

N. Heredia Carballo
IGME, C/Matemático Pedrayes 25, 33005 Oviedo, Spain
e-mail: n.heredia@igme.es

L. Márquez · A. Márquez-Aliaga · P. Plasencia
Departamento de Geología, Facultad de Biología, Instituto Cabanilles, Universidad de Valencia, 46100 Burjassot, Valencia, Spain
e-mail: leopoldo.marquez@uv.es

A. Márquez-Aliaga
e-mail: ana.marquez@uv.es

P. Plasencia
e-mail: pablo.plasencia@uv.es

configuration developed and the compressive tectonics definitively gave way to a large-scale transtensional and extensional regime, and the initial, or tectonic phase, of many basins in different microplates, including Iberia. These new conditions finally brought to continental break-up, the north-directed subduction of the Paleotethys oceanic ridge beneath Eurasia (Stampfli and Borel 2002; Stampfli et al. 2013; Druguet et al. 2014), and the opening and westward expansion of the Neotethyan ocean (Angiolini et al. 2013 and references therein) (Fig. 3.1b). More broadly, the latest Carboniferous-Early Permian extension was marked by the development of a lateral mega shear system connecting the Alleghanian Orogen to the Urals, through a "middle earth" intra-Pangea wrench zone, most likely located between the Iberian Peninsula and the Bohemian massif (e.g. Arthaud and Matte 1977; Gutiérrez-Alonso et al. 2011; Murphy et al. 2009, 2010; Scotese 1984, 2003; Aubele et al. 2012). The onset, the evolution and development of the Late Paleozoic rifting phases produced several small extensional sub-basins, filled by terrestrial sediments: it was the local response to the progressive collapse and dismantling of the Variscan belt, in late to post-orogenic extension, wrenching and thinning of the orogenic lithosphere (Burg et al. 1990; Faure and Pons 1991; Faure et al. 2002; Van Den Driessche and Brun 1989; Von Raumer et al. 2013). Such tectonic activity controlled both the subsidence and the post-orogenic magmatism (ca. 310–295 Ma) affecting SW Europe (e.g. Arche and López-Gómez 1996; Bruguier et al. 2003; Cassinis et al. 2003; Cortesogno et al. 1998; Dallagiovanna et al. 2009; Decarlis et al. 2013; Fernández-Suárez et al. 2000; Gutiérrez-Alonso et al. 2011; Maino et al. 2012; Pereira et al. 2014; Ronchi et al. 2008; Valle Aguado et al. 2005).

A first generalized subsidence stage, still with tectonic influence, would indicate the beginning of a mature phase in the rifting evolution of the basins, i.e. the transition from tectonic to thermal subsidence (Van Wees et al. 1998; McCann et al. 2006; Murphy et al. 2009). This transitional stage was associated to the first marine incursions, although still without covering the whole basins (Ziegler and Stampfli 2001). Marine incursions were first into narrow corridors and later surrounding the highest areas of the flanks (Allen and Allen 2005; Vargas et al. 2009; Escudero-Mozo et al. 2015). The evolution of these basins during the rifting stage normally shows important interruptions in the sedimentary record, as it will be shown later in the case of the Iberian Basin. A later generalized subsidence represented by extensive marine platforms devel-

A. Martín-Algarra · A. Pérez-López · C. Viseras
Dpto. de Estratigrafía y Paleontología, Facultad de Ciencias, Universidad de Granada, Avda. Fuentenueva, s/n, 18071 Granada, Spain
e-mail: agustin@ugr.es

A. Pérez-López
e-mail: aperezl@ugr.es

C. Viseras
e-mail: viseras@ugr.es

A. Martín-Algarra · A. Pérez-López
Instituto Andaluz de Ciencias de la Tierra (CSIC-Universidad de Granada), Avda, de las Palmeras 4, 18100 Armilla (Granada), Spain

F. Martín-González
Área de Geología ESCET, Universidad Rey Juan Carlos, C/Tulipán s/n, 28933 Móstoles, Madrid, Spain
e-mail: fidel.martin@urjc.es

M. Marzo · F. Ortí · E. Ramos
Department de Mineralogia, Petrologia i Geologia Aplicada, Universitat de Barcelona, 08008 Barcelona, Spain
e-mail: mariano.marzo@ub.edu

F. Ortí
e-mail: f.orti@ub.edu

E. Ramos
e-mail: emilio@ub.edu

R. Mercedes-Martín
SZALAI Grup S.L, P.O. Box 1005 07314 Caimari, Mallorca, Spain
e-mail: rmercedesgeo@gmail.com

F. Pérez-Valera · J. A. Pérez-Valera
Departamento de Ciencias de la Tierra y del Medio Ambiente, Facultad de Ciencias, Universidad de Alicante, 03690 San Vicente Del Raspeig (Alicante), Spain
e-mail: fperez@ua.es

J. A. Pérez-Valera
e-mail: japerezv@ua.es

F. Pérez-Valera
Centro de Estudios Avanzados en Ciencias de la Tierra, Universidad de Jaén, Campus Las Lagunillas s/n, 23071 Jaén, Spain

R. Salas
Departament d´Petrología i Geoquímica, Facultat de Geología, Universitat de Barcelona, Barcelona, Spain
e-mail: ramons@ub.edu

Á. Suárez-Rodríguez
IGME León, Parque Científico de León, Avda. Real 1, 24006 León, Spain
e-mail: a.suarez@igme.es

T. Ubide
School of Earth and Environmental Sciences, Faculty of Science, The University of Queensland, Brisbane, Australia
e-mail: t.ubide@uq.edu.au

B. Valero Garcés
Instituto Pirenaico de Ecología-CSIC, Avda. Montañana 1005, 50059 Saragossa, Spain
e-mail: blas@ipe.csic.es

H. Vargas
REPSOL, C/Méndez Álvaro 44, 28045 Madrid, Spain
e-mail: henar.vargas@repsol.com

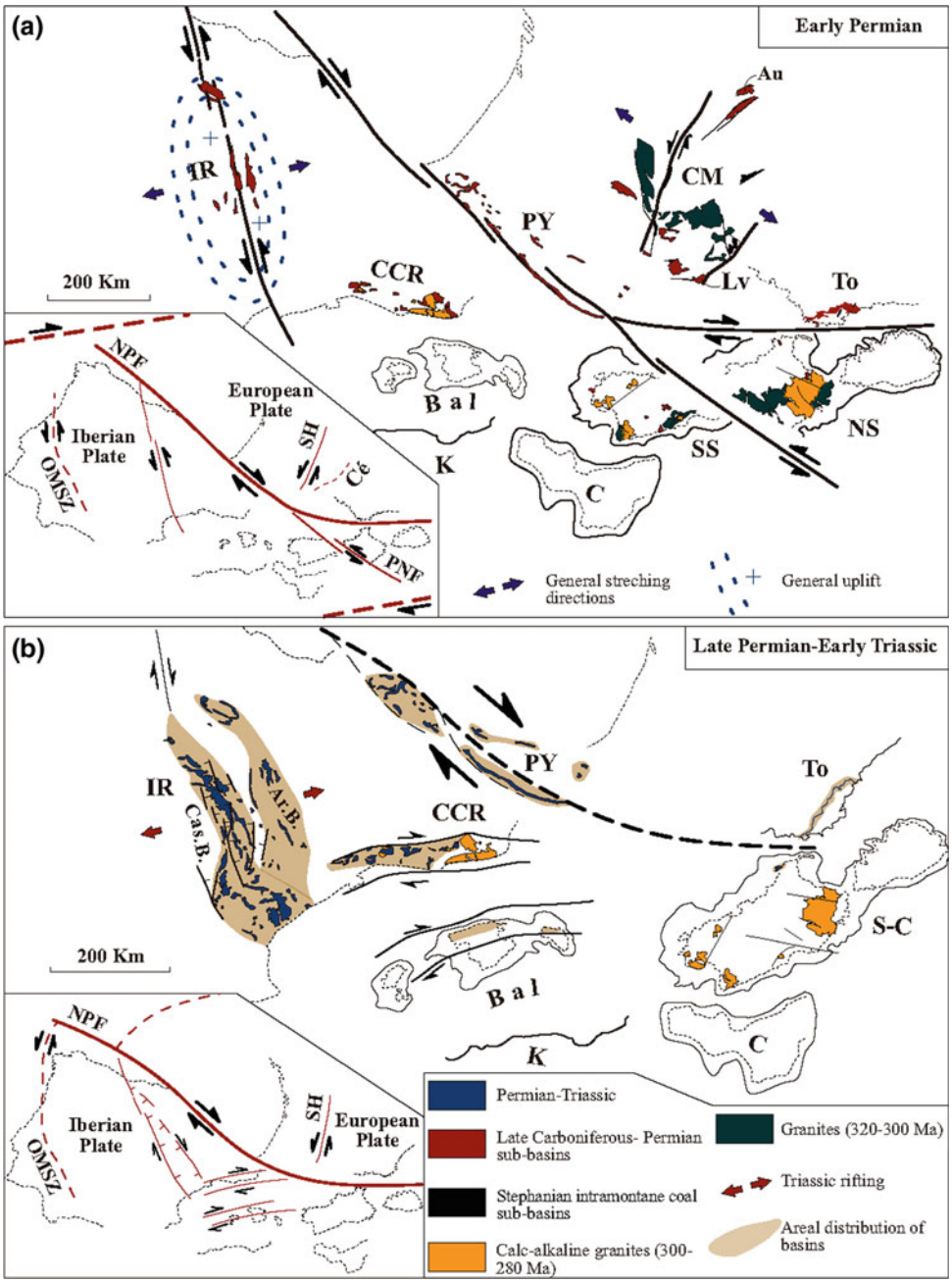

Fig. 3.1 Paleogeographical maps of Iberia of the western Europe for **a** the Late Carboniferous-Early Permian and **b** Late Permian-Early Triassic times, inspired on Matte (2001) and Domeier et al. (2012). Insets detail the southwestern European sector. The main strike–slip structures are sketched in the little marginal box (Faure et al. 2009; De Vicente et al. 2009): Cé: Cévennes Fault; NPF: North Pyrenean Fault; PNF: Permian Nuoro Fault; SH: Sillon–Houiller Fault. OMSZ: Ossa–Morena Zone. Major basins and localities: Ar.B.: Aragonese Branch; Au: Autun Basin; Bal: Balearic Islands; C: Calabria; Cas.B.: Castilian Branch; CCR: Catalan Coastal Ranges; CM: Central Massif; IR: Iberian Ranges; K: Kabilies; Lv: Lodève Basin; NS: North Sardinia; PY: Pyrenees; SS: South Sardinia; To: Toulon–Cuers

opment was mainly related to the thermal activity in the basins (thermal subsidence), and represents the postrift or passive margin stage (dealt with in Chap. 4.2.2), which extended from latemost Triassic to Middle Jurassic times.

3.2 The Pyrenean Basin

López-Gómez J, De La Horra R, Ronchi A, Gretter N, Barrenechea J, Lloret J, Arche A, Borruel-Abadía V, Heredia Carballo N, Martín-González F, Suárez-Rodríguez A, Cadenas P, Fernández-Viejo G, Sopeña A, Galán-Abellán B, Sánchez-Moya Y, Díez JB, Rodríguez-Méndez L, Cuevas J, Tubía JM, Martín-Chivelet J, Escudero-Mozo MJ, Ortí F, Pérez-López A, Lago M, Galé C, Ubide T, Valero Garcés B and Gisbert Aguilar J

The present-day Pyrenean Ranges, extending E-W from the Mediterranean Sea, in the Catalonian coast, to the Basque-Cantabrian Cordillera, or western Pyrenees, is the result of around 84 Ma of progressive inversion and deformation of previous Mesozoic basins (Capote et al. 2002; Barnolas and Pujalte 2004). These previous Mesozoic basins were Permian to Cretaceous extensional to transtensional rift

systems, and were developed in two main rift–postrift cycles: Permian–Late Jurassic and Late Jurassic–Late Cretaceous, although later Cenozoic deformation masked the original rifting structure of these basins. The geodynamic development of the Permian-Triassic initial rifting phase is described here following the two structural units of Muñoz's (2002) configuration of the Pyrenees: Basque-Cantabrian Pyrenees, and Aragonese-Catalan Pyrenees (Fig. 3.2). The limit between both main units is represented by the Pamplona fault (also called Estella-Dax or Navarre Diapirs Line), a structure representing an important transtensional displacement (Vergés 2003; Larrasoaña et al. 2003).

3.2.1 The Initial (Tectonic) Rifting Phase

Gretter N, De La Horra R, Lloret J, Arche A, Ronchi A, López-Gómez J, Barrenechea J

In the Pyreneean basin, the extensional regime in response to the progressive collapse and dismantling of the Variscan belt, progressively acquired a transcurrent component, leading to a more transtensional regime, along Early Permian times. The direct result of such tectonics was the development of a series of elongate half-graben intramontane basins (Arche and López-Gómez 1996; López-Gómez et al. 2002; McCann et al. 2006; Pereira et al. 2014; Valero-Garcés 1993). These troughs were filled not only with alluvial fan slope breccias and, towards the depocenters, with fluvio-lacustrine sediments, but also with various kinds of volcanic and volcaniclastic products. In fact, the Late Carboniferous calc-alkaline volcanic activity (e.g. Bixel 1984; Lago et al. 2004a, b; Galé 2005; Pereira et al. 2014) played an important role and accompanied the birth and evolution of every Pyrenean Late Paleozoic basin. For this reason the thick volcaniclastic deposits at the base of the basin infill, justifies the presence of faults, deep enough to reach the asthenosphere, providing conduits to these important outpourings. The following progressive declining of the calc-alkaline magmatism in most of the southern Variscides and the consequent mid-Permian magmatic gap (e.g. Deroin and Bonin 2003; Muttoni et al. 2003; Gutiérrez-Alonso et al.

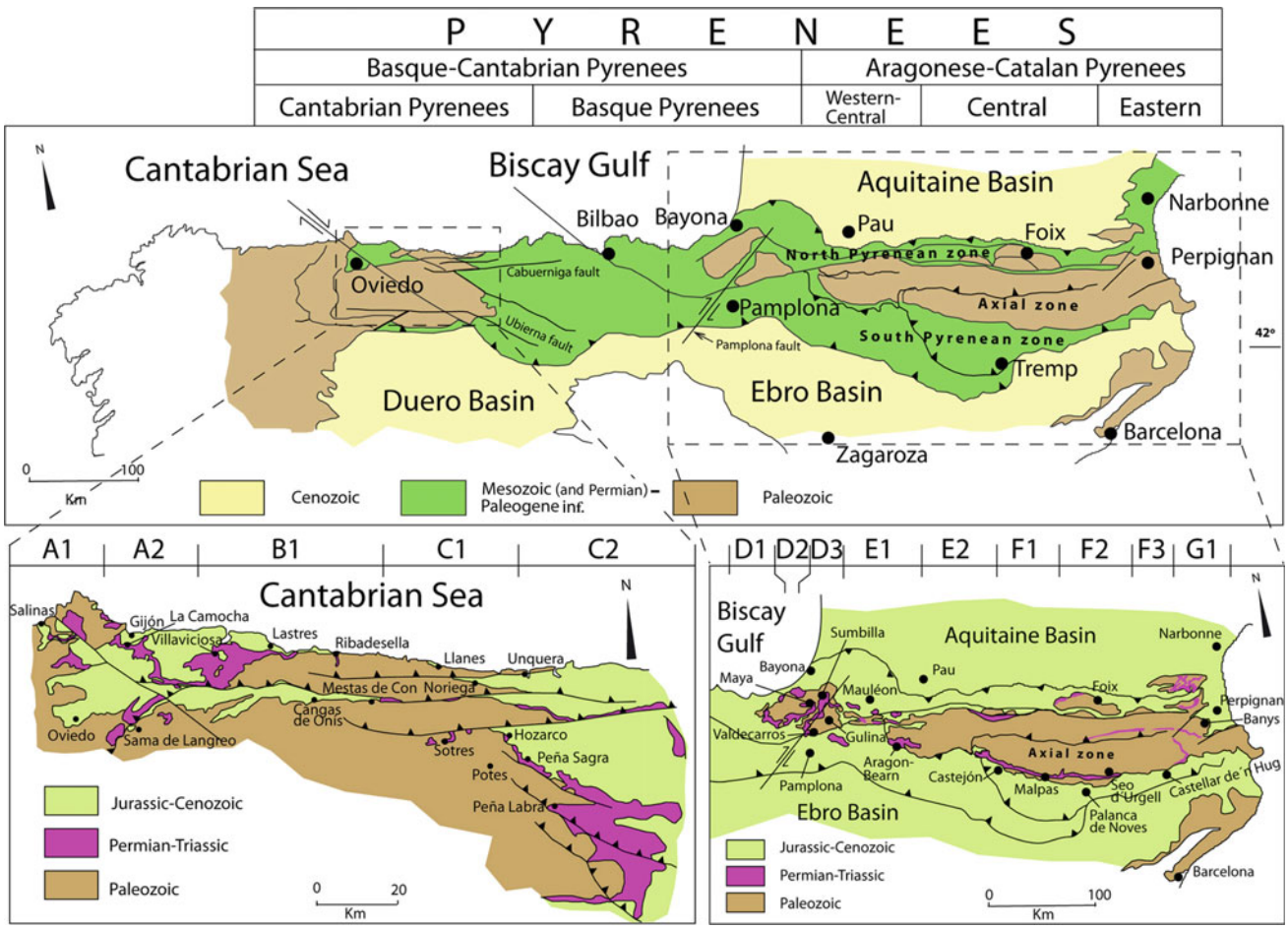

Fig. 3.2 The Pyrenees. Location of the Permian and Triassic outcrops and scheme of the described lithological units in the main representative sections in the different subdivided areas (Main lithological areas based on Barnolas and Pujalte 2004). Subdivision zones in the Pyrenees based on Muñoz (2002). Sectors A1 to G1 are here subdivided as those where the most representative sections are located

2008a, b; Angiolini et al. 2013) has been related to the main phase of a general strike-slip tectonic event, which probably led to an intra Pangea reorganization. A renewed Late Early to Late Permian extension, marked by clastic sedimentation of extensive red beds in the European domain, together with an alkaline magmatism, continued in Triassic times. Although this configuration affected most sectors of Paleoeurope, in the Pyrenees and eastern Iberian plate this regime led to the development of symmetric basins bounded by lystric faults, probably as the response to dextral strike-slip movements at the margins of the Iberian Microplate and the crustal collapse of the overthickened roots of the Variscan orogen (Arche and López-Gómez 1996; de Vicente et al. 2009). Here the extension was not accompanied by volcanic activity; as a matter of fact, the late Paleozoic volcanism, whose paroxysm extended from the latest Carboniferous to the Early Permian, seems to stop by the middle Guadalupian epoch. Moreover, a recovery of the isotherms occurred at the same time and general subsidence rates were moderate to low, decreasing with time in all enlarged sedimentary basins.

3.2.2 Sedimentation During the Permian-Triassic Initial Rifting Phase

López-Gómez J, De La Horra R, Ronchi A, Arche A, Gretter N, Barrenechea J, Lloret J and Borruel-Abadía V

The beginning of the Permian-Triassic small basins in the Pyrenees, as in the rest of Iberia, was related to the fragmentation of southern Variscan Europe and western Tethys as a result of the initial break-up of Pangea (López-Gómez et al. 2002). Although most of the Permian-Triassic rift basins in the Pyrenees followed a similar development, some structural differences allow distinguishing the Basque-Cantabrian and the Aragonese-Catalan Pyrenean basins as separate sub-basins. As a consequence of the initial tectonic control in basin development and the later Cenozoic deformation, the outcrops of these basins show today a distribution related to seven main areas (Figs. 3.2 and 3.3a): A to D in the Basque-Cantabrian zone, and E to G in the Aragonese-Catalan zone.

Figure 3.3a allows recognition of the main sedimentary pulses and the intervening uplifting-erosion periods during the Permian-Triassic time interval. A remarkable characteristic is that similar time-equivalent sedimentation and erosion intervals are broadly recognized in most of the Pyrenean basin areas indicating a common geodynamic response (López-Gómez et al. 2019). It resulted from complex multistage process as the result of both the Variscan and the Pyrenean/Alpine? orogenic cycles. So, depending on the authors, the estimated ages and differentiated stratigraphical units, and the different observed areas, up to four main sedimentary pulses, separated by interruption/erosion stages, can broadly be identified in this first rift (synrift) period: (i) Latest Carboniferous to Early Permian (Sakmarian?), (ii) Early Permian (Artinskian to Kungurian?), (iii) late Early Permian (Kungurian?) but expanding to Middle Permian (Wordian?) or even Late Permian (Wuchiapingian?) times, and (iv) Triassic (from late Olenekian to Norian). This latter one surely also interrupted by pulses without sedimentation and erosion, but the absence of precise-age determinations of the rocks can not confirm or refuse this idea.

These sedimentary pulses preserve the signatures of the late Paleozoic Pangea break-up during the progressive dismantling of the Variscan chain up to the Triassic diffused extension. These pulses are separated by unconformities representing periods of tectonic activity, uplift, interruption in sedimentation and erosion. As it is discussed later, they are also included in different TSU and transpression, transtension and extension tectonic events. The first three sedimentary pulses record volcanic episodes that allow a precise dating of the events in different areas of the Pyrenean basin (e.g. Bixel 1987; Briqueu and Innocent 1993; Lago et al. 2002; Rodríguez-Méndez et al. 2014; Denèle et al. 2012; Pereira et al. 2014; Gretter et al. 2015). It is also important to indicate that the Basque-Cantabrian Pyrenees area shows some different stratigraphic successions when they are compared with the rest of the Pyrenean Basin areas. As discussed later, this is probably due to erroneous interpretations related to the lack of precise-age determinations in the Cantabrian area.

In the end of the last episode (Olenekian to Norian), the basins were inter-connected during the mature phases of the rifting, during the beginning of the transition from tectonic to thermal subsidence that lasted until the Late Triassic, when large dolomitic and evaporitic deposits were accumulated (Calvet et al. 1993; Ortí et al. 1996; Espina et al. 2004). This stage of beginning of thermal subsidence continued through the Jurassic, when shallow water marine deposits formed the dominant facies in the basins completing the first Mesozoic synrift-postrift phase.

3.2.2.1 Basque-Cantabrian Pyrenees

The Variscan Heritage

Heredia Carballo N, Martín-González F and Suárez-Rodríguez A

The Variscan orogenic belt that crops out in the western Iberian Peninsula forms the Iberian Massif (Figs. 3.2 and 3.4). In the northwestern sector of this massif (the external Cantabrian Zone), the Variscan orogeny finished in Late Carboniferous (Gzelian)-Early Permian (Asselian) times, developing a characteristic arc shaped orogen (Asturian Arc)

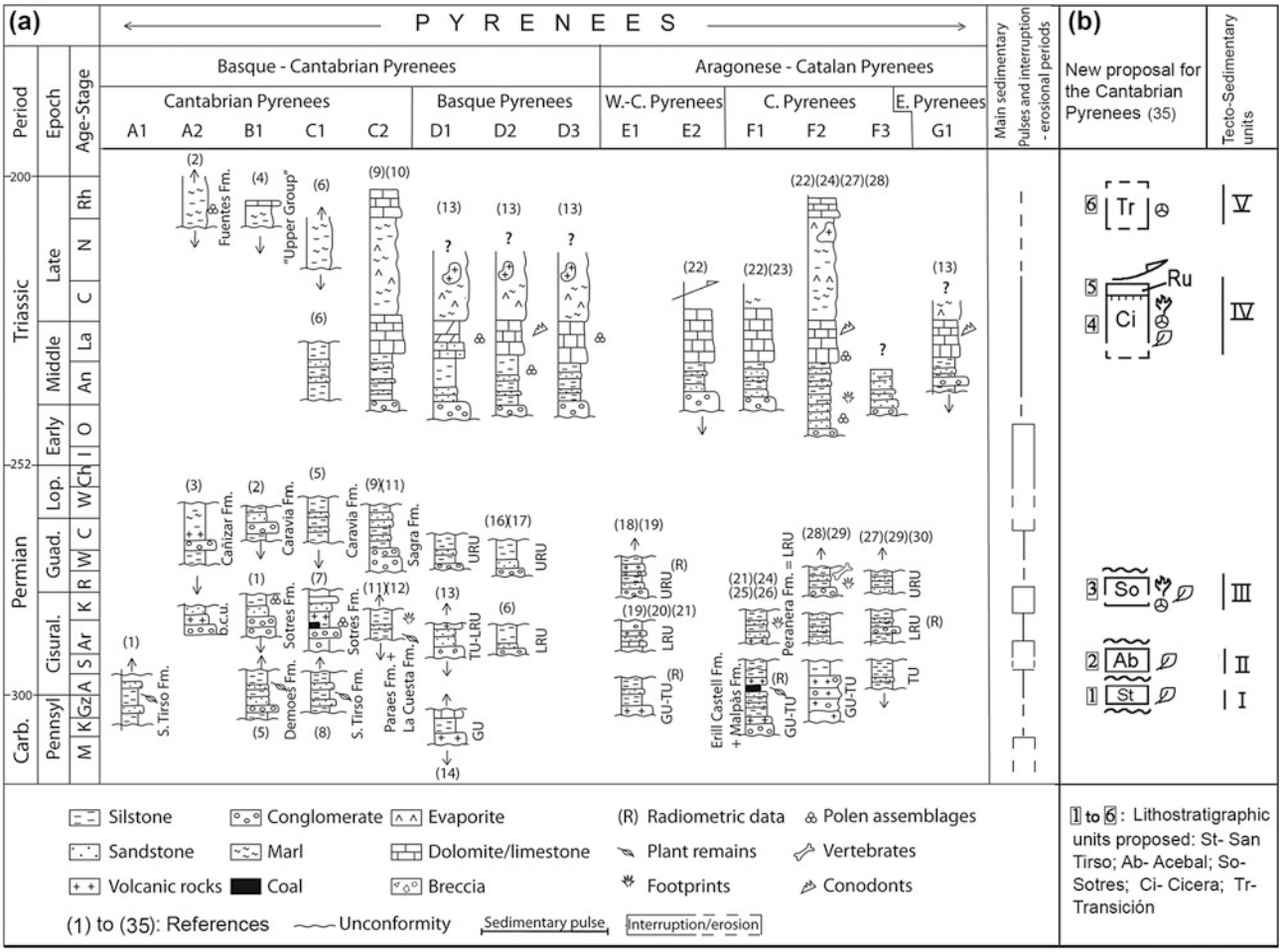

Fig. 3.3 **a** The most representative Permian and Triassic selected sectors and sections in the Pyrenees. Type sections: A1—Gamonedo; A2—La Camocha—La Collada; B1—Caravia—Villaviciosa; C1—Sotres; C2—Peña Sagra; D1—Maya; D2—Valcarlos; D3—Gulina; E1—Aragon—Bearn; E2—Castejón; F1—Erill-Castell–Malpàs; F2—La Seu d´Urgell–La Trava; F3—Catellar de n´Hug-Camprodón; G1—Banys D´Arles–Massarac. See Fig. 3.2 for location of the sections. Selected references for the type sections: 1—Martínez García (1999); 2—Martínez García (1991); 3—Pieren et al. (1995); 4—Manjón et al. (1992); 5—Martínez García (1999); 6—Sopeña et al. (2009); 7—Juncal et al. (2016a, b); 8—Gervilla et al. (1978); 9—García-Mondejar et al. (1989); 10—Maas (1974); 11—Gand et al. (1997); 12—Robles and Pujalte (2004); 13—Calvet el al. (1993); 14—Denèle et al. (2012); 15—Lasheras et al. (1999); 16—Müller (1973); 17—Valero-Garcés (1994); 18—Valero (1974); 19—(Valero Garcés and Gisbert Aguilar 1992); 20—Pereira et al. (2014); 21—Lago et al. (2004a, b); 22—Voigt and Haubold (2015); 23—Fréchengues and Peybernès (1991); 24—Gisbert (1983); 25—Lloret et al. (2016); 26—Mujal et al. (2016a); 27—Gisbert et al. (1985); 28—Müller (1969); 29—Gretter et al. (2015); 30—Bixel and Lucas (1987); 31—Martí and Barrachina (1986)–(1987); 32—Mey et al. (1968); 33—Martínez García et al. (1998); 34—Fréchenges et al. (1990); 35-López-Gómez et al. (2019). The subdivided areas (from A1 to G1) correspond to the ones indicated in Fig. 4.9. Other symbols: Ca—Cabranes Fm., b.c.u—Basal Conglomeratic Unit, Ar—Arroyo Fm, Pa—Paraes Fm., La—La Cuesta Fm., GU—Grey Unit, TU—Transition Unit, LRU—Lower Red Unit, URU—Upper Red Unit. **b** A new stratigraphic organization proposed by López-Gómez et al. (2019) for the Permian and Triassic sedimentary record of the Cantabrian Pyrenees by . It includes new tecto-sedimentary and lithostratigraphic units

(Merino-Tome et al. 2009; Gutiérrez-Alonso et al. 2011) (Fig. 3.4). Shortly after, this orogen collapsed and the related extensional tectonics allowed the development of post-orogenic Permian basins and the emplacement of the last calc-alkaline Variscan magmas in upper crustal levels. These magmas even reached the earth surface, like in the Villaviciosa basin, where volcanic intercalations are abundant (Suárez-Rodríguez 1988; Valverde-Vaquero 1992) (B in Fig. 3.4). This post-orogenic magmatism can be observed in the eastern Cantabrian Zone, where the small plutons of Peña Prieta, Pico Jano, Pico Iján and the igneous complex of Infiesto were emplaced (Fig. 3.4). This magmatism took place between 297 and 292 Ma (Asselian-Sakmarian) (Gallastegui et al. 2004). In late Early Permian times, the volcanism decreases and the basin infill is mainly sedimentary with source areas located in nearby areas. Related to this collapse a subhorizontal cleavage is formed, which offset the Variscan structures, being better developed in the Carboniferous slate formations of the inner part of the Asturian Arc (Pisuerga-Carrión Region) (Aller et al. 2004).

The Variscan and late-Variscan structures of the Asturian Arc control the main Permian normal faults and therefore the related Permian basins. In Fig. 4.12 the probable extension of the Permian basins is shown, located under Mesozoic rocks in the western end of the Basque-Cantabrian Region of the Alpine Pyrenean Orogen (Martín-González and Heredia 2011). Noticeably, the Villaviciosa and La Justa-Aramil basins, among others, located in the central part of the Cantabrian Zone, have a predominant NE–SW orientation (A and B in Fig. 3.4) parallel to Variscan thrusts; while those located at the easternmost part, such as those on the Picos de Europa Region and the northern part of the Pisuerga-Carrión Region (Sotres-Pandébano, Cueto Turis, Peña Sagra and Peña Labra basins) have E–W (C in Fig. 3.4) to NW–SE trends (D, E and F in Fig. 3.4), related to Variscan thrusts and late-Variscan faults respectively (López--Gómez et al. 2019).

Extensional tectonics during the Early Permian was not generalized in the Cantabrian Zone, giving rise to narrow and isolated continental basins with very local very local depocenters. This extensional tectonics became generalized during the Triassic, related to the Pangea fragmentation, occupying the sedimentary basins wider areas.

A Geodynamic Approach

Cadenas P and Fernández-Viejo G

From latest Carboniferous to Early Permian, a dextral translation of Africa relative to Europe gave rise to the development of a conjugate shear system that transected the Variscan fold belt and its northern foreland, leading to the beginning of the break-up of Pangea (Arthaud and Matte 1977). Collapse of the Variscan orogen was accompanied by regional uplift, subsidence of an array of transtensional and pull-apart basins, and widespread magmatism (Ziegler and Stampfli 2001). Once the tectonic and magmatic activity abated in the Variscan domain during the Late Permian and the Triassic, the thermal subsidence of the lithosphere and the southwestward propagation of the preexisting Norwegian-Greenland and Tethys rifts dominated the evolution of the Variscan domain during the Late Triassic (Fig. 3.5a, b). Those rifts, together with the formation of an ESE trending rift system connecting both, initiated the future Iberian-Eurasian plate boundary (Ziegler 1990; García-Mondéjar 1989). Within this context, Western and Central Europe, including the Variscan domain of Iberia, were transected during the Triassic by a complex

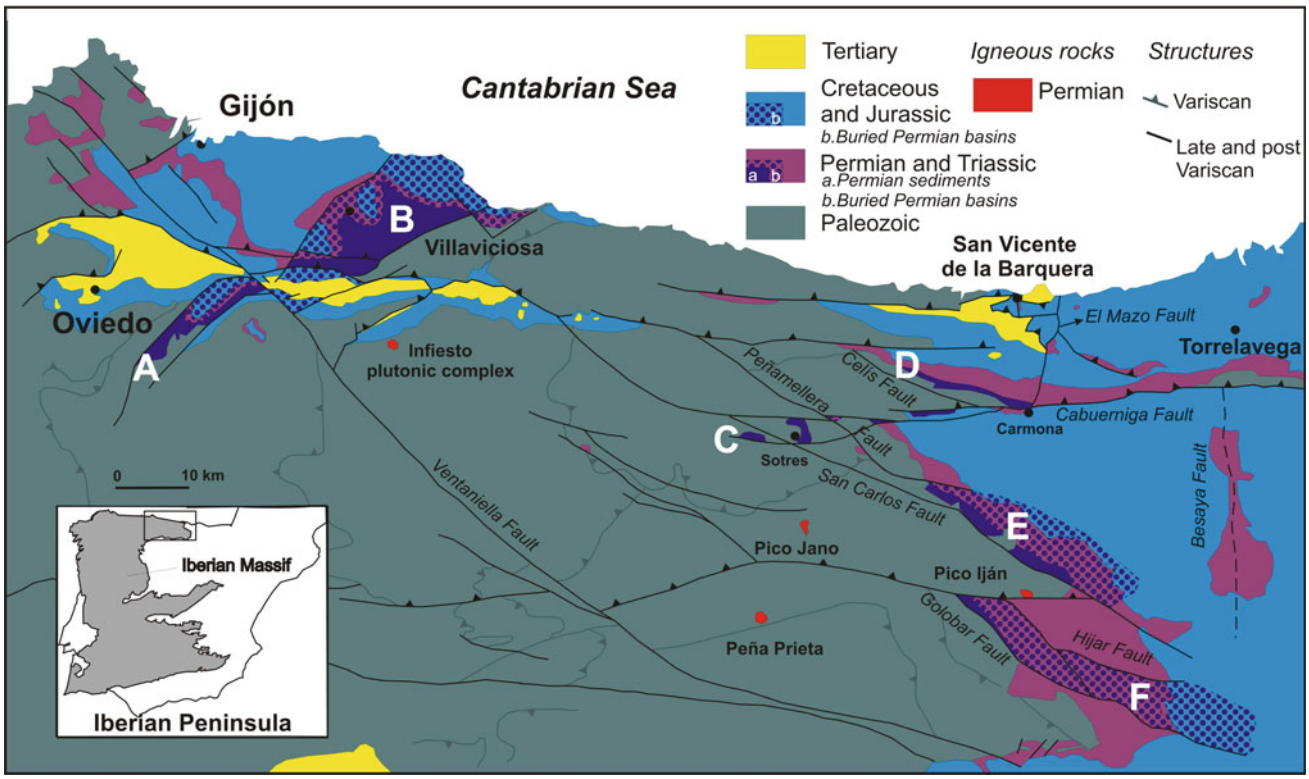

Fig. 3.4 Geological sketch map of the eastern Cantabrian Zone and surroundings. This sketch only shows the location of the basins containing exposed and well-dated Permian rocks and its related post-Variscan normal faults. Variscan, late Variscan and/or Alpine faults and the main outcrops of Lower Permian post-orogenic plutonic rocks are also shown

and multidirectional rift system, with some elements superimposed on Permo-Carboniferous fractures (Ziegler 1990; Stampfli 1991) (Fig. 3.5b). The Bay of Biscay rift and the Iberian rifts initiated as part of this extensional system in the Middle Triassic (Ziegler 1990; Salas et al. 2001) (Fig. 3.5b).

Early extensional stages started in the Permian, leading to the development of several small-scale basins in the western area of the current Pyrenean-Cantabrian domain, whose patchy remnants (Fig. 3.5c, d) recorded a continental rifting lasting for 90 Ma. It predates the main Lower Cretaceous hyperextensional event, during which major rift basins within the Bay of Biscay rift system developed (Tugend et al. 2014), evolving to lithospheric breakup and a short-lived seafloor spreading period in the Bay of Biscay (Sibuet et al. 2004; Vissers and Meijer 2012). Some remnants of the initial Permo-Triassic rift event can be found within the two major Mesozoic basins in the western Pyrenean-Cantabrian area, the Asturian Basin and the Basque-Cantabrian Basin (Fig. 3.5c). Recent studies into the continental platform of the North Iberian margin (Cadenas et al. 2018) also indicate that syncline basins developed off the Galicia coast (Fig. 3.6). Borehole Galicia B2 (Lanaja 1987), drilled at the westernmost part of the Cantabrian platform (Fig. 3.6), shows these minor troughs as infilled by a syn-rift unit, including Triassic deposits, and a post-rift unit, including Aptian deposits.

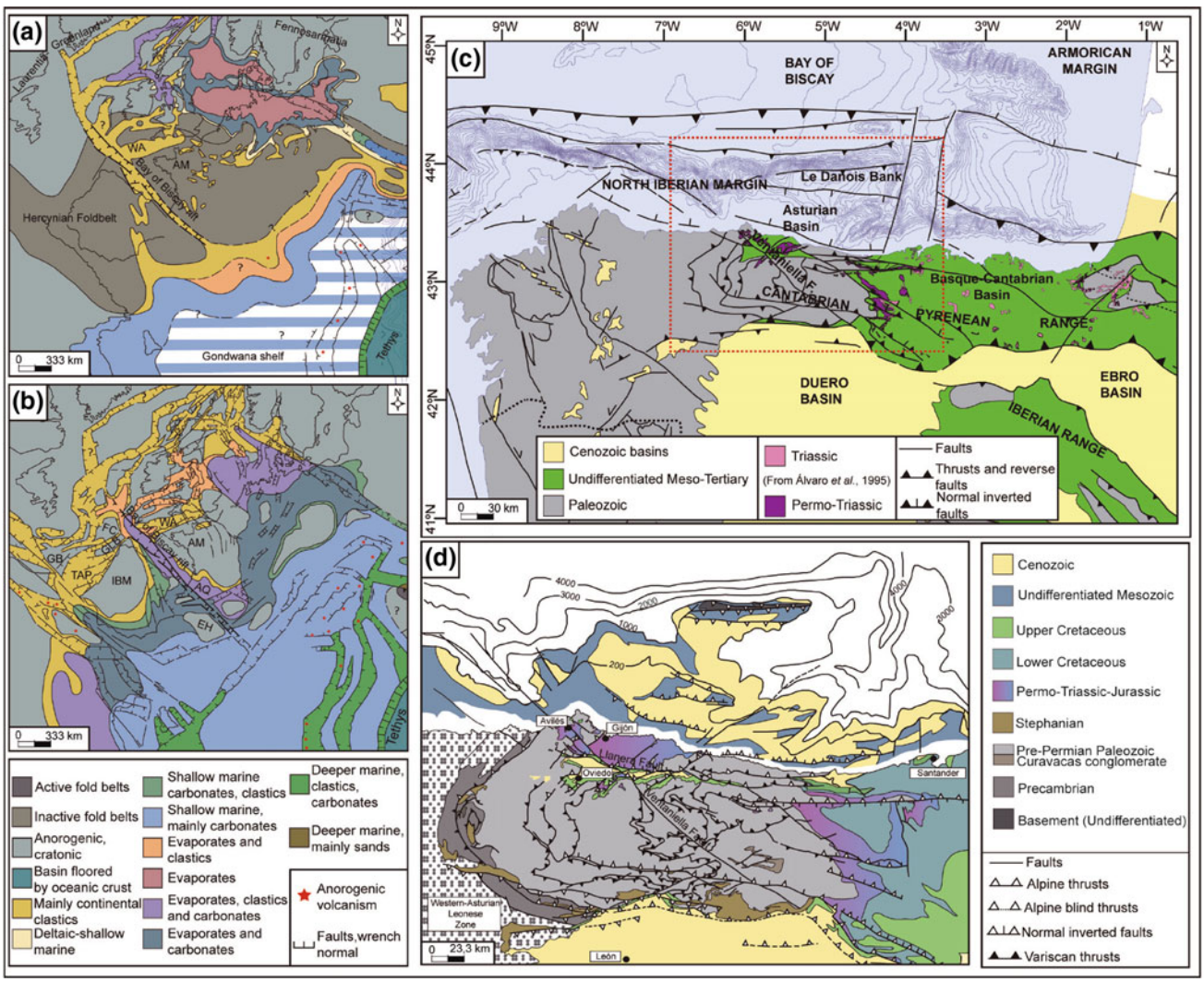

Fig. 3.5 **a**, **b** Geodynamic context in the Late Permian and the Middle Triassic, respectively, showing the location of the Bay of Biscay rift (from Ziegler 1988a, b). **AM**: Armorican Massif, **AQ**: Aquitaine Basin, **EH**: Ebro High, **FC**: Flemish Cap, **GB**: Grand Banks, **GLB**: Galicia Bank, **IBM**: Iberia Meseta, **TAP**: Tagus Abyssal Plain, **WA**: Western Approaches Trough; **c** geotectonic map of the Asturian and Basque-Cantabrian domains displaying the main outcrops of the Permo-Triassic successions within the Asturian and the Basque-Cantabrian basins, taken from Álvaro et al. (1995). The red square delineates the area displayed in detail in D; **d** geological map of the Asturian-Cantabrian and westernmost part of the Basque domains showing in detail the Permo-Triassic rocks (modified from Pulgar et al. 1999)

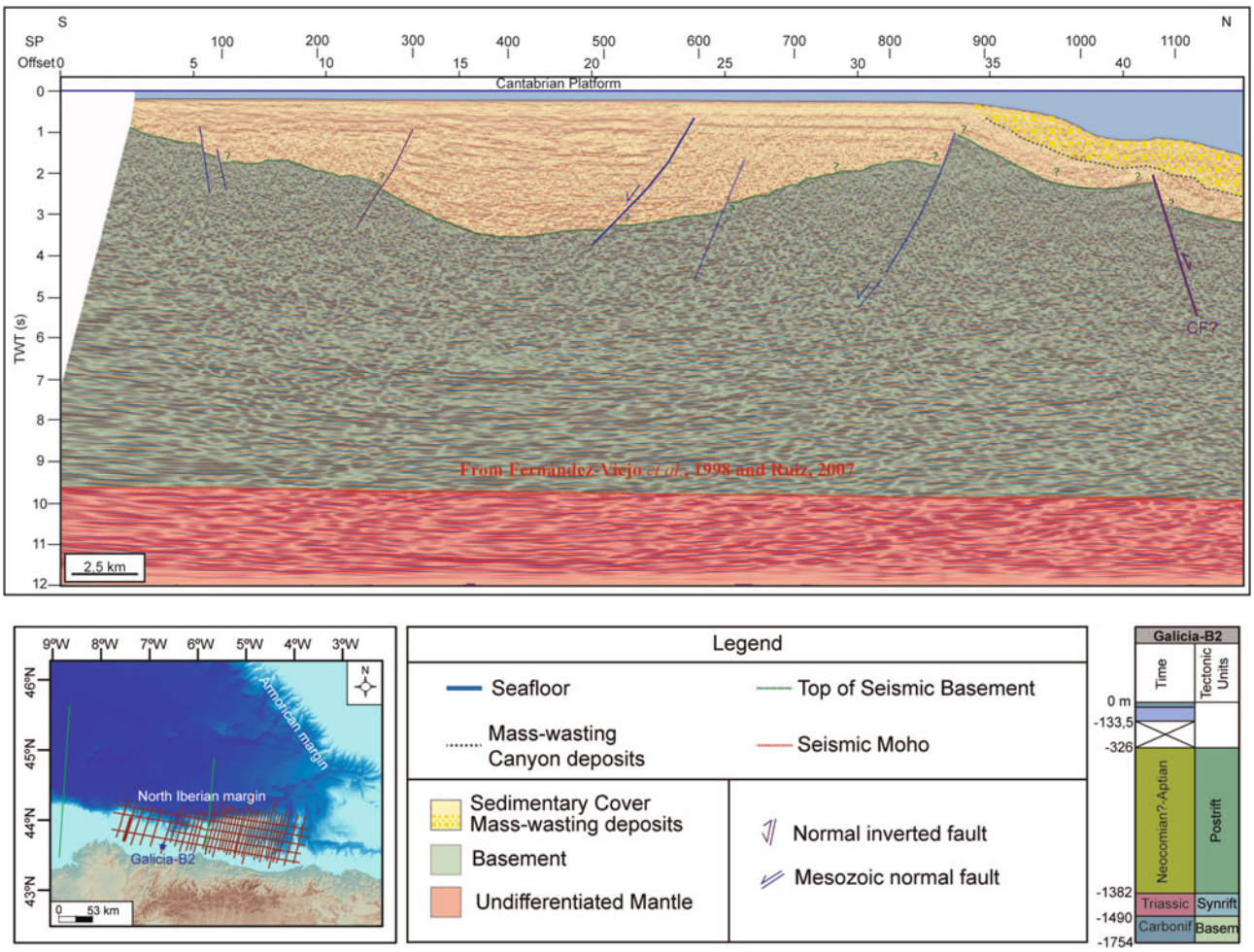

Fig. 3.6 Time migrated seismic reflection profile crossing the westernmost part of the Cantabrian platform. The figure shows a syncline rift basins located in Seismic Moho from Fernández-Viejo et al. (1998) and Ruiz (2007). In the lower left, the location of the seismic line within the reflection dataset used to interpret structural and stratigraphic features across the North Iberian margin. Refraction profiles used to define the seismic Moho in the western corner are traced in green. Galicia B2 is posted as a blue star. Its stratigraphic section borehole report, evidencing the presence of Triassic rocks, and the interpreted tectonic units, are shown in the lower right corner. **CF**: Cantabrian Fault, and **SP**: Splay fault, have been taken from Fernández-Viejo et al. (2014)

The offshore Asturian Basin sits on a depressed area formed between Le Danois Bank and the Cantabrian continental platform (Cadenas and Fernández-Viejo 2017; López-Gómez et al. 2019) (Fig. 3.5c). The presence of diapirs and halokynetic-related structures affecting the seismic sequences has been attributed to the rise of Triassic evaporites (Boillot et al. 1979; Cadenas and Fernández--Viejo 2017). Some Permo-Triassic remnants are preserved onshore, close to the Asturian coast (Fig. 3.5c, d). These outcrops include Late Stephanian, Permian and Triassic successions unconformably overlain by Jurassic red beds (Martínez-García 1981). In the eastern sector, the structure is dominated by a set of NE-SW and NW-SE syn-sedimentary normal faults (Suárez-Rodríguez 1988). Relying on an isopach map, Suárez-Rodríguez (1988) inferred that the thickness of the trough increases towards the NW. Two NE–SW depressions have been recognized, whit intensive volcanism and the syn-sedimentary activity indicating a transtensive continental rifting. Three faults systems, formed during the late Variscan orogeny, have been recognized affecting Mesozoic sediments within the Asturian area: (i) a NE–SW trending fault system, (ii) NW–SE structures, including the Cantabrian or Ventaniella fault (Julivert 1960; Martínez-Álvarez 1968) (Fig. 3.5c, d), and (iii) an ENE-WSW to ESE–WNW fault system, including the Llanera fault (Fig. 3.5d). All show evidences of a distinctive reactivation to various extents during the subsequent Late Jurassic to Late Cretaceous extension and during Cenozoic compressional tectonic events.

The Basque-Cantabrian Basin crops out extensively west of the Pyrenees (Figs. 3.2 and 3.5c). The evidences of Permo-Triassic extension are found in the western area

where normal faults and syn-sedimentary activity, including great sedimentary thickness variations, have been recognized displaying horst-graben configurations (Espina 1997; Suárez-Rodríguez 1988; Lepvrier and Martínez-García 1990).

Tectonically speaking, both basins can be considered to have a late Hercynian heritage, because they developed along late Variscan lineaments (Arche and López-Gómez 1996). This intracontinental Permo-Triassic rift episode seems to have been a low magnitude rift. Minor segmented troughs were structured by NE–SW bounding faults developed during a transtensional period which was accompanied by bimodal volcanic rocks. Intense volcanism of alkaline type supports the interpretation of a continental rift setting (Martínez-García and Tejerina 1985).

The same context has been proposed for the Iberian Range basins (De Vicente et al. 1996). With a high degree of mechanical coupling between the brittle and the ductile parts of the crust, small basins developed in what has been referred to as "proximal domain" in terms of architectural rift classification (Tugend et al. 2014). It can be highlighted that the main direction of extension at this period would be aproximately NE–SW (Cadenas et al. 2018). It was probably a limited rift zone trending NW–SE with a low strain rate accommodated by brittle deformation and stretching of the crust. Later, with the advance of the Atlantic rifting and reactivation of these earliest weakness zones, mayor rift basins developed during the subsequent rifting periods that evolved to lithospheric breakup and seafloor spreading in the Bay of Biscay.

The Beginning of Sedimentation in the Basque-Cantabrian Pyrenees

López-Gómez J, De La Horra R, Ronchi A, Arche A, Gretter N, Barrenechea J, Sopeña A, Lloret J, Borruel-Abadia V, Galán-Abellán B, Sánchez-Moya Y and Díez JB

The beginning of sedimentation in the Basque-Cantabrian Pyrenean Basin (A1 to D3 areas in Fig. 3.2) took place on a very irregular topography with a relief up to 500 m between troughs and swells (García-Mondejar et al. 1989; Espina 1994). This initial configuration and the later activity of the faults allowed irregular sedimentation in the isolated Late Carboniferous and Permian basins. As a result, some areas of the western Basque-Cantabrian Basin were active during the Late Carboniferous but did not record Permian or even Triassic sediments, and vice versa. Although the main sedimentary pulses are well recognized not only in the Basque-Cantabrian zone, but also in the Aragonian-Catalan zone of the Pyrenean Basin (Fig. 3.3a), some of these cycles are very incomplete, and even not recorded in this realm.

There are not many detailed stratigraphical works about Permian and Triassic rocks in the Basque-Cantabrian basin. Unfortunately, some of these works even induce to confusion due to the absence of precise ages to locate some units in time and space. Some stratigraphic review works (Martínez-García 1991; Calvet et al. 1993; López-Gómez et al. 2002; Sopeña and Sánchez-Moya 2004; Robles and Pujalte 2004; Espina et al. 2004) have tried to organize the complex mosaic of units, sometimes with numerous local names, but still without a precise stratigraphical frame. Figure 3.3a (A1–D3) shows a classical stratigraphical synthesis of the Permian-Triassic record in the Basque-Cantabrian Pyrenees based on tens of works. However, a recent effort based on new chronostratigraphic data (López-Gómez et al. 2019) has allowed to define a new stratigraphic succession for the Cantabrian area. Fig. 3.3b shows a comparison between this new and the classical stratigraphic succession.

Present-day main faults in the Basque-Cantabrian Basin trend WNW–ESE. They were initially related to the extensional collapse phase of the Variscan orogeny, during the Late Carboniferous-Early Permian (Fig. 3.2). During that time, intermontane terrestrial basins were developed in the northern border of the Iberian plate in response to tectonic readjustments to transtensional faulting in the Chedabucto-Gibraltar and Bay of Biscay areas (López-Gómez et al. 2002). Current sedimentation mainly consisted in slope breccias, alluvial fans, and lacustrine deposits associated with volcaniclastic rocks of calc-alkaline affinities (Denèle et al. 2012) (e.g. San Tirso and Demues formations, or Grey and Transition units in the Cantabrian and Basque areas, respectively) (Fig. 3.3a, A1–D3). Transtensional activity finally ceased and it was followed by a period of uplift, tilting and erosion. An extensional cycle of sedimentation started during the Kungurian (e.g. Sotres Fm, Juncal et al. 2016a, b, in the Cantabrian area, and Lower Red Unit, in the Basque area) (Robles et al. 1987; García-Mondéjar et al. 1989; Mamet and Martínez-García 1995; Gand et al. 1997). After a period of uplift, tilting and erosion, a new cycle of sedimentation started during the Middle Triassic.

This first Mesozoic record is represented by the Buntsandstein facies, consisting of conglomerates, sandstones and siltstones, related to alluvial deposition (Fig. 3.3, A1–D3). It may reach 400–900 m in thickness (Carreras et al. 1979; García-Mondéjar et al. 1989; Robles and Pujalte 2004), although Alpine tectonics may have contributed to local erroneous thickness estimations. This sedimentary record was accumulated in extensional basins with a main E–W orientation. The succession, when complete, shows two parts. The lower one begins with homogeneous and well-rounded conglomerates, 10–90 m in thickness, and grade upwards into cross-bedded, coarse-grained sandstones. The upper part consists of red fine-grained sandstone, silts

and mudstones. Although this continental succession shows similar lithology, it is important to remark that the age of the upper part of this sedimentary record in the Basque area is Anisian (Calvet et al. 1993), while in the Cantabrian area it is late Ladinian-early Carnian (Sopeña et al. 2009), that is, they belong to different sedimentary cycles.

3.2.2.2 Aragonese-Catalan Pyrenees

The Aragonese-Catalan Pyrenean sector represents the eastern area of the two structural units of Muñoz's (2002) configuration of the Pyrenees (Fig. 3.2). In turn, this structural unit is also subdivided into three areas: Western-Central, Central and Eastern. In some of these areas, isolated sub-basins are also described here due to their particular development and paleogeographic significance.

The Western-Central Area

Rodríguez-Méndez L, Cuevas J and Tubía JM

The fading of Variscan compressional tectonics in the Western-Central area of the Aragonese-Catalan Pyrenees resulted in the onset of a new extensional tectonic regime that led to the formation of Stephanian-Permian basins, mainly scattered along the southern border of the Axial Zone. They are small isolated continental basins that trend parallel to the east-west elongation of the belt. Although they are little known in detail, a general common structure is recognized, in which 2 or 3 sub-basins connected by a paleohigh constitute each basin. Two main basins are distinguished in the Western-Central Pyrenees: the Aragón-Bearn (E1) in the west and the Castejón-Laspaúles basin (E2) to the east (Figs. 3.2 and 3.3). The Aragón-Bearn basin is generally divided in the Oza and Anayet sub-basins, to the west and east respectively (Fig. 3.7). Locally derived continental successions fill the basins, which renders difficult the correlation even within a basin. Nevertheless, four main lithostratigraphic units are distinguished for the Stephanian-Permian of this area of the Pyrenees: the Grey Unit, the Transition Unit, the Lower Red Unit and the Upper Red Unit, from base to top respectively (Gisbert 1984).

In the Castejón-Laspaúles basin, the Upper Red Unit is absent and the Transition Unit appears as discontinuous outcrops, whereas the Aragón-Bearn basin preserves one of the most complete sedimentary records, with the four stratigraphic units well developed (Fig. 3.7). As previously stated, one of the main questions regarding the stratigraphic evolution of the Stephanian-Permian basins is the deficient correlation between the biostratigraphic and the absolute ages in the interlayered volcanic rocks. In this regard, Rodríguez-Méndez et al. (2016) have reported differences of at least 17 Ma between the paleontology-based and the absolute ages in the Aragón-Bearn basin.

The Grey Unit is a volcano-sedimentary complex formed by shales, coal and brecciated conglomerates with interlayered volcanic flows. It shows a diachronic base and a lateritic roof. Plant-bearing limestones from the eastern part of the Aragón-Bearn basin (Anayet sub-basin) yield an upper Stephanian to Autunian age (Ríos et al. 1987). U-Pb ages of 278 ± 5 and 272 ± 3 Ma (Cisuralian-Kungurian) have been reported for rhyolites and dacites interlayered in the Anayet sub-basin (Briqueu and Innocent 1993).

The Transition Unit is composed by alternating layers of shales, sandstones and oolitic limestones of grey colours. The Grey and Transition units crop out only in the easternmost part of the Aragón-Bearn basin (Anayet sub-basin) with 50–200 m of maximum thickness (Rodríguez-Méndez et al. 2016). In the Castejón-Laspaúles basin the Grey and Transition units reach a maximum thickness of 550 m (Valero Garcés and Gisbert Aguilar 2004).

The Lower Red Unit consists of well-stratified, cross-bedded red sandstones, and occasionally conglomerates. Lava flows, dykes and laccoliths crop out interbedded within this unit in the Aragón-Bearn basin. "Saxonian" to "Thüringian" ages are proposed for this unit (Lago et al. 2004a). The Lower Red Unit shows a thickness of around 200–250 m in both basins (Rodríguez-Méndez et al. 2016; García Senz and Ramírez Merino 2009), although it eventually reaches 400 m (Teixell et al. 1994).

The Upper Red Unit is formed by three thinning-upwards megasequences of red conglomerates, sandstones and minor shales that crop out only in the Aragón-Bearn basin. Alkaline basalts are interbedded within this unit (Fig. 3.7). The Upper Red Unit exhibits the biggest sedimentary record, with a maximum thickness of 1500 m in the Oza sub-basin (Teixell et al. 1994). The Upper Red Unit is absent in the Castejón-Laspaúles basin, where a Triassic continental succession cover unconformably the Lower Red Unit (Mey 1968) (Fig. 3.3). The Triassic deposits comprise basal coarse-grained sandstones and conglomerates, black, red or green mudstones, containing veins of gypsum, siltstones and yellowish dolomitic marls (Buntsandstein facies). The total succession can be represented by two fining-upwards megasequences with important thickness changes. In some areas of the Western-Central Pyrenees, the lower sequence, or B1 (Gisbert 1983) of the Buntsandstein facies, is not present, suggesting a structural high, but a precise paleogeographic reconstruction is still not clear (López-Gómez et al. 2002). A rapid, normal vertical transition to calcareous Muschelkalk facies is a common stratigraphic characteristic in this area.

The Aragón-Bearn and the Castejón-Laspaúles sub-basins were inverted during the Late Cretaceous to Tertiary Pyrenean compression (Fig. 3.8a, b). The Castejón-Laspaúles basin was transported towards the south and

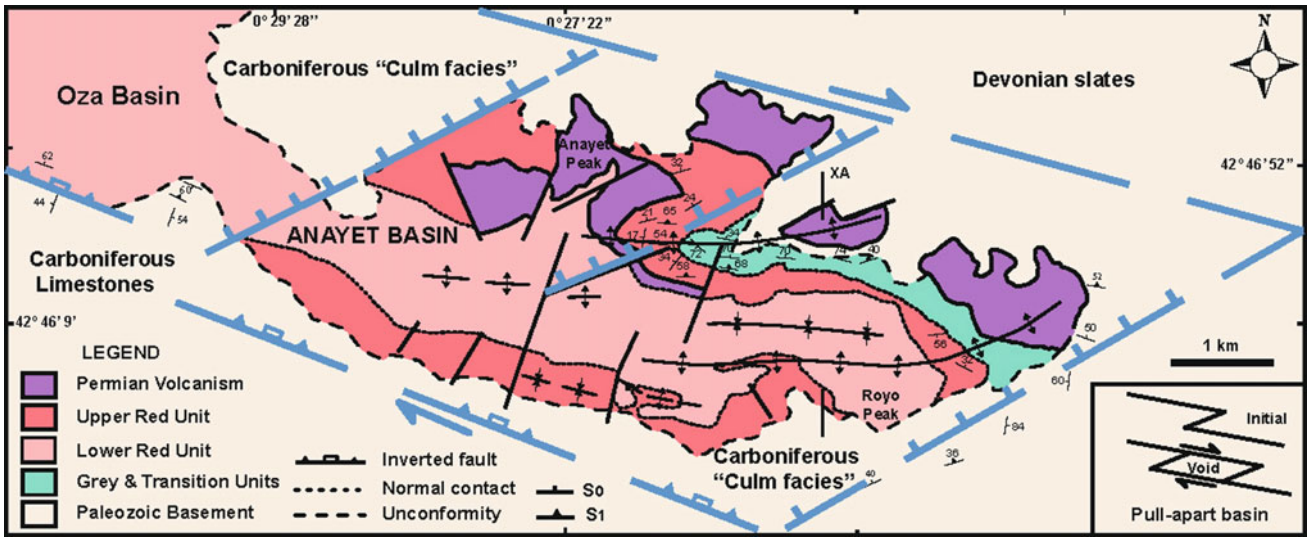

Fig. 3.7 Geological map of the Anayet sub-basin (Aragón-Bearn basin) with the distribution of the main lithostratigraphic units. The margin and the intrabasinal faults of the pull-apart system responsible for the opening of the basin are indicated. The Grey and Transition units are here represented together

strongly deformed by frontal, thrust-related folds of an antiformal stack, the so-called "têtes plongéants" (Seguret 1972), where the Paleozoic basement is also involved (Fig. 3.8b). In contrast, the Aragón-Bearn basin shows a less severe deformation, dominated by south vergent WNW–ESE angular folds of kilometric wavelength with axial plane cleavage (Rodríguez-Méndez et al. 2016; Teixell et al. 1994; Teixell and García-Sansegundo 1994). Despite the marked influence of the Pyrenean inversion in the present configuration of the Anayet sub-basin, detailed mapping of the area still allows a pull-apart geometry to be identified for the basin opening (Fig. 3.7). The Anayet sub-basin shows a lozenge-shaped geometry with a WNW–ESE elongation that might be considered as an inherited structural feature from the former basin margin faults (Fig. 3.9). The northern margin fault is poorly exposed but its location is underlined by a WNW–ESE alignment of volcanic rocks interlayered with the Permian sediments (Fig. 3.7). N 50° E-trending transverse faults divide the basin and determine the existence of several paleo-highs and depocenters (Figs. 3.7 and 3.9). The western paleo-high constitutes the limit between the Anayet and Oza basins. The central fault was sealed by the deposition of the Lower Red Unit and the western one by the Upper Red Unit. The eastern transverse fault is the sole extensional fault, as indicated by the presence of the oldest units in the sedimentological record (Fig. 3.9). The orientation of the transverse normal faults at right angles to the expected extensional fractures in a strike-slip system, suggests that the intrabasinal faults were Variscan fractures reactivated during the opening of the basin. Moreover, a dextral movement of the edge wrench fault is supported by the westward migration of the depocenters. The Grey Unit shows increasing thickness towards the north (see the cross section in Fig. 3.9), which indicates that the opening of the Anayet sub-basin started under transtensional conditions.

Stephanian and Permian Lakes in the Aragon-Bearn Basin

Valero Garcés B and Gisbert Aguilar J

Reactivation of Variscan faults during the Stephanian transtensional phase originated the late Variscan basins in the Pyrenees (Bixel and Lucas 1983, 1987) that were filled with thick volcanoclastic and volcanic material, and alluvial fan and lacustrine sediments (Gisbert 1981, 1983, 1984; Gisbert et al. 1985; Lucas 1985, 1989; Lucas et al. 1996; Valero Garcés and Gisbert Aguilar 1992, 1994, 2004). Although lacustrine formations are spatially and temporally restricted, they have special significance in the geotectonic evolution of these basins. The Aragón-Bearn basin (E1 in Figs. 3.2 and 3.3a) provides the best examples for lake variability in transtensional settings during late Variscan times in the Pyrenees. This basin was composed of two sub-basins (Oza-Baralet, Fig. 3.7, and Campo de Troya-Midi d'Ossau), both asymmetrical, with preferential subsidence on their eastern side (Lucas 1985; Valero Garcés 1991, 1993) (Fig. 3.7). During the compressive cycle, a thick volcanic and volcaniclastic sequence was deposited (Valero Garcés 1991, 1994). Lake environments including carbonate, swamps and clastic deposition occurred in the lower member of the Transition Unit, TU (late Stephanian-Early Permian). Lakes are absent in the lower red clastic series (the Lower Red Unit, LRU). A change from

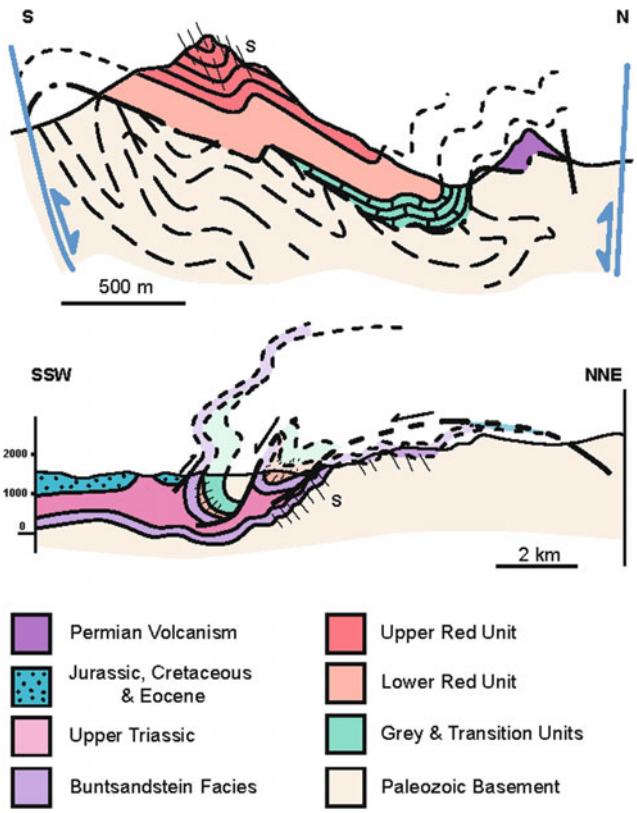

Fig. 3.8 Cross sections showing the main structural features in: the upper part the eastern part of the Anayet basin (from Rodríguez-Méndez et al. 2016), and in the lower part the Castejón-Laspaúles basin (from Seguret 1972). The section of the E Anayet area is located as XA in Fig. 3.7

a main E–W dextral shear during the Stephanian to a sinistral shear over a set of faults oriented NNE–SSW and ENE–WSW during the Permian, would be responsible for a gradual change toward an extensional setting during Late Early-Middle-(?) Late Permian (Fig. 3.3). This extensional cycle is represented by three fining-upward alluvial megasequences (that constitute the Upper Red Unit, URU), with some intercalated lava flows, sills and intrusive bodies with alkaline affinities (Bixel 1984). Numerous thin calcareous pedogenic horizons and seven decameter-thick units with carbonate are present in these megasequences. The limestone layers (up to 40 m thick) are the most widespread, and crop out at the top of the first megasequence and at the bottom of the second megasequence. A gypsum unit (ca. 50 m thick) appears at the top of the first megasequence in the northwestern area of the basin, while dolostone units appear at the top of the second megasequence towards the easte of the basin.

The Central Area

Gretter N, Arche A, Lloret J, De la Horra R, Ronchi A, López-Gómez J and Barrenechea J

The stratigraphic subdivision of the Late Paleozoic continental succession filling the Central and Eastern Pyrenean basins (Figs. 3.2 and 3.3) has been a matter of discussion over the last few decades (e.g. Arche and López Gómez 1996; López Gómez et al. 2005; Van Wees et al. 1998; Vargas et al. 2009). The latest syntheses followed the approach that has proven to be valuable in the rest of Western Europe: the tectono-stratigraphic subdivision. This view is based on a number of well differentiated "tectono-stratigraphic units" (TSU_s), as emphasized by many authors (e.g. Virgili et al. 2006; Cassinis et al. 2008, 2012; Gretter et al. 2013) and, more broadly, strenghthened by: (i) radiometric age data, (ii) paleontological investigations (macrofloras, microfloras and tetrapod footprints), and (iii) tectono-stratigraphical arguments and correlations. Although applying this perspective to the Central and Eastern Pyrenees areas is not easy, it is possible to distinguish three main TSUs, separated by marked unconformities and gaps of as yet uncertain duration (see Bourquin et al. 2011; Cassinis et al. 1995, 2012; Virgili et al. 2006 and references therein) (Fig. 3.10).

The lower TSU_1 (Late Carboniferous–Middle Permian *p.p.*, sensu Cassinis et al. 2012; Virgili et al. 2006) is mainly characterized by fine-to-coarse fluvio-lacustrine and volcanic deposits of calc-alkaline acidic to intermediate composition, lying unconformably over the Variscan basement. Its architecture involves four lithostratigraphic units; from oldest to youngest (nomenclature of Gisbert 1981):

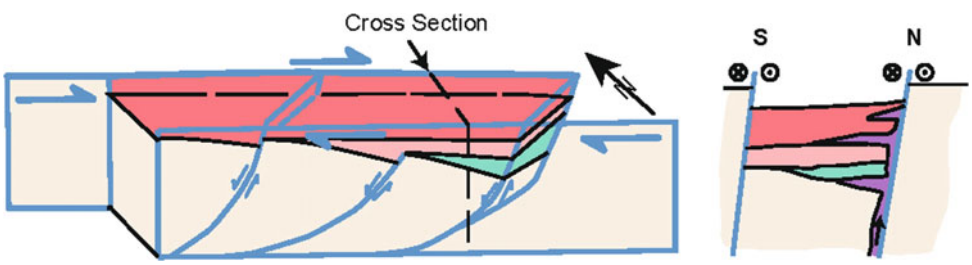

Fig. 3.9 Pull-apart model responsible for the opening of the Anayet sub-basin. The N–S cross-section shows the role of the northern margin fault of the basin as the feeding channel for the volcanic rocks

(1) Grey unit (GU): this represents the first deposits defined primarily on its lithological characteristics and partly on paleobotanical contents. It is mostly made up of volcanic and volcaniclastic rocks. This unit shows polygenic slope breccias at the base (Aguiró Fm. of Mey et al. 1968 and Nagtegaal 1969), grey sandstones and conglomerates characterizing the apical part of alluvial fans bodies, with laminated lacustrine sediments. These facies are laterally interspaced by volcaniclastic and pyroclastic bodies (dacitic to rhyolitic in composition), together with several andesitic and rhyolitic lavas (Erill Castell Fm of Mey et al. 1968). It rests unconformably over the basement and, on the basis of fossil floras, is Stephanian B-C (Gzhelian) in age. New radiometric age determinations on intrusive and extrusive rocks by Pereira et al. (2014) provided a late Kasimovian-early Gzhelian age (307.4 ± 1.4 Ma − 301.5 ± 1.9 Ma).

(2) The Transition Unit (TU) ("Permien alternant" by Broutin et al. 1994) may correspond to the upper part of the Erill Castell Fm and the Malpas Fm of Mey et al. (1968) and Nagtegaal (1969). It is mostly characterized by a detrital succession of volcanic and volcanoclastic sequences, grading upwards to grey sandstones and microconglomerates alternating with grey and reddish siltstones. Reddish/greenish coarse-grained siltstones, with thin levels of carbonate nodules, can also be found at the top of this succession. Unlike other areas, in the Seu d´Urgell zone, the TU rests conformably over the underlying GU. Owing to the poor macrofloristic content, the age of the TU is still the subject of uncertainty. However its attribution to the early-Middle Autunian (Broutin and Gisbert 1985), or better to the Latest Gzhelian-late Asselian, is not only very plausible but also emphasized by the 297.2 ± 3.3 Ma age recently obtained from the Erill Castell ignimbrites (Pereira et al. 2014).

(3) The Lower Red unit (LRU) is probably equivalent to the Peranera Fm described by Mey et al. (1968), Nagtegaal (1969) and Roger (1965) in the Western-Central Pyrenees. It is dominated by alluvial fan sediments and meandering river flood-plain deposits, including channels, overbank fines and paleosols. This succession generally constitutes a fining upwards sequence and characterizes the lower part of the unit, which grades upwards to red debris flow and stream flood deposits (Lloret et al 2018). Volcaniclastic bodies commonly occur at the base of the unit. Inferred age is Autunian to post Autunian (i.e. Sakmarian–Artinskian–Kungurian). Floras and plant remains confirm an Early Permian age (Dalloni 1930; Virgili 1958; Roger 1965), and the so-called "Flora of Gotarta" (Broutin and Gisbert, 1985), but also tetrapod ichnoassociations as well as several invertebrate trace fossils suggest an Artinskian age for the lower part of the LRU (Mujal et al. 2016a, b, c). In addition, recent radiometric age determinations on ignimbritic samples collected in Castellar de n'Hug area (Fig. 3.3) yielded an Artinskian age (290.0 ± 1.2 Ma and 285.6 ± 1.5 Ma; Pereira et al. 2014) Above the LRU, the onset of the Upper Red Unit (URU) is defined by an angular unconformity sealing a gap of uncertain duration (Gisbert 1981, 1983; Gretter et al. 2015). The biostratigraphic data and the absolute age determinations in this region of the Pyrenees are apparently contradictory in some cases, which remain to be solved.

(4) The Upper Red Unit (URU) is mainly composed of red conglomerates, sandstones and siltstones with carbonate nodules and lacustrine deposits, arranged in two fining upwards megasequences with a number of interbedded volcanic bodies in the lower part (Gisbert 1983; Gretter et al. 2015). On the basis of vertebrate remains and regional correlations, its age could be referred to a generic Middle Permian, possibly Wordian (Mujal et al. 2016a). As it is bounded by two unconformities, the URU could be considered as a sequence in itself. Actually, it is quite likely to consider it lying between the upper TSU_1 and TSU_2. Up to now, however, neither the biostratigraphical nor the tecto-sedimentary data can decide if the URU belongs to the TSU_1 or represents the base of the TSU_2.

The TSU_2 (Late Middle?–Late Permian, sensu Cassinis et al. 2012) is apparently missing in the Pyrenees. In the rest of SW Europe it begins with prevalently fluvial detritic red beds marked again by a stratigraphical discontinuity. It is mostly dominated by alluvial deposits and almost everywhere in SW Europe completely devoid of volcanics (Cassinis et al. 2012).

The TSU_3 (Lower–Middle Triassic) rests unconformably over the underlying older Permian rocks and can be directly correlated to the Germanic Buntsandstein. On top of the URU, the fluvial Buntsandstein facies (Bunter Formation of Mey et al. 1968) started with a coarse-grained oligomictic quartz-rich conglomerate, followed by sandstones and shales in a fining upwards sequence. The lowermost facies of the Buntsandstein (e.g. the Iguerri member of Nagtegaal 1969) shows a deeply erosive base and sandstones of gravel braided fluvial systems and channel sand-sheets (Gretter et al. 2015; Lloret et al. 2018). The dark red fine clastics above this first coarse unit are composed of reddish sandstones, bioturbated mudstones and siltstones of a playa lake environment. Near the top, siltstones and claystones locally change into dark red fine levels until the contact with the Muschelkalk sequence. The contact between the upper fine deposits and dolomites of the first marine incursion probably

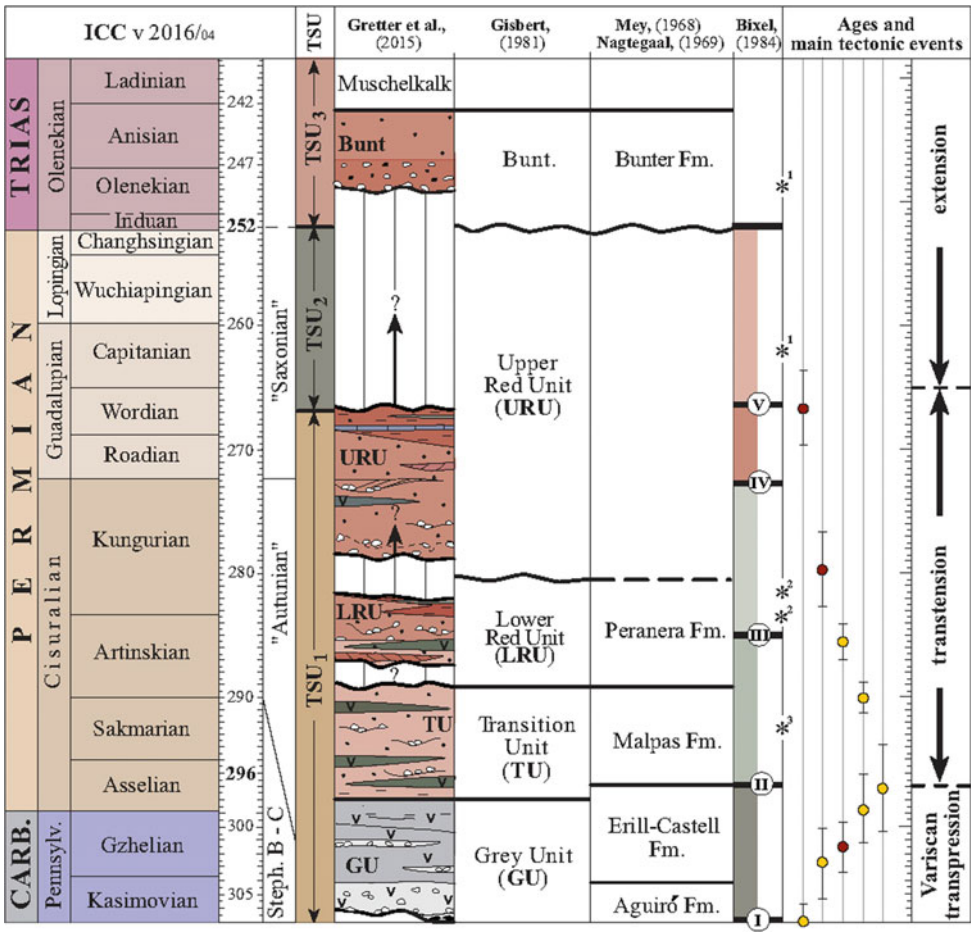

Fig. 3.10 Synthetic Late Paleozoic-Early Mesozoic lithostratigraphic scheme based on Gisbert (1981), Mey et al. (1968), Nagtegaal (1969) and Gretter et al. (2015). Magmatic episodes are taken from Bixel (1984). Radiometric age assessment in the central-eastern Pyrenees comes from both intrusive (red circles) and volcanic (yellow circles) rocks (Pereira et al. 2014); from oldest to youngest: 307.4 ± 1.4 Ma, 302.6 ± 2.6 Ma, 301.5 ± 1.9 Ma, 298.6 ± 2.5 Ma, 297.2 ± 3.3 Ma, 290.0 ± 1.2 Ma, 285.6 ± 1.5 Ma, 279.6 ± 3.0 Ma, 266.7 ± 3.1 Ma. The five starred points in the relative age column, mark the paleofloras as from (1) Broutin et al. (1988), (2) Broutin and Gisbert (1985) and (3) Dalloni (1930). In particular, from oldest to youngest: "*Gerri de la Sal*" flora (3), "*Gotarta*" flora (2), "*Castellar de n'Hug*" flora (2), "*Palanca de Noves*" microflora (1) "*Baro*" microflora (1). Tectonic events are taken from Carreras and Druguet (2014)

represents a hiatus that lasts until the late Anisian (Escudero-Mozo et al. 2014). Although palynological data, together with other palynomorph assemblages from the basal part of the coarse fluvial Buntsandstein deposits have been attributed to a "Thuringian age" (e.g. Broutin et al. 1988; Calvet et al. 1993; Díez 2000; Díez et al. 2005), new different types of spores and pollens allow correlating this associations with the Early Triassic levels (i.e. late Olenekian, Mujal et al. 2016a).

The complex interplay of tectonics and sedimentation in the transtensional sub-basins of the Central Pyrenees area (F1–F3 in Figs. 3.2 and 3.3), strongly influenced the deposition and architecture of syn-extensional sediments. In fact, the Late Carboniferous-Early Permian strike-slip sub-basins, here represented by the Erill-Castell, Estac, Gramós and Castellar de n'Hug-Camprodon troughs, formed under the general extensional regime and transtensional faulting in the range of the first post-Variscan rifting (Saura and Teixell 2006) (Fig. 3.11a–d). The restored structural sections (e.g. Hartevelt 1970; Poblet 1991; Saura 2004; Saura and Teixell 2006; Teixell 1992, 1998) revealed that most of these sub-basins formed initially as grabens or half-grabens elongated along an E–W direction (see Saura and Teixell 2006). The southern basin-bordering faults exhibit normal slickensides that were active during Stephanian-Early Permian times, and reactivated as the present-day thrusts in the Cenozoic. Unfortunately, the Cenozoic deformations partially tampered with the primary features of the late Variscan structures, during the most recent polyphase reactivation during the Pyrenean folding phases (Eocene) and the post-Pyrenean deformations (Oligocene-Miocene) (e.g. Hartevelt 1970; Saura and Teixell 2006; Sibuet et al. 2004). Two of the most important of these sub-basins are described below.

The Erill Castell Sub-basin

The Erill Castell sub-basin in the Malpàs-Sort area (Figs. 3.3 and 3.11b) has been defined as a half-graben trough (e.g. Mey 1968; Poblet 1991; Saura and Teixell 2006), produced by the continental extension occurred in Late Carboniferous–Early Permian times. The Stephanian-Permian continental succession, as defined by the depositional units of Gisbert (1981), reaches considerable thicknesses (up to 1000 m) and is unconformably covered by the Buntsandstein facies, during the Early Triassic (Lloret et al. 2018). Also in this particular case, the entire succession is rather complex due to the interplay of tectonism, volcanism and clastic sedimentation. Deposition and erosion processes were controlled by alternating periods of tectonic activity, culminating with extended erosive events marked by angular unconformities.

The most important stratigraphic features are, from base to top:

- The Grey Unit (up to 500 m thick) is mostly characterized by clastic sedimentation with coal levels affected by an intense volcanic activity, mostly represented by andesites that crop out in the central-western part of this sub-basin. The GU also includes collapse breccias, conglomerates, coarse sandstones, in addition to the interbedded volcanic tuffs and ashes.
- The Transition Unit reaches 146 m in this area and consists of greenish/greyish sandstones, conglomerates, coal levels, dark siltstones and fresh-water lacustrine limestones, organized in thin levels. Coal seams are only present in the western sector of the basin. The TU gets thinner to the east (only 16 m thick in La Mola d'Amunt sector). A 20 m thick coarse conglomerate level, first described by Lloret et al. (2018), characterizes the upper portion of the TU. An erosive base and a weak positive sequence to the top characterize this level in the Castellars sector.
- In the Lower Red Unit (lower Permian) the sedimentary record changes radically to reddish conglomerates, sandstones and siltstones of fluvial origin. In the west side of the Erill Castell sub-basin (Fig. 3.11b) the vertical succession is continuous with an average of 80 m in thickness (Gotarta and Malpàs sectors). In the central sector the LRU disappears due to the presence of a basement structural high. Finally, the LRU becomes thicker to the east, reaching 481 m.
- The Upper Red Unit does not apparently appear in this sub-basin.

The sedimentary fill ends with the Buntsandstein facies (Lower-Middle Triassic), up to 290 m thick in the central sector. This unit is separated by an unconformity from older units and is composed of coarse-to-fine fluvial (at the base) and playa-lake deposits (at the top). The thicknesses of LRU and the Buntsandstein are strongly variable due to the angular relationship between them.

The stratigraphic succession of the Erill Castell sub-basin (Fig. 3.11b) records different paleoenvironments and paleoclimates. The evolution starts with a humid period (coal levels in the GU), passing through a semi-humid interval, evidenced by the extensive fluvial system of the LRU, to more arid conditions, as inferred by the playa-lake deposits of the Buntsandstein facies.

The Gramós Sub-basin

According to the most recent structural reconstructions (Hartevelt 1970; Teixell 1998; Saura and Teixell 2006; Gretter et al. 2015), the Gramós sub-basin, (Figs. 3.3F2 and 3.11c) sets out to be an asymmetric graben, bounded by extensional normal faults (Fig. 3.11d). The main synsedimentary structure, active during the deposition of the TSU_1 and defining the southern margin of the basin, probably corresponded to the present-day Orri thrust. Accordingly, the related complex structural network controlled the sedimentation of the Stephanian-Permian succession. In particular, the Late Carboniferous-Early Permian sequence unconformably rests over the Variscan basement through a clear angular unconformity. During this period, sedimentation took place in volcanic, alluvial, lacustrine and playa-lake environments. The volcano-sedimentary record of the GU and TU, representing the base of the TSU_1 (Fig. 3.10), was thus deposited as a consequence of increasing subsidence associated with crustal faulting. The main structural lineaments, besides controlling the lateral changes in thickness, facilitated the rise of hot igneous materials from the asthenosphere, considered as the source of the coeval calc-alkaline volcanism, testifying an active syn-sedimentary tectonic regime. Volcanic activity, mostly represented in the form of interbedded pyroclastic deposits, lasted from these basal units up to the base of the URU, though decreasing in frequence upwards. Several minor internal erosive surfaces affect the TSU_1. These surfaces can probably be attributed to minor alternating stages of tectonic activity; the most important one marks the passage from the LRU to the URU. Accordingly, debris flow bodies at the base of the URU, suggest deposition in proximal areas of alluvial fan systems. Their deposition was controlled by structural factors close to the footwall slope area. Steepening of gradients as a consequence of a new minor tectonic pulse would result in erosion of the upper part of the LRU (angular unconformity) followed by supply of clastics (debris flows) sealing the unconformity. In particular these facies commonly occur in the western sector of the Gramós sub-basin. There, the normal fault network probably created a scarp system, several tens of metres high. It is also clear that this sector experienced increasing subsidence from the Early to Middle

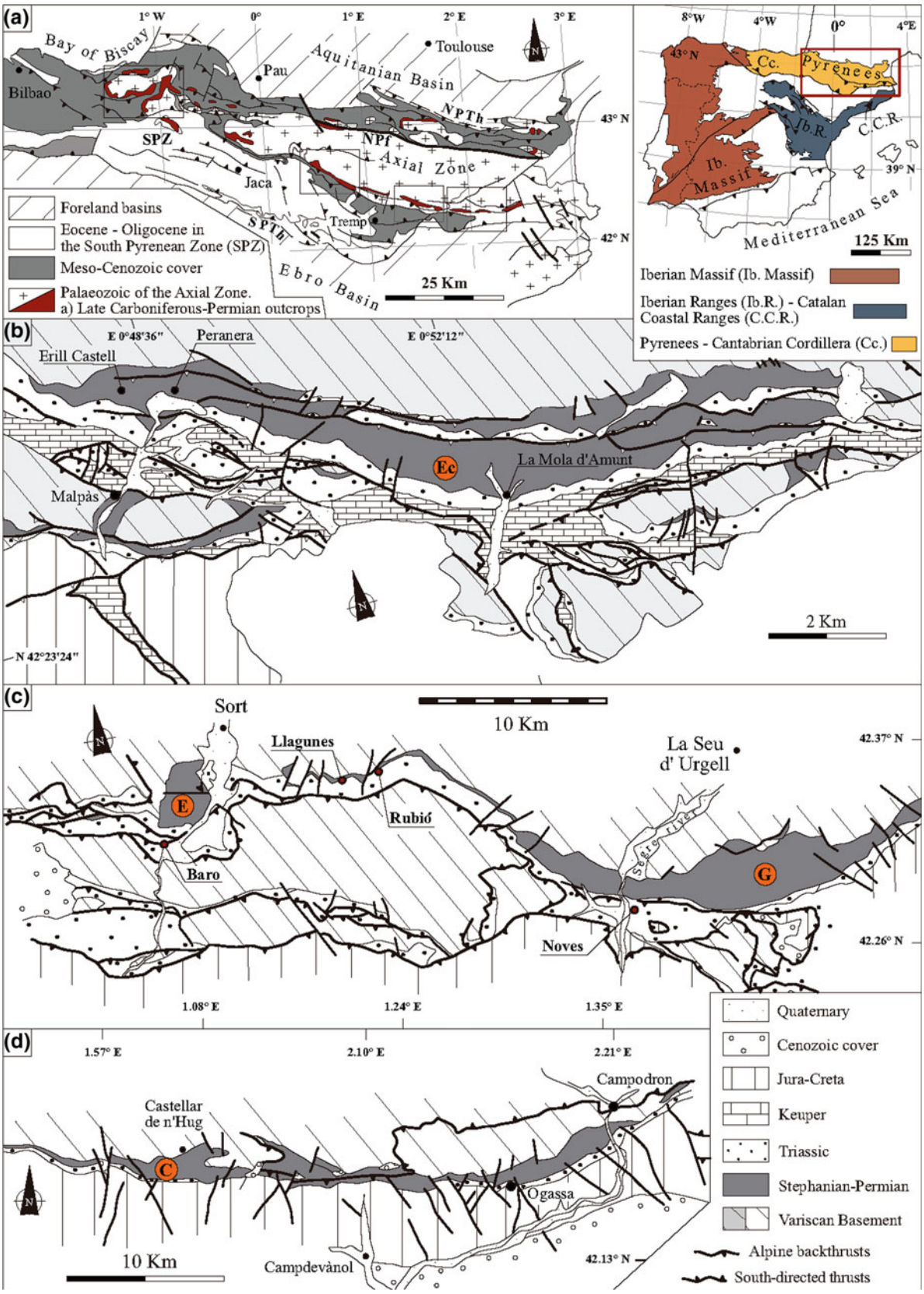

Fig. 3.11 **a** Late Carboniferous-Permian sub-basins settled within the tectonic framework of the Pyrenees (modified from Oliva Urcia et al. 2012). Inset location map shows the present-day Iberian basins and ranges. NPf: North Pyrenean Fault, NPth: North Pyrenean Frontal Thrust, SPth: South Pyrenean Frontal Thrust. Simplified geological maps of **b** Malpàs area (Ec: Erill Castell sub-basin), **c** Sort-La Seu d'Urgell area (E: Estac sub-basin, G: Gramós-Prats d'Aguiló sub-basin) and **d** Castellar de n'Hug-Camprodon area (C: Castellar de n'Hug sub-basin); all these sketched maps modified from Hartevelt (1970) and Saura and Teixell (2006)

Permian, which implies high deformation rates. A progressive reduction in tectonic activity probably affected the deposition of the URU; a meandering river fluvial system followed a braided one and thick playa deposits finally closed this sedimentary cycle.

From the Latest Carboniferous to the Middle–Late (?) Permian, the subsidence of the Gramós sub-basin probably shifted clockwise to the southwest (Gretter et al. 2015). On a smaller scale, this fact may reflect a coeval regional rotation of blocks, taking place in the wider transtensional regime. A modern analogue example can be found in the San Andreas system (California) (e.g. Allen and Allen 2005; Dibblee 1977; Nicholson et al. 1986), where rotation of blocks near the intersection of the two most important faults, controls the shape of areas experiencing extension, paleodrainage and evolution of subsidence in a similar manner to that observed in the studied area.

In Late Permian–Early Triassic times a new extensional tectonic phase led to the development of symmetric basins filled by alluvial–fan conglomerates followed by sandy braided rivers deposits (Buntsandstein facies) (Fig. 3.10). Therefore, above the TSU_1, a hiatus whose duration is difficult to estimate represents a major erosional surface that characterizes the base of the Buntsandstein facies and the onset of the TSU_3. In the Catalan Pyrenees, the Late Permian sediments or a part of them (corresponding to the TSU_2 in other western European sectors) seems not to be preserved, totally or partly eroded together with the Lowermost Triassic deposits or not deposited at all. More broadly this event has been explained in the earliest Triassic as a period of by-pass (Bourquin et al. 2011). The top of the Permian is characterized by an unconformity overlain by braided river sediments, deposited under an arid climate. At the scale of western and southwestern Europe, this arid episode could be attributed to the Early Olenekian (Smithian) (Durand 2008; Bourquin et al. 2007), where a break in sedimentation of Late Olenekian-Early Anisian duration is often observed.

The Eastern Area

Arche A and López-Gómez J

The Permian-Triassic rifting phase is only partially represented in this area of the Pyrenean Basin. It was probably an elevated area where Permian sediments were not deposited. Most representative sections are located around Massarac and Banys d´Arles sections (G1 in Figs. 3.2 and 3.3a). The first Mesozoic sedimentary record is probably of Anisian age, and represents the youngest sediments of this rifting phase. They consist of red siltstones, sandstones and some intercalated conglomerate levels (Calvet and Anglada 1987). They lie on weathered granitic basament with a thin basal breccia and their upper part may reach an early Ladinian age, so included in the B1 or upper Buntsandstein sedimentary cycle of Gisbert's (1983) nomenclature. A 8–18 m thick unit of variegated marls and thin stromatolitic layers marks the transition to the Muschelkalk facies.

3.2.3 The Middle–Late Triassic Mature Rift Phase in the Pyrenean Basin

López-Gómez J, Martín-Chivelet J, Escudero-Mozo MJ, Ortí F and Pérez-López A

A new period of subsidence covering most of the Middle and Late Triassic defined a phase of mature rifting in the Pyrenean Basin. The subsidence affected broader areas in comparison to the previous initial rifting phase (García-Mondejar et al. 1989; Calvet et al. 1993, 2004) and determined the entrance of marine waters into the basin from the Tethys Sea (i.e. from the East). This marine transgression gave rise the installation of the Middle Triassic carbonate ramps (Muschelkalk facies) and the later development of Upper Triassic marl-evaporite shabkha systems (Keuper facies). The sea waters invaded the area in the early Ladinian (i.e. notably later than in other basins of Iberia, Escudero-Mozo et al. 2014) and the development of the carbonate ramp was limited to the eastern and central parts of the basin (the Aragonese-Catalan and the Basque Pyrenean sectors), being absent in the Cantabrian area (Fig. 3.3a).

3.2.3.1 The Middle Triassic Carbonate Ramps (Muschelkalk Facies) in the Pyrenean Basin

López-Gómez J, Martín-Chivelet J and Escudero-Mozo MJ

The Muschelkalk facies in the Pyrenean basin is represented by a single carbonate ramp of Ladinian-earliest Carnian age (Calvet et al. 1993, 2004). This is a remarkable difference in relation to other areas of Iberia, such as the Catalan Ranges and the Iberian Basin, where another older ramp system, Anisian in age, exists. The carbonate ramp was developed on the Catalan–Aragonese and the Basque sectors, but not in most of the Cantabrian one (Fig. 3.3a). From west to east, three main outcrop zones exist: Basque Pyrenees, Malpás-Pedraforca-Nogueres-Cadí area, and Eastern Pyrenees (Fig. 3.3a, D1–D3, F1–F3 and G1, respectively).

In the Basque Pyrenees this carbonate unit reaches 70 m in thickness and is constituted by three different lithologies, from bottom to top: marly dolomites, gray limestones, and thin-bedded limestones and dolomites (Müller 1973; Calvet and Anglada 1987; Calvet et al. 1993; Calvet and Marzo 1994). Sedimentological studies indicate subtidal-supratidal environments (Calvet et al. 2004). Based on foraminifera,

conodont and pollen associations a Ladinian-early Carnian age has been proposed for this unit (Calvet et al. 1993; Calvet and Tucker 1995).

In the Malpás-Pedraforca–Nogueres–Cadí area, this carbonate unit is basically represented by gray limestones in the lower part and gray limestones and dolomites in the upper part, and reaches up to 80 m in thickness (Roger 1965; Robles and Llompart 1987) (Fig. 3.12). Sedimentological studies indicate subtidal-supratidal deposional environments for this unit (Calvet and Anglada 1987; Calvet and Marzo 1994). Sections in this area are strongly affected by post-sedimentary tectonics related to the Pyrenean orogeny. As result, these sections are usually incomplete, especially in its lower part. Data obtained from palynological assemblages (Calvet and Marzo 1994), foraminifera (Fréchengues et al. 1990; Márquez et al. 1990; Fréchengues and Peybernès 1991; Calvet and Marzo 1994) and conodonts (Calvet and Anglada 1987; March 1991) indicate a Ladinian age for this carbonate unit.

The Eastern Pyrenees sector shows few and incomplete sections basically constituted by dolomites and gray limestones that mostly indicate tidal flat environment sedimentation (Fréchengues et al. 1990). Based on conodont studies, these sections are considered Ladinian in age (Calvet and Marzo 1994).

3.2.3.2 The Upper Triassic (Keuper) Sedimentary Record

Ortí F and Pérez-López A

The general successions of the Keuper facies (lower, middle, and upper Keuper) were initially described in eastern Iberia (Ortí 1974). However, these successions are relatively similar in all the Triassic basins of the Iberian plate (Fig. 3.13). They are mainly formed by a lower evaporitic succession (lower Keuper unit, K1 unit) and an upper evaporitic succession (upper Keuper units, K4 and K5 units), all of them of marine origin (Utrilla et al. 1992; Ortí et al. 2014). A major difference, however, is the intercalation in some basins of a non-evaporitic, clastic series (middle Keuper units, K2 and K3 units) between the two evaporitic ones. This intercalation only occurs in the basins surrounding the present reliefs of the Iberian Massif (Prebetic-Subbetic basin, central and southern sectors of the Iberian basin, and partly in the Basque-Cantabrian basin), whereas it is absent in the basins located far from the Iberian Massif (Catalan, Ebro, Pyrenean and Balearic basins, and eastern part of the Iberian basin) (Ortí et al. 2017).

Age attributions of the Keuper facies in the Pyrenean basin have been based on palynological assemblages, indicating a Carnian to Norian, or Carnian to Rhaetian age (Calvet et al. 1993). This age is younger than in the other Triassic basins in eastern Iberia, so the possibility that a stratigraphic gap (Carnian *pro parte* and/or Norian *pro parte*) affects the stratigraphic record of the Keuper facies in the northern basins of Iberia is open to debate.

The Keuper succession in the Aragonese-Catalan sector of the Pyrenean Basin (Fig. 3.2) crops out in the External Sierras and the Nogueres structural units. From base to top, the Keuper succession is formed by the Canelles Fm, the Boix Fm and the Avellanes Fm in the External Sierras, and by the Adons Fm, the Boix Fm, the Senterada Fm and the Avellanes Fm in the Nogueres Unit (Salvany and Bastida 2004) (Fig. 3.14). The correlation of all these units with those of the Catalan basin is as follows according to Salvany and Bastida (2004): the Canelles Fm and the Adons Fm correlate with the Miravet Fm; the Boix Fm correlates with the Molar Fm; and the assemblage of the Senterada Fm and the Avellanes Fm correlates with the Gallicant Fm (Fig. 3.14).

The Canelles Fm, up to 45 m thick, is formed by laminated gypsum beds with some carbonate interbeds. The Adons Fm, up to 100 m thick, is composed of green claystone layers and carbonate beds grading upward into variegated, red claystones and minor carbonate. The Boix Fm, less than 100 m thick in the External Sierras but some hundred metres thick in the Nogueres Unit, is characterized by red to variegated claystones, laminated gypsum beds and reddish masses of gypsum breccias (Fig. 3.15). At the subsurface, this unit intercalates salt masses as suggested by borehole data in the External Sierras, in the South Pyrenean Zone. The thickness of this saline unit is close to 430 m. Klimowitz and Torrescusa (1990), however, attributed this unit to the lower Keuper. The Senterada Fm, of 50–250 m thick, is composed of white layers of laminated gypsum bearing some dolomitic intercalations (Nogueres Unit). The Avellanes Fm, of up to 100 m thick, is composed of marls and carbonates.

No sure Keuper succession appears to exist in the Basque-Cantabrian basin. However, a number of outcrops including those of Aguilar de Campoo and Reinosa show alternations of clay and gypsum layers which are similar to the cycles characterizing the K1 unit of the Iberian basin. Moreover, units very similar to the K3, K4 and K5 units of the Iberian basin crop out in the Poza de La Sal diapir, where the top (K5) unit of this succession is overlain by the Imón Fm (Salvany 1990; Gómez et al. 2007), which is equivalent to the Isábena Fm in the Eastern Pyrenees (Arnal et al. 1994). In other diapirs of this basin, some opencast workings of thick gypsum units again suggest the presence of the K5 unit of the Iberian basin.

3.2.4 Permian-Triassic Magmatism in the Pyrenean Basin

Lago M, Galé C, Ubide T and Gretter N

Since the end of the Paleozoic to the end of the Mesozoic, three main tectono-magmatic cycles have been identified in the

Fig. 3.12 The Middle Triassic carbonate platform (Muschelkalk) in the Malpàs area (centre of the picture), Aragonese-Catalan Pyrenean Basin. Upper Buntsandstein facies in the right side of the lower part of the picture

Pyrenees: Late Carboniferous–Permian, Late Triassic-Early Jurassic, and Cretaceous (Albian-Santonian) (Fig. 3.16). The first magmatic cycle in SW Europe was associated to a period of widespread basin formation in SW Europe (e.g. Dallagiovanna et al. 2009; Galé 2005; Lago et al. 2004a, b; Maino et al. 2012, 2013; McCann et al. 2006). It was related to the end of the Variscan Orogeny, which induced a generalized strike-slip tectonic regime in the Pyrenees (i.e. Ziegler 1982, 1988a, b), and probably also generated mantle upwelling leading to partial melting of the thickened lithosphere or the asthenosphere (Cebriá et al. 2000; Lago et al. 2004a, b). The strike-slip regime favoured the development of W-E trending small basins infilled with continental detrital deposits and coeval volcanics during the Pennsylvanian and the Permian (Arthaud and Matte 1977; Ziegler 1988a, b; Cassinis et al. 2000). The influence of the regional tectonics in the development of this cycle is evidenced by the composition and origin of the associated magmatism. The Permian tectono-magmatic cycle is defined by two compositionally different and temporally consecutive magmatic episodes. First, a calc-alkaline and evolved magmatism (andesites to rhyolites) took place during the Pennsylvanian to Cisuralian interval still under syn-orogenic conditions (Lago et al. 2004a, b; Pereira et al. 2014). The origin of this magmatism is ascribed to melting of lithospheric material (Lago et al. 2004a, b). Afterwards, the magmatism switched to transitional and alkaline affinities, and less evolved compositions (trachyandesites, basalts and dolerites). Sourced from an asthenospheric source, this event benefitted from the transtensional tectonic regime prevailing from the Guadalupian to the Lopingian (Lago et al. 2004a, b; Galé 2005). The increasing influence of asthenospheric melts during this cycle is related to a shift towards extensional tectonics, thinning of the crust and upwelling and partial melting of the mantle beneath the Pyrenees at the end of the Paleozoic (Lago et al. 2004a, b; Galé 2005).

In detail, at the Aragonese-Catalan Pyrenean scale, extensive volcanism and dyke emplacement into the intramontane sub-basins took place in five episodes (from Late

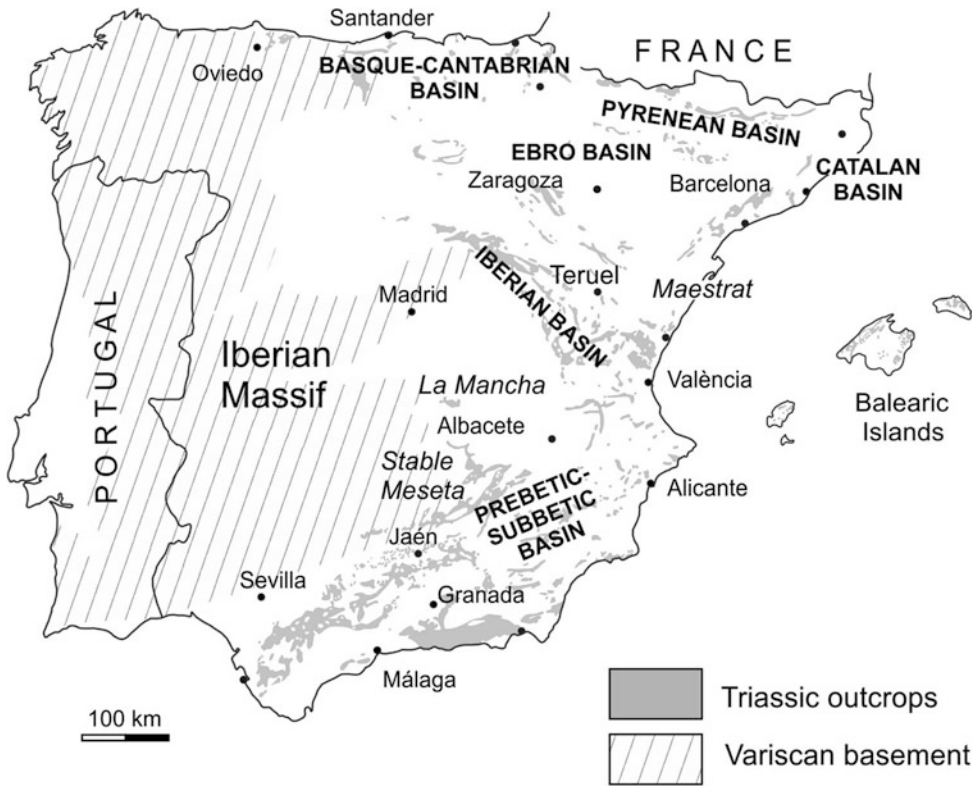

Fig. 3.13 Distribution of Triassic basins in eastern Iberia

AGE	TRIASSIC BASINS										
	Stable Meseta	Prebetic-Subbetic	Iberian					Catalan	Ebro	Pyrenean	
			Southern	Central (Iberian Ranges)		Maestrat				External Sierras	Nogueres
NORIAN-RHAETIAN	Unnamed dolostones	Zamoranos Fm	Imón Fm					Imón Fm	Suprakeuper	Isàbena Fm	
	K4-K5 undifferenciated	K5	Ayora Fm (K5)	Upper evaporitic series (Upper Keuper)	Valencia Keuper Group	Upper anhydritic unit		Gallicant Fm	Upper anhydrite unit (K-3)	Avellanes Fm	
		K4-K5 undifferenciated									Senterada Fm
		K4	Quesa Fm (K4)			Intermediate claystone unit		Molar Fm	Detrital Intermed. unit (K-2)	Boix Fm	
CARNIAN	K3	K3	Cofrentes Fm (K3)	Detrital intermediate series (Middle Keuper)		— — — ?					
	K2	K2	Manuel Fm (K2)								
	K1	K1	Jarafuel Fm (K1)	Lower evaporitic series (Lower Keuper)		Lower saline unit		Miravet Fm	Lower saline unit (K-1)	Canelles Fm	Adons Fm
LADINIAN	Buntsandstein facies	Cehegín Fm + Siles Fm	Cañete Fm (M3)			M3		Upper Muschelkalk (M3)	Upper Muschelkalk (M3)	Upper Muschelkalk	

Jaén Keuper Group

Fig. 3.14 Nomenclature and distribution of the stratigraphic units forming the Keuper successions in the Triassic basins of eastern Iberia

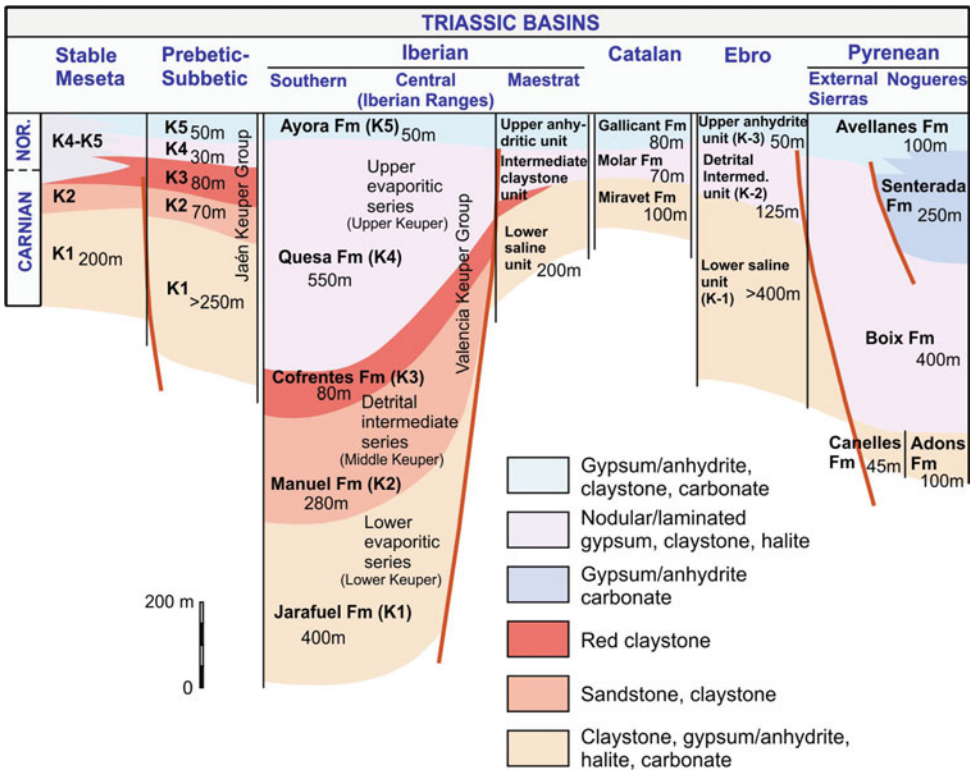

Fig. 3.15 Reference successions of the Keuper units in eastern Iberia. Scheme out of scale. The base of the Imón Fm represents the top of the successions.

Carboniferous to Middle (?) Permian). Magmatism covered a wide range of rock types, ranging from calc-alkaline pyroclastic rocks of rhyolitic-andesitic composition to alkaline basalts. Recent age determinations revealed that magmatism was active from ca. 307 Ma to ca. 266 Ma and was affected by a complex and prolonged history of melt crystallization (Pereira et al. 2014). In particular, the earliest phase of volcanic activity (1st volcanic episode, Bixel 1984, 1987) occurred in the Upper Carboniferous, when extrusives included pyroclastic rocks of rhyolitic composition andbasic calc-alkaline of potassic andesitic lavas interbedded in the Grey Unit. Hyperpotassic, calc-alkaline acid andesites and dacites are considered to affect the basal Autunian (early Cisuralian) and represent the 2nd volcanic episode of Bixel (1984, 1987). The hyperpotassic character is mostly due to assimilation of peraluminous material by the calc-alkaline potassic magma (Debon et al. 1995). The 3rd volcanic episode, of Autunian age (here interpreted as Artinskian-Kungurian), is mainly composed of peraluminous potassic rhyolites bearing sanidine and almandine. Calc-alkaline andesites of the 4th volcanic episode (Bixel 1984, 1987) bear minerals of alkaline affinity, such as chromiferous diopside and edenite-pargasitic amphibole (Debon et al. 1995). This transitional volcanic episode may range between the "upper Autunian and lower Saxonian" (over the Cisuralian-Guadalupian boundary). The final 5th volcanic episode, emplaced under the basal conglomerates of the Buntsandstein facies is exclusively composed of alkaline basalts bearing olivine and titanium-rich augite (Lago et al. 2004a, b; Galé 2005).

3.3 The Catalan Basin

López-Gómez J, Barrenechea J, Galán-Abellán B, De La Horra R, Arche A, Marzo M, Borruel-Abadía V, Escudero-Mozo MJ, Martín-Chivelet J, Mercedes-Martín R, Salas R, UbideT, Galé C and Lago M

As most of its coetaneous basins in the Iberian plate, the Catalan Basin records the change from a Pangean configuration and compressive tectonic regime inherited from the Variscan orogeny, to a Mesozoic general extensional tectonic setting accompanied by continental break-up and westward expansion of the Tethys ocean (López-Gómez et al. 2002). Later, during the Cenozoic, a Paleogene topography generated by thrusting was offset by erosion and isostatic subsidence resulting in a high mountain range. However, its present-day configuration is the outcome of Neogene tectonic subsidence, surface erosion and sedimentation (López-Blanco et al. 2000; Gaspar-Escribano et al. 2004). As a result, the Catalan Coastal Ranges and Catalan Margin, which corresponds to the northeastern part of the extensional margin bounding the Valencia Trough, is a NE–SW structure dominated by longitudinal, near vertical basement faults trending NE–SW to ENE–WSW and by a

AGE	MAGMATISM	TECTONIC REGIME
Pennsylvanian (Late Carboniferous)	Calc-alkaline intrusives (granitoids)	Thickenned crust Syn-orogenic
Cisuralian (Early Permian)	Calc-alkaline volcanics	Transtensional
Guadalupian (Middle Permian)	Transitional	Transtensional
Lopingian (Late Permian)	Alkaline	Transtensional-extensional
Late Triassic –Early Jurassic	Tholeiitic	Extensional
Albian – Santonian (Cretaceous)	Alkaline	Extensional

Fig. 3.16 Evolution of the composition of the magmatisms related to different tectonic regimes in the Pyrenean basin

set of strike-slip faults trending NW–SE (Anadón et al. 1979; Guimerà 1984, 1988; Bartrina et al. 1992; Roca et al. 1999) (Fig. 3.17a, b).

At the end of the Permian and throughout the Triassic, the Catalan basin was situated in the southernmost area of the ancient megacontinent of Laurasia. This basin started its development during the Middle-Late Permian due to widespread extension in that plate (Galán-Abellán et al. 2013) and evolved as a NE-SW oriented rift basin with conjugate NW-SE fault systems. This elongated structure was separated from neighboring basins by the Girona, Lleida and Montalbán-Oropesa highs (Calvet and Tucker 1988; Calvet and Marzo 1994; Morad et al. 1995; see also Ebro Basin in Sect. 3.5).

Mainly during the Permian but also in the Triassic, the sedimentary filling of the Catalan Basin was controlled by the development of grabens separated by Paleozoic highs. During this time, the activity of the NW–SE fault system divided the basin into different paleogeographic domains or sub-basins (from SW to NE): Priorat–Baix Ebre, Prades and Gaia-Garraf, and Montseny domains (Marzo 1980; Marzo and Calvet 1985) (Fig. 3.18). Subsidence in these grabens was not coetaneous causing thickness differences in the sedimentary record (Marzo 1980; Calvet and Marzo 1994). Presence of substantial sedimentation discontinuities in the graben during the Permian-Triassic time-interval indicates repeated periods of tectonic activity (Galán-Abellán et al. 2013). Five sedimentary cycles, mainly based on these discontinuities, separate different periods of rift evolution: cycles 1 to 3 represent Permian–Early Triassic continental syn-rift sedimentation, and cycles 4 and 5 record the Middle-Late Triassic westward incursion of the Tethys sea in the basin, represented by the sedimentary record of the so-called Muschelkalk and Keuper facies. This latter, or mature phase, indicates the transition to a thermal subsidence of rift development affecting more extensive areas.

3.3.1 Sedimentation During the Permian-Triassic Initial Rifting Phase

López-Gómez J, Barrenechea J, Galán-Abellán B, De La Horra R, Arche A, Marzo M and Borruel-Abadía V

This phase of Catalan basin evolution is mostly represented in the Prades and Garraf sub-basins, while practically absent in the Montseny sub-basin (Figs. 3.17, 3.18). The three sedimentary cycles that filled these sub-basins were of terrestrial origin. Detailed sedimentological analyses of these rocks can be found in Marzo and Anadón (1977), Anadón et al. (1979), Marzo (1980, 1986), Calvet and Marzo (1994), and Galán-Abellán et al. (2013). Further published works are the palynological studies of Solé de Porta et al. (1987) and Díez et al. (2012), the detailed petrological study of Gómez-Gras (1993), and the magnetostratigraphy study of Dinarès-Turell et al. (2005).

Basic stratigraphic nomenclature was initially established by Marzo (1980), and later complemented by Galán-Abellán et al. (2013), as summarized in Fig. 3.18. The three Permian–Early Triassic sedimentary cycles of this syn-rift phase represent relatively short periods of sedimentation related to subsidence pulses and separated by partially quiescent periods. Both situations were common in the Prades and Garraf sub-basins, but differences are observed in the Montseny sub-basin, where the first cycle was not recorded.

The beginning of sedimentation unconformably lies on a folded Devonian-Carboniferous basement (Colodrón et al. 1979). It mostly consists of gravels and sandstones related to alluvial fans and superimposed braided fluvial systems indicating marked control of basin border faults (Marzo 1980). A low-angle unconformity separates these rocks from the second Early Triassic sedimentary cycle (Figs. 3.18 and 3.19). This new cycle of sedimentation

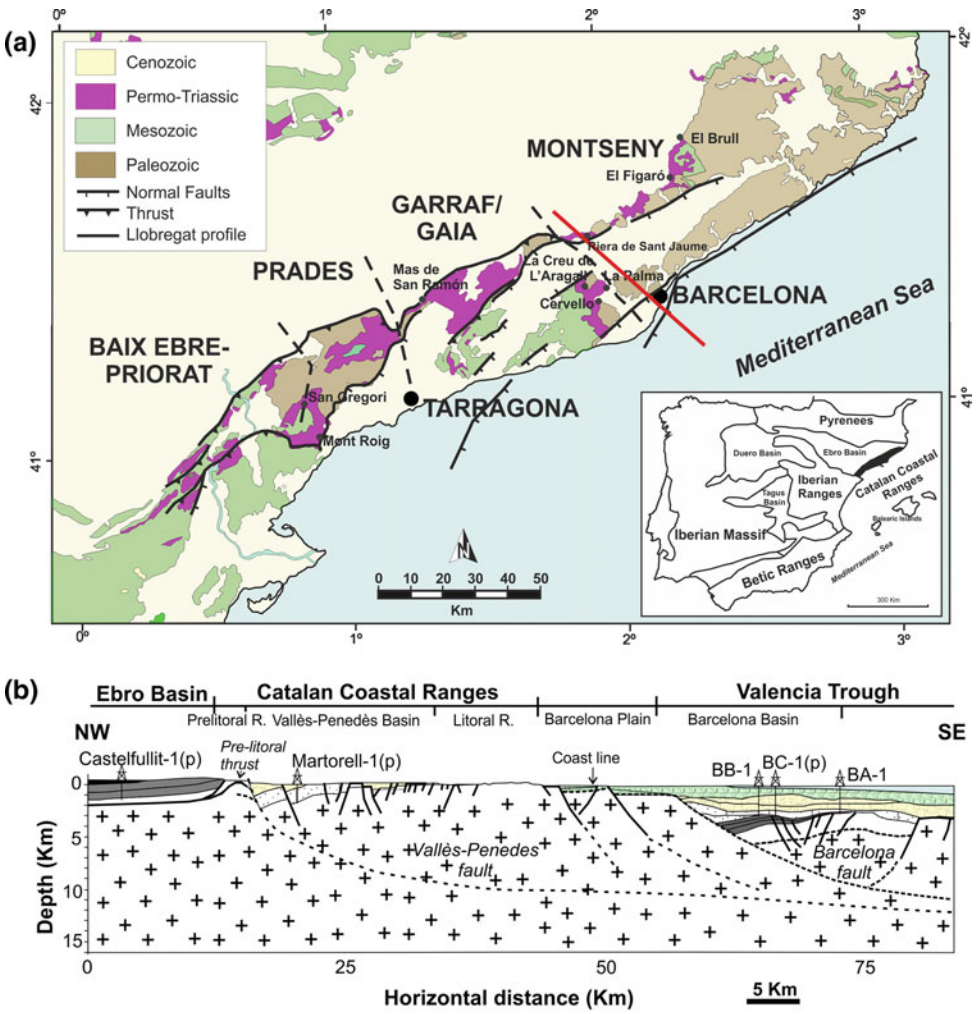

Fig. 3.17 **a** The Catalan Coastal Ranges and location of the main faults and Permian-Triassic outcrops. Paleogeographic domains or subbasins (from Marzo 1980, and Marzo and Calvet 1985) from SW to NE: Priorat–Baix Ebre, Prades and Gaia-Garraf, and Montseny. **b** Structural cross section across the central Catalan Coastal Ranges (modified from Gaspar-Escribano et al. 2004)

clearly reflects both climate and tectonic controls on sedimentation of the Catalan basin. The globally arid and semi-arid Early Triassic climate in NE Iberia (Borruel-Abadía et al. 2015) and the still active local tectonic control gave rise to the different sedimentary characteristics of the three main sub-basins (Figs. 3.18 and 3.20). Sedimentation of this cycle broadly represents the development of braided fluvial systems in the central Garraf sub-basin and aeolian dune fields with isolated braided fluvial systems in the Prades sub-basin, while the Montseny sub-basin was basically elevated and shows a reduced sedimentary record (Galán-Abellán et al. 2013).

After a period of interruption, a third cycle of continental sedimentation took place in the early Anisian. This sedimentary record, mostly representing distal fluvial systems (ASM and FSM in Fig. 3.18), was progressively related to low topographic reliefs in the Catalan basin, without clear subsidence rate differentiation. This new tectonic characteristic in the basin provided the necessary conditions for the first incursion of the Tethys Sea in Iberia, represented in sedimentary terms by the Muschelkalk facies.

3.3.2 Middle Triassic Carbonate Ramps in the Catalan Basin

Escudero-Mozo MJ, Martín-Chivelet J, López-Gómez J and Marzo M

During Anisian, new tectonic conditions determined a broader and more homogeneous subsidence in the Catalan basin, despite local fault movements still controlling depocenters. Under these conditions (and favoured by them) marine waters invaded the basin in a generalized transgressive episode. That episode was going to drastically change the paleogeography and the sedimentation of the basin, thence becoming dominated by shallow marine environments within vast carbonate platforms. These conditions broadly prevailed for ten million years, during which two thick carbonate rock bodies, corresponding to the Muschelkalk facies accumulated in the basin: lower Muschelkalk and upper Muschelkalk units, respectively. This interval of carbonate deposition was: (1) heralded by a period of evaporite-carbonate-lutite deposition (Röt facies) that reflects the progressive incoming of the sea during the

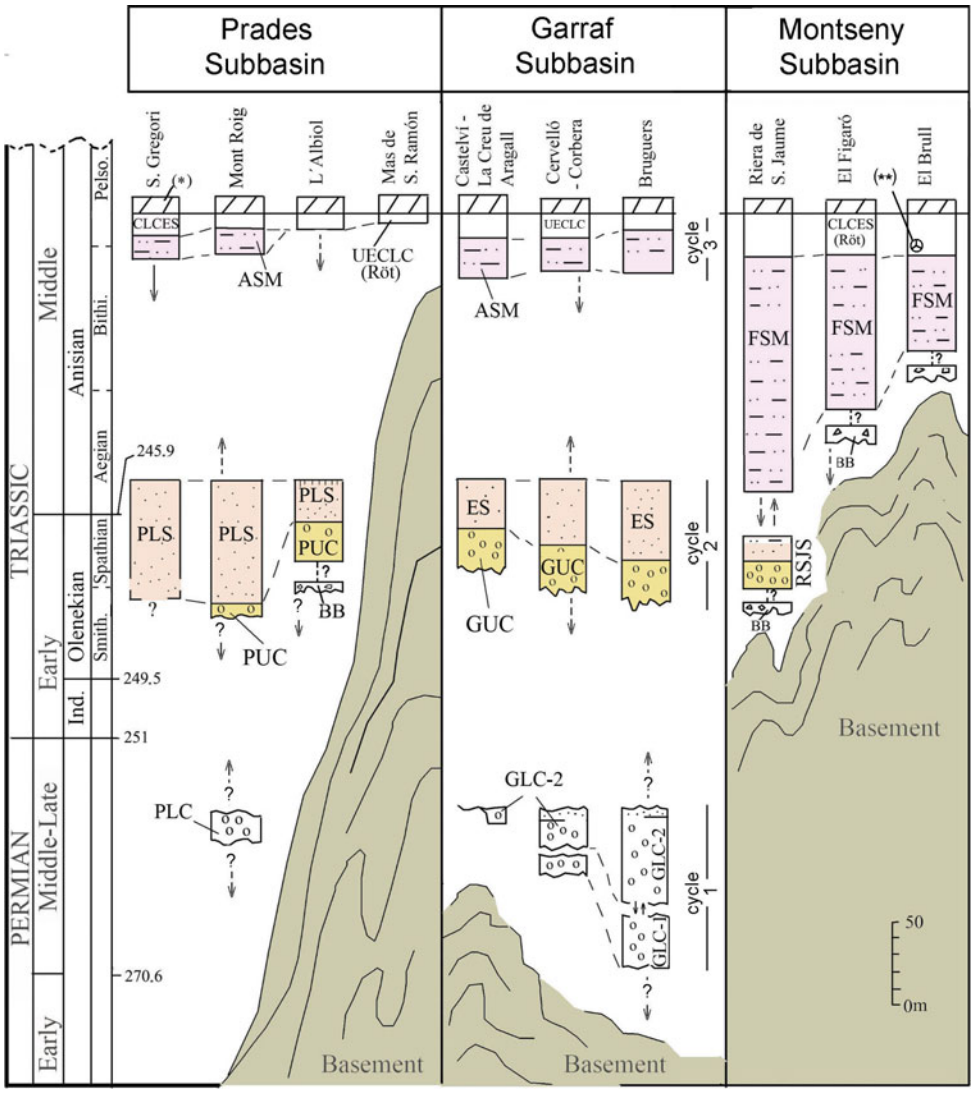

Fig. 3.18 Scheme of the continental Permian and Lower-Middle Triassic sedimentary successions in the three subbasins of the Catalan Ranges; including lithological units, unconformities and hiatuses. Units: PLC—Prades Lower Conglomerates; GLC 1-Garraf Lower Conglomerates 1; GLC 2—Garraf Lower Conglomerates 2; BB—Basal Breccias; PUC—Prades Upper Conglomerates; GUC—Garraf Upper Conglomerates; PLS—Prades Lower Sandstones; ES—Eramprunyà Sandstones; RSJS—Riera de San Jaume Sequence; ASM—La Creu d´Aragall Sandstones and Mudstones; UECLC—Upper Evaporite, Carbonate and Lutite Complex (Röt facies); FSM—El Figaró Sandstones and Mudstones. *Muschelkalk. **Polen assemblage (Díez et al. 2012). Stratigraphical nomenclature from Marzo (1980) with modifications from Galán-Abellán et al. (2013)

middle Anisian; (2) interrupted by a new period of mixed sedimentation in the latest Anisian (the so-called middle Muschelkalk); and (3) postdated in the early Carnian by the development of the large evaporitic systems represented by the Keuper facies (Virgili 1958; Calvet et al. 1990; Calvet and Marzo 1994; Mercedes-Martín et al. 2013; Escudero-Mozo et al. 2015).

During the middle Anisian to earliest Carnian interval two major transgressive-regressive cycles took place in the basin (Fig. 3.21). The first one occurred during the middle to late Anisian and is recorded by the Röt facies, the lower Muschelkalk and part of the middle Muschelkalk units. The second cycle, latest Anisian—early Carnian in age, is represented by the upper part of the middle Muschelkalk, the upper Muschelkalk and the lower part of the Keuper facies.

The first transgressive episode, which occurred in the middle Anisian (Pelsonian), allowed the development of a wide ramp, dominated by shallow environments corresponding to the inner to middle ramp. Depositional conditions were quite uniform in the entire basin and the thickness of the carbonate body ranges from 70 m in the Gaia-Montseny area to 120 m in the Baix-Ebre (Fig. 3.21).

This transgression was limited to the north by a NE–SW fault system that defined the border of the subsiding basin. However, it was open towards the NE, connected to the Paleotethys, constituting the seaward corridor of the Iberian Basin (Escudero-Mozo et al. 2015) (Fig. 3.22). Sedimentary and sequence stratigraphy analyses indicate that the Catalan basin acted as a single basin during the Anisian with a main depocenter located in the Baix-Ebre area, where the deepest facies and the thickest successions were accumulated. Subsidence was still locally controlled by main faults, but thermal relaxation also allowed the beginning of a new flexural subsidence, the mature rifting phase, previous to the general post-rift subsidence during the Jurassic.

During the late Anisian, a rapid regressive episode progressively marked the final evolution of the lower

Fig. 3.19 Permian and continental Lower-Middle Triassic units in the Mont-Roig section (Prades subbasin). The unconformity between PLC and PUC (cycles 1 and 2) is shown in the inset. See figure 3.18 for the nomenclature of the units

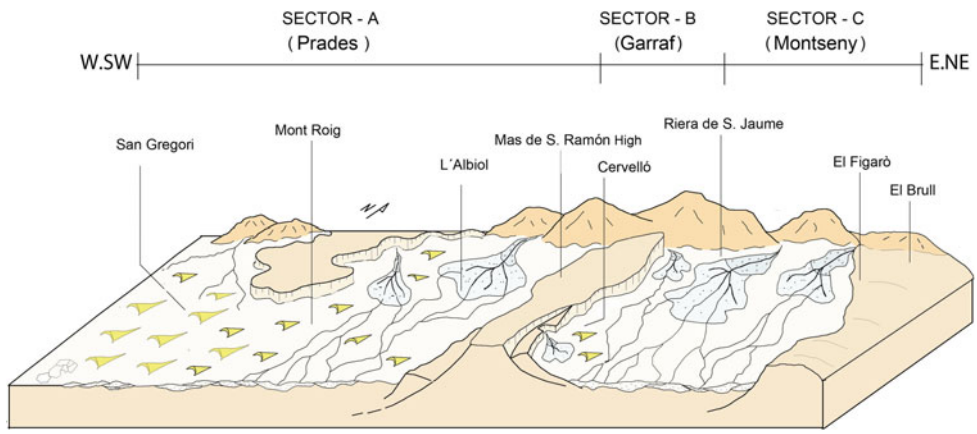

Fig. 3.20 Sketch reconstruction of the grabens and highs in the Catalan basin and their sedimentary environments during the Spathian (Late Early Triassic). Location of the differentiated subbasins and sectors are indicated. River systems flow from the northern elevated areas towards the south, but most of them were interrupted by aeolian dune fields, mainly in the southern areas. Paleozoic highs constituted barriers between the areas of subsidence in the three subbasins. Modified from Galán-Abellán et al. (2013)

Muschelkalk carbonate ramp and permitted the deposition of the mixed facies of the middle Muschelkalk. This sedimentary record is divided in four units showing different evaporite-coastal to fluvial environments along the basin. The presence of alluvial fan deposits in the NE and some volcanic deposits to the SW suggest a tectonic reactivation of the basin during this period (Mitjalva and Martí 1986; López-Gómez et al. 1998; Sanz et al. 2012).

The second transgressive-regressive cycle started in the late Anisian, with a rapid trasgressive event that determined the installation of a new carbonate ramp (upper Muschelkalk, late Anisian to earliest Carinan in age). This marine transgression could be related to the opening of the Neotethys (Escudero-Mozo et al. 2015). Five different members have been described in the upper Muschelkalk. The first two members (late Anisian) and the last one (late Ladinian-early Carnian) show similar lithological and stratigraphic features throughout the basin, whereas the middle members (Ladinian) show important differences regarding facies and thickness (Escudero-Mozo et al. 2015).

Three main evolutive phases can be differentiated during the end of the Anisian and the beginning of the Ladinian. A first one was characterized by the installation of a shallow carbonate ramp, with high microbial carbonate production in

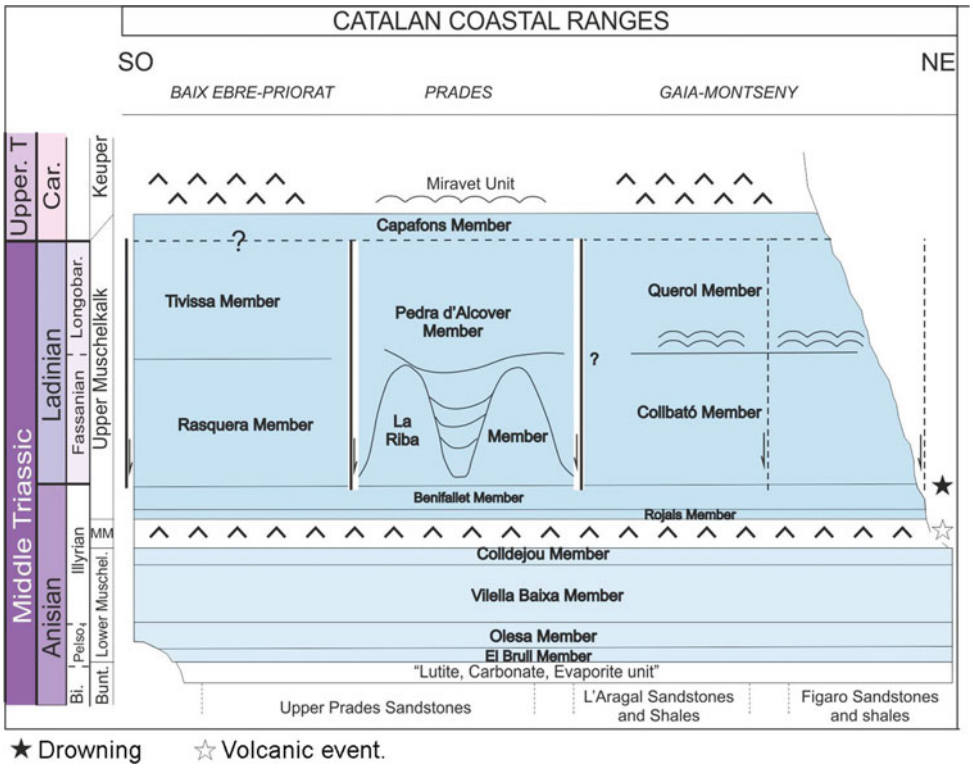

Fig. 3.21 Lithostratigraphical units defined for the Middle Triassic carbonate ramps in the Catalan Coastal Ranges (Calvet and Ramón 1987; Ramón and Calvet 1987; Calvet et al. 1990) related to the three main paleogeographical areas in which the basin is subdivided

the subsiding areas of the basin during the late Anisian. The second represents a period of a rapid subsidence, controlled by NW–SE faults, mainly developed during the latest Anisian. These faults compartmentalized the Catalan basin generating three sub-basins with different subsidence rates (Mercedes-Martín et al. 2013). This tectonic subsidence episode extended until the latest Ladinian, when the widespread deposition in tidal flats environments of the Capafons Member and the Keuper facies throughout the whole basin represented a homogenization of the basin and a deceleration of the subsidence rates in this area. During the latest Anisian the Baix-Ebre and Prades domains represented a single basin controlled mainly by tectonic subsidence with a depocenter located in the Prades domain (Fig. 3.17a). The third phase took place during the Anisian-Ladinian transition and was characterized by a new tectonic reactivation of the basin, represented by the separation of the Baix-Ebre and Prades domains (Mercedes-Martín et al. 2014a) and by a rapid sea-level rise that in the Baix–Ebre domain caused the drowning of the previous carbonate setting and the installation of the deepest marine conditions in this area. The regional character of this event suggests that it was linked to the main paleogeographic changes that were occurring in the western Tethys (Escudero-Mozo et al. 2015).

The Gaia-Montseny (northern domain) represents the less subsident domain of the Catalan basin (Fig. 3.17a). As in the other domains, its development was controlled by fault activity, which started later in this domain, during the latest Anisian. Notably, although this domain has been traditionally considered as a single one, recent studies indicate that the Gaia-Montseny domain could be subdivided into two different sub-basins with different subsidence rates (Mercedes-Martín et al. 2013).

3.3.3 Ladinian Rifting Accommodation and Microbialite Development in the Catalan Basin

Mercedes-Martín R and Salas R

The evolution of subsidence during the Triassic strongly advocates that the Ladinian stage was a period of widespread and rapid syn-rift subsidence in the eastern part of the Iberian plate where extensive carbonate successions deposited at this time (Tucker et al. 1993; Mercedes-Martín et al. 2014b).

In the Triassic Catalan basin, the second carbonate unit (Ladinian) of the Muschelkalk facies was subdivided by Mercedes-Martín et al. (2014b) into two transgressive-regressive sequences (T-Rs) corresponding to two low-angle, microbial-dominated carbonate ramps (Fig. 3.23). T-Rs1 is characterised by stromatolite deposits (at least 7 m thick) developed in the inner ramp setting, and thrombolites (averaging 40 m in thickness) accumulated in the middle-outer ramp environments (Mercedes-Martín et al.

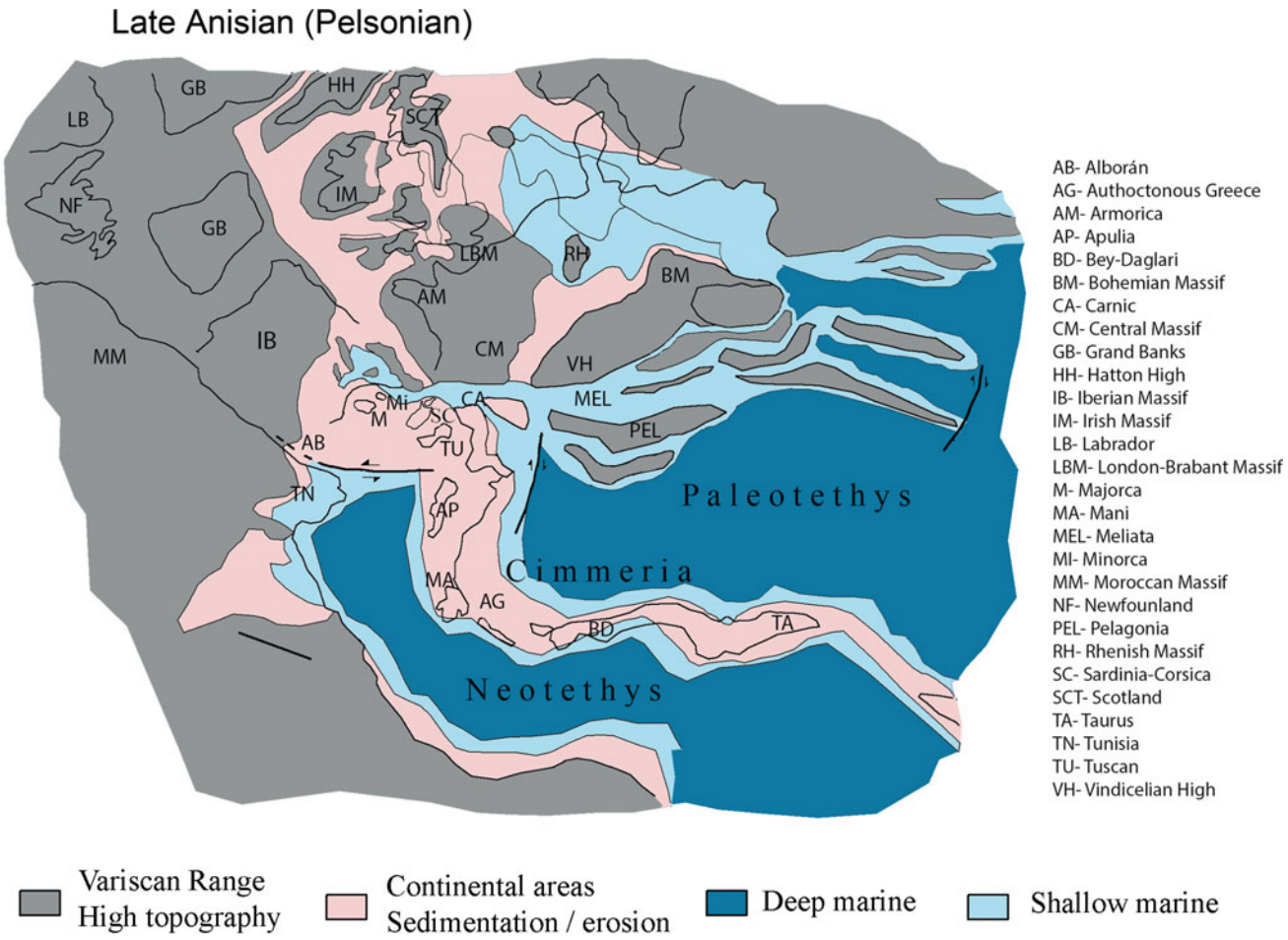

Fig. 3.22 Paleogeographic reconstruction of the westernmost Tethys realm for the Anisian (Pelsonian). Modified from Escudero-Mozo et al. (2015)

2013; 2014a, b). The second T-Rs, or T-Rs2, is mainly characterised by the occurrence of ooidal-muddy laminites (up to 3 m thick) in the inner ramp environment, and internal shoals and sheltered lagoons of coarse-grained to muddy carbonates in the middle ramp. Both T-Rs are bounded by a regional subaerial unconformity whose origin was attributed to a prominent sea-level drop of at least 50 m (Calvet and Tucker 1995; Mercedes-Martín et al. 2014b). This unconformity is characterised by deep paleo-valley incisions (up to 60 m), karst features and common collapse breccia fillings.

According to subsidence analysis carried out over stratigraphic sections from three different domains of the Triassic Catalan basin, a rapid total subsidence attaining 470 m was recorded during the Ladinian (Mercedes-Martín et al. 2014b). Fault-controlled half-graben development particularly affected the middle-outer ramp environments producing rapid pulses of syn-rift subsidence and increased gains in accommodation space collectively controlling the architecture of the microbial deposits (Mercedes-Martín et al. 2014a, b). Domed stromatolites and mounded thrombolite bodies developed during stages of increasing accommodation rates, whereas stratiform stromatolites and biostromal thrombolite morphologies grew in association with periods of low accommodation rates.

The total subsidence evaluation of Mercedes-Martín et al. (2014b) is in agreement with the quantitative subsidence analysis previously performed by Vargas (2002) and Vargas et al. (2009) for the Triassic deposits of the areas of the Iberian and Ebro basins. Although the syn-rift compartmentalisation of the Ladinian basin played a crucial role governing the macro-scale morphology of microbial reefs, it was hypothesised that hydrothermal fault-controlled fluid circulation and episodic conditions of dysoxia/anoxia could have favored microbial carbonate precipitation (Mercedes-Martín et al. 2014a).

3.3.4 The Keuper Facies in the Catalan Basin

Ortí F and Pérez-López A

The sedimentary record of the Keuper facies in the Catalan basin is only partially represented when it is compared with the one recorded in the SE Iberian microplate (Fig. 3.15). The sedimentary record in the Catalan basin is constituted by the Miravet Fm at the base (equivalent to the K1 unit of the Iberian Basin), the Molar Fm (equivalent to the K4 unit) and the Gallicant Fm (equivalent to the K5 unit) (Salvany and Ortí 1987) (Fig. 3.24). The Miravet Fm, up to 90–100 m in thickness, is comprised of an alternation of grey claystone beds and laminated and nodular gypsum beds. In some paleohighs, however, only thin successions of claystone, marls and carbonate are present. The Molar Fm is characterized by abundant gypsum layers (mainly laminated gypsum, but nodular gypsum also) in association with red claystones. A pyroclastic layer (1 m thick) forms the base of the unit. The Gallicant Fm is constituted by claystones, carbonates and minor nodular gypsum (Figs. 3.15 and 3.24).

3.3.5 The Triassic Alkaline Magmatism of the Catalan Coastal Ranges: Insights into the Opening of the Neotethys Ocean

Ubide T, Galé C and Lago M

In the Catalan Coastal Ranges the onset of the Tethyan rift was accompanied by intraplate alkaline volcanism (Mitjavila and Marti 1986; Lago et al. 1996; Sanz et al. 2012) emplaced into basins controlled by two main fault systems: SW–NE and N–S (Calvet and Ramón 1987; Bourquin et al.

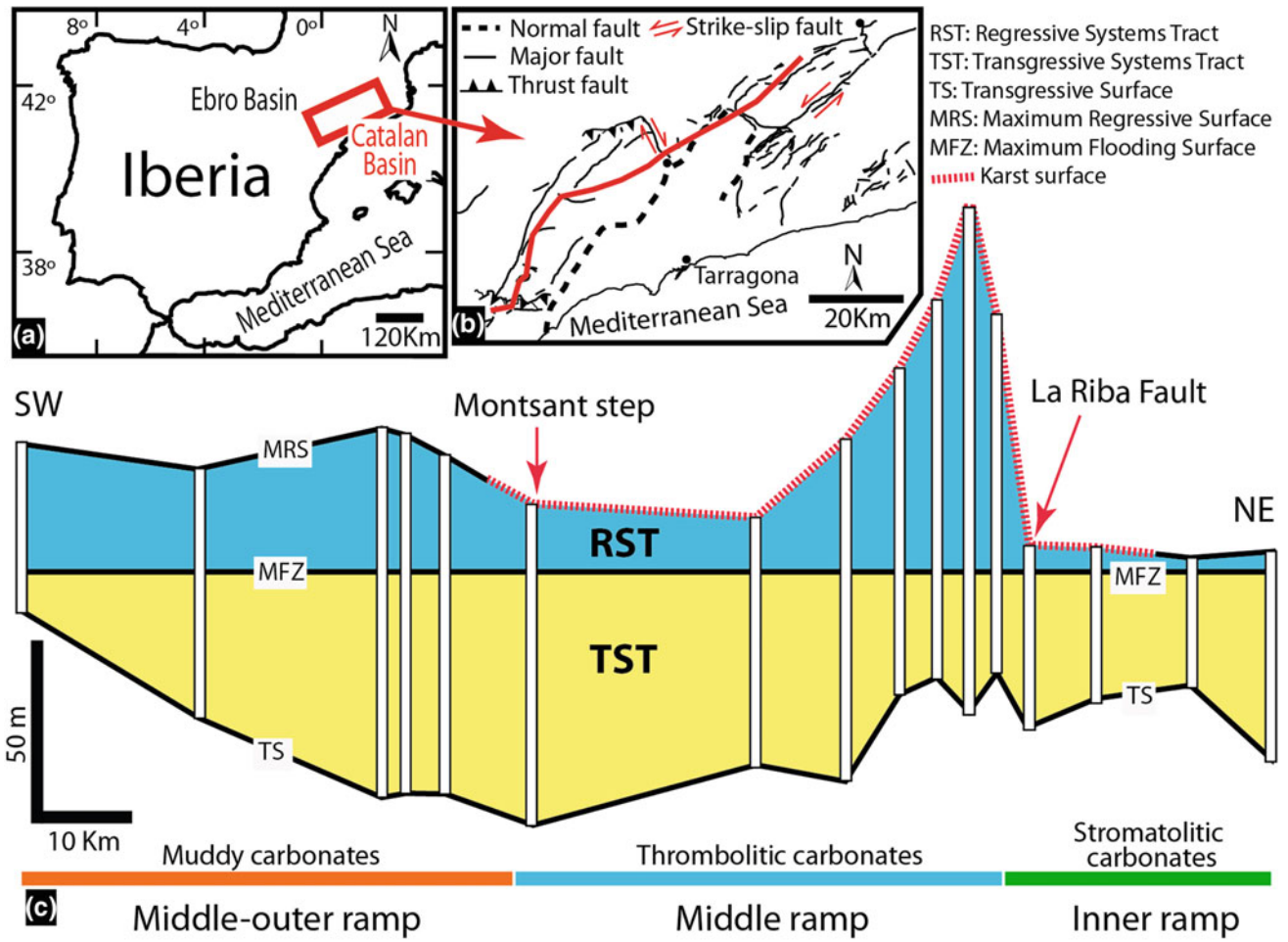

Fig. 3.23 Lateral evolution of accommodation space during the Ladinian in the Catalan basin. **a** Map of Iberia showing the location of the Triassic Catalan basin in the red square. **b** Detail of A displaying the major structural features. Red solid line shows the profile in (**c**). **c** Variations of the accommodation space in the first Transgressive-Regressive Sequence during the Ladinian. Stratigraphic thicknesses are plotted against the MFZ (maximum flooding surface). Note that accommodation increases in the surrounding of La Riba Fault and Montsant step where microbial carbonates (see bottom) developed widely across the inner and middle ramp settings

2011 and references therein). Lago et al. (1996) included this volcanism into a Triassic alkaline magmatic province related to the opening of the Neo-Tethys sea in SW Europe. This province was also linked to magmas of similar age in the Iberian Ranges and the Northern Range of Majorca in Spain, and Corbières and Écrins-Pelvoux in France.

This volcanism is represented by isolated outcrops that occur in three geographic sectors. The Beceite thrust and the Baix Ebre and Burgar faults, delineate the western and the central sectors respectively (Fig. 3.17a, b). In both sectors the volcanic rocks were emplaced between the top of the Middle Triassic, or upper Muschelkalk (M3 Unit) of late Ladinian-early Carnian age (Escudero-Mozo et al. 2015), and the Upper Triassic deposits (Sanz et al. 2012). In the eastern sector the sill of Vandellós-Tivissa intrudes the middle part of the Middle Triassic deposits, or middle Muschelkalk (M2 Unit) (Mitjavila and Marti 1986; Sanz et al. 2012).

Two volcanic stages are identified in the western and central sectors. The oldest has been interpreted as a hydromagmatic event, with associated volcanic structures like maars and ring and tuff cones (Sanz et al. 2012). This stage comprises lapilli tuffs crosscut by lava flows, dikes and sills. From a stratigraphic point of view, these volcanics overlay the top of the Middle Triassic deposits (M3 Unit) and are probably coeval with the deposition of the Miravet Fm (Carnian) (Fig. 3.21). The second stage is mainly composed of sills intruding the Upper Triassic sequences (Miravet, Molar and Gallicant Fms) that could eventually reach the surface generating lapillistone deposits. These volcanics have been interpreted as the result of strombolian activity coeval with the deposit of the Molar and Gallicant Fms (Norian) (Sanz et al. 2012).

The rocks have primitive composition and alkaline affinity, and they include mantle xenoliths of lherzolite and websterite. Sanz et al. (2012) proposed an origin related to low degrees of partial melting of the asthenospheric mantle. This hypothesis suggests local upwelling and melting of the mantle during the Late Triassic in this area, probably in response to the extensional tectonic regime generated by the opening of the Neo-Tethys sea.

3.4 The Balearic Basins

López-Gómez J, Barrenechea J, De La Horra R, Arche A, Ronchi A, Marzo M, Borruel-Abadía V, Ramos E, Bourquin S, Arribas J, Gómez-Gras D, Escudero-Mozo MJ, Martín-Chivelet J, Goy A, Ortí F and Pérez-López A

The present-day location of the Balearic promontory has been related to the development of the Valencia Trough during the Oligocene and Middle Miocene (Bourrouilh 1973; Pomar 1979; Sabat et al. 1988; Roca and Guimerà

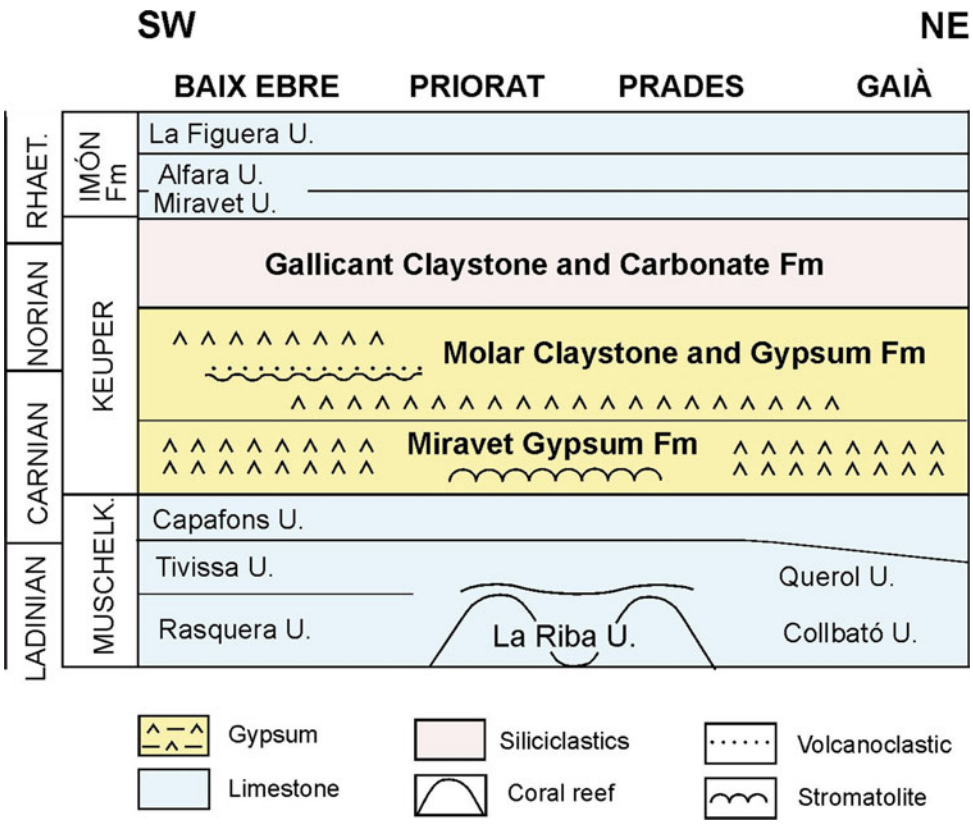

Fig. 3.24 Stratigraphy of the Keuper units in the Catalan basin. Basin sectors: Baix Ebre, Priorat, Prades and Gaià. Simplified from Calvet and Marzo (1994). Scheme out of scale

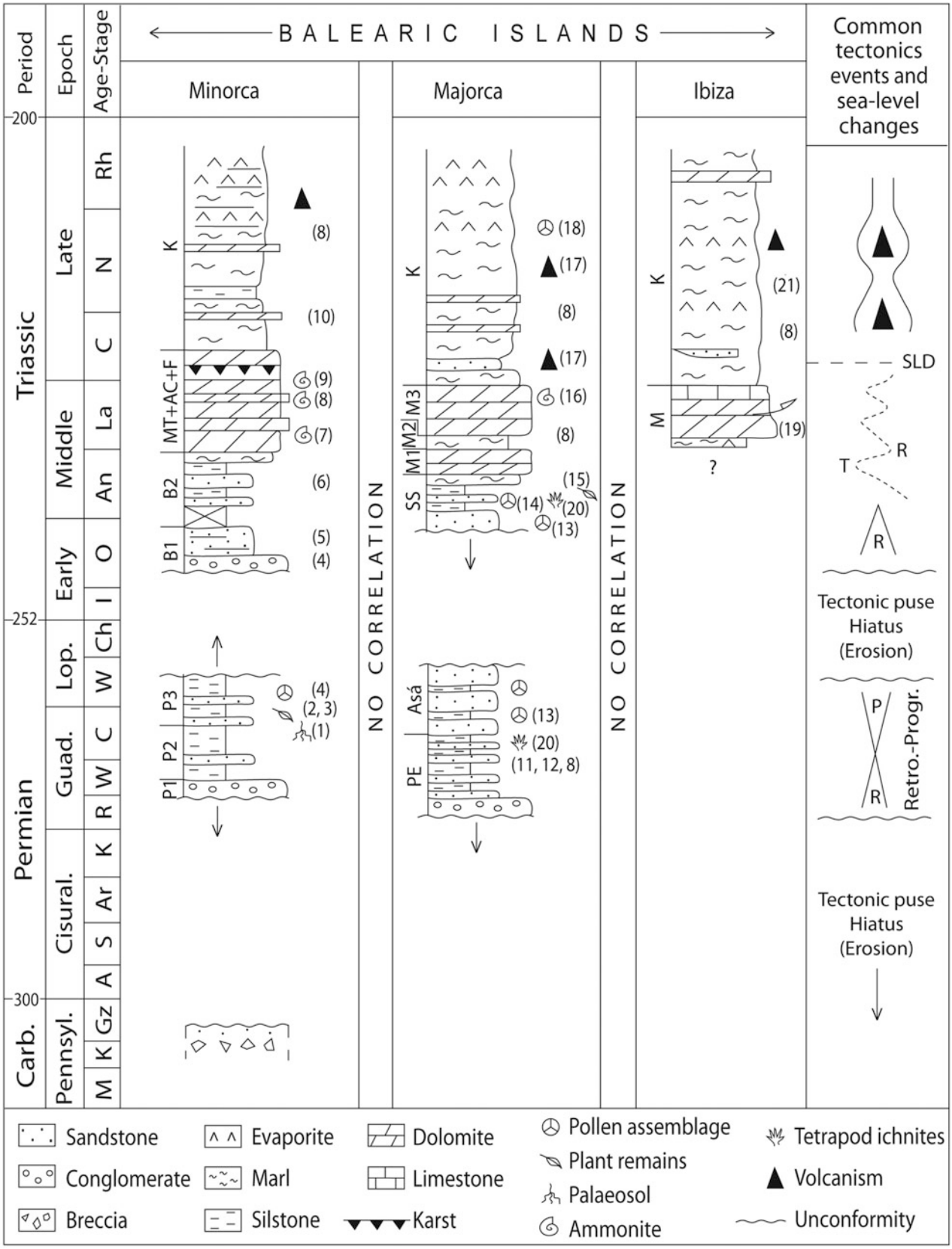
Period
Epoch
Age-Stage
BALEARIC ISLANDS
Minorca
Majorca
Ibiza
Common tectonics events and sea-level changes
Triassic
Permian
Carb.
Late
Middle
Early
Lop.
Guad.
Cisural.
Pennsyl.
Rh
N
C
La
An
O
I
Ch
W
C
W
R
K
Ar
S
A
Gz
K
M
200
252
300
K
MT+AC+F
B2
B1
P3
P2
P1
M3
M2
M1
SS
Asá
PE
M
?
(8)
(10)
(9)
(8)
(7)
(6)
(5)
(4)
(4)
(2, 3)
(1)
(18)
(17)
(8)
(17)
(16)
(8)
(15)
(14)
(20)
(13)
(13)
(20)
(11, 12, 8)
(21)
(8)
(19)
NO CORRELATION
NO CORRELATION
SLD
T
R
R
Tectonic puse
Hiatus
(Erosion)
P
R
Retro.-Progr.
Tectonic puse
Hiatus
(Erosion)
Sandstone
Conglomerate
Breccia
Evaporite
Marl
Silstone
Dolomite
Limestone
Karst
Pollen assemblage
Plant remains
Palaeosol
Ammonite
Tetrapod ichnites
Volcanism
Unconformity

◀ **Fig. 3.25** Sketch of the Permian and Lower-Middle Triassic siliciclastic (Buntsandstein facies) sedimentary record in the Balearic Islands. 1—Gómez-Gras and Alonso-Zarza (2003); 2—Broutin et al. (1992); 3—Bercovici et al. (2009); 4—Bourquin et al. (2011); 5—Linol et al. (2009); 6—Rosell et al. (1988); 7—Goy (1995); 8—Rodríguez-Perea et al. (1987); 9—Escudero-Mozo et al. (2014); 10—Hirsch (1977); 11—Gómez-Gras (1993); 12—Ramos (1995); 13—Ramos and Doubinger (1989); 14—Grauvogel-Stamm and Álvarez-Ramis (1995); 15—Álvarez-Ramis et al. (1995); 16—Bouzá (1981); 17—López-Gómez et al. (2017); 18—Lago et al. (1988); 19—Boutet et al. (1982); 20—Calafat et al. (1986–87); 21—Rangheard (1972)

1992; Bartrina et al. 1992). This promontory represents the northeastern prolongation of the Betic Cordillera (Gelabert et al. 1992; Barón et al. 2004), and forms the eastern border of the Valencia Trough Basin, an almost symmetrical domain to the Catalan-Valencia domain, which represents the western border (Fontboté et al. 1990; Roca 1992). Since the 1970s, the Cenozoic tectonic development of the Balearic Islands has been described in detail and is also presented later in this book. However, we lack detailed descriptions of the location and development of the first post-Variscan basins shaped by Permian-Triassic rifting.

3.4.1 Sedimentation During the Permian-Triassic Initial Rifting Phase

López-Gómez J, De La Horra R, Barrenechea JF, Arche A, Ronchi A, Marzo M, Borruel-Abadía V, Bourquin S and Ramos E

The Late Carboniferous configuration of the equatorial westernmost Tethys domain at the eastern border of Pangea was the consequence of a succession of compression and extension motions associated with strike-slip faulting and block rotations (Matte 1991; Franke 2000; Edel et al. 2014). Later, Permian-Triassic extension during the first steps of the break-up of Pangea gave rise to horsts and graben in the Balearic islands area that were initially infilled with clastic sediments of continental origin (Rodríguez-Perea et al. 1987; Calafat 1988; Rosell and Elízaga 1989; Ramos 1995; Bourquin et al. 2011). Sediment thickness variations in these basins contribute significantly to locating and understanding detachment levels of later thrust systems during the Alpine orogeny (Gelabert et al. 1992). However, the different orientations of ancient fault systems on the islands point to different initial structures, mainly in Minorca (Maillard et al. 1992).

Despite the supposed similar initial development of these basins, most outcrops in Minorca and Majorca islands show clear differences in their infill during Permian and Triassic rift evolution. These characteristics suggest the different durations of some tectono-sedimentary stages in the basins, or even non coetaneous stages, perhaps as the consequence of different paleogeographic evolution in each case. Despite being evident in the Permian-Triassic continental record, these paleogeographic differences also appear in the first Mesozoic transgression of the Tethys sea in the Balearic island basins during the Middle Triassic, represented by the Muschelkalk facies (Escudero-Mozo et al. 2014).

In Fig. 3.25 we provide a synthetic sketch of the Permian and Triassic sedimentary record of Minorca, Majorca and Ibiza, indicating main common tectonic events and sea-level changes. These data were obtained in different studies including our own work. A first observation is the lack of outcrops of Permian age in Ibiza, while the Permian sedimentary record of Minorca and Majorca is well represented in the northern part of the islands. These records show rocks of Guadalupian-Lopingian age, probably of the Wordian-Wuchiapingian time-interval (Ramos and Doubinger 1989; Broutin et al. 1992; Bercovici et al. 2009). The sedimentary record of these rocks has been mainly examined during the second half of the last century, but only a few works have detailed their sedimentary characteristics. These sedimentary studies of Permian rocks in Majorca (Bourrouilh 1973; Calafat 1988; Gómez-Gras 1993; Ramos 1995; Arche et al. 2002) have revealed the alternating development of braided and meandering fluvial systems. Substantial lateral thickness variations exist in this island, with a double sedimentary record compared to the Minorca basins (Rosell et al. 1988; Arribas et al. 1990; Gómez-Gras and Alonso-Zarza 2003; Linol et al. 2009; Bourquin et al. 2011).

The Lower-Middle Triassic continental sedimentary record, or Buntsandstein facies (Rodríguez-Perea et al. 1987) of the Balearic Islands again lacks outcrops in Ibiza (Rangheard 1972). The age of the rocks is Olenekian-early Anisian (Bourrouilh 1973; Álvarez-Ramis et al. 1995; Álvarez-Ramis and Grauvogel-Stamm 1996; Juárez-Ruiz and Wachtler 2015). These sediments were deposited in the Majorca and Minorca basins following a long period of tectonic activity and erosion. They basically consist of red sandstones in the lower part, and mudstones with intercalated sandstone levels at the top, and have been interpreted in both islands as braided fluvial systems evolving to distal alluvial sedimentation in the upper part (Rodríguez-Perea et al. 1987; Rosell et al. 1988; Calafat 1988; Brandes and Tiedt 1991; Gómez-Gras 1993; Ramos 1995; Bourquin et al. 2011). These sedimentation processes were the prelude to the first incursions of the Tethys in the islands, represented by different units of the Muschelkalk facies.

3.4.1.1 Composition of the Permian Sandstones in Minorca and Its Geodynamic Significance

Arribas J and Gómez-Gras D

As manifested in other areas of Iberia (i.e. Iberian Ranges; Arribas 1985), sandstone composition of the Permian record in Minorca is characterized by sedimentoclastic petrofacies (quartzoarenites and sublithoarenites) (Fig. 3.26a) outlining recycling processes from the Paleozoic substratum and suggesting a "recycled orogen" geotectonic provenance (Rosell et al. 1988; Gómez-Gras 1993). In addition, the overlying Buntsandstein facies maintain this recycled character at the base of the sequence, with a quartzoarenitic composition, suggesting greater maturation of sediments by recycling of Upper Permian deposits (Fig. 3.26b). In the upper part of the Buntsandstein facies, a progressive influence of plutonic sources can be deduced by a progressive increment of feldspar grains in framework sandstones (subarkoses) (Fig. 3.26b). This fact denotes an important change towards a "basement uplift" geotectonic provenance type. An important feature in the Minorca record is that the change in composition (i.e. sources) between Late Permian and Lower-Middle Triassic is retarded and occurs during deposition of the upper part of the second cycle (Rosell et al. 1988; Gómez-Gras 1993). However, in the Iberian Basin this change occurs in the lower part of the upper sedimentary cycle.

3.4.2 The Middle-Late Triassic in the Balearic Islands

Escudero-Mozo MJ, Martín-Chivelet J, López-Gómez J, Goy A, Ortí F and Pérez-López A

During the Late Middle and Late Triassic time interval, the Balearic Islands spanned together with the rest of the Iberian plate the latitudes 8°N to 15°N (Perri et al. 2013). The exact paleogeographic location of these islands is however still a matter of debate, although they were close to the rest of Iberia and probably connected with its basins (Edel et al. 2014). General plate reorganization involved syndepositional extensional tectonics and frequent sea-level oscillations during that time affecting the Early Mesozoic sedimentation in Western and Central Europe (Biddle 1984; Brandner 1984; Gianolla and Jacquin 1998). As a result, the Tethys sea advanced westwards during the late Anisian-Ladinian in different incursions to encircle the Iberian Massif and covering the eastern area of the Iberian plate and the surrounding areas as the present-day Balearic Islands, Corsica and Sardinia (Ziegler and Stampfli 2001). These first marine sediments resulted in carbonate ramps (Muschelkalk facies) development (Escudero-Mozo et al. 2014). They were interrupted during the early Carnian (Julian) when sporadic continental fluxes, arising during humid stages from the elevated areas of the Iberian Massif, may have crossed different subsiding trough systems in the E Iberian plate reaching the Balearic Islands (Fig. 3.27). This humid pulse, related to the Carnian Pluvial Event (CPE), was correlated with the sedimentary record of the same event occurred in the Iberian plate (López-Gómez et al. 2017) and defined by Arche and López-Gómez (2014). This pulse was however short, and again during new periods of falling sea-level and desiccation, "Keuper salts" were deposited in areas of rapid subsidence during the Carnian and Norian.

3.4.2.1 Middle Triassic Carbonate Ramps in the Balearic Islands

Escudero-Mozo MJ, Martín-Chivelet J, López-Gómez J and Goy A

Middle Triassic outcrops exist in the three main islands: Majorca, Minorca and Ibiza, although in the latter they are restricted to the easternmost part of the island and show a very incomplete and fragmentary record, strongly affected by later tectonics. This structural complexity is not only limited to Ibiza, but also exists in the other two islands (Gelabert et al. 1992), making difficult the reconstruction of the Middle Triassic carbonate ramps sedimentary record. In spite of it, very interesting works that created the basis of the present-day knowledge were published in the past century (Darder 1914; Virgili 1952; Bourrouilh 1973; Colom 1975; Rodríguez-Perea et al. 1987; Llompart et al. 1987).

Despite their present-day proximity, Majorca and Minorca show remarkably different sedimentary successions for the late Anisian to early Carnian interval (Fig. 3.25). The Minorca succession is characterized by the lack of a middle

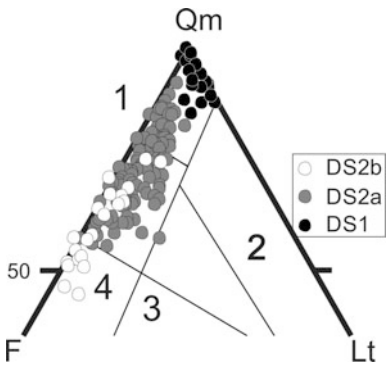

Fig. 3.26 Sandstone composition plotted in a QFR diagram (quartz, feldspar and rock fragments, based on Pettijohn et al. 1973) from the Permian and Lower-Middle Triassic siliciclastic (Buntsandstein facies) sedimentary record of Minorca. Modified after Rosell et al. (1988)

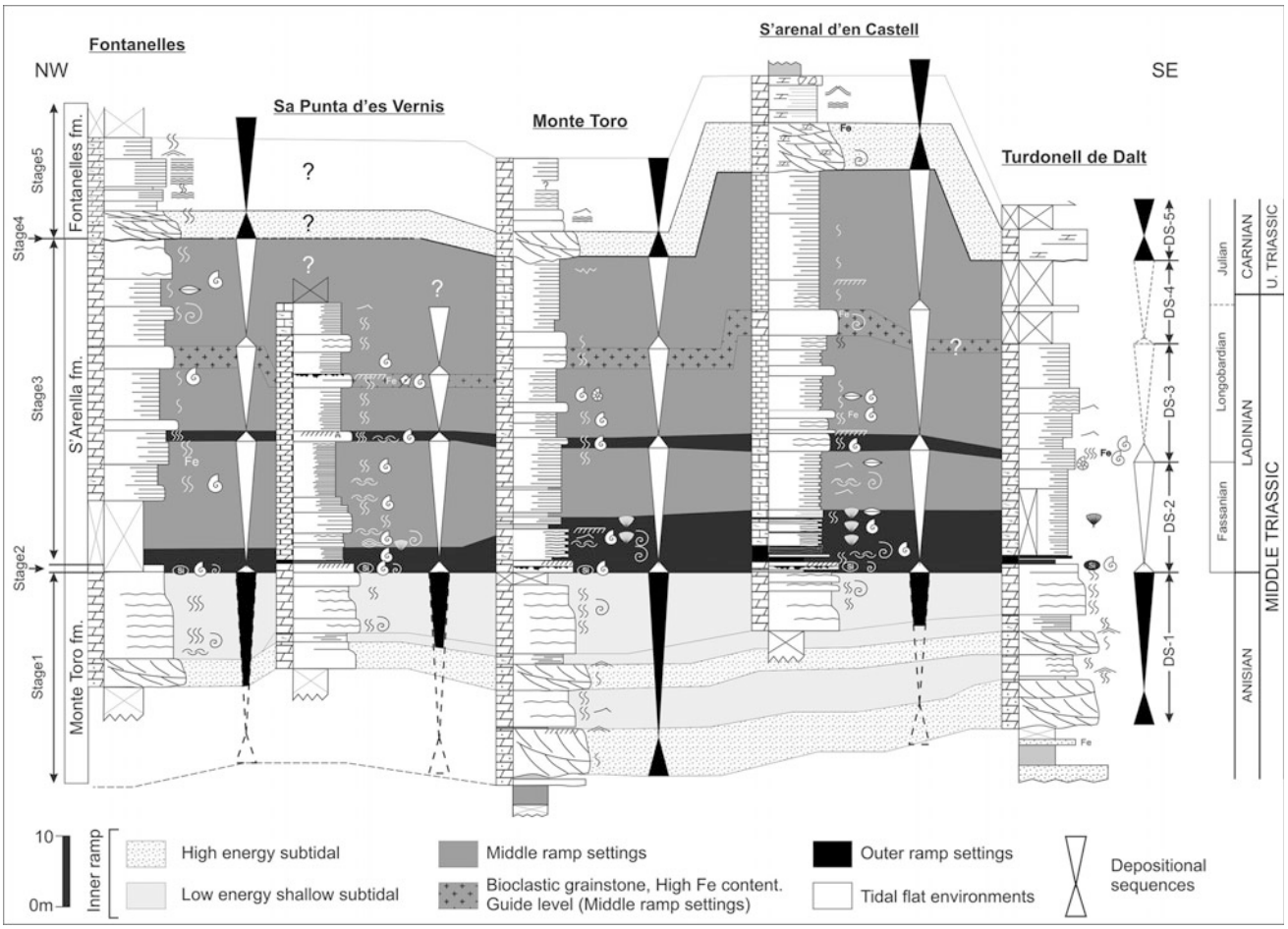

Fig. 3.27 Sequence stratigraphy of the Middle Triassic carbonate succession (Muschelkalk facies) of Minorca. Modified from Escudero-Mozo et al. (2014)

Anisian carbonate ramp, and by a prominent latest Anisian to earliest Carnian ramp, similarly to some areas of the Iberian Basin (the so-called "Levantine-Balearic Muschelkalk" by López-Gómez et al. 1998). However, in Minorca there was a third carbonate ramp of early Carnian (Julian) age that did not develop in the Iberian basin.

Based on sequence stratigraphy analysis the Muschelkalk facies succession of Minorca has been recently studied in detail by Escudero-Mozo et al. (2014). A total of five depositional sequences represent the whole succession that, in some cases, these authors compare with similar third order sequences defined in other basins of the western Tethys realm (Fig. 3.28). Sedimentary characteristics of the sequences include an evolution from shoal to inner and middle ramp environments, from base to top respectively. This latter sequence is capped by an unconformity and karst with siliciclastic input. This input is lower Carnian (Julian) in age and corresponds to a global humid episode described as Carnian Pluvial Event (CPE) by Simms and Ruffell (1989) or Carnian Humid Episode (Ruffell et al. 2016). In the Balearic Islands it was recently recognized by López-Gómez et al. (2017), who related this event with a continental (fluvial) equivalent in the Iberian plate.

The Muschelkalk facies rocks of Minorca have to date the richest ammonoid faunas of the same interval in Spain (Virgili 1952; Llompart et al. 1987; Rodríguez-Perea et al. 1987; Goy 1995; among others), and a detailed revision has been described in Escudero-Mozo et al. (2014). This fossil content indicates a late Anisian to early Carnian age for these rocks and allows detailed correlations with other areas (Fig. 3.27).

The Majorca succession shows two carbonate ramps, late Anisian and latest Anisian to Ladinian in age, and thus has a comparable record to those of the Catalan Ranges and the central part of the Iberian Ranges (Escudero-Mozo el al. 2014), areas traditionally framed within the "Mediterranean Muschelkalk type" of López-Gómez et al. (1998).

There are very few modern studies on the Majorca Muschelkalk. Rodríguez-Perea et al. (1987) described several outcrops and compared them with well-known sections of the Catalan Coastal Ranges. Later, Álvaro et al. (1991)

subdivided this carbonate succession in four subunits that broadly considered equivalent to the Muschelkalk record of Minorca. The sections of northern Majorca (Tramuntana area) show the thickest sedimentary record of the Muschelkalk in the Balearic Islands.

In that area, the contact with the Keuper facies is transitional (Álvaro 1987). In the lower part of this latter facies it is possible to recognize the above mentioned CPE, however, in this island this event was recorded by continental sediments with intercalated volcanic rocks (López-Gómez et al. 2017). The Majorca record represents the transition from clear fluvial systems developed in E Iberia, represented by the K2 Unit defined by Ortí (1974), to a carbonate platform subaerial exposure, and pervasive karstification in Minorca during the CPE. In a later episode, represented by the K3 Unit (Ortí 1974), a marine evaporite succession expanded again westwards covering both exposed and continental areas (Fig. 3.28). Therefore, E Iberia and the Balearic Islands represented a continental-marine transition during the short, but global, CPE.

3.4.2.2 The End of the Mature Rifting Phase: The Keuper

Ortí F and Pérez-López A

The Triassic rocks in the Balearic Islands display similar Germanic facies as in the Iberian Peninsula (Rodríguez-Perea et al. 1987). However, the small dimensions of the outcrops and the complex tectonics make it difficult to characterize the Keuper facies and to correlate them with the Iberian units.

The Keuper facies consists of lutites, sandstones and evaporites of late Carnian-Norian age (Boutet et al. 1982; Escudero et al. 2014), with some intercalated volcanogenic rocks (Navidad and Álvaro 1985). In the Keuper facies of Majorca, basaltic and volcanoclastic rocks with lutitic intercalations are common (Fig. 3.25). Rodríguez-Perea et al. (1987) described a succession, almost 300 m thick, of red lutites and marls with siltstones or fined-grained sandstones and laminated gypsum beds in the upper part.

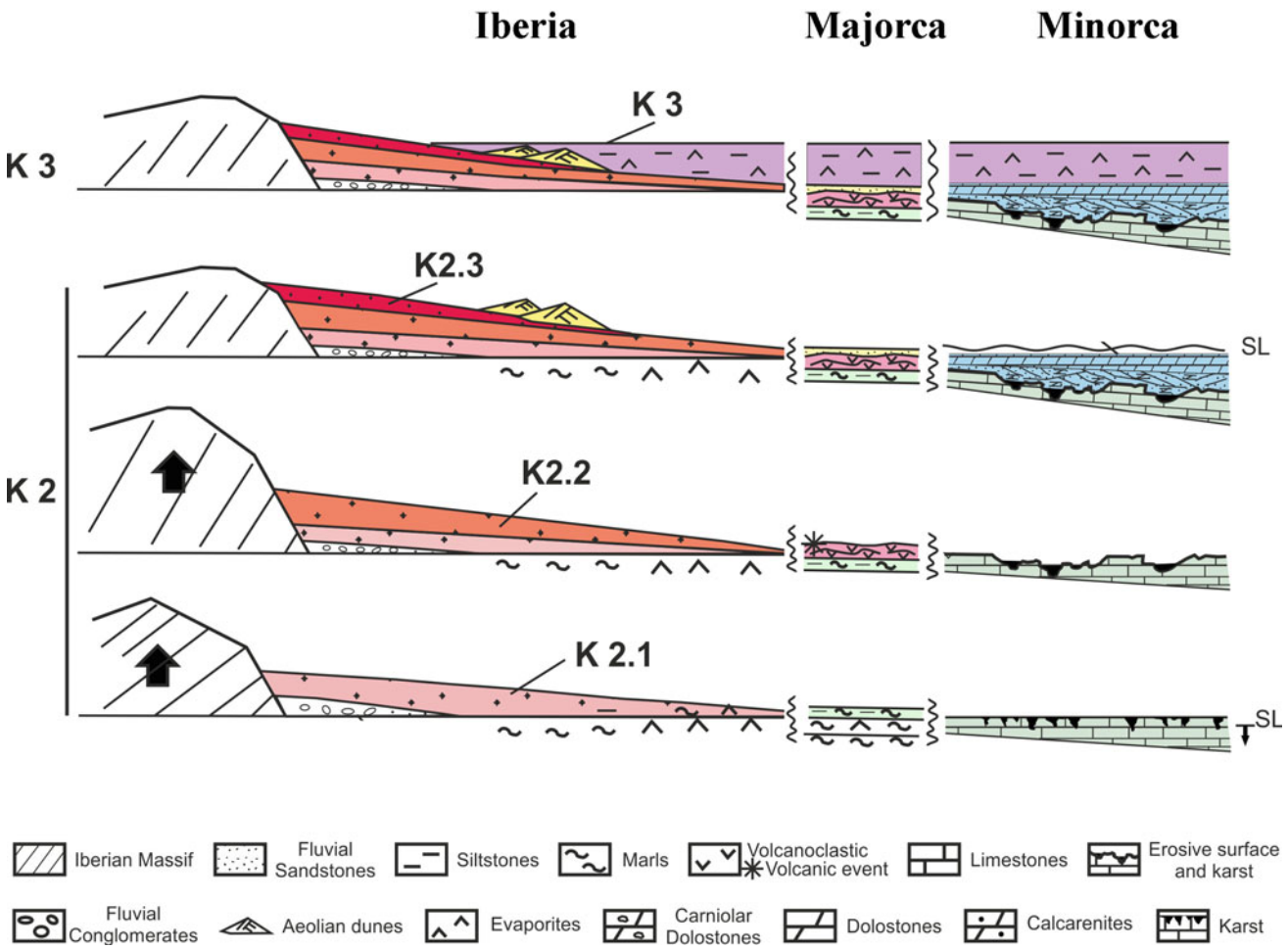

Fig. 3.28 Early Carnian (Julian) sketch of the continental-marine sedimentary record connection during the Carnian Pluvial Episode (CPE) in the Iberia, Majorca and Minorca realms. Modified from López-Gómez et al. (2017)

The Keuper facies successions of Ibiza (80 m thick) and Minorca (100 m thick) are similar, although thinner than those of Majorca. These Keuper deposits were referred as the "Upper Pelitic Unit" by Rodríguez-Perea et al. (1987) and have been interpreted as supratidal, intertidal coastal environments, shallow lagoons and continental deposits. The sedimentation of these deposits was interrupted by volcanic episodes.

3.4.3 The Triassic Alkaline Magmatism in the Balearic Islands

Lago M, Galé C and Ubide T

In the Balearic Islands, the onset of the Tethyan rift was accompanied by intraplate alkaline volcanism (Lago et al. 1996). This volcanism can be linked to magmas of similar age in the Iberian Ranges and Catalonian Coastal Ranges in Spain, and Corbières and Écrins-Pelvoux in France. Most outcrops are located in the Northern Range of Majorca (Navidad and Álvaro 1985; Rodríguez-Perea et al. 1987; Lago et al. 1996; López-Gómez et al. 2017) but isolated outcrops are also found in the islands of Minorca (Bourrouilh 1973) and Ibiza (Beausigneur and Rangheard 1968) (Fig. 3.25).

In the Northern Range of Majorca island, two Triassic magmatic units were described by Sanz et al. (2013). Most magmatic rocks belong to the main unit which consists of lava flows, pyroclastic deposits and hypovolcanic sills emplaced within Carnian-Norian sediments (Keuper facies). The lava flows and sills are alkali basalts and show fine-grained holocrystalline microporphyritic textures, defined by scarce microphenocrysts of olivine and titanium-rich augite, embedded in a doleritic groundmass composed of plagioclase, titanoaugite, olivine, titanomagnetite and accessory apatite. Ultramafic cm-sized xenoliths are common in these rocks. The xenoliths have a medium- to coarse-grained granoblastic texture composed of olivine an spinel (Lago et al. 1996; López-Gómez et al. 2017). The top of this unit includes tuff deposits linked to a general erosive event (Sanz et al. 2013). This unit shares common lithostratigraphic and compositional features with contemporary outcrops located in the NW margin of the Iberian Chain and the Catalonian Coastal Ranges and represents a pluriepisodic continental volcanism of Carnian-Norian age (Sanz et al. 2012, 2013).

The second unit comprises three hypovolcanic sills emplaced within the Felanitx Fm, at Cala Tuent. These sills show evidence of magma interaction with the host shallow marine sequence, suggesting that magma emplaced into unconsolidated sediments and therefore can be considered geologically coeval with the host rocks (e.g. Lago et al. 2012), i.e. of Norian age (Sanz et al. 2013). The composition of this unit is more evolved than the previous one, with higher contents of silica and potassium in bulk rock, and higher modal proportions of plagioclase (Navidad and Álvaro 1985). In addition, Enrique (2012) described a teschenite sill intruding the Upper Triassic limestones and there are reports of dykes of uncertain origin and age cross-cutting the Buntsandstein facies (Anisian) or even the Mal Pas Fm (Hettangian) (Sanz et al. 2013).

In Minorca Island, only one dolerite dyke has been found to intrude the Buntsandstein facies (Bourrouilh 1973). There are also irregular masses of volcanic rocks interbedded with the red siltstone levels of the Muschelkalk facies (Rosell et al. 1989). These rocks have not been studied yet and their relationship with the Triassic volcanic rocks of Majorca or Ibiza is unclear.

Finally, the Triassic magmatic rocks of Ibiza Island consist of lava flows and hypovolcanic sills emplaced within Keuper facies (Carnian-Norian). Their composition ranges between alkali basalts and andesites (Beauseigneur and Rangheard 1968) and could be equivalent to the main magmatic unit described in Majorca.

The primitive composition and alkaline affinity of the Triassic magmatism in the Balearic Islands, together with the occurrence of ultramafic xenoliths, suggest that this volcanism is related to the Triassic alkaline magmatism of the Catalonian Coastal Ranges. Furthermore, the lithostratigraphic features and age of emplacement of both magmatisms are equivalent. These similarities suggest a common origin for the magmas, related to local upwelling and melting of the asthenospheric mantle, as proposed by Lago et al. (1996 and references therein) and Sanz et al. (2012).

3.5 The Ebro Basin

Arche A, López-Gómez J, Arribas J, Vargas H, Gaspar-Escribano J, Martín-Chivelet J and Escudero-Mozo MJ

The Permian-Triassic Ebro basin was a structure located in NE Iberia (Fig. 3.29) that initiated its development during the Middle–Late (?) Permian and was completed by Triassic times (Vargas et al. 2009). In this section it is referred to as the Ebro basin and is not to be mistaken for the Cenozoic Ebro basin superimposed on the older basin as a much younger Alpine structure. This Permian-Triassic Ebro basin was bounded by Paleozoic highs along its northern margin (Pyrenean high), eastern margin (Girona-Catalan high) and southwestern margin (Ateca-Montalbán high). It was a semi-enclosed basin connected to the adjacent Iberian and South Catalonian basins via a narrow passage in its southeastern corner, in the Maestrat-Priorat region.

Nowadays, its Permian-Triassic infill only crops out along the Aragonian Branch of the Alpine Iberian Ranges, NE of the Ateca-Montalbán-Maestrat high (Fig. 3.29). It mostly lies under Cenozoic Ebro basin sediments and it is only recognized in exploratory wells and electric logs (Jurado 1989, 1990). The original configuration of the basin is now distorted by intense compressive Alpine deformation along its borders.

During the Early and Middle Triassic evolution of the Ebro basin it was not connected to the Iberian basin and sediment fluxes to these basins came from different source areas. By Late-Middle Triassic (Ladinian) times, the Girona-Catalan and Ateca-Montalbán highs were almost totally drowned by a marine transgression of the Neo-Tethys Sea and the NE and Central Iberia basins were unified (Escudero-Mozo et al. 2015).

The oldest sediments of the Ebro Basin have been located near its SE corner in the Caspe-1 exploratory well (Vargas et al. 2009) and are of Early Permian age. Coeval sediments may be present in other exploratory wells but, if this is the case, they were deposited in isolated, small basins as their counterparts in the Iberian basin (López-Gómez et al. 2002) (Fig. 3.30).

Middle-Late(?) Permian sediments are found lying unconformably on the Paleozoic basement in the central part of the Ebro basin, east of a lineament running NE–SW from Bujaraloz-1 to Sariñena-1 wells (Figs. 3.29 and 3.30). These sediments consist of conglomerates and red lutites, probably deposited in one or more narrow graben basins during an extensional period, but a differentiated Ebro basin had not yet developed. Along the Aragonian Branch of the Iberian Ranges, conglomerate bodies of limited lateral extension crop out in the troughs of an energetic paleorelief carved on the Paleozoic basement. Overlying red siltstones are missing as the result of either erosion or non-deposition. The latter branch comprises the Feliciana Fm, described by Marín (1974) in the Montalbán region, and the Araviana Fm (DS1 of Arribas 1984, 1985) in the Moncayo region, and are interpreted as proximal alluvial fan deposits.

After several periods with different duration of uplift, tilting and partial erosion in each domain of the Ebro basin (Figs. 3.29 and 3.30), continental sedimentation restarted in the SE of the basin independently of the Iberian basin to the south. The first marine transgression commenced in the middle Anisian, during the beginning of the mature rifting phase. Marine sediments consisted of two major transgression-regression cycles made of carbonate, evaporite and siltstone deposits, including the Ebro basin in the Mediterranean Triassic sedimentary record type (two carbonate levels of Anisian and Ladinian age) (Sopeña et al. 1988; Muñoz et al. 1995; López-Gómez et al. 1998; Escudero-Mozo et al. 2014). Upper Triassic (Carnian-Norian) evaporite sediments, or Keuper facies, are present only in the central part of the Ebro basin and consist of a lower interval of halite and anhydrite, a middle one of siltstones and an upper one of anhydrite (Jurado 1989, 1990).

The Ebro basin was clearly differentiated since Late Early Triassic (Olenekian) times as part of a general extension

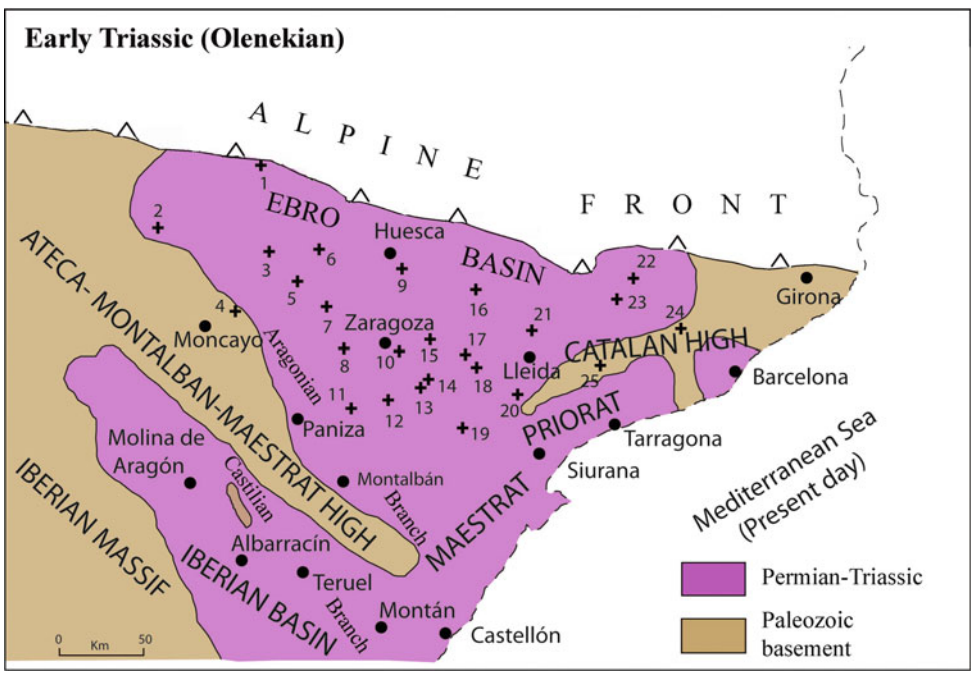

Fig. 3.29 The Ebro Basin at the Olenekian, Early Triassic. Other contiguous basins also shown. Oil wells used as control points: 1—Sanguesa-1, 2—Arnedo-1, 3—Ejea-1, 4—Magallón-1, 5—Tauste-1, 6—Valpalmas-1, 7—Zuera-1, 8—Zaragoza-1, 9–Huesca-1, 10.—Monegrillo-1, 11.—Lopín-1, 12.—La Zaida-1, 13.—Ebro-1, 14.—Bujaraloz-1, 15.—Ebro-2 16.—Monzón-1, 17.—Ballobar-1, 18.—Fraga-1, 19.—Caspe-1, 20.—Mayals-1 21.—Lérida-1, 22.—Sanahuja-1, 23.—Guisona-1., 24.—Castellfullit-1, 25.—Senant-1. Data from IGME (1987)

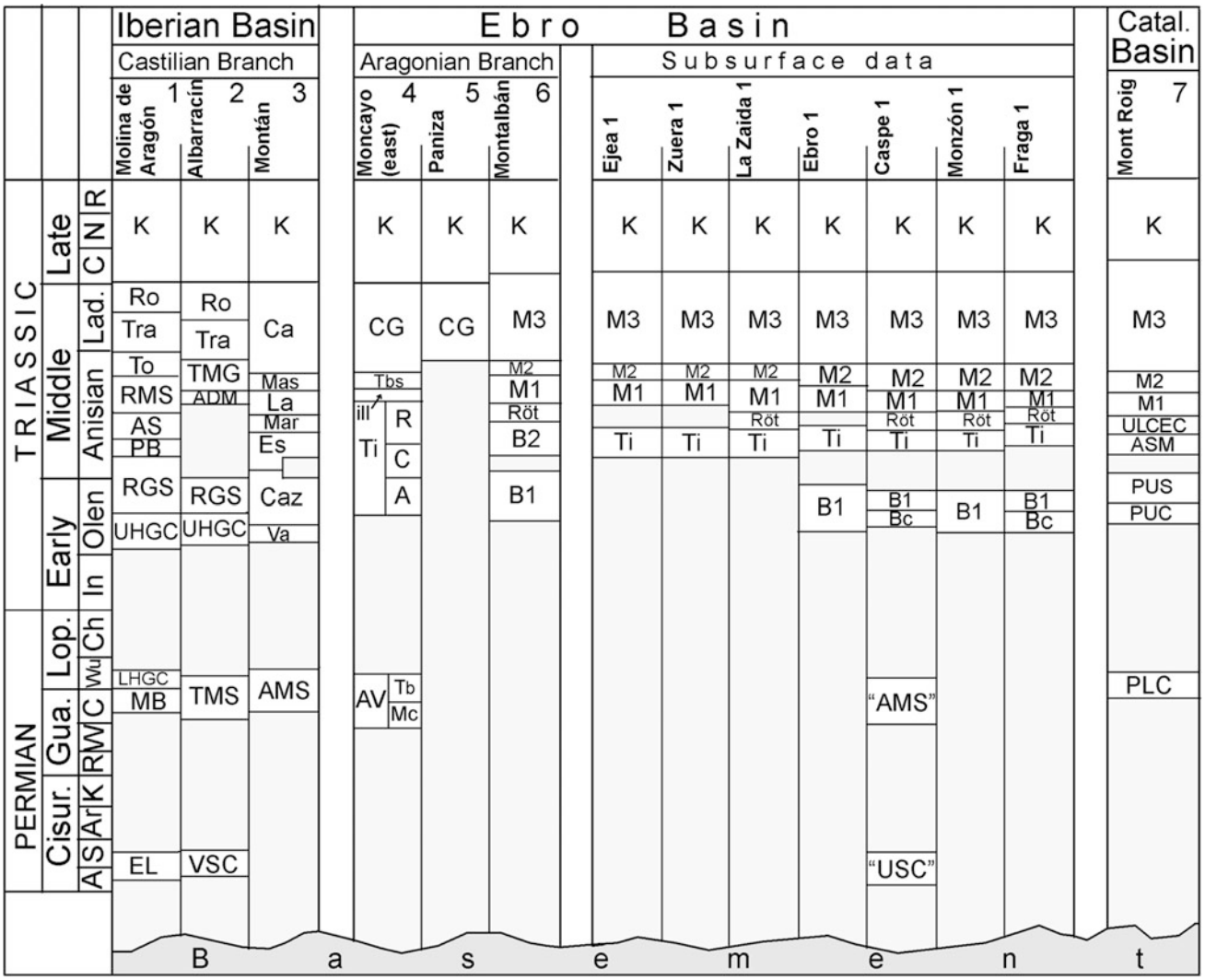

Fig. 3.30 Correlation between the lithostratigraphical units of the Iberian, Ebro and Catalan basins. Permian units: EL—Ermita Layers, LHGC—"Lower" Hoz de Gallo Conglomerates; MB—Montesoro Beds, VSC—Volcano-Sedimentary Complex, TMS—Tormón Mudstones and Sandstones, AMS—Alcotas Mudstones and Sandstones, AV—Araviana (Tb—Tabuenca, Mc—Moncayo), PLC—Lower Prades Conglomerates. Triassic Units: UHGC—"Upper" Hoz de Gallo Conglomerates, RGS—Rillo de Gallo Sandstones, PB—Prades Beds, AS—Arandilla Sandstones, RMS—Rillo Lutites and Sandstones, To—Torete Mudstones and Sandstones, Tra—Tramacastilla Dolomites, Ro—Royuela Dolomites, Marls and Limestones, Ro—Royuela Dolomites, Marls and Limestones, K—Keuper, TMG—Tramacastilla Mudstones and Gypsum, ADM—Albarracín Dolomites and Marls, Va—Valdemeca Conglomerates, Caz—Cañizar Sandstones, Es—Eslida Sandstones and Mudstones, Mar—Marines Clays, Marls and Mudstones, La—Landete Dolomites, Mas—Mas Sandstones, Marls and Gypsum, Ca—Cañete Dolomites and Limestones, Ti-Tierga Sandstones and Mudstones (Members: A—Aranda, C—Carcalejos, R-Ranné), ill—Illueca Dolomites, Tbs—Trasobares Mudstones and Marls, CG—Carbonate Group, B1—"Lower unit of the Buntsandstein", B2—"Upper unit of the Buntsandstein", M1—"Lower Muschelkalk", K2—"Middle Muschelkalk", K3—"Upper Muschelkalk", Röt—"Röt facies", PUC—Prades Upper Conglomerates, PUS—Prades Upper Sandstones, ASM—Aragall Sandstones and Mudstones, ULCEC—Upper Lutitic, Carbonatic, Evaporitic Complex. See Fig. 3.28 for their location

process in the Iberian microplate. It was a complex rift basin bounded by normal faults dipping towards the SW along its SW margin and poorly defined normal fault systems along its NE (Girona-Catalan high) and N (Pyrenean high) margins, both of them obscured by intense alpine deformation.

3.5.1 Sedimentation During the Permian-Triassic Initial Rifting Phase

Arche A, López-Gómez J, Arribas J, Vargas H and Gaspar-Escribano J

The oldest Triassic sediments in the Ebro Basin were deposited around a depocenter in its central part (Caspe-1, Ballobar-1 and Fraga-1 wells, in Figs. 3.29 and 3.30), thinning out towards the north and northwest and being absent along the Catalan high. These sediments consist of red sandstones and siltstones with complex amalgamated units of sandy braided river origin. Towards the SE corner of the basin, aeolian sediments have been identified at this level in the Montalbán region (Soria et al. 2011) and in the La Zaida-1, Caspe-1 and Monegrillo-1 wells (our interpretation) (Figs. 3.29 and 3.30). Aeolian-fluvial associations have been identified at this level in the adjacent South Catalan basin (Baix Ebre and Prades sub-basins, in Fig. 4.25) (Marzo 1986; Galán-Abellán et al. 2013) and in the SE Iberian Basin (López-Gómez et al. 2012).

A new stage of extension marked by a basal erosive surface led to the deposition of alternations of red sandstones and siltstones of fluvial origin in a basin showing differential subsidence (Vargas et al. 2009). The depocenter shifted to the north along the Pyrenean border and a secondary one developed in the Moncayo region. This cycle has been termed Tierga Fm in the Aragonian branch (DS2 of Arribas 1984, 1985) and can be correlated with the Eslida Fm of the Iberian basin (Arche and López-Gómez 1999a, b) (Figs. 3.29 and 3.30). It has been dated as Anisian according to macroflora and palynological assemblages found near the top of the formation in the Aragonian branch (Díez et al. 1996, 2007). The Tierga Fm (lateral equivalent to Eslida Fm) has been identified across the subsurface of the Cenozoic Ebro basin through electric logs of exploratory wells.

3.5.1.1 Composition and Origin of Sediments

The first depositional sequence (DS1, conglomerates and lutites of Araviana Fm) unconformably overlies an Early Paleozoic succession (mainly Cambrian) (Fig. 3.30). It is characterized by a basal conglomeratic unit that suddenly evolves to lutitic deposits with paleosols and minor sandstone levels. The following depositional sequence (DS2, Tierga Sandstones Fm) rests with an apparent conformity over the previous depositional sequence, and it is constituted mainly by a succession of coarse- to medium-grained channelized sandstones with interbedded lutitic intervals.

Composition of coarse-grained sediments (conglomerates and sandstones) drastically differs between these two sequences (Arribas 1984, 1985; Arribas et al. 2007; Ochoa et al. 2007). DS1 has a quartzolithic character, its sediments constituted by local supplies from the erosion of metasediments (Late Paleozoic). Recycled quartz grains and metasedimentary rock fragments are the main clastic components. Framework in sandstones from DS2 and successive sequences is quartzofeldespathic, with a clear dominance of monomineralic clasts (quartz plus feldspar). The amount of feldspar increases towards the top of the Permo-Triassic succession. This fact is interpreted as the consequence of new supplies from the erosion of crystalline rocks (plutonites) diluting local metamorphiclastic supplies.

The great difference in composition between DS1 and the rest of overlying DSs (Fig. 3.31) has been used to interpret DS1 as equivalent to the Upper Permian "Saxonian facies" outcropping in the Castilian branch (Arribas 1984, 1985), and representing the start of the Alpine sedimentation cycle in the Iberian Range (Arribas et al. 2007).

3.5.2 Sedimentation During the Triassic Mature Rifting Phase

Arche A, López-Gómez J, Vargas H, Martín-Chivelet J, Escudero-Mozo MJ and Gaspar-Escribano J

Continental sedimentation in the Ebro basin ended in middle Anisian times and a shallow marine-coastal sedimentary cycle (loosely termed Röt facies) started. This new cycle shows a main depocenter in the center and northern parts of the Permo-Triassic Ebro basin and a secondary one along the Aragonian branch, separated by an elongated area across the SW and NE parts of the basin, where fluvial sediments of the Tierga Fm are directly covered by the marine carbonates, or Muschelkalk facies, as in wells Zuera-1, Senant-1, Guisona-1, Sanahuja-1 Castelfullit-1, La Zaida-1 and Lopín-1 (Figs. 3.29 and 3.30). In the Aragonian branch this sedimentary record has been termed Cálcena Fm (Arribas 1984, 1985) and can be correlated with the Marines Fm of the Iberian Ranges (López-Gómez and Arche 1992) and the Upper Lutitic-Evaporitic complex of Marzo (1980), or Boundary clays of Virgili (1958), both in the Southern Catalan basin. Siltstones and variegated clays are found in the Aragonian branch depocenter while anhydrite, halite and red clays dominate the more subsiding central-northern Ebro basin depocenter.

Above these shallow marine deposits, during the beginning of the Pelsonian (middle Anisian), a definitive westward transgression of the Tethys sea covered the Ebro basin following wide corridors linked with the open sea across the central-south Catalan basin (Fig. 3.22). It was represented by carbonates of shallow marine ramps, so-called M-1 Unit

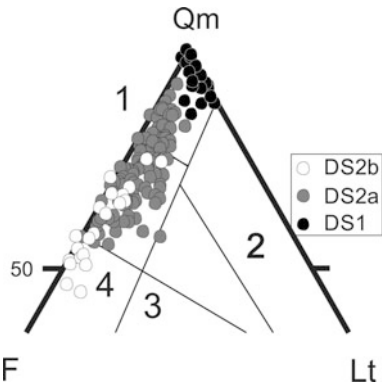

Fig. 3.31 Sandstone composition petrofacies from Permo-Triassic deposits in the Aragonese branch of the Iberian Ranges. DS1: Araviana Conglomerates and Silstones Fm; DS2a: Lower part of Tierga Sandstones Fm; DS2b: Upper part of Tierga Sandstones Fm. Fields defined by Dickinson (1985): 1—Stable Craton; 2—Recycled Orogen; 3—Magmatic Arc; 4—Basement Uplift. Qm: monocrystalline quartz; F: feldspars; Lt: lithic fragments

or lower Muschelkalk facies in the Catalan basin (Virgili 1958; Calvet and Marzo 1994). Present-day outcrops of this Middle Triassic marine episode in the Ebro basin are only located in the southernmost area of the basin, in the NE of the Aragonian branch (Fig. 3.29). This carbonate unit and the undelying Röt facies would constitute the first transgressive-regressive cycle (T.R.-1) defined by Escudero-Mozo et al. (2015) in neighbour basins. After a progressive retreat of the Tethys Sea and the incoming of continental fluxes in the western areas of the basin, represented by the so-called middle Muschelkalk (lutites, carbonates and evaporitic facies), a new transgression of the Tethys Sea began at the end of the Illyrian. The new record of carbonate sediments is probably related with a general re-configuration of the Tethys Sea with an important propagation of the Neotethys due to the sudden northward displacement of Cimmeria (cf. Escudero-Mozo et al. 2014) (Fig. 3.22). Those carbonates are represented by the upper Muschelkalk or M-3 Unit. An abrupt and intense relative sea-level rise that occurred during the Anisian-Ladinian transition caused partial drowning of the carbonate ramps and led to deposition of the deepest facies (outer ramp) of the Middle Triassic in the basin. After this episode, carbonate production was recovered and the evolution of the carbonate ramps continued, within a slow and multi-episodic shallowing-up trend, until the Ladinian to Carnian transition, when carbonate deposition was replaced, after about 5.5 my by the mainly evaporitic sedimentation of the Keuper facies (Fig. 3.15). The upper limit of the second transgressive-regressive cycle (T.R.-2) can be located above this drastic sedimentological change (Escudero-Mozo et al. 2015). Those evaporitic marine conditions dominated sedimentation during the rest of the Carnian and the Norian (Keuper facies).

3.6 The Iberian Basin

De La Horra R, López-Gómez J, Arche A, Barrenechea J, Borruel-Abadía V, Galán-Abellán B, Sopeña A, Sánchez-Moya Y, Vargas H, Escudero-Mozo MJ, Martín-Chivelet J, Ortí F, Pérez-López A, Lago M, Galé C, Ubide T, Luque J, Alonso-Azcárate J, Márquez-Aliaga A, Goy A, Márquez L and Gaspar-Escribano J

The present-day Iberian Chain is a wide zone of intraplate deformation that records the tectonic inversion produced during the Pyrenean orogeny of the basins previously developed during the initial Alpine cycle extensional phase (Arche and López-Gómez 1996; Salas et al. 2001; Sopeña and Sánchez-Moya 2004; de Vicente et al. 2009). This Permian-Mesozoic extensional regime is generally associated with the break-up of Pangea and the multiphase destruction of the Variscan orogen. As a result, the Iberian basin evolution is deeply influenced by the pre-extension structure inherited from the late Variscan orogeny (Sopeña et al. 1988; Vargas et al. 2009; de Vicente et al. 2009).

3.6.1 Tectonics and Sedimentation During the Beginning of the Basin

De La Horra R, Arche A, López-Gómez J, Sopeña A, Sánchez-Moya Y, Barrenechea JF, Galán-Abellán B, Borruel-Abadía V and Vargas H

Many aspects of the geodynamic situation of the Variscan orogen during the Carboniferous and its transition to the Permian are still controversial and out of the scope of this chapter. Still under debate are the origin and evolution of the Ibero-Armorican orocline (Martínez-Catalán et al. 2007; Gutiérrez-Alonso et al. 2008a, b), the identification of the intra-Pangea shear zone separating Gondwana from Laurasia that could explain a Pangea B configuration (Weil et al. 2001; Muttoni et al. 2009; Domeier et al. 2012; Aubele et al. 2012), and the nature of the transition between the end of the Variscan orogeny and the beginning of the extension that later produced the break-up of Pangea (López-Gómez et al. 2002; Sopeña and Sánchez-Moya 2004; Franke 2006; Wagner and Álvarez 2010).

More widely investigated and accepted is the evolution of the Iberian basin, which can be explained by two major rifting cycles followed by post-rift periods of thermal subsidence (Sopeña et al. 1988; Arche and López Gómez 1996; Van Wees et al. 1998; Vargas et al. 2009). The first main rift cycle took place from the Early Permian to the Middle Triassic (Sopeña and Sánchez-Moya 1997; Vargas et al. 2009). The second main cycle spanned the Late Jurassic to

Early Cretaceous and has been linked to the separation of Africa from Europe and the simultaneous anticlockwise rotation of the Iberian Plate (Sánchez Moya and Sopeña 2004; Rosenbaum et al. 2002). We will focus here on the first of the main rift cycles which, based on the age of the sedimentary filling, tectonic setting and geometries of the basins, magmatic manifestations and sedimentologic characteristics, has been subdivided into three tecto-sedimentary phases: (A) Latest Carboniferous to Early Permian, (B) Middle-Late Permian, and (C) Lower to Middle Triassic (Fig. 3.32).

3.6.1.1 Latest Carboniferous-Early Permian

It is most widely accepted that a regime of oblique collision between Gondwana and Laurasia during the Late Paleozoic was responsible for the Variscan orogeny, dominated by dextral transpression (Arthaud and Matte 1977; Martínez-Catalán et al. 2007). This situation produced the westward displacement of Gondwana relative to Laurussia and favored the opening of the Paleotethys (Ziegler 1988a, b; Stampfli et al. 2001; Franke 2006; Martínez Catalán et al. 2007). Such transpressional conditions persisted during the last stages of the Carboniferous and until the Sakmarian

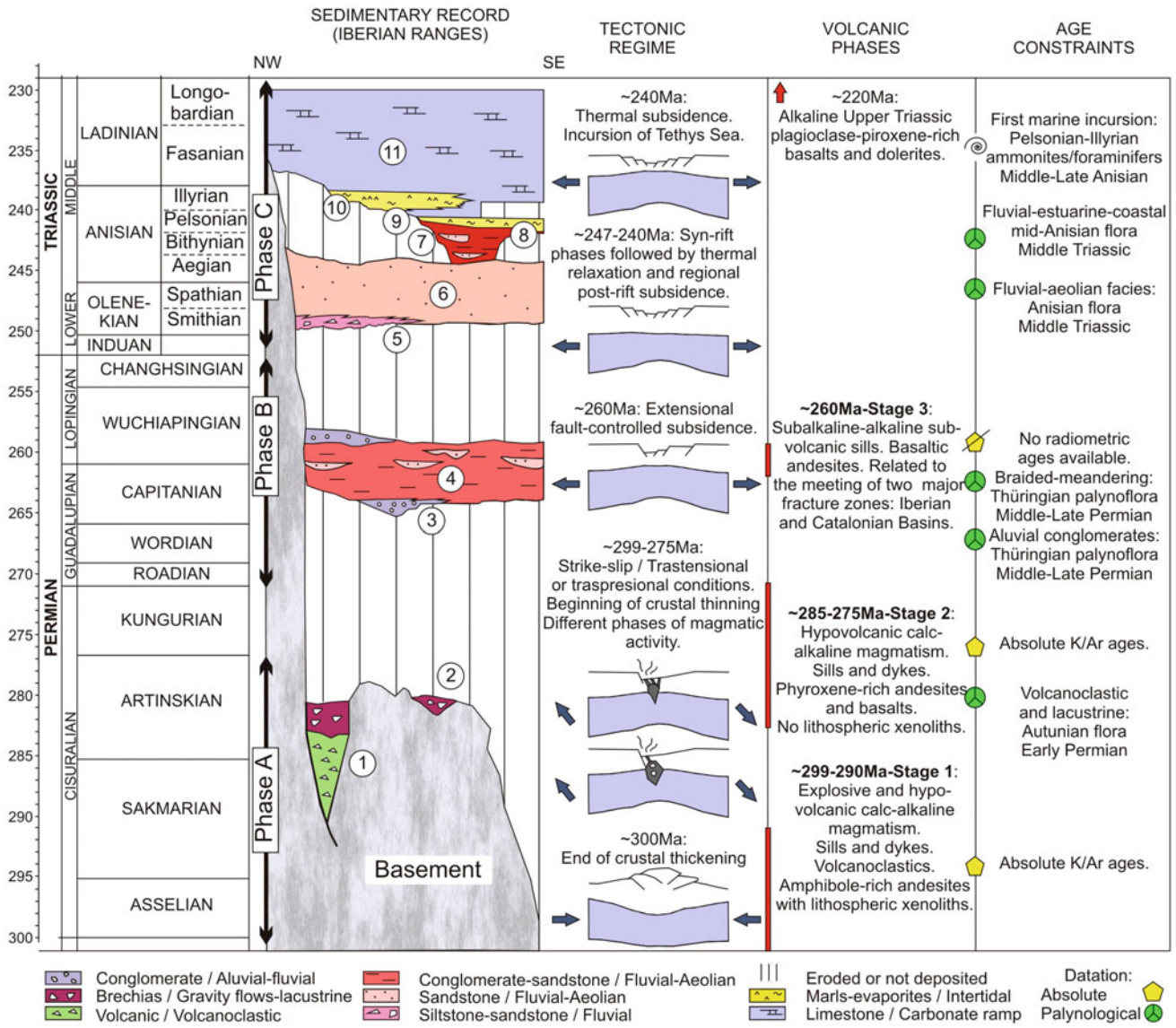

Fig. 3.32 Permian-Triassic sedimentary record at the beginning of the break-up of Pangea. Igneous activity, age constrains, and inferred tectonic regimes are also included. See text for references and Fig. 3.33 for a paleogeographical interpretation of each tectosedimentary phase. Units: (1) Andesites of Cañamares, Volcanic-volcanoclastic complex of Pálmaces, Ermita Fm, (2) Pálmaces sandstones Fm, Pálmaces mudstones Fm, Retiendas sandstones Fm, Tabarreña breccias Fm, (3) Boniches conglomerates Fm, (4) Alcotas and Montesoro siltstones Fms, Noviales Mudstones, Sandstones and Conglomerates Fm, Hoz del Gallo Conglomerates Fm, (5) Chequilla and Valdemeca units, (6) Cañizar and Rillo de Gallo Fms, (7) Cercadillo, Arandilla, and Eslida Fms, (8) Marines Fm, (9) Albarracín and Landete Fms, (10) Torete Siltstones Fm, El Mas Fm, (11) Cañete, Tramacastilla, and Royuela Fms

(Lower Permian) in northwestern areas of Iberia. In this region, a compressive NNE–SSW paleostress field has been inferred from paleomagnetic data (Weil et al. 2001; Domeier et al. 2012). However, for the Iberian Ranges, there are still doubts about when the change occurred from the compressive tectonic regime inherited from the Variscan orogeny to the extensional Alpine rifting that subsequently gave rise to the Iberian basin. Some authors still relate the latest Carboniferous-Early Permian stage to the end of the Variscan cycle representing the collapse of the Variscan orogen (Doblas et al. 1994; Capote et al. 2002). According to others, instead, the basins created during this period are best assigned to the beginning of an Alpine cycle of extensional tectonics (López-Gómez et al. 2002). The present-day configuration of these basins and the lack of precision in age assignation based on its paleontological record make it difficult to resolve these controversies. The small basin of Henarejos is a good example of this dilemma (Sopeña and Sánchez-Moya 2004; Arche et al. 2007; Wagner and Álvarez 2010). Certainly, the Late Carboniferous-Permian transition needs re-assessment through new structural and paleontological reviews. This section offers an overview of the main features of the basins created during this period.

In the Iberian Range area, continental deposits lying unconformably on the folded Variscan basement filled-up isolated and small basins preferentially preserved at the SE margin of the Central System and in the northwestern and central areas of the Castilian and Aragonese branches (Fig. 3.33). These new basins were small (2–10 km long), sometimes rhomb-shaped, and bounded by deep normal faults. Their continental sedimentary record is variable, sometimes thick (more than 1000 m), and highly heterogeneous, including slope breccias, alluvial fan, fluvial and lacustrine deposits.

The age of these deposits has been established as Autunian (Early Permian) in some basins based on conchostraca and macro- and microflora data (Sopeña et al. 1977; Wagner et al. 1985; Broutin et al. 1999). Most important is the

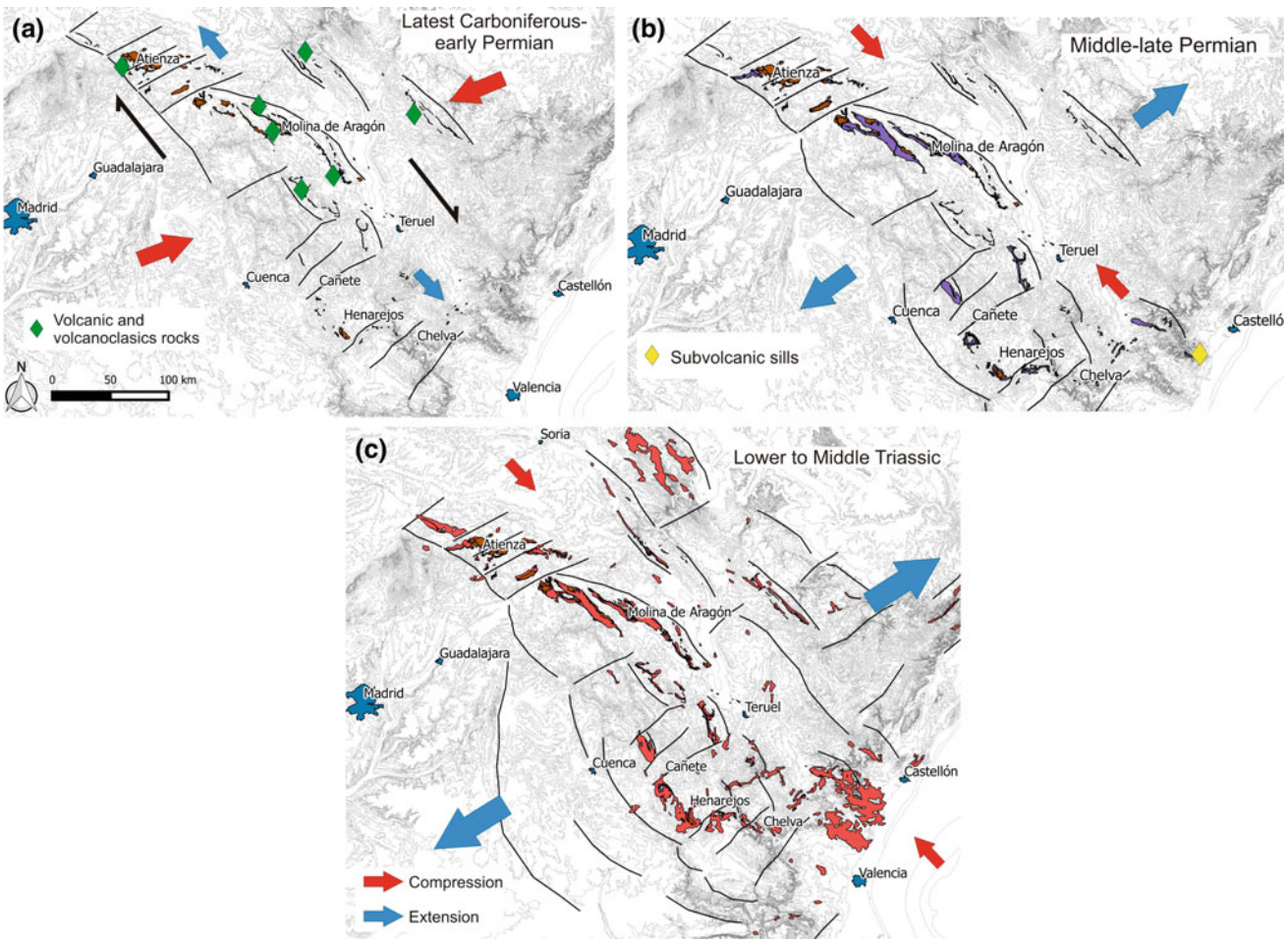

Fig. 3.33 Tectosedimentary evolution of the Iberian basin in **a** latest Carboniferous-Early Permian phase, **b** Middle-Late Permian phase, and **c** Lower to Middle Triassic phase. Probable geometries of the fault systems and stress regime are interpreted. Present-day outcrops for each phase are colored in brown (**a**), purple (**b**), and orange (**c**)

presence of an extensive record of short-lived volcanic episodes that produced thick andesitic lava flows and pyroclastic rocks. Absolute ages of these deposits indicate a maximum age interval of 299–275 Ma (Lago et al. 2005). Such calc-alkaline volcanism dated as Stephanian-Early Permian shows two stages: (i) a first stage whose hypovolcanic magmatism and explosive eruptions are characterized by amphibolic andesites incorporating deep crust xenoliths and indicating existence of crustal-scale faults (Lago et al. 2005); and (ii) a second stage represented by the intrusion of sills and dykes of a more basic composition (pyroxenic andesites and basalts) and a minor presence of xenoliths (Fig. 3.32).

The geographically aligned basins (Fig. 3.33), their geometric characteristics, intense subsidence, deep border faults, and type of volcanism, likely point to a relationship with strike-slip tectonics closely linked to the crustal roots of the Variscan orogen (López-Gómez et al. 2002; Sopeña and Sánchez-Moya 2004). Pull-apart basins at releasing bends are the best tectonic configuration to explain these features (de Vicente et al. 2009). A still open question is whether these basins were created under a regional transpressional or transtensional regime. However, if we consider paleomagnetic indicators, oblique transpressional conditions are not to be discarded definitely (Weil et al. 2001).

3.6.1.2 Middle-Late Permian

A marked change in tectonic regime is observed in the Middle-Late Permian interval. Under a clear extensional regime, larger basins related to normal faults and half-graben geometries accommodated continental deposits (Arche and López-Gómez 1996; Vargas et al. 2009; López-Gómez et al. 2002; Sopeña and Sánchez-Moya 2004). The vertical development of this infill in most of the basins starts with transverse alluvial fans and ends with fluvial systems developed into extensive floodplains with intercalated lacustrine environments (Sopeña et al. 1988; López-Gómez et al. 2002). Lying unconformably on the Variscan basement or, locally, on Early Permian rocks, alluvial fan deposits are composed of clast-supported conglomerates of mainly well-rounded, quartzite clasts that transitionally change to red mudstones and siltstones, with intercalated red to pink sandstones beds, conglomerate lenses, and paleosol levels, in a sandy or mixed braided and meandering fluvial system developed on wide floodplains (Arche and López-Gómez 2005; De la Horra et al. 2008, 2012).

The age of this stage was established through palynological assemblages as Thüringian (Doubinger et al. 1990; Sopeña et al. 1995; De la Horra et al. 2012). This imprecise time unit can be broadly correlated with the Capitanian (Middle Permian) and Wuchiapingian (Late Permian). Magmatic manifestations are practically absent. Only some intercalated sills of basaltic andesites have been described in the southeastern area (Fig. 3.33). Due to their alteration, radiometric dating of the sills has not been possible but a Middle-Late Permian age has been inferred. Further, field data suggest that emplacement took place shortly after sedimentation of the continental deposits and the geochemical affinity of the sills is similar to that of other Middle-Late Permian magmatism rocks in the western Tethys, e.g. those from the Pyrenees (Lago et al. 2012).

A widespread extensional regime of this period is clear. Middle-Late Permian deposits are geographically distributed throughout the Iberian basin, which at that moment was subdivided by SW–NE alignments into sub-basins, 25–65 km long, controlled by NW–SE fault systems. These merge laterally, show arcuate geometries (Fig. 3.33), and have been interpreted as listric boundary faults controlling asymmetric half-graben (Arche and López-Gómez 1996).

As in all western and central European basins, Permian and Triassic rocks are clearly separated by a sedimentary hiatus that corresponds at least to the late Lopingian, and probably lasted until Olenekian times (Bourquin et al. 2007). In the Iberian basin, this hiatus is represented by an angular unconformity.

3.6.1.3 Early to Middle Triassic

The Triassic rocks of the Iberian Basin contain the three facies broadly corresponding to the three Germanic type units: Buntsandstein, Muschelkalk and Keuper. However, these divisions lack chronostratigraphic value. Here, we focus on the Buntsandstein facies, represented by siliciclastic units of continental origin. These units have been extensively investigated since the 1970s and classified into formation categories according to lithostratigraphic criteria (see reviews by Sopeña et al. 1988; López-Gómez et al. 2002; Sopeña and Sánchez-Moya 2004; Arche and López-Gómez 2006).

During this phase, the extensional development of the rift is indicated by widespread NW–SE faults that have been interpreted as listric boundary faults controlling the hangingwall geometry and sedimentation type. In selected areas, field mapping reveals well developed listric basin-boundary faults and complex synthetic and antithetic rollover structures (Arche and López-Gómez 1996; Sopeña and Sánchez-Moya 1997). A similar situation may be observed in the present-day rifts of East Africa, with half-graben infilled by deposits of fluvial systems, lakes, and alluvial fans (Ebinger 1989). Examples of these boundary faults are the Somolinos fault and the Serranía de Cuenca fault (Sopeña and Sánchez-Moya 1997; Arche and López-Gómez 1996; de Vicente et al. 2009).

At the base of the Triassic sequences it is common to find sandy, matrix- and clast-supported, subrounded to subangular quartzite conglomerates and interbedded sandstones (Ramos 1979). In the different sub-basins, the base of these deposits shows a drainage system crosswise to the basin

margin with a rather radial pattern. However, at the top, paleocurrents parallel the basin axis and point SE. These continental deposits were initially interpreted as alluvial fans and gravelly braided fluvial systems (Ramos 1979). However, it is important to note the presence of sandstone beds of very well-rounded grains and isolated ventifacts that, along with other sedimentological evidence, has been related to markedly arid climate conditions contrasting with the seasonal and humid climate of the previous stage (Bourquin et al. 2007; De la Horra et al. 2011; López-Gómez et al. 2012; Borruel-Abadía et al. 2015). In the absence of direct age data, their stratigraphic location points to the lower Olenekian (Lower Triassic), a time of arid climate conditions at the scale of western Europe.

On top of the basal conglomerates, a sandy unit is most representative of the continental Triassic in the Iberian basin due to its spectacular outcrops. Although its name changes from one geographic area to another (Rillo de Gallo Fm, Cañizar Fm) its basic sedimentary features are consistent and allow lithostratigraphic correlations (López-Gómez et al. 2012). These rocks lie unconformably on the Variscan basement and on Permian rocks, or otherwise conformably on the conglomerate deposits. Thickness ranges from 80 to 140 m and is mainly composed of red sandstones (subarkoses) of different grain size, and scarce subrounded quartzite clasts. The rocks have been interpreted as deposited by sandy braided fluvial systems showing punctate aeolian reworking (López-Gómez et al. 2012). However, at the SW Ebro basin margin (Montalbán area), most deposits are of aeolian origin (Soria et al. 2011). In the SE Iberian basin, a pollen and spore assemblage recovered from the top of this succession suggests an early Anisian age (Doubinger et al. 1990). Thus, most of the unit may be assigned to the Late Olenekian although the age is considered Late Smithian by López-Gómez et al. (2012). As reported in earlier studies, lateral facies changes between units indicating different lithologies and environments are a common feature in the Iberian Basin (Sopeña et al. 1988).

Transitionally on top of these sandy units there are other continental deposits which, again, have been given as different formation names (e.g. Arandilla Fm, Cercadillo Fm, Eslida Fm) depending on their geographical location (Arche and López-Gómez 2006; López-Gómez et al 2002). In contrast with the older sandy units, these rocks consist of alternating red sandstones and thick beds of siltstones. The sandstones are fine- to coarse-grained arkoses and subarkoses (Alonso-Azcárate et al. 1997). Siltstones contain insects, abundant bioturbation, root prints and paleosols, vertebrate footprints and plant remains (Béthoux et al. 2009; Gand et al. 2010; Borruel-Abadía et al. 2014). Formation thickness ranges from a few meters to >600 m in different depocenters. These rocks have been interpreted as sandy braided and meandering fluvial systems crossing wide floodplains with small lakes and ponds (Ramos 1979; Arche and López-Gómez 1999a, b). At the SW Ebro basin margin (Montalbán area), some sequences show aeolian deposits. Plant remains and vertebrate footprints point to an Anisian age but a mid-Anisian palynological association has recently offered a precise datation (Juncal et al. 2016a, b).

Semigraben compartmentalization of the Iberian basin is indicated by generalized subsidence of Early to Middle Triassic stage sub-basins, the widening of their sedimentation areas, their variable thicknesses, the asymmetric shape of isopac maps, and their geometric characteristics (Van Wees et al. 1998; Sopeña and Sánchez-Moya 2004; Vargas et al. 2009). Under conditions of simple-shear extension, active extension prograded away from the original boundary faults and younger continental units were deposited away from the center of the basin (Vargas et al. 2009). The combination of dextral E–W shear with main NW–SE faults produced a main ENE–WSW stretching (García-Lasanta et al. 2015). At the end of this stage, branches of previous rift systems became finally connected (e.g., Catalan, Ebro and Iberian basins) allowing fauna migrations along thousands of km across the European plate. The stage of maximum widening of the rift basins, or mature stage of rifting, started with the incursion of the Tethys Sea in the Iberian basin (Escudero-Mozo et al. 2014).

The evolution of the first rifting cycle until the first marine incursion can be summarized by the following tectono-sedimentary features: (i) short-duration syn-rift stages between long hiatuses in the sedimentary record; (ii) an Early Permian initial stage of late Variscan strike-slip faults reactivation characterized by small basins (±10 km), rapid subsidence, and volcanism of calc-alkaline affinity; (iii) a Middle-late Permian stage of lateral extension and alluvial to fluvial sedimentation in medium-sized basins (±25–65 km) with very local volcanism of alkaline affinity; (iv) a Late Early to Middle Triassic extensional phase of diachronic filling of fluvial-aeolian deposits in larger basins of different rift systems that became finally interconnected; and (v) a post-rift stage of rapid Middle Triassic marine transgression of the Tethys sea following corridors between the still elevated areas.

3.6.2 Middle–Late Triassic Mature Rifting Phase in the Iberian Basin

Escudero-Mozo MJ, Martín-Chivelet J, López-Gómez J, Arche A, Pérez-López A, Ortí F, Márquez-Aliaga A, Goy A and Márquez L

The mature rifting phase in the Iberian basin started during the Anisian (Middle Triassic) and prolonged until almost the end of the Late Triassic. This phase was characterized by an

enlargement of the sedimentation area due to the beginning of subsidence of the rift flanks (Van Wees et al. 1998). Therefore, this mature phase was affected by the onset of thermal subsidence, but still under the tectonic control of the main faults (Arche and López-Gómez 1996). It was basically represented by the westward marine transgression of the Tethys affecting the eastern half of the Iberian plate. As a result, a succession of carbonate deposits, or Muschelkalk facies, was recorded in this area until the end of the Middle Triassic, when a generalized and prolonged regressive event allowed Keuper facies deposition. This event extended until the beginning of the postrift stage at the end of the Triassic, when dynamics of the basin started to be controlled by thermal subsidence (Vargas et al. 2009).

3.6.2.1 The Middle Triassic Carbonate Ramps (Muschelklak) in the Iberian Basin

Escudero-Mozo MJ, Martín-Chivelet J, López-Gómez J, Arche A, Márquez-Aliaga A, Goy A, Márquez L, Plasencia P and Sánchez-Fernández D

The middle Anisian to early Carnian time interval in the Iberian basin was characterized by the installation of extensive shallow marine settings in response to the combined effect of a generalized regional subsidence and a sea level-rise. The high relative sea-level together with the climatic conditions favoured the development of shallow marine settings with carbonate deposition, for which carbonate microbial production had a very significant role. That accumulation of carbonate deposits conforms the Muschelkalk facies which, in the SE Iberian basin, is represented by two carbonate units, the Landete Fm and the Cañete Fm (López-Gómez et al. 1993), middle-upper Anisian and upper Anisian–Ladinian in age, respectively (Escudero Mozo et al. 2015, Fig. 3.34). These two units are stratigraphically separated by a mixed siliciclastic-evaporite unit (Mas Fm of López-Gómez et al. 1993). Abundant stratigraphic and sedimentological work on these units has allowed reaching the current knowledge of these units (e.g. Pérez-Arlucea and Sopeña 1985; Arribas 1985; Arche and López-Gómez 1996; Sopeña et al. 1988; Sopeña and Sánchez-Moya 2004; García-Gil 1990; Pérez-Arlucea 1992; López-Gómez et al. 1993, 1998; Escudero-Mozo et al. 2015). These units, together with the uppermost part of the Buntsandstein facies and the lower part of the Keuper facies, represent two major transgressive-regressive cycles (in the sense of Escudero-Mozo et al. 2015), each of them defined by the installation, development and demise of a vast carbonate ramp.

The first carbonate ramp (Landete Fm) developed in the central part of the Iberian basin (Fig. 3.34). It reaches a thickness of 60 m and pinched out towards the basin margins. It mainly consists of shoal calcarenite facies, subtidal bioturbated muds and peritidal microbial facies, all affected by an intense and pervasive dolomitisation. The marine transgression was rapid and from the NE through a narrow NE–SW corridor across the Catalan and Ebro basins (Escudero-Mozo et al. 2015) (Fig. 3.22). The marine carbonates onlap over older units including different Buntsandstein units (Fig. 3.34). The exception is the northern basin areas, where a transitional lower contact exists over the Buntsandstein facies, defined by a mixed lutite-evaporite-carbonate unit (Röt facies). The carbonate ramp recorded two depositional sequences (Escudero-Mozo et al. 2015) until the late Anisian (Illyrian), when a rapid regressive episode determined its demise and replacement by continental to coastal settings with siliciclastic and evaporitic sedimentation, these represented in the lower part of the Mas Fm (Fig. 3.34).

The second carbonate ramp, represented by the Cañete Fm (Figs. 3.34 and 3.35), consists of severely dolomitised carbonate deposits, including outer, middle and inner ramp (lagoon to tidal flat) facies (López-Gómez et al. 1993, 1998; Escudero-Mozo et al. 2014, 2015). The initiation of the ramp resulted from a new generalized transgression that started in the late Anisian. It was more extensive than the former, covering all the areas of the previous ramp but also others that had prevailed emerged until now, and onlaps on older units reaching the Paleozoic basement westward of the basin (López-Gómez et al. 1998). Interestingly, this transgressive pulse derived during the Anisian-Ladinian transition in an abrupt deepening event, which caused local drowning and widespread deposition of open marine (middle to outer ramp) facies. After this rapid relative sea-level rise, a much slower and progressive shallowing episode took place. This trend lasted more than 4 my and was punctuated by two additional transgressive pulses, which allow defining three successive depositional sequences (Figs. 3.34 and 3.35). Carbonate deposition finished with the demise of the carbonate ramp and gradual but rapid change into the hypersaline conditions that led to Keuper facies deposition, starting at the Ladinian-Carnian transition. The evolution of this ramp has been related to the progressive opening of the Neotethys and the paleogeographic changes that occurred in the western Tethys domain during the late Anisian to early Carnian interval (Escudero-Mozo et al. 2015). The integration of biostratigraphical studies, which allowed to recognize the *Eoprotrachyceras curionni, E.vilanovai* and *E. hispanicum* biozones (Goy 1995; Escudero-Mozo et al. 2015), and sequence stratigraphy, lead to precise inter-basinal correlations between the Iberian Ranges, Catalan Coastal Ranges and Minorca (Escudero-Mozo et al. 2014, 2015) (Fig. 3.34).

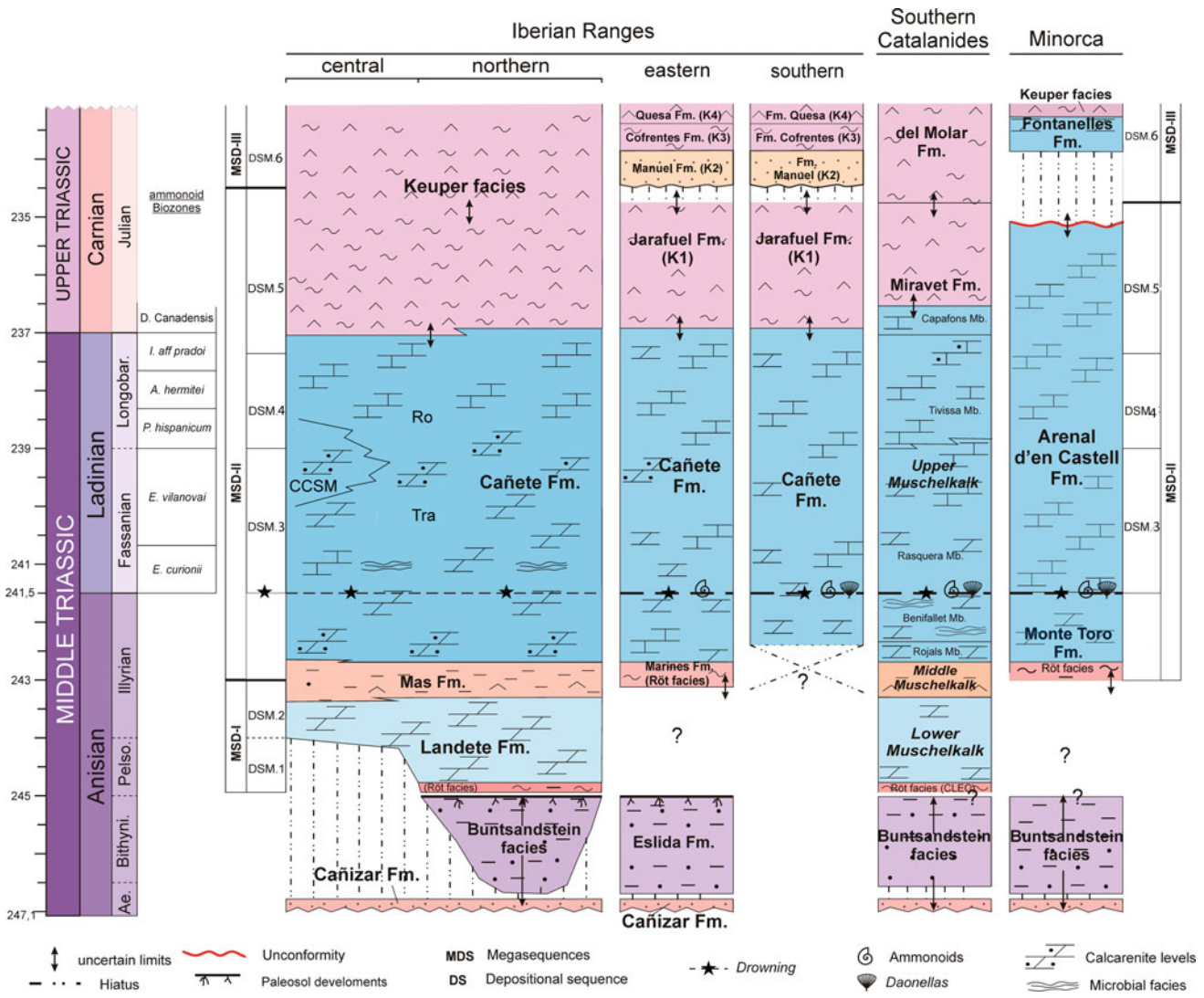

Fig. 3.34 Depositional sequences of the Muschelkalk facies sedimentary record and the Iberian basin and the Catalan and Minorca basins. Modified from Escudero-Mozo et al. (2015). Laterally equivalent units: Ro—Royuela Dolomites, Marls and Limestones, Tra—Tramacastilla Dolomites and Marls (Pérez-Arlucea 1992); CCSM—Cuesta del Castillo Sandstones and Mudstones (García-Gil 1990)

3.6.2.2 Evolution of the Keuper Evaporites

Ortí F and Pérez-López A

The SE domain of the Iberian microplate records the most complete succession of Keuper facies sedimentation and is taken here as reference for the successions in the other basins (Fig. 3.13). The Keuper facies in eastern Iberia belong to two 3rd-order depositional sequences. The most commonly accepted arrangement of units in these sequences is that of Pérez-López (1996): the older sequence is formed by the lower Keuper (K1 unit) and the younger sequence is formed by the assemblage of the other Keuper units (K2, K3, K4, K5 units) and also by the base of the dolomitic, shallow marine Imón Fm, of late Norian age (Fig. 3.14), already considered to mark the beginning of the postrift stage. A different unit arrangement was assumed by Suárez (2007), to whom the older sequence is formed by the K1, K2 and K3 units, and the younger one is comprised of the K4 and K5 units and the Imón Fm at the top.

The lower Keuper unit (K1 unit in the Iberian basin and the equivalent units in the other basins) represents a mosaic of shallow-water chloride ponds and sulfate salinas irregularly distributed in an evaporitic mudflat. The predominant host sediment in this evaporitic mudflat was grey claystone.

The middle Keuper units (K2 and K3 units in the basins surrounding the Iberian Massif) represent a fluvial, siliciclastic intercalation in the platform, which interrupted evaporite sedimentation. The paleoclimatic meaning of the siliciclastic episode represented by the K2 unit, of middle Carnian age, has been explained by Arche and López-Gómez (2014) as a short-lived (>1 Ma) humid event, the

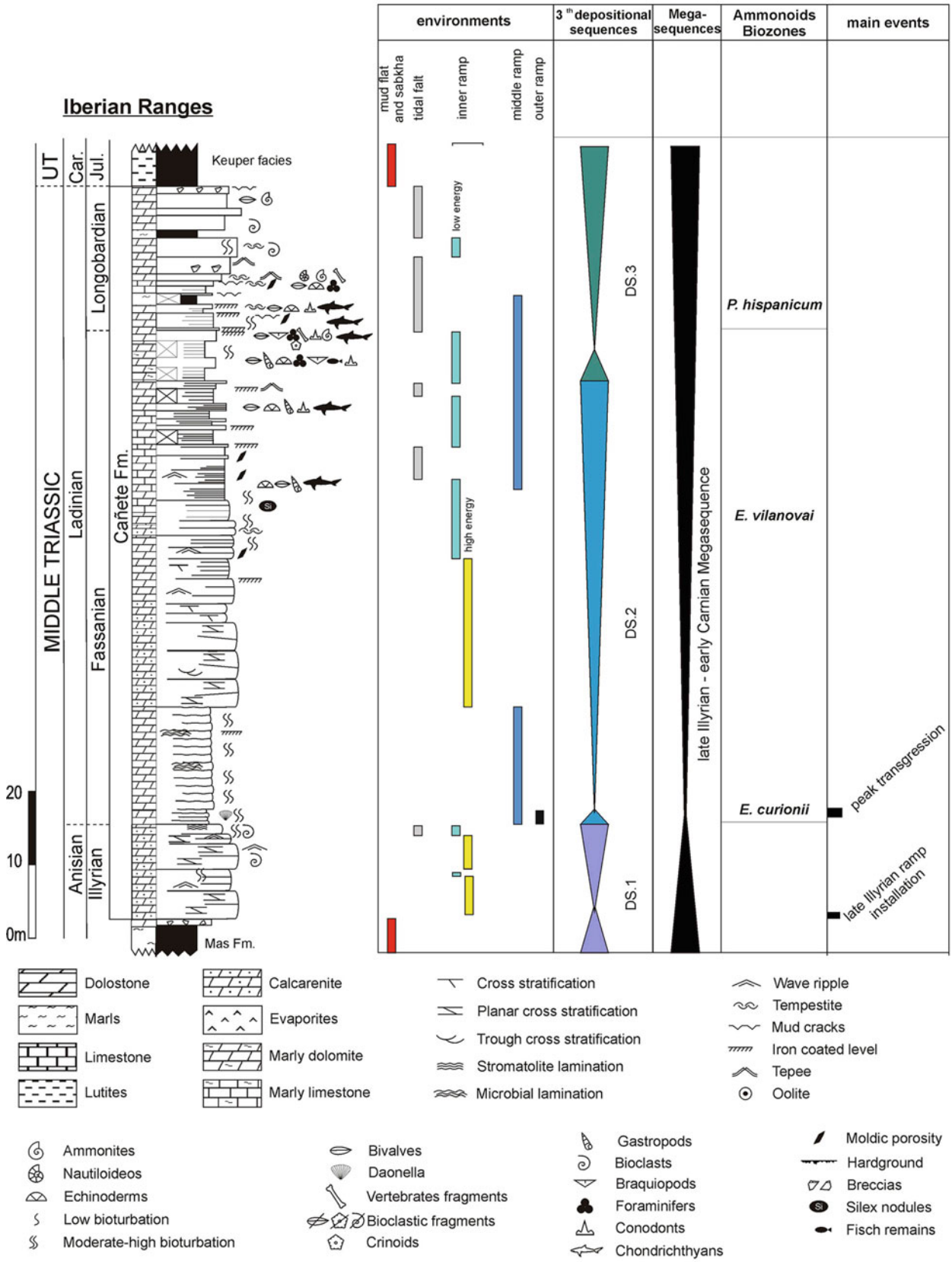

Fig. 3.35 Sequence stratigraphy of the Middle Triassic carbonate succession (Muschelkalk facies) in the Iberian Ranges. Modified from Escudero-Mozo et al. (2014)

"Carnian Pluvial Event" (CPE) or "Carnian Humid Episode" (see Chap. 3.6.2.3.). In association with the episode, other events such as rifting reactivation, sea-level (eustatic) fall, intense volcanic activity, and doming of the Iberian Massif also occurred in Iberia (Arche and López-Gómez 2014; López-Gómez et al. 2017).

The upper Keuper units (K4 and K5 units in the Iberian basin, and the equivalent units in the other basins) represent a renewed evaporitic platform. Sedimentation in this platform again began as an evaporitic mudflat (K4 units), which evolved into sulfate lagoons at the platform scale (K5 units). The evaporitic sedimentation ended with the shallow marine carbonatic platform represented by the Imón Fm.

It is interesting to consider the maximum thicknesses reached by the Keuper evaporite units in the Triassic basins of eastern Iberia (Fig. 3.15). For the lower Keuper evaporites (K1 and equivalent units) it was almost 400 m in La Mancha sector of the Iberian basin and about 450 m in the Ebro basin. For the K4 unit and equivalent units of the upper Keuper it was 550 m in La Mancha sector of the Iberian basin and 430 m in the External Sierras of the Pyrenean basin. For the K5 unit and equivalent units of the upper Keuper it was over 250 m in the Nogueres structural unit of the Pyrenean basin (Fig. 3.15). These values are considerably thicker than the maximum values (<200 m in general; commonly 100–150 m) of the three Triassic carbonatic units (lower and upper Muschelkalk units, and Imón Fm) which alternated with the evaporitic ones during the Middle-Late Triassic (Ortí et al. 2017, 2018). High maximum values are also known for the other Triassic evaporite units in eastern Iberia. These values reach up to 600 m for the middle Muschelkalk unit (Mas Fm; Anisian) in the Maestrat sector of the Iberian basin, and for the "Anhydrite Zone" (or Lécera Fm; Rhaetian-Hettangian) that reaches 500 m in the Ebro basin and 1000 m in La Mancha sector of the Iberian basin. All these values indicate that the Triassic evaporite units in eastern Iberia, including the Keuper ones, were controlled mainly by reactivation pulses of the Triassic rifting. Also the clastic K2 unit of the middle Keuper, which is almost 300 m thick in the La Mancha sector of the Iberian basin, seems to belong to this category of subsident units. These reactivation pulses alternated with deceleration pulses of the extensional activity. During these deceleration pulses, the carbonatic units were sedimented on the Iberian platform.

The reference succession of the Keuper facies units, which is dated Carnian-Norian, corresponds to the Valencia and southern La Mancha sectors (Figs. 3.15 and 3.36). In the outcrops of the Valencia sector, the succession is composed of the lower Keuper unit (Jarafuel Fm or evaporitic K1 unit), the middle Keuper units (Manuel Fm or detrital K2 unit; Cofrentes Fm or detrital K3 unit), and the upper Keuper (Quesa Fm or evaporitic K4 unit; Ayora Fm or evaporitic K5 unit) (Ortí 1974, 1982–83). The carbonatic Imón Fm (Norian) overlies de K5 unit. At the subsurface of the southern La Mancha sector, this Keuper succession, up to 700 m thick, was firstly mentioned by Castillo (1974) and then described in detail by Suárez (2007) by means of wireline studies in deep boreholes. At the subsurface of the eastern sector of the basin, i.e. the Maestrat sector, several deep boreholes show a complete, little disturbed Keuper succession formed by three units with a total thickness of 280 m. These units are the lower saline unit (K1), the intermediate claystone unit (K4), and the upper anhydritic unit (K5), (Lanaja 1987; Bartrina and Hernández 1990) (Fig. 3.14). Probably, no record of the K2 and K3 units exists in this Maestrat sector.

The lower Keuper unit (K1) is characterized in the outcrops of the Valencia sector by monotonous alternations of laminated gypsum beds and grey claystone beds. These alternations also intercalate irregularly some layers of sandstones, marls and carbonates (Ortí 1974). At the subsurface of the southern La Mancha sector, the K1 unit is a bedded halite unit formed by 4th- or 5th-order shallowing upwards sequences, about 5–25 m thick, with a total thickness up to 380 m (Suárez 2007). These sequences are formed by clay-halite cycles at the metre-scale and the decametre-scale. Scarce sulfate is observed in association with these cycles.

The K2 unit (Manuel Fm) is formed in the southern sectors of the basin by a succession of claystones and channelled fluvial sediments, which are derived from the Iberian Massif to the west (Ortí 1974; Arche and López Gómez 2014). At the subsurface, the unit reaches up to 280 m in thickness (Suárez 2007). The age of this unit is early Carnian/Julian (Arche and López-Gómez 2014).

The K3 unit (Cofrentes Fm) is formed by red-coloured, massive claystones and some carbonate beds. The thickness of the unit is relatively homogeneous both at the surface (up to 50 m) and the subsurface (up to 80 m; Suárez 2007).

The K4 unit, 60–70 m thick in the outcrops of the Valencia sector, is a poorly stratified assemblage of massive, red claystones bearing abundant nodular gypsum beds. At the subsurface of the southern La Mancha sector, this unit intercalates salt layers and reaches up to 550 m in thickness (Suárez 2007). The unit was subdivided in three subunits by Suárez (2007): basal (K4a) and top (K4c) subunits, which are formed by claystone layers and anhydrite layers; and central (K4b) subunit, which is mainly composed of salt. The three subunits show cycles at the metre-scale and the decametre-scale, which are clay-halite cycles in the K4a subunit and clay-anhydrite cycles in the other two subunits.

The K5 unit is characterized mainly by white, bedded gypsum, although some claystone and carbonate beds can be found interbedded in the sulfates of this unit. The thickness of the unit, up to 50 m, is relatively homogeneous both in outcrop and at the subsurface.

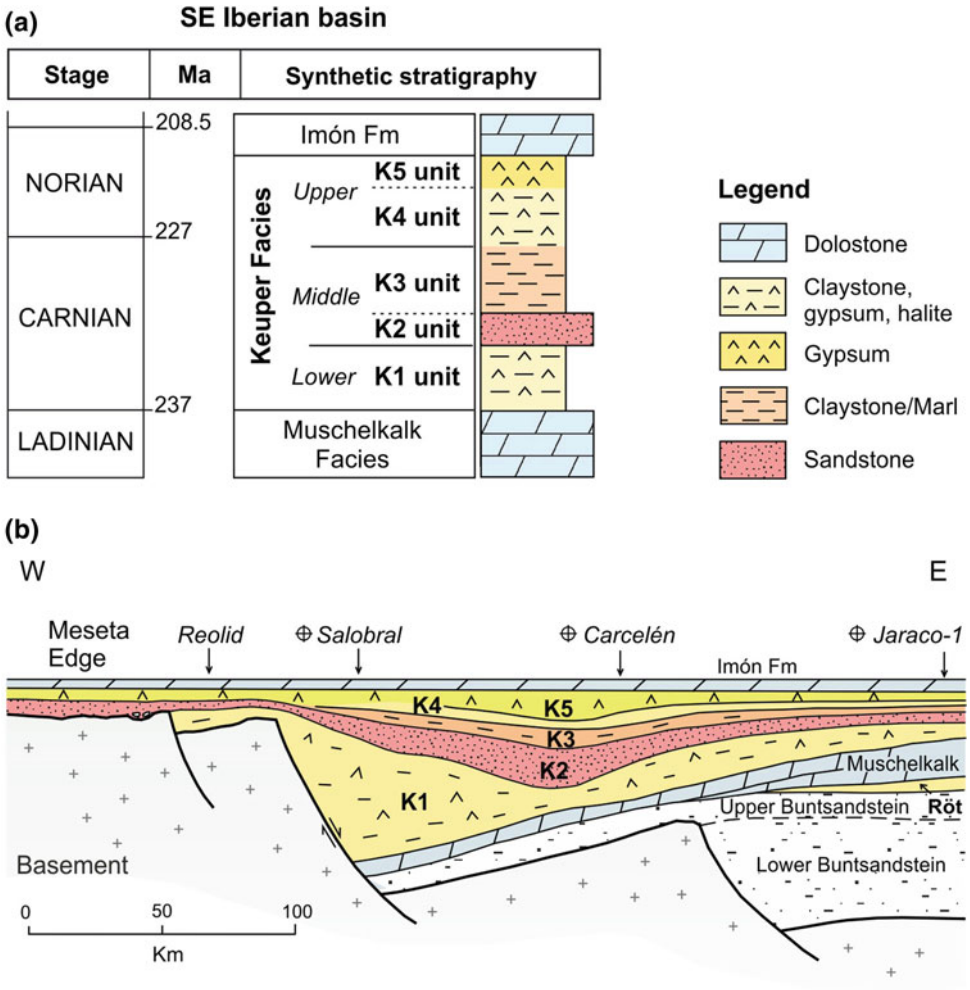

Fig. 3.36 **a** Reference succession of the Keuper units in eastern Iberia. Stratigraphic section representative of the southern sectors (Valencia and La Mancha sectors) of the Iberian basin. Scheme out of scale. **b** Cross-section in the southern sector of the Iberian basin (La Mancha and Valencia sectors, W to E). Datum is the top of the Imón Fm. Modified from Arche and López-Gómez (2014)

In the SE Margin of the Iberian Massif (so-called Stable Meseta) (Figs. 3.13, 3.14 and 3.15), the Keuper succession is formed by the 'Lower red mudstones and sandstones unit' (Lrms) at the base, which is equivalent to the K1 unit, by the Red Sandstone unit (Rs), equivalent to the K2 unit, and by the other units of the Iberian basin, i.e. the K3, K4 and K5 units (Arche and López-Gómez 2014). The basal Lrms unit lies unconformably and onlaps on the Paleozoic basement.

Age attributions of the Keuper facies units in eastern Iberia have been based almost exclusively on palynological associations found in some units. The majority of the palynological assemblages in the Prebetic-Subbetic, Iberian, Catalan, and Ebro basins are characterized by *Camerosporites secatus* accompanied by *Vallasporites ignacii*, *Pseudoenzonalasporites summus,* and the genus *Paracirculina* (Solé de Porta and Ortí 1982; De Torres and Sánchez1990; Arche and López-Gómez 2014). This assemblage belongs to the "*Camerosporites secatus* phase" of Visscher and Krystyn (1978), and specifically to the *secatus-densus* palynological zone, which dates the middle-late Carnian according to Besems (1981a, b). In domains located to the west and southwest of the Iberian basin, however, some palynological assemblages of the upper Keuper units have been dated as Norian, as in the NE Central System (Hernando 1977), and also in the Stable Meseta in SE Spain (Besems 1981a, b). Thus, it is commonly assumed that in the Prebetic-Subbetic and the Iberian basins, the lower and middle Keuper units are Carnian in age, and the upper Keuper units are Norian (Arche and López-Gómez 2014).

All the evaporite units forming the Keuper successions in eastern Iberia have a marine origin, which is supported by the isotopic compositions of sulfur, oxygen and strontium ($\delta^{34}S_{CDT}$, $\delta^{18}O_{SMOW}$, $^{87}Sr/^{86}Sr$) in sulfates (Utrilla et al. 1992; Ortí et al. 2014; 2017), and on the bromine content in chlorides (Ortí et al. 1996). These units were accumulated as platform evaporites in settings such as chloride ponds, sulfate salinas, sulfate lagoons, and sabkhas. At the scale of the whole platform, these settings constituted either claystone-rich evaporitic mudflats (K1 and K4 units) or sulfate salterns bearing carbonate (K5 unit). The terms 'evaporitic mudflat' and 'saltern' are used sensu Warren (2006).

3.6.2.3 The Carnian Pluvial Episode

Arche A, López-Gómez J, Martín-Chivelet J, Barrenechea JF, De la Horra R and Escudero-Mozo MJ

The Triassic period was marked by the different geodynamic processes related to the break-up of the Pangea supercontinent. Among these processes, igneous activity was a key factor. It is well-known that intense volcanic activity related to Siberian traps during the Permian-Triassic transition marked one of the most significant changes of the Phanerozoic, including global climate and ecosystem changes that led to the notorious mass extinction (Benton 2003; Erwin 1993; Galfetti et al. 2007; Payne and Krump 2007; Sun et al. 2012; Hochuli and Frank 2006). However, other igneous episodes during the Triassic such as the emplacement of the Wrangelia igneous province could have also provoked drastic changes on Earth (Nakada et al. 2014; Ruffell et al. 2016; Mueller et al. 2016, among others). Emplacement of the Wrangelia igneous province took place during the Julian-Tuvalian interval (early Carnian), and may have been the trigger for abrupt carbon dioxide-induced warming and associated increased rainfall. Notwithstanding, its duration, global impacts and relatively rapid termination are not fully understood and require further intercalibrated terrestrial and marine data (Wignall 2015).

As a consequence of this episode, regional basins experienced dramatic changes reflected in their sedimentary records. Carbonate platforms developing in the tropics were abruptly interrupted, while river systems occupied vast surfaces on land and left widespread sand-rich levels across coastal regions (Berra 2012). This humid episode was initially described by Simms and Ruffell (1989, 1990) as the Carnian Pluvial Episode (CPE), and later coined as Carnian Humid Episode (CHE) by Ruffell et al. (2016). Synchronicity between the Wrangelia igneous province and the CPE was noted by Xu et al. (2014). In addition, Dal Corso et al. (2012) specifically related the carbon isotope excursion of Carnian age to the Wrangellia event. The CPE is therefore considered today a global event and has been described in many different basins (Mutti and Weissert 1995; Rigo et al. 2017; Preto et al. 2010; Kozur and Bachmann 2010; Roghi et al. 2010; Bialik et al. 2013; Arche and López-Gómez 2014).

In the Iberian microplate, the CPE has been described by Arche and López-Gómez (2014). The sedimentary record of this humid episode broadly corresponds to the Manuel Fm n described by Ortí (1974) in E and SE Spain. This is one of the five formations comprising the so-called Valencia Group, equivalent to the Keuper facies, and is also described as part of this facies in the chapters of this book dealing with the Iberian and Betic basins (see Chap. 3.6.2.2.). Sedimentary studies of the Manuel Fm by Fernández (1977), Fernández and Dabrio (1978), De Torres and Sánchez (1990), Fernández et al. (2005) and Arche and López-Gómez (2014), among others, related this unit to the development of mostly braided and meandering fluvial systems, and with some aeolian reworking in its uppermost part (Arche and López-Gómez 2014). River systems point east, towards the Tethys Sea (Fig. 3.37), and in river head areas, they directly cut into the Paleozoic basement (Fig. 3.38).

This humid episode is probably not recorded as a single pulse. In both marine and continental environments, some authors (Breda et al. 2009; Stefani et al. 2010; Kolar-Jurkovsek and Jurkovsec 2010; Roghi et al. 2010; Arche and López-Gómez 2014) have described the episode as indicated by three or four separate humid fluctuations. Although details are still not fully understood, there is a clear relationship between this event and the tectonic reorganization of the Tethys domain, including closure of the Paleotethys (Ziegler 1988a, b), a sea-level fall (Haq and Al-Qahtani 2005), and the general development of rift branches related to the break-up of Pangea (Ziegler and Stampfli 2001).

In a recent work, López-Gómez et al. (2017) establish correlations in the continental-marine sedimentary record for this Late Triassic CPE in E Iberia and Majorca and Minorca Islands. This study was focused on facies analysis and identified allogenic controls on both continental and marine records. In this transition, the east of Iberia shows a terrestrial (mainly fluvial) sedimentary record, while its lateral equivalent record in Majorca is represented by distal fluvial environments with volcanic intervals. In a more distal area, in Minorca, this event is represented by an exposed and karstified marine carbonate surface (see Fig. 3.28). Tectonic activity developed NNE–SSW and NW–SE conjugate fault lineaments in eastern Iberia. Sedimentation in this area was controlled by this tectonic episode allowing volcanic activity at the fault lineaments junction, in the Majorca area. As a result, a paleogeography of elevated and subsiding blocks, which controlled both continental and marine sedimentation, was shaped (Fig. 3.39).

3.6.3 Permian and Triassic Magmatism in the Iberian Basin

Lago M, Galé C and Ubide T

The intense crustal stretching that accompanied the break-up of Pangea at the end of the Paleozoic, favoured magma ascent of magmas through the crust. During the Permian, rising magmas intruded and infilled half-graben basins developed in what would later constitute the Iberian Chain (Lago et al. 2004a, b, 2005).

The Permian magmatism in the Iberian basin is really well recorded with more than 500 outcrops of magmatic

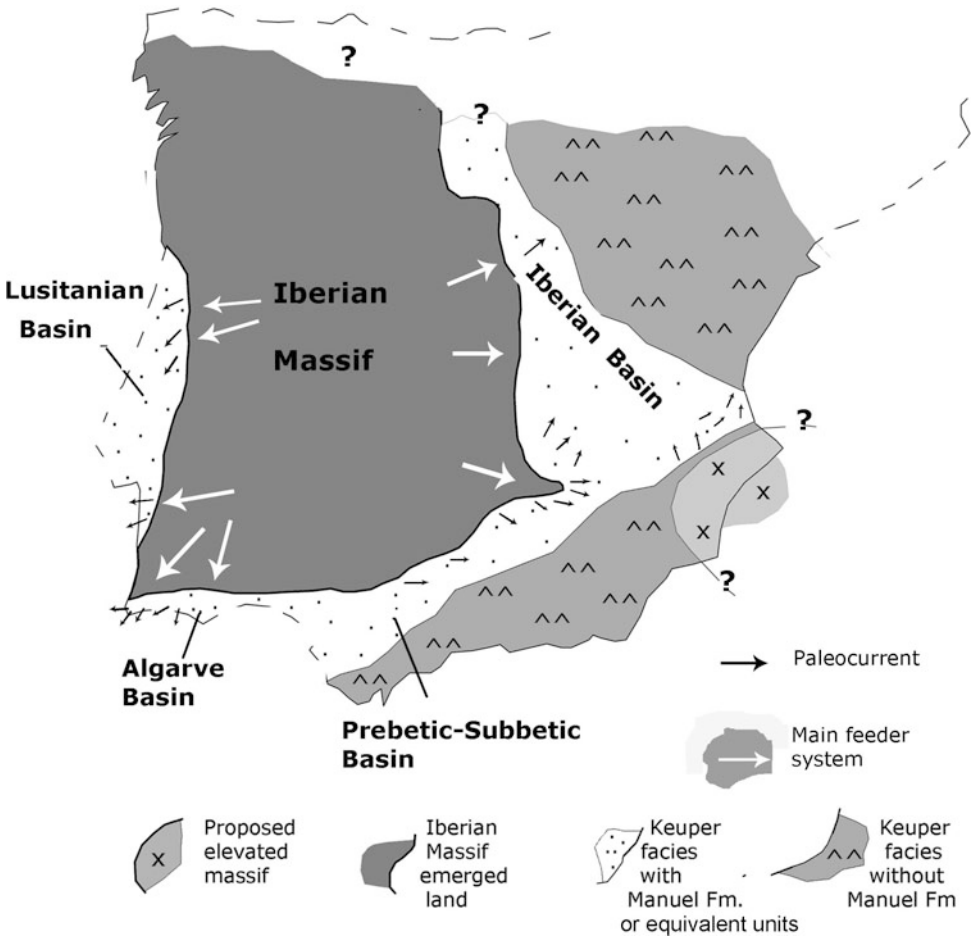

Fig. 3.37 Elevated massifs and sedimentary basins around Iberia during the deposition of the Manuel Fm. and coeval units in Portugal. Black arrows indicate average paleocurrent measurements. White arrows represent inferred feeder systems in the elevated Iberian Massif. Modified from Arche and López-Gómez (2014)

rocks along the entire belt. This magmatism comprises hypovolcanic intrusions, lava flows and volcanoclastic deposits. Rock compositions range from gabbro to rhyolite, and are most commonly andesite. The geochemical affinity is subalkaline (calc-alkaline) (Lago et al. 2004a, b, 2005; Majarena et al. 2017). Pluriepisodic events have been recognized but the age of emplacement of those episodes has not been established yet (Lago et al. 2004a, b, 2005). Available radiometric ages range between 287 ± 12 and 283 ± 2.5 Ma (Cisuralian) and have been obtained in representative outcrops with different radiometric methods. Namely, at Atienza (whole-rock K-Ar, Hernando et al. 1980), Loscos (K-Ar in biotite, Lago et al. 1991; Ar/Ar in biotite, Perini and Timermann 2008), Fombuena (K-Ar in biotite, Conte et al. 1987) and Sierra de Pardos (U-Pb zircon geochronology, Majarena et al. 2017). The influence of assimilation processes and lithospheric melts in the origin of these magmas is evidenced by their geochemical composition (cf. Lago et al. 2004a, b). The common presence of xenoliths of metapelites and granitoids, and inherited minerals of crustal origin (Lago et al. 2004a, b, 2005; Majarena et al. 2015, 2017) supports the hypothesis of crustal assimilation.

Lago et al. (2012) reported, for the first time, the occurrence of volcanic rocks in the Middle-Late Permian sequences (Guadalupian-Lopingian) of the Iberian Ranges. These comprise a hypovolcanic intrusion of basic to intermediate alkaline magma in the Alcotas Fm. The enriched mantle geochemical signature of these rocks is not shared by other Middle-Upper Permian igneous rocks in the western Tethys and is also different from the crustal signature of the Lower Permian magmatism in the Iberian Ranges (Lago et al. 2012).

In summary, a widespread subalkaline magmatism of lithospheric origin was emplaced during the Cisuralian (Lower Permian) in the Iberian Ranges, followed by a very scarce alkaline magmatism of enriched mantle origin emplaced during the Guadalupian-Lopingian (Middle-Late Permian).

Alkaline magmatic rocks were emplaced in the SE part of the Iberian Ranges during the Late Triassic (Lago et al. 1996, 2000). This magmatism comprises more than 100 outcrops of hypovolcanic bodies exposed following a NW–SE regional direction, from Villel (Teruel) to Altura (Castellón). Some of these bodies belong to individual sills, separated into segments due to Alpine tectonics. Most sills intrude Keuper facies rocks (K1 to K4 members) although

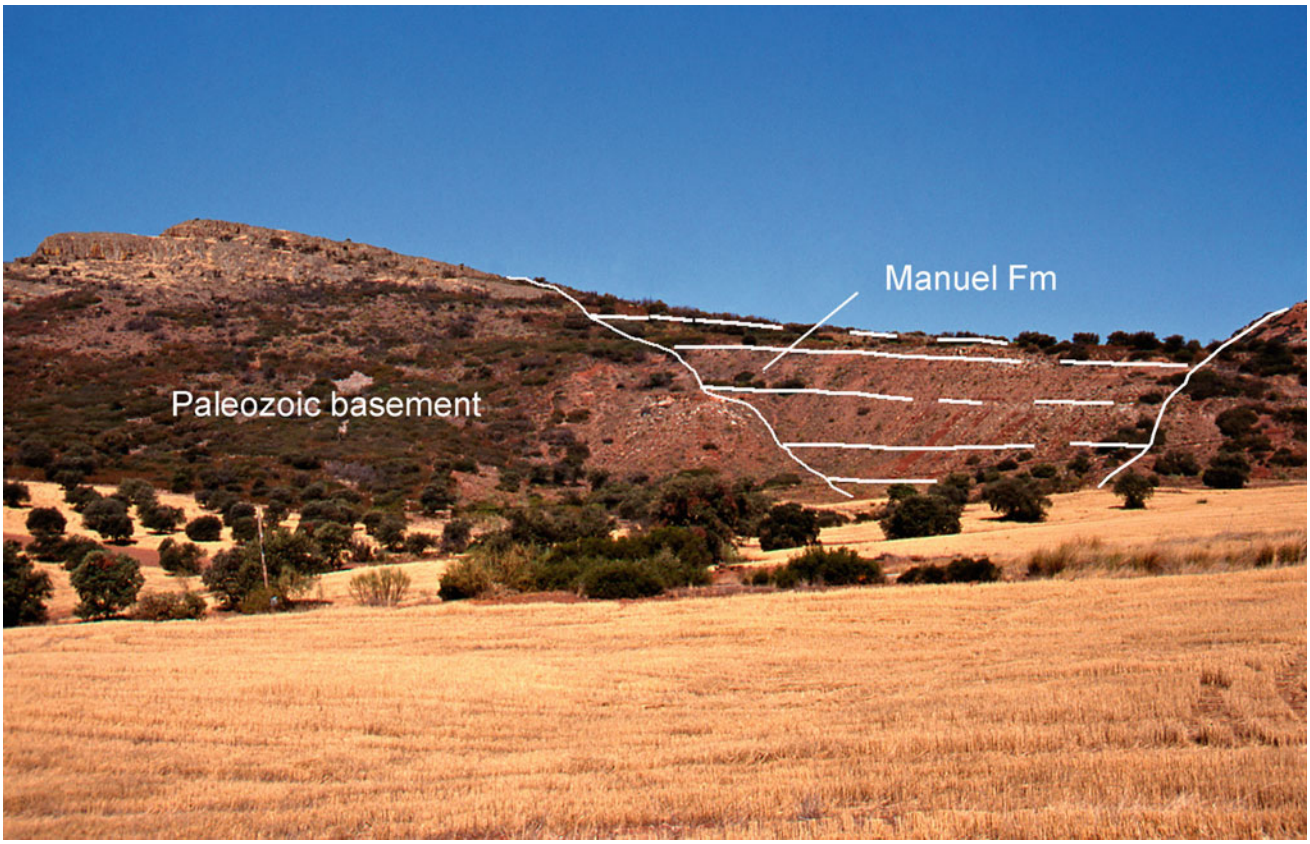

Fig. 3.38 The Manuel Fm (or K2) lying unconformably on the Paleozoic basement in central-eastern Spain, near Albaladejo, in the so-called Stable Meseta. This area was near the main feeder system of these continental deposits related to the Carnian Humid Episode (CPE). Modified from Arche and López-Gómez (2014)

some examples were emplaced into Buntsandstein facies deposits (i.e. Pina de Montalgrao and Albentosa outcrops). These outcropsare composed of dolerites which usually show fluidal structures in the top of the sills and also low grade contact metamorphism of the host rock (i.e. Lago et al. 1996, 2000). The composition of these alkaline dolerites is basaltic and they have a geochemical signature similar to an enriched lithospheric mantle (Lago et al. 2000). Crustal xenoliths of granitoids, metapelites and granulites are common in these sills, suggesting that magmas ascended through a fracture system related to an extensional tectonic regime that affected different levels of the lithosphere (Lago et al. 2000). The alignment of magmatic outcrops is related to the reactivation of Late Variscan deep faults that favoured the upwelling and partial melting of the underlying mantle.

The magmatic activity in the SE sector of the Iberian Ranges was reactivated during the Jurassic (Gómez 1979; Martínez et al. 1998 and references therein). It consists of multiepisodic volcanism emplaced into the calcareous units of the Lower and Middle Jurassic (Martínez et al. 1998). Like the Triassic magmatism, the Jurassic episodes have basaltic composition and alkaline affinity. However, the geochemical signature of the Jurassic magmas indicates an asthenopheric mantle source. The composition of the magmatism in the Iberian Ranges was closely related to the onset and development of the Neoethys rifting Martínez et al. 1998) as summarized in Fig. 3.40.

3.6.4 A Comparison of the Iberian and Ebro Basins During the Permian and Triassic

Arche A, López-Gómez J, Vargas H and Gaspar-Escribano J

The Permian and Triassic basins of the Iberian microplate were developed on a folded and thrusted basement intruded by granitic bodies. This was the result of a continent-continent collision between Laurussia and Gondwana at the end of the Carboniferous that created the Variscan Orogen (Arthaud and Matte 1977; Dewey and Burke 1973; Matte 1988), a region characterized by overthickened lithosphere, considerable shortening, deep crustal roots and high topographic relief.

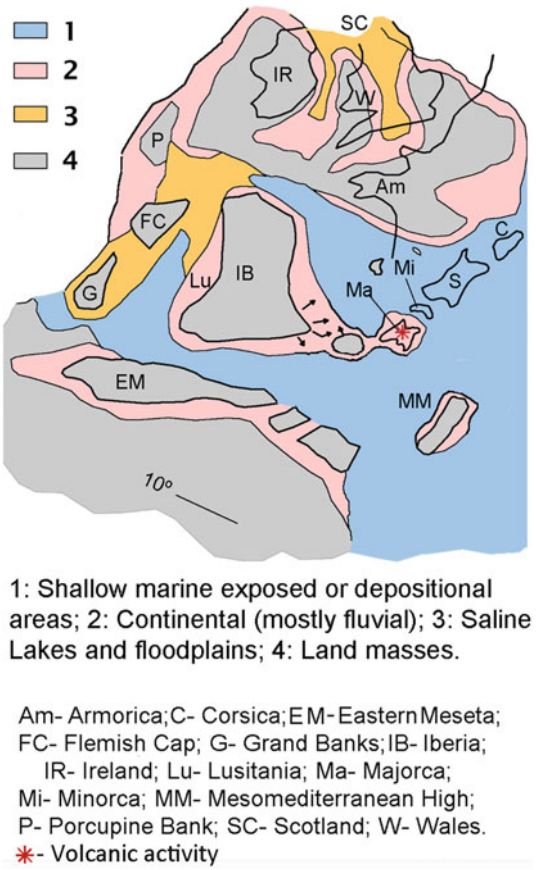

Fig. 3.39 Julian paleogeographic reconstruction in the western Tethys domain showing the deposition area of the Manuel Fm (K-2), which represents the Carnian Pluvial Episode (CPE). Modified from López-Gómez et al. (2017)

High relief and thick crust are stable while compression lasts at the edges of the orogen, but folding and thrusting ceased in most of southern Europe by Late Carboniferous times (Malavielle et al. 1990; Seranne 1992). Following its cessation, gravitational instability starts after 15–20 my (England 1982; Houseman et al. 1981) and the lithospheric roots of the collision chain collapse. This process led to a period of extensional tectonics and high heat flux during which a series of linear rift basins (half-graben and graben) developed in Central and NE Iberia (Arche and López-Gómez 1992, 1996, 1999b, 2005; Doblas et al. 1994; Van Wees et al. 1998; Vargas et al. 2009; López-Gómez et al. 2012; Galán-Abellán et al. 2013).

3.6.4.1 Periods of Ebro and Iberian Basins Evolution and Their Comparison

The sedimentary record of Permian and Triassic age of the Iberian and Ebro basins is subdivided by angular unconformities that indicate energetic syn-sedimentary tectonics. Thick wedges of terrestrial sediments were accumulated in basins bounded by normal faults during the Permian and the Early-Middle Triassic. Calc-alkaline volcanic rocks associated with the Early Permian sediments are abundant in the Iberian basin, the Ateca-Montalbán-Maestrat high and the SW Ebro basin (Sopeña et al. 1988; Arche and López-Gómez 1999a, b; Lago et al. 2004a, b).

The first phase of rifting, or initial tectonically-driven rifting, had a first episode in the Early Permian when a series of small, isolated half-graben basins were created in both areas, most of them underfilled by alluvial fan sediments, that eventually evolved into permanent lakes such as in the Molina de Aragón area or the Caspe-1 well (Fig. 3.41) (Ramos 1979; Arche et al. 2007). This episode is coeval with a volcanic and thermal event (Lago et al. 2004a, b) that is recorded all over the Iberian microplate.

The second episode of the initial-tectonic rifting phase, of Late Middle Permian–Late Permian age, created more extensive half-graben linked axially and a basin boundary fault system along the SW margin of the Iberian basin. Upper Permian sediments are present in the central Ebro basin (Jurado 1989, 1990) but there are insufficient subsurface data to delineate the rift basins in this domain.

At the beginning of this episode, the Iberian basin was filled by transverse alluvial fans fed directly from the upifting footwall block. As rifting progressed, new accommodation space was created, which led to a reorganization of the basin geometry, a migration of the depocentre to the NE, the creation of antithetic normal faults in the hanging wall and the creation of full-graben. Drainage shifted to an axially-fed fluvial network sourced in the NW corner of the basin (Arche and López-Gómez 1999b).

The third episode of extension during the initial or tectonic rifting phase, of Early-Middle Triassic age, had a more complex evolution and represented the transition to the mature rifting stage in the Iberian microplate. Extension progressed to the NE, but accommodation rate slowed down, leading to overfilling of the fluvial basins during the Early Triassic. Complex amalgamated braided fluvial deposits filled the basins and partially overlapped the Paleozoic highs. Renewed extension during the Early Middle Triassic led to substantial differential subsidence in the Iberian and Ebro basins, asymmetric distribution of active fluvial channels and large migrations of the depocentres (Arche and López-Gómez 1999b).

The basin boundary faults for the Iberian and Ebro basins have been partially reconstructed using balanced sections affected by alpine deformation and isopach maps for each period of extension. They consist of arcuate segments, laterally linked and offset by transversal fault systems trending at high angles. They are interpreted (Arche and López-Gómez 1996) as simple shear, listric fault systems (Fig. 3.41) becoming horizontal at a depth of 12–15 km, close to the extensional models of Wernicke (1981) and Wernicke and Burchfield (1982) for the Basin and Range province.

Fig. 3.40 Composition of the Early Permian-Middle Jurassic magmatism in the Iberian Chain

AGE	MAGMATISM		TECTONIC REGIME
	Nature	Xenoliths	
Pliensbachian-Bajocian (Lower-Middle Jurassic)	Alkaline/ Astenospheric mantle source		Extensional Rift third stage
Upper Triassic	Alkaline/ Sublithospheric mantle source	Crustal: granitoids granulites, metapelites	Extensional Rift second stage
Guadalupian-Lopingian	Transitional to alkaline/ Astenospheric mantle source	scarce	Extensional Rift first stage
Cisuralian (287-283 Ma)	Calc-alkaline/ Lithospheric melts and assimilation processes	Crustal: granitoids, metapelites	

Folding in the hanging wall block of these extensional structures (roll-over anticline of Gibbs 1984) led to the formation of antithetic and synthetic fault fans, isolating a non-deformed basement high in between extending basins. This structural evolution can explain the formation of the Ateca-Montalban-Maestrat high and the linked evolution of the Iberian and Ebro basins during the Triassic.

In Anisian times, the SW basin boundary fault system (Serranía de Cuenca fault system) became inactive, sedimentation ceased along large tracts of the Iberian basin and subsidence and sedimentation shifted to its NE margin at the newly created Ebro basin (Arche and López-Gómez 1996).

The mature rifting phase started in Central and NE Iberia during the middle-late Anisian, indicating that the lithosphere was stable after the collapse of the Variscan Belt, and cooling and contraction started to be the dominant processes.

The onlapping of the Tethys Sea on the eastern part of the Iberian basin started when cooling brought this part of the Variscan basement below sea level and a transgression pulse prograding from east to west occupied the newly created accommodation space. Four successive episodes or transgressive-regressive cycles developed during the mature rift period, covering wider areas than the sediments of the preceding syn-rift period: two of Anisian-Ladinian age, composed of shallow-water carbonates and evaporites (Muschelkalk Facies), and another two of Carnian-Norian age, composed of marine evaporites and mudstones (Keuper Facies), just before the beginning of the post-rift event.

Each cycle onlapped on wider areas of the eastern Iberian microplate than the preceding one as a consequence of the progressive cooling of the lithosphere that created larger subsiding areas with time (Arche and López-Gómez 1992). The Ateca-Montalban-Maestrat high was drowned and flooded by marine sediments during the early Ladinian. Most of the similar Paleozoic highs also disappeared in this period, and the Iberian, Ebro and Catalan basins were interconnected in a single one (Escudero-Mozo et al. 2015).

3.6.4.2 The Nature of Subsidence During the Permian and Triassic in the Central and NE Iberian Microplate

Quantitative subsidence studies by Gaspar-Escribano et al. (2001) for the Ebro basin, Van Wees et al. (1998) and Vargas et al. (2009) for the Iberian and Ebro basins using back-stripping methods have yielded details on the creation and evolution of these basins beyond the classic paleogeographic studies. Forward modeling using both one-layer and two-layer configurations of the lithosphere (Vargas et al. 2009) has demonstrated that the latter always provides the best fit between predicted and observed data (Fig. 3.42). As a consequence, the simple shear, arcuate listric fault model of extension proposed by Arche and López-Gómez (1992, 1996) is favored against others proposing deep seated, rectilinear basin boundary faults.

Another fact revealed by this kind of analyses is that the rifting episodes can be subdivided into a rapid, initial rifting pulse followed by a period of slow subsidence associated to stratigraphic gaps and angular unconformities, lasting 5–10 Ma (Fig. 3.43) (Vargas et al. 2009).

The fluvial architecture of the Permian-Triassic alluvial deposits of the Iberian and Ebro Basins is controlled by the interaction of subsidence rates and changes in regional base levels (López-Gómez et al. 2010), specially lateral tilting of floodplain surfaces. Extension rates and its temporal and spatial variations in the upper part of the lithospheric plate (δ and β stretching factors) exerted a first-order control on the fluvial styles: amalgamated with low rates and complex with high rates. The changes in extension rates in the lower lithospheric layer show no relation to the fluvial styles.

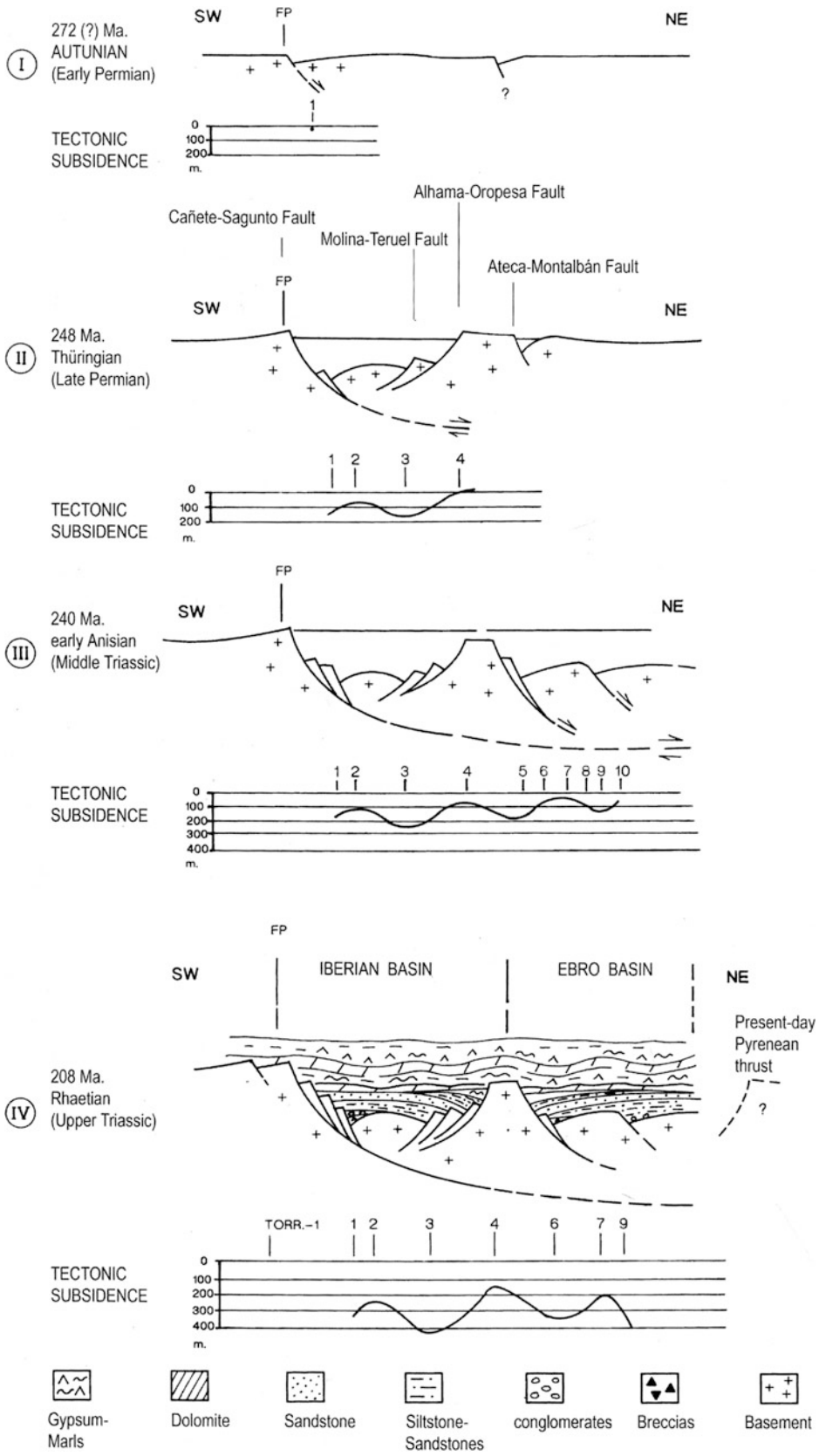

Fig. 3.41 Comparison of subsidence values in the Iberian and Ebro basins during the Permian. Numbers represent sections: 1-Cañete (Ca), 2—Chelva (Che), 3—Chovar-Eslida (Cho-Es), 4—Teruel (Ter), 5—Alhama (Alh), 6—Caspe 1, 7—Bujaraloz 1 (Buj-1), 8—Monegrillo 1 (Moneg-1), 9—Ebro 2, 10—Monzón 1 (Monz-1). FP—"Fixed Point". Geographical locations in Figs. 3.29 and 3.33. Modified from Van Wees et al. (1998)

The sedimentary record of the Permian-Triassic basins of Central and NE Iberia show an evolution from the stage of collapse of a thickened lithosphere after the Hercynian orogeny to another of crustal extension of a thinned lithosphere and finally to one of cooling and contraction that brought part of the Hercynian basement below sea-level by Mid-Triassic times. This process has been interpreted by Menard and Molnar (1988) in the French Alps and the Massif Central as an evolution from a thickened Tibet-type hercynian chain into a thinned Basin-and-Range province in about 60 Ma; our data in Iberia agree with this interpretation.

3.6.5 Mineralogical and Geochemical Indicators of the Biotic Crisis in the Iberian Basin During the Break-up of Pangea

Barrenechea JF, Galán-Abellán B, Borruel-Abadía V, Luque J, Alonso-Azcárate J, De la Horra R and López-Gómez J

As mentioned before, the development of the Iberian basin during Permian-Triassic times was related to successive rifting episodes (Arche and López-Gómez 1996) in the context of the break-up of Pangea. During this period of

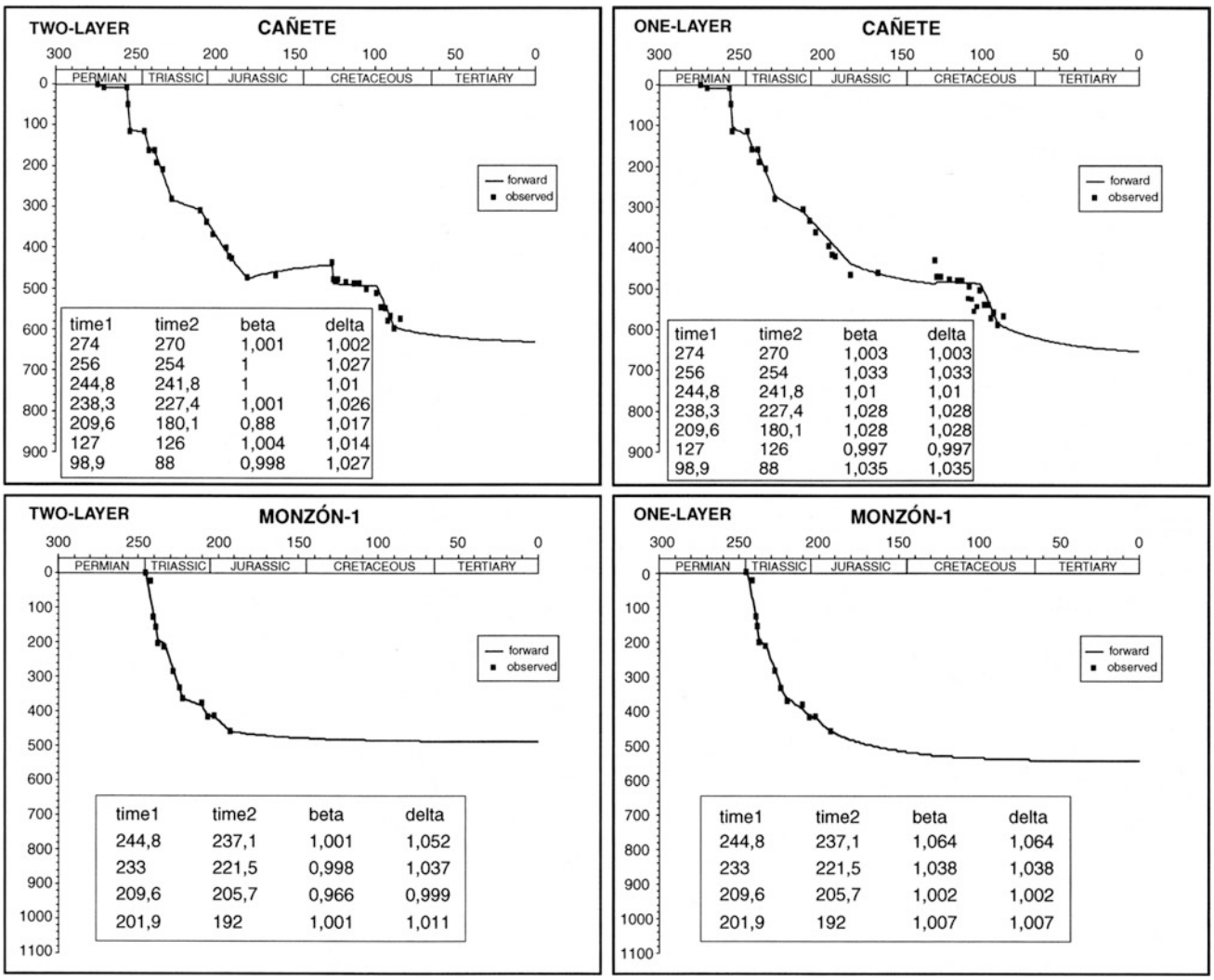

Fig. 3.42 Comparison between two-layer and one-layer stretching models in two selected sections of the Iberian and Ebro basins. It can be deduced how the two-layer modelling fits much better for the sections of the Iberian basin, whilst differences between both modelling methods are not so evident for the Ebro basin selected wells. Geographical locations in Figs. 3.29 and 3.33. Modified from Vargas et al. (2009)

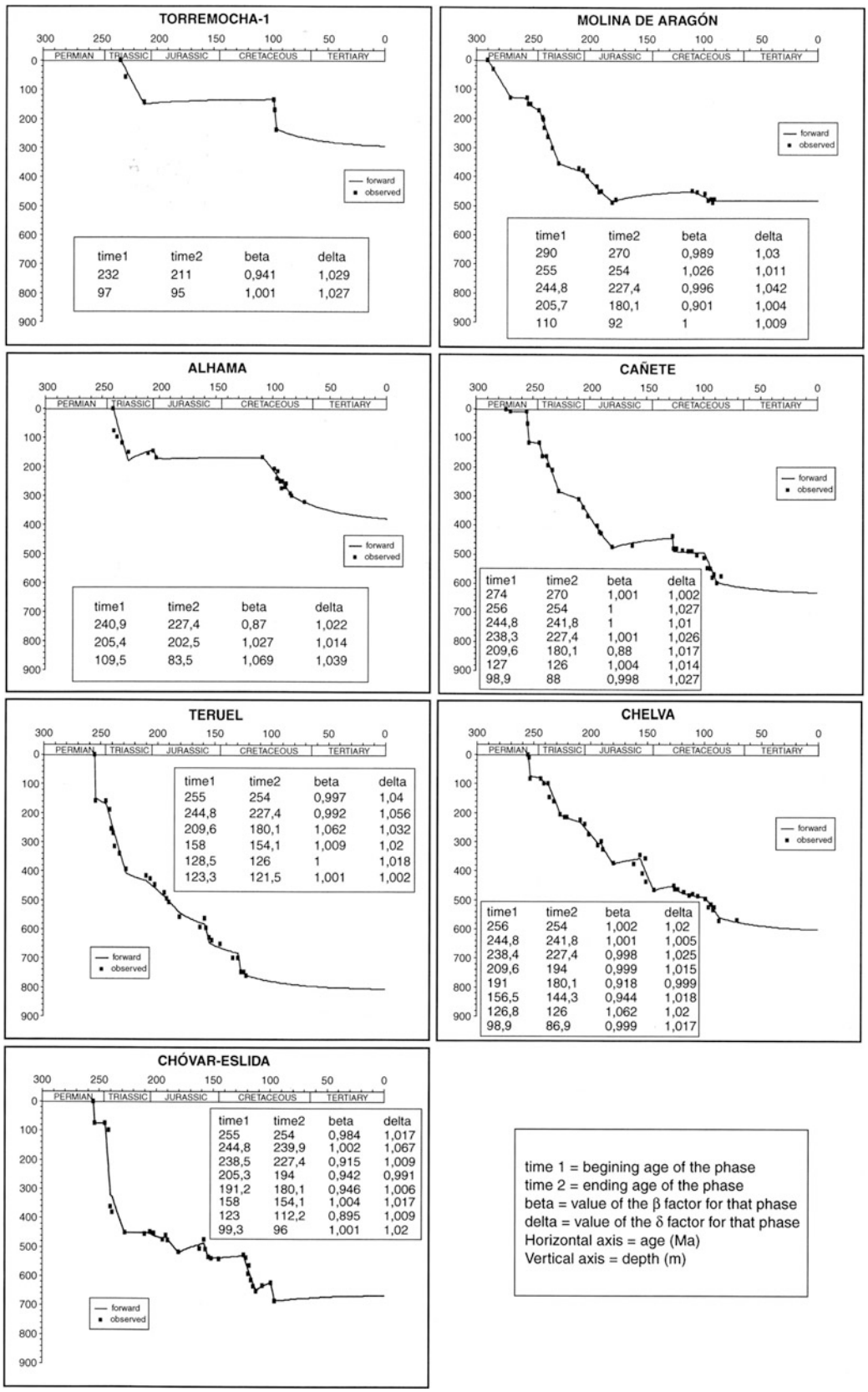

Fig. 3.43 Forward modelling curves and β and δ values for selected sections of the Iberian Ranges. Geographical locations in Figs. 3.29 and 3.33. Modified from Vargas et al. (2009)

widespread extension there were different biotic crisis events on a global scale, including the end Guadalupian extinction (Zhou et al. 2002; Jost et al. 2014) and the largely known End Permian Mass Extinction (EPME), which killed off most forms of marine and terrestrial life (Benton 2003; Erwin 2006). The causes of the EPME are still debated, but there is broad acceptance of its relation with Siberian Traps volcanism, that would have increased CO_2 and CH_4 emissions leading to enhanced global warming and acidity (Payne and Kump 2007; Algeo et al. 2011; Romano et al. 2013). The damaged environmental conditions were intermittently extended until the Smithian-Spathian (end of Early Triassic) life crisis (Galfetti et al. 2007; Sun et al. 2015), thus resulting in a delayed recovery of life.

The Permian-Triassic transition is not detectable in the sedimentary record of the Iberian basin (or in most coeval continental successions in SW Europe). However, the effects of the biotic crisis on these emerged areas of the western Tethys can be envisaged from the detailed multidisciplinary study of several sections across these units. The characteristics of the Middle-Late Permian (Alcotas Fm) and Early-Middle Triassic (Cañizar and Eslida Fms) sedimentary rocks have been described in previous sections (see Fig. 3.32). The most remarkable feature is the lack of any record of organic activity (bioturbation, plant and fossil remnants, presence of paleosols, etc.) in the basal part of the Cañizar Fm (C1–C4 in Fig. 3.44). The distributions and relative thicknesses of these units were controlled by complex interaction between NE–SW boundary faults and a subordinate system of NNE–SSW faults (Arche and López-Gómez 1996; Van Wees et al. 1998).

Recently, the mineralogical and geochemical characterization of these units has revealed the presence of Sr-rich aluminum phosphate-sulfate minerals (APS), a rather scarce constituent of sedimentary rocks (Dill 2001). These APS were first reported in the Iberian basin by Benito et al. (2005). Several studies have shown that these phosphate-sulfate minerals are stable at low pH and relatively oxidizing conditions (Vieillard et al. 1979; Stoffregen and Alpers 1987; Gaboreau et al. 2005). Therefore, if the timing of APS formation is close to the sedimentation process, they can be used as paleoenvironmental markers of such acidic and oxidizing conditions.

APS minerals occur as tiny (1–5 μm) disseminated, euhedral, pseudocubic crystals or as polycrystalline aggregates (up to 300 μm) that replace metapelite fragments (Galán-Abellán et al. 2013) in mudstone, siltstone and sandstones. Their idiomorphic nature and delicate stepped faces allow discarding a detrital origin. Textural relationships show that APS minerals predate the precipitation of diagenetic quartz and illite cements, and that the replacement of metamorphic rock fragments and detrital micas occurred before the main compaction of the sedimentary pile. Accordingly, Galán-Abellán et al. (2013) concluded that the formation of APS minerals took place during early diagenetic stages, shortly after sedimentation and most probably under the influence of acid meteoric waters.

Based on element mapping of randomly selected areas in thin sections using an electron microprobe, Borruel-Abadía et al. (2016) proposed a method to quantify the relative abundance of these APS minerals. Their results are plotted in Fig. 3.44 and show that in all the sections examined there is a notable increase in APS minerals contents at the base (subunits C1–C4) of the Cañizar Formation (Early-Middle Triassic), relative to contents in underlying (Alcotas Fm.) and overlying (C5–C6 subunits and Eslida Fm.) rocks. This homogeneous distribution pattern of APS abundance across the basin suggests stratigraphic control of their formation. It should also be highlighted that APS occurred in all the samples analyzed, although their proportions in Permian and middle Triassic rocks are low. According to Borruel-Abadía et al. (2016) relative APS proportions reflect the duration and intensity of the acidification process, because once they precipitate these mineral phases are highly insoluble. Thus, the variation curves in Fig. 3.44 support the hypothesis of enhanced acidic environmental conditions during sedimentation of the basal part of the Cañizar Fm, where low-pH ground waters would promote the dissolution of detrital phosphates and precipitation of APS minerals. The lack of any record of organic activity in these units strongly suggests that APS can act as indicators of the damaged environmental conditions that produced the delayed recovery of life after the EPME event. In the underlying and overlying units, these acidic conditions would have been much less marked.

The ultimate causes of increased acidification remain unclear. However, the most likely explanation so far attributes this to the environmental effects of volcanic aerosols in a context of active rifting and extensional tectonic activity. According to López-Gómez et al. (2012), the transition from subunits C4 to C5 (Cañizar Fm) corresponds to the Spathian-Anisian transition and could be related to the coeval Hardegsen unconformity of central-western Europe. This change in the Iberian Range is marked by lower APS contents and by the first signs of biotic recovery, including bioturbation, paleosol development and plant remains (Béthoux et al. 2009; Gand et al. 2010; Borruel-Abadía et al. 2014). It also reflects climate change from an arid to a sub-humid period (Borruel-Abadía et al. 2015), and even a change in provenance as indicated by U-Pb detrital zircon geochronology (Sánchez-Martínez et al. 2012). Hence, the tectonic reactivation associated with this unconformity seems to have controlled both the development of highs and corridors, and the environmental and climate evolution of the basin.

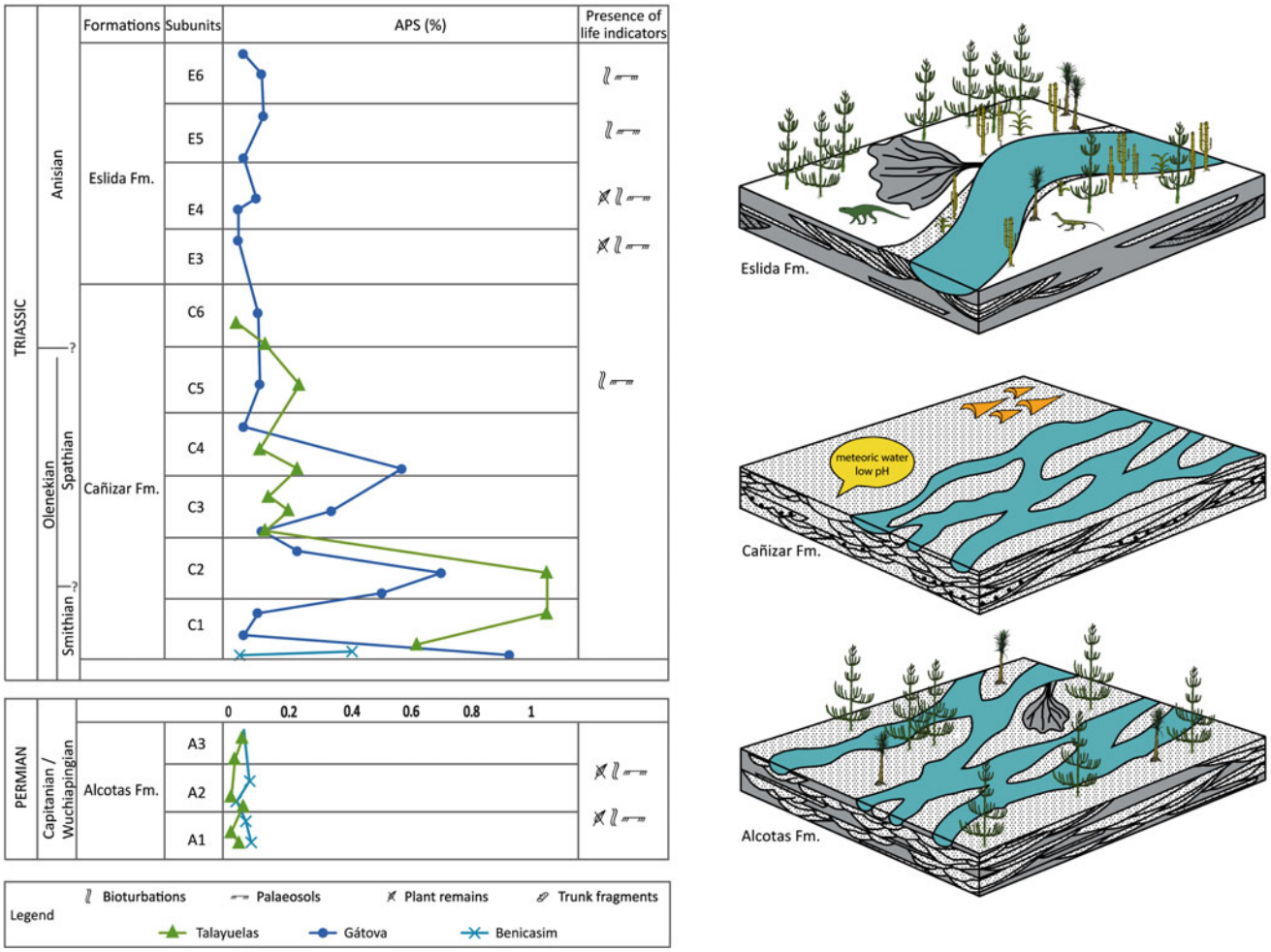

Fig. 3.44 Variation of the APS-mineral content of the Alcotas, Cañizar and Eslida formations, comparison with the presence of life indicators (bioturbation, paleosols and plant remains) and paleoenvironmental reconstruction of these formations. Geographical locations in Figs. 3.29 and 3.33. Modified from Borruel-Abadía et al. (2016)

3.7 The Betic Basin

Pérez-López A, Martín-Algarra A, Pérez-Valera F, Pérez-Valera JA and Viseras C

3.7.1 Triassic Tectonic Context of the Betic External Zones

A wide variety of Triassic facies exists in the Betic Cordillera (Fig. 3.45), with epicontinental Germanic and marine Alpine facies along with continental facies related to both of them (Blumenthal 1927; Schmidt 1935; Fallot 1948; Simon and Kozur 1977; Busnardo 1975; Roep 1972; Fernández 1977; Delgado et al. 1981, 2004; Martín-Algarra 1987; Pérez-López 2000; Pérez-López and Pérez-Valera 2007). This facies variety is recorded by different lithofacies and thickness of the successions, which were controlled by variable subsidence rates in the different internal vs. external tectonostratigraphic terranes of the Betic orogen and by their proximal to distal relations with respect to the open marine areas of the Neotethys.

In Triassic time, the different tectonostratigraphic terranes occupied distinct paleogeographic locations within subsiding graben closer to, or farther from rising faulted continental areas around them. The main continental areas conditioning the paleogeography of the Triassic Betic basin were the Iberian Variscan Massif and the Mesomediterranean Microcontinent (Pérez-López and Pérez-Valera 2007), both being isolated by faulting from Pangea, which finally disintegrated in independent plates in Jurassic-Cretaceous time (Fig. 3.46).

The sediments deposited in the Triassic Betic basins mainly formed on an epicontinental shallow to moderately deep sea affected by alternating episodes of subsidence

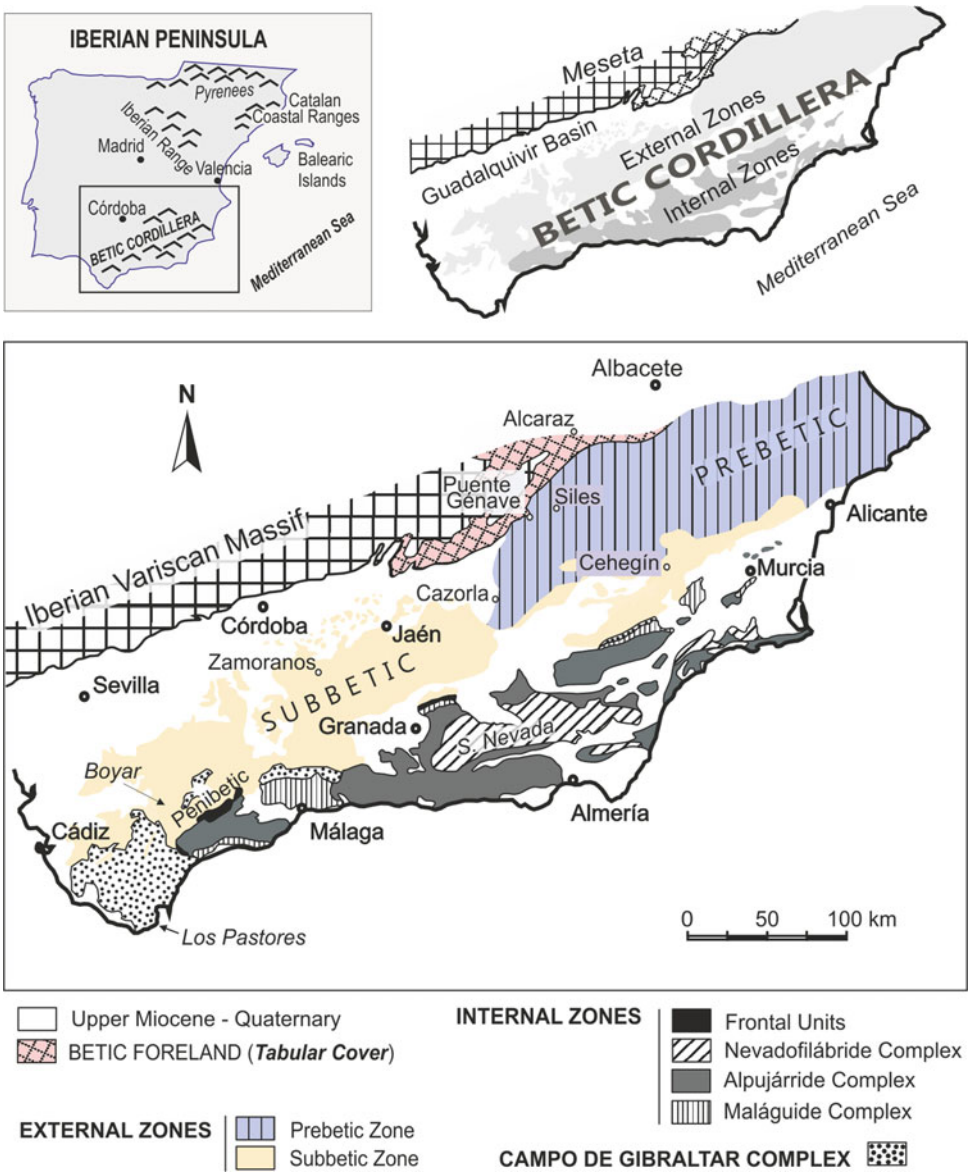

Fig. 3.45 Geological sketch map of the different tectonic units in the Betic Cordillera (S Spain). Modified from Pérez-López and Pérez-Valera (2007)

during the rifting phase. The extensional regime in SE Iberia existed since at least the Early Triassic. Extension progressed from E to W over time, in connection to younger antithetic normal faults that were created along the South-Iberian margin of the Iberian Massif. During the Permian-Late Triassic (early Norian), sedimentation took place in synrift terrestrial basins and, consequently, the Betic epicontinental platform was compartmentalised by fault systems which conditioned strong subsidence changes in different graben. Finally, from the Jurassic onwards, oceanic crust appeared locally (Vera 2001), thus defining the two continental margins that limited the Betic basin. These margins evolved differently to give rise to the South-Iberian paleomargin (now constituting part of the present-day Betic External Domain) and the Mesomediterranean paleomargin (now constituting part of the present-day Internal Domain). The Triassic sediments predating the formation of both margins were quite different. Those deposited on the South Iberian crust were related to the other Permian-Triassic basins of Iberia, and show epicontinental facies with many common stratigraphic and geodynamic evolutionary features.

The Triassic sediments related to the South-Iberian paleomargin, called "Southiberian Triassic" (Pérez-López and Pérez-Valera 2007), consist of two main facies belts, proximal and distal. The proximal facies belt is exclusively made of continental redbeds, defined as Hesperian Triassic by Sopeña et al. (1983) for the whole of Iberia. The distal facies belt consists of the epicontinental or Germanic facies that are now present in the External Zones (Prebetic and Subbetic), with the threefold classic division in: Buntsandstein (rarely exposed due to tectonics, Pérez-Valera et al.

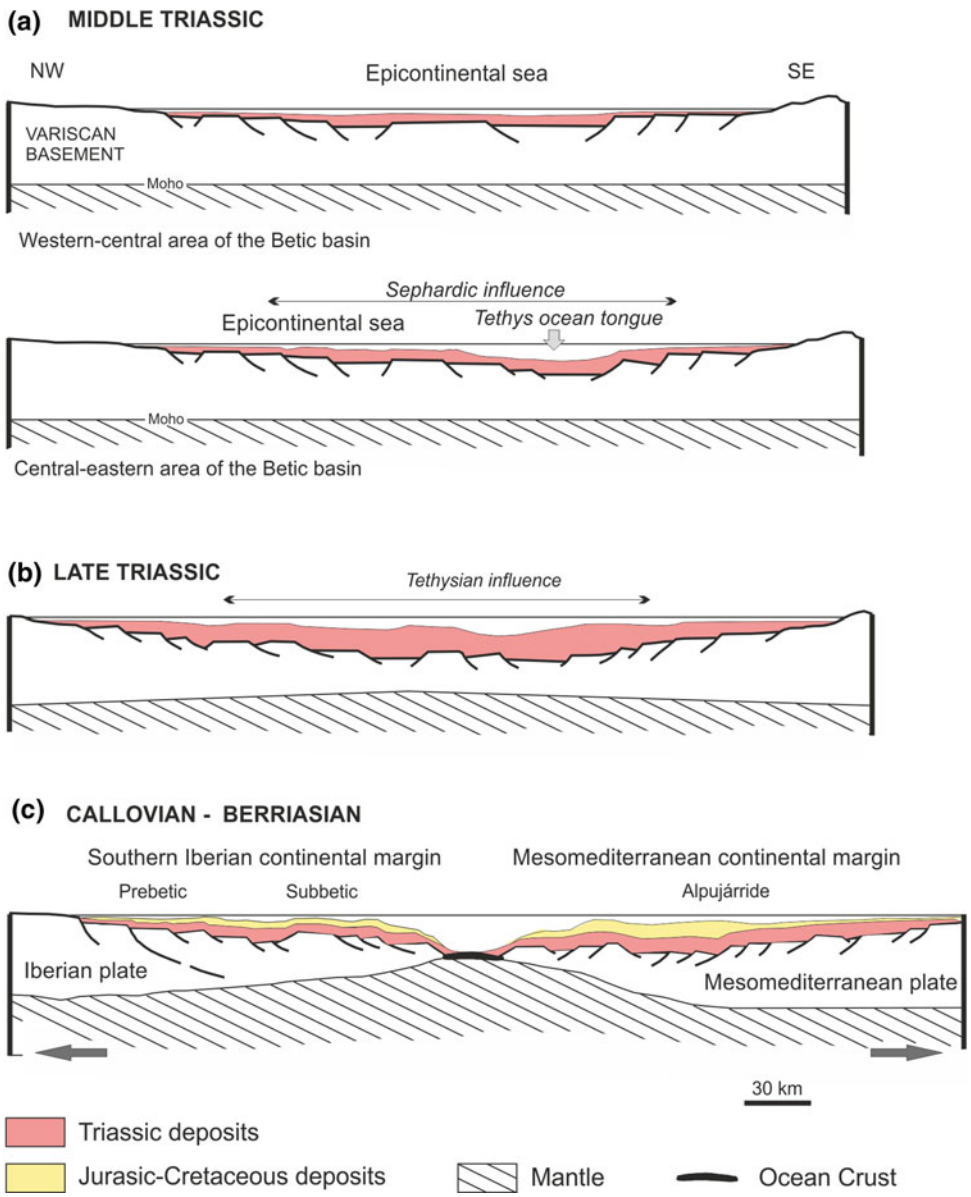

Fig. 3.46 Three-steps development of the Betic basin. A: Initial rifting and sedimentation stage of the Triassic deposits on an epicontinental platform. B: Deposition of thick carbonate units showing major Tethysian influence. C: Differentiation of two continental margins when ocean crust was created after the Triassic period. Modified from Pérez-López and Pérez-Valera (2007)

2000), representing the initial or tectonic rifting phase, and Muschelkalk and Keuper that constitute the mature rifting phase.

3.7.2 From Initial to Mature Rifting Phases

The Hesperian Triassic comprises Buntsandstein and Keuper facies but lack completely the carbonate Muschelkalk facies (Fernández et al. 1994). It crops out widely north of the central sector of the Betic Cordillera along the southeastern edge of the Variscan Iberian Massif, forming its unfolded sedimentary cover, the so-called "Tabular Cover", therefore properly outside of the Betic orogen. It is mentioned in recent publications by the name of TIBEM ("Triassic of the Iberian Meseta", Viseras et al. 2011; Henares et al. 2014, 2016). Fernández et al. (1994), Pérez-López and Pérez-Valera (2007), Arche and López-Gómez (2014) made a correlation between these redbeds and the Keuper facies units in the Prebetic Domain of the External Zones (Fig. 3.47). An important lateral increase in thickness has been well reported from the Tabular Cover to the Prebetic, where deep wells have cores of more than 1000 m of almost undisturbed Keuper facies (Carcelén and El Salobral wells, Ortí et al. 1996). Towards the S, the vast outcrops of Subbetic Triassic rocks clearly reveal enormous original stratigraphic thickness, especially in the Keuper facies.

Pérez-López (1991, 2000), Pérez-Valera (2005) and Pérez-Valera and Pérez-López (2008) synthesized the Triassic stratigraphy of the Prebetic and Subbetic

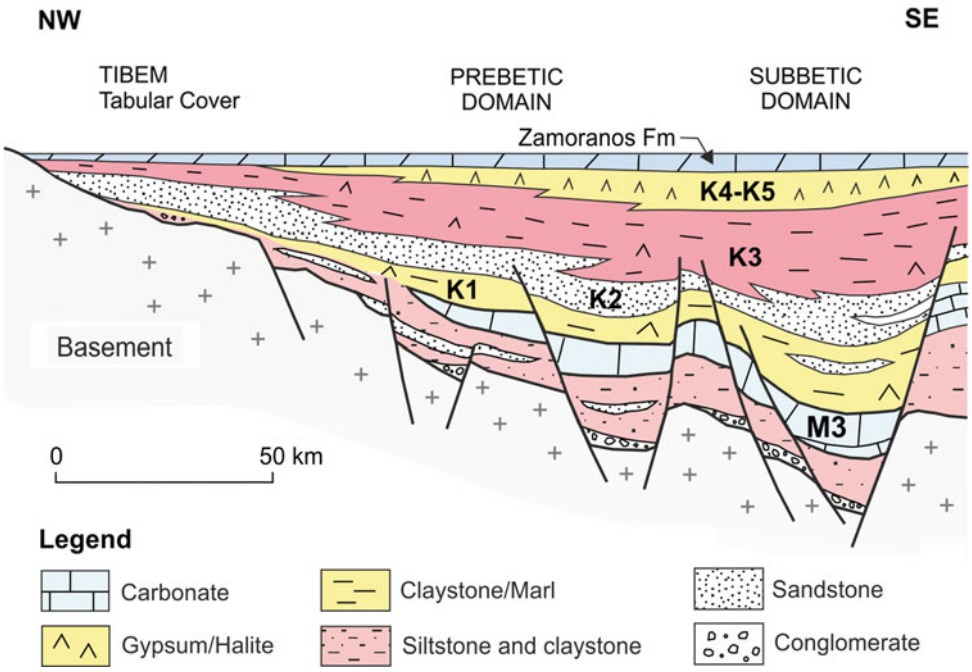

Fig. 3.47 Paleogeographical reconstruction of the Triassic basins along a Tabular Cover (TIBEM)–Betic basin profile, where it is possible to make a correlation between the main Triassic units in several domains controlled by the rifting phase. Modified from Pérez-Valera and Pérez-López (2008)

tectonostratigraphic units by distinguishing (Fig. 3.48): one package of Muschelkalk carbonates, which is defined by two formations (Cehegín Fm and Siles Fm, Fig. 3.49); five detrital and evaporitic formations constituting the Jaen Keuper Group; and finally, one upper carbonate formation of Norian age (Zamoranos Fm). This general stratigraphic frame can be maintained with only few variations up to the tectonic units lying close to the front of the Internal Zones. Nonetheless, there exist important lateral changes in sediment thickness, and a general trend of facies change towards more open marine environments southwards and eastwards in the Triassic Betic basin, showing progressively more pronounced Alpine influences.

The Muschelkalk carbonates, which are absent in the Hesperian Triassic, are already present in the outermost Prebetic tectonic imbricate units, showing a gradual increase in thickness towards the interior of the basin. They also show slightly more proximal features in the Prebetic (Siles Fm) than in the External and Medium Subbetic (Cehegin Fm), where they are much thicker although display the same sequential evolution (Fig. 3.49).

Towards the innermost part of the Subbetic domains a marked reduction of stratigraphic thickness is recorded in moderately disturbed Keuper successions of some tectonic units of the southernmost part of the western Medium Subbetic (Boyar) or the Penibetic, where the whole Keuper units' stratigraphy is preserved in ca. 100 m of succession. In some units close to the Internal-External zones' boundary (Tariquides of Los Pastores-Gibraltar: Durand-Delga et al. 2007), the Keuper facies are progressively replaced by dolomitic Alpine-like facies of Hauptdolomit type during the latest Carnian to Norian, including some alternance of marly-limy beds of Rhaetian age (Martín-Algarra et al. 1993). Muschelkalk facies are usually absent in inner Subbetic units due to tectonic causes but, when present, like in the westernmost Internal Subbetic (or Penibetic: Meleguetín Fm, Martín-Algarra 1987), their thickness is the greatest (sometimes over 200 m) and some of its facies display resemblances with the so-called Alpine Muschelkalk of the Alps and, in particular, with the Reifling Fm (H.J. Gawlick, pers. com. to AMA in 2004). Clearly, facies variability is due to differential subsidence in each of the sub-basins, while occupying different positions with respect to the open sea.

3.7.2.1 Storm Deposits in a Complex Epicontinental Platform

The Muschelkalk carbonates of the Betic basin were deposited during the late Anisian to the Ladinian in an epicontinental platform showing a transgressive-regressive megasequence evolution (Pérez-Valera and Pérez-López 2008). Most sediments formed in coastal and shallow-marine environments that were scattered across a wide platform with a complex paleogeography, with lagoons and restricted inland seas rapidly evolving in time due to changing wave energies related to currents and storm effects (Pérez-López et al. 2011). The most widespread sediment was originally lime mud, although bioclastic deposits are also common.

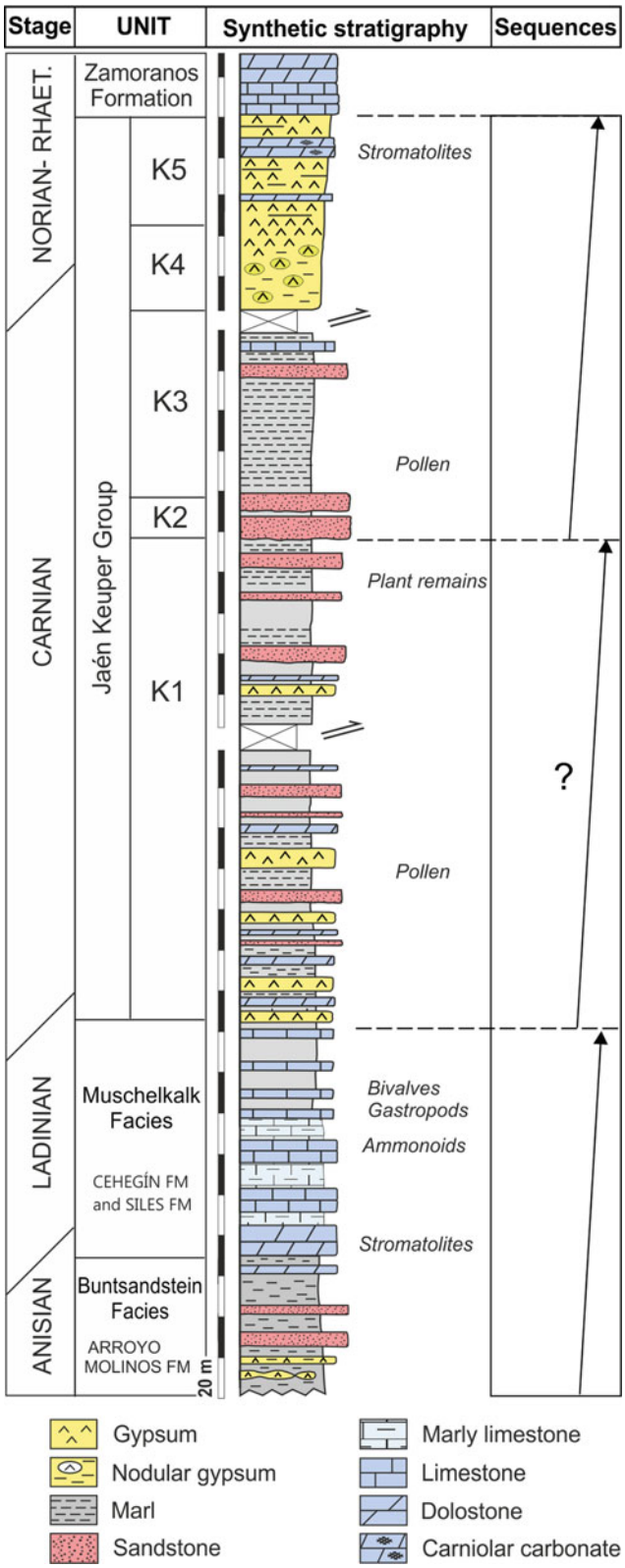

Fig. 3.48 Lithostratigraphic units of the epicontinental Triassic of the Betic External Zones. Unit thickness is approximate and the duration of the visual gaps due to dettachment faults in unknown

Microbial carbonates characterize the lower stratigraphic units and change upwards to bioclastic beds (occasionally bearing algae) as the most significant lithofacies of the upper units. According to available facies models (Pérez-Valera and Pérez-López 2008) there is no evidence of a seaward reef or an oolitic-bioclastic sandy barrier, and muddy sediments grade from deep-water to intertidal environments. It is evident that there were emerged areas or supratidal zones within this complex epicontinental platform. This context defines the variability of sedimentary environments like a mosaic of extensive lagoons and tidal flats.

In addition, the Triassic Betic basin was located at paleolatitudes where hurricanes were certainly common (Pérez-López and Pérez-Valera 2012). Platform evolution is now reflected in storm deposits, which are frequent and the most significant high-energy deposits in the epicontinental carbonate platform. Nonetheless, storm deposits are not present in all sections due to the complex paleogeography of the basin and to tectonic disturbances of the original succession.

The lithofacies, thickness and type of tempestites present in different sections help to understand the sea level evolution and subsidence changes during the transgressive-regressive megasequence evolution mentioned above. These features are more variable in the lower part of the carbonate sections than in the upper one. Besides, there was a rifting phase pulse during the deposition of these lower carbonates, which accounted accordingly for a bypass-zone tempestite model: pot and gutter casts related to storms developed during the transgressive stage, when siliciclastic coastal flats were flooded and transformed in wide carbonate ramps with a well-defined profile at the edge of the epicontinental basin (Fig. 3.49). In the subsequent highstand stage, the typical graded tempestite beds with laminations were deposited in shoreface zones. In this latter stage, stratigraphic successions display shallowing-upward sequences in which storm deposits are scarce towards the top. The presence of protected environments conditioned the sedimentation of the winnowed storm deposits that define the winnowed tempestite model (Pérez-López and Pérez-Valera 2012). Frequently these restricted lagoons or inland seas were interconnected to the open ocean, since cephalopods appear in some successions in upper stratigraphic positions.

The sediments of the highstand phase were deposited when the platform started to compartmentalize into lagoons, perhaps forming a “mosaic” of lagoons or inland seas. This shallow and complex paleogeography was related to differential subsidence, which lead to a shallow depth of the platform over a long time span. Subsidence permitted stabilization of shallow environments in time but not space. Finally, a fall in sea level conditioned the deposition of Keuper coastal facies across the entire region.

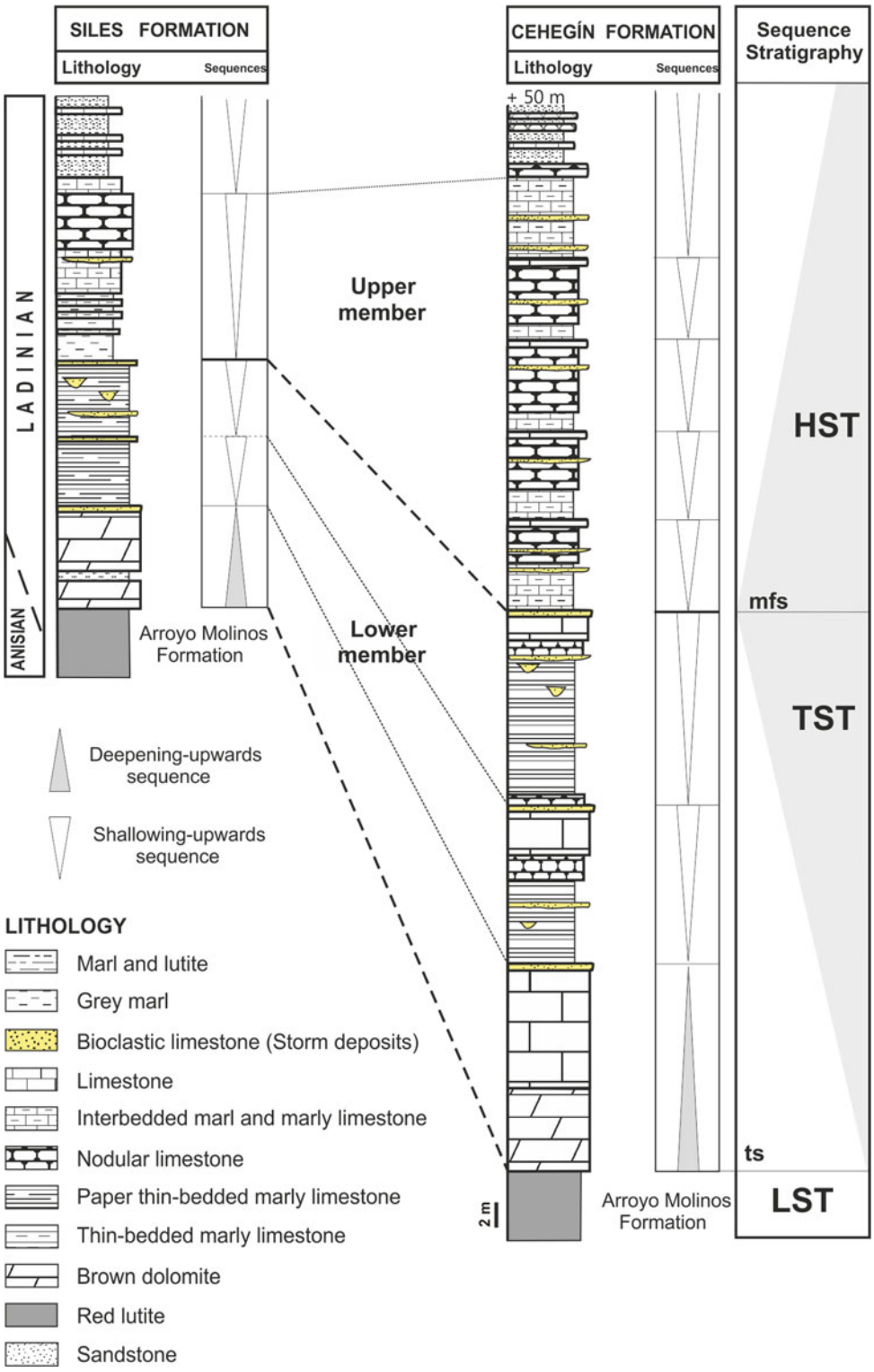

Fig. 3.49 Stratigraphy of the two formations which define the Muschelkalk carbonates in the Betic External Zones: The Siles Fm was defined in the proximal areas close to the Iberian Massif; and the Cehegín Fm was defined in the deeper areas of the Triassic platform. Depositional sequences are indicated; LST: Lowstand System Tract, TST: Transgressive System Tract, HST: Highstand System Tract. Modified from Pérez-Valera and Pérez-López (2008)

3.7.3 Eustatic and Tectonic Control During the End of the Mature Rifting Phase of Keuper Facies Sedimentation

The lower Keuper unit (K1 unit) shows thicknesses in the order of hundreds of meters and is made entirely of interbedded facies deposited in a coastal-plain depositional system where a metastable equilibrium existed between sea level change, sediment supply and subsidence related to tectonics. This unit consists of a multi-coloured clayey succession with thin intercalations of carbonates, gypsum and fine-grained sandstones (Figs. 3.48 and 3.50). Locally, lignite beds appear higher in this unit; dark clay horizons bearing Carnian pollen are sometimes present and also rare thin levels of oolitic limestone and sandy/bioclastic limestone with Carnian bivalves (e.g. Martín-Algarra et al. 1993, 1995). The thickest packages of gypsum, which occur in the lower Keuper unit, have intercalations of layered carbonates with evaporitic pseudomorphs. Locally, extremely thin (10–20 cm) sand layers have horizontal or ripple lamination. In some places, thicker sand packages (from 1 to 5 m) show erosive bases, cross-stratification and horizontal bedding or ripples towards the top of the sequences. Finally, associated with the sediments of this unit, halite deposits also exist that, despite not crop out, can be inferred from the many saline springs and gullies frequently draining these deposits, which make evident that the seawater was never far from the K1 unit depositional environment.

This variability in the lower Keuper sediments does not display a clear trend of facies evolution, preventing sequence to be applied. They can be very thick monotonous alternations of claystone, gypsum, sandstone, carbonate and mixed facies beds, but no regular cyclicity can be ascertained. Subsidence was significant but sea level was more or less locally constant, which produced frequent spatial variations of sedimentary environments. These deposits were

Fig. 3.50 K1 unit outcrop characterized by alternations of beds of different nature, with variegated colour (picture taken at the southern Jaen province)

expansive because they reached the western edge of the basin, where they were deposited above the first continental sediments over the Variscan basement (Stable Meseta).

The base of the K2 unit regionally corresponds to an erosional surface that is interpreted as a major discontinuity. Above this surface, the succession shows mainly the following facies trend (Fig. 3.48): sandstone, red clay and gypsum to the top. The deposition of K2 was certainly related to a major sequence boundary which was probably associated with a combination of eustatic and climatic phenomena related to the Carnian Pluvial Event (Arche and López-Gómez 2014). This allowed widespread deposition of fluvial sandstone in and around the Iberian continent, also at its southern margin.

The major sediment storage occurred during the transgressive phase related to the deposition of the K3 unit (constituted mainly by red clay). This was due to an increase in accommodation space associated with a relatively rapid rise in the base level (Pérez-López 1996). In the lowstand and highstand phases, the eustatic movements were masked by local tectonic factors, which to some degree more directly controlled the sedimentation in these phases.

The upper Keuper facies sediments consist mainly of claystone with nodular gypsum (K4 unit) and laminated gypsums to the top (K5 unit). The presence of evaporites, as significant facies in the upper part of the Keuper facies units, is interpreted as evidence of a marine influence in this coastal depositional system during the Norian, due to a relative rise in the sea level (Fig. 3.51). This evaporitic facies are correlatable to other Triassic basins in the Iberian Peninsula (Ortí et al. 2017).

3.7.4 Neotethys Opening and Development of the New Sephardic Province

The epicontinental basins with Germanic facies of the Iberian Peninsula were at some time in their history connected

Fig. 3.51 Gypsum, as the main lithology of the Keuper facies successions, marks the marine influence in all basins due to a relative sea level rise (picture from the southern Jaen province)

to the Tethys, as demonstrated by the fossils found in the Muschelkalk carbonates and, locally, in the lower part of some Keuper sections (Martín-Algarra et al. 1995). Sopeña et al. (1983) observed in some of the Muschelkalk facies outcrops in Cataluña, Valencia, Castellón and Teruel a particular biofacies, other than the Germanic with Alpine influence. Previously, Hirsch (1972, 1975, 1977) coined the term "Sephardic province" to distinguish a vast paleogeographic area comprising many sectors of the Iberian Peninsula and the E Mediterranean regions (Fig. 3.52). This author found an "evolution autonomy" of species, which was independent with respect to that of the Tethyan regions but with some Alpine influence in its fauna, as well as a diachronic migration of bivalves from the Middle East to the "circummediterranean terrains" (Hirsch and Márquez-Aliaga 1988; Márquez 2005). It seems reasonable to assume that the endemic fauna of the Sephardic province reached the Iberian central-eastern platforms via the Betic basin during transgressive stages and, actually, the faunal assemblages of different shallow platforms of the Betic basin were probably

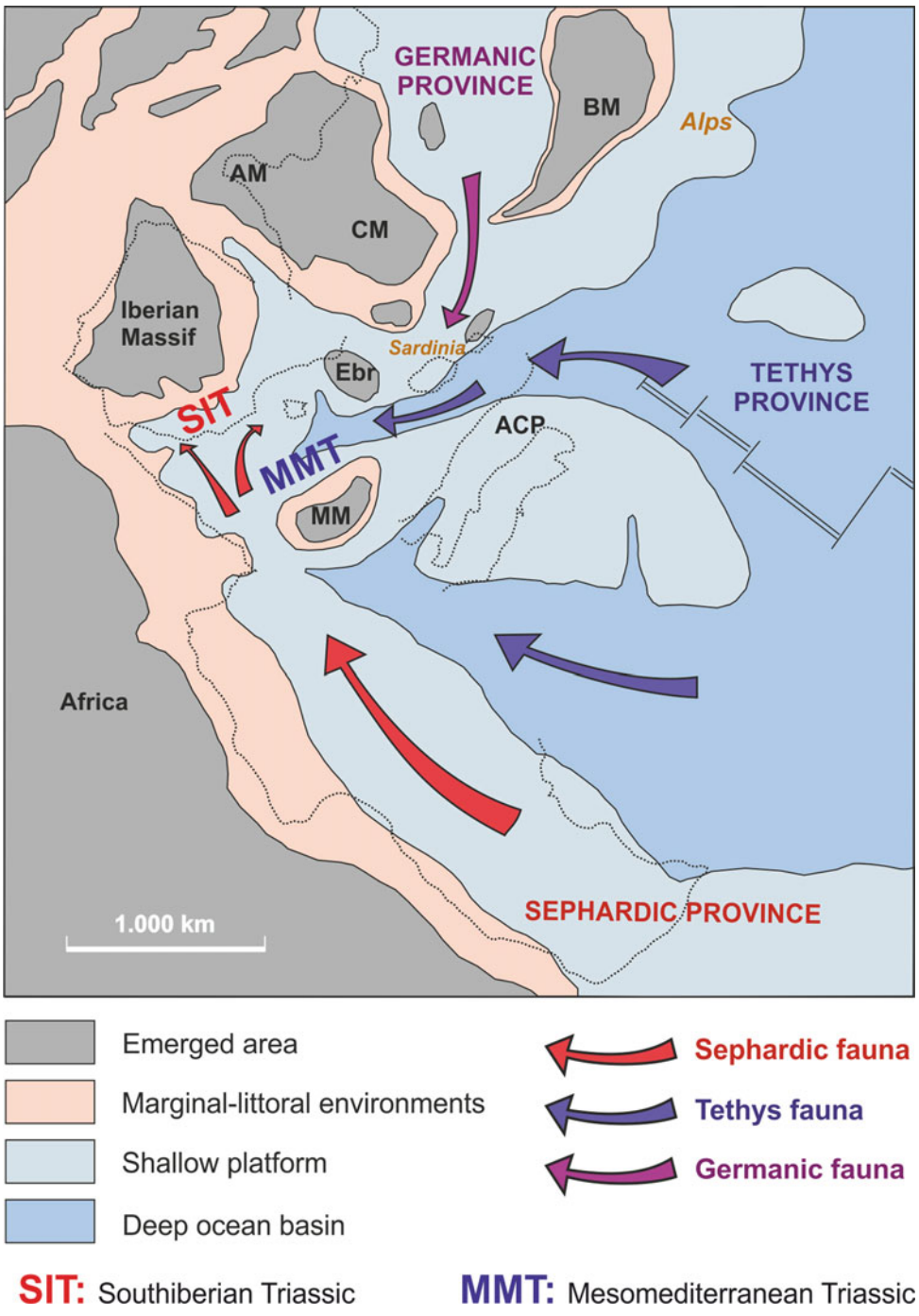

Fig. 3.52 Paleogeographical reconstruction of the westernmost Tethys area for the Middle Triassic. Faunal movements are indicated with arrows. AM: Armorican Massif; BM: Bohemian Massif; CM: French Central Massif; Ebr: Ebro Massif; MM: Mesomediterranean Massif; ACP: Apennine Carbonate Platform. *Main Sources* Márquez-Aliaga and Hirch (1988), Decourt et al. (1993), Pérez-López et al. (2003), Martín-Algarra and Vera (2004), Márquez (2005) and Pérez-Valera (2015)

not so different to each other, as Ladinian fossils characteristic of the Sephardic province have been collected in different Betic domains, either external (Prebetic, Subbetic) or internal (Alpujárride, Maláguide).

Presence of the foraminifers *Lamelliconus ventroplanus* (Oberhauser), *Lamelliconus cordevolicus* (Oberhauser), *Lamelliconus procerus* (Liebus), in the lower Ladinian carbonates of the Betic Cordillera (Pérez-López et al. 2005), suggests the arrival of these fauna from similar assemblages of the Sephardic domain, which in Israel appear in levels dated as "late Fassanian" (early Ladinian) (Benjamini 1988). These species were to become very important in Alpine basins by the late Ladinian (Márquez 2005). At the end of the Ladinian, before the regression related to the development of the Keuper facies, a wide shallow platform became established allowing a generalized colonization by bivalve faunas typical of the Sephardic province, including: *Costatoria kiliani* (Schmidt), *Pseudoplacunopsis teruelensis* (Wurm), *Gervillia joleaudi* (Schmidt), among other species (Márquez-Aliaga and Ros 2003).

Cephalopod assemblages (ammonoids and nautiloids) found in the Betic External Zones have recently allowed the construction of a biostratigraphical framework for the Ladinian stage (Pérez-Valera 2015; Pérez-Valera et al. 2016). The species are mostly from the Sephardic province, as *Gevanites epigonus*, *Protrachyceras hispanicum* and *Picardiceras picardi*, although also ammonoids of broader geographical distribution appear, e.g. *Eoprotrachyceras curionii* and nautiloids as *Germanonautilus bidorsatus*. These fossil associations indicate that the opening of the Neotethys, and the associated sea level rise, caused the development of the Sephardic southern platform and other platforms with their endemisms. Thus, during the Ladinian, the Southiberian area was a paleogeographical region open to faunal exchange between the Germanic, Tethyan and Sephardic provinces (Fig. 3.52).

3.7.5 Magmatism and Tectonic Signatures in the Sediments

The study of several sections reveals that subsidence controlled by tectonics varied across hundreds of kilometres in southern Spain according to thickness variations in stratigraphic successions. These variations are especially evident in the Muschelkalk carbonate units of the Subbetic Zone,

Fig. 3.53 Load structure probably caused by seismic shaking (Muschelkalk facies carbonates at the lower part of the Cehegín Fm)

although the influence of the tectonics is recorded also in the different thickness of the Keuper facies units. Besides, several features are present in the Triassic successions that indicate tectonic activity as magmatism and sedimentary structures related to earthquakes.

Muschelkalk carbonates harbour signatures of tectonically controlled sedimentation. Many syndepositional deformational structures such as slumps, slide planes or parallel shear surfaces induced by earthquakes were recognised in the lower member of the Cehegín Fm (Muschelkalk facies). Internal breccias associated with these structures were also detected, which were deposited in what was a muddy carbonate ramp context that developed during the transgressive stage of Ladinian age. Bioclastic limestone beds with soft-sediment deformational structures are also present in the lower member of the Cehegín Fm, as load structures or ball-and-pillow structures that could have a tectonic origin (Fig. 3.53). The latter structures are thus interpreted as seismites.

In the tempestites of the Muschelkalk carbonates, some bioclastic grainstones, floatstones or rudstones display features of dewatering processes, which can be related to tsunamites and seismic activity. Despite this, sometimes their primary origin is not easy to recognize. When examining supposed storm deposits, tsunamites and seismites cannot be ruled out. The different subsidence of each area and these peculiar syndepositional deformational structures of the Muschelkalk carbonates point to tectonic activity, associated with the rifting phase, in the Triassic epicontinental platform during the Ladinian of the Betic basin.

The rifting phase is also recognized by the presence of volcanic rocks, specially in the upper part of the Keuper facies deposits (K3 unit). Numerous outcrops of subvolcanic rocks appear in siliciclastic sediments. Morata (1990) described some intrusions of magma in red clays with significant water content. Whole-rock geochemical characteristics and primary mineralogical compositions allow defining a tholeiitic affinity for the Triassic magmatism, although some bodies are transitional to alkaline (Morata et al. 1997). Tholeiitic magmatism was generated during this Triassic extensional stage. After this magmatic event, and as a consequence of an increment of the extensional regime with important continental lithosphere thinning, transitional alkaline magmatism occurred (Portugal-Ferreira et al. 1995).

Magma genesis was plausibly triggered by extensional tectonic activity, marking the onset of a tectono-magmatic cycle that from the post-Variscan rifting phase progressively evolved, by ascent of the asthenosphere, toward continental breakup and opening of the Neotethys and the Atlantic and Alpine Tethys oceans, accompanied by intrusion/extrusion of basic magmas along their continental margins (Puga et al. 2010).

References

Alibert C (1985) A Sr-Nd isotope and REE study of Late Triassic dolerites from the Pyrenees (France) and the Messejana Dyke (Spain and Portugal). Earth Planet Sci Lett 73: 81–90. https://doi.org/10.1016/0012-821x(85)90036-6

Algeo TJ, Chen Z, Fraiser M, Twitchett RJ (2011) Terrestrial-marine teleconnections in the collapse and rebuilding of Early Triassic marine ecosystems. Palaeogeography, Palaeoclimatology, Palaeoecology 308: 1–11

Allen PA, Allen JR (2005) Basin analysis: Principles and applications, second ed. Blackwell, Oxford

Aller J, Álvarez-Marrón J, Bastida F, Bulnes M, Heredia N, Marcos A, Pérez-Estaun A, Pulgar JA, Rodríguez-Fernández LR (2004) Zona Cantabrica: Estructura, Deformación y Metamorfismo. In: Vera JA (ed) Geologia de España SGE-IGME. pp 42–47

Alonso-Azcárate J, Arche A, Barrenechea JF, López-Gómez J, Luque J, Rodas M (1997) Palaeogeographical significance of the clay minerals in the Permian and Triassic sediments of the SE Iberian Ranges. Palaeogeography, Palaeoclimatology, Palaeoecology 136: 309–330

Álvaro M (1987) La tectónica de cabalgamientos de la Sierra Norte de Mallorca (Islas Baleares). Bol Geol Min 94: 34–41

Álvaro M, Del Olmo P, Battle A (1991) Sóller [map] (1:50 000) MAGNA Hoja 670, Segunda serie. IGME Report and Map, p 62

Álvaro M, Apalategui O, Baena J, Balcells R, Barnolas A, Barrera JL, Bellido F, Cueto LA, Díaz De Neira A, Elízaga E, Fernández-Gianotti JR, Ferreiro E, Gabaldón V, García-Sansegundo J, Gómez JA, Heredia N, Hernández-Urroz J, Hernández-Samaniego A, Lendínez A, Leyva F, López-Olmedo FL, Lorenzo S, Martín L, Martín D, Martín-Serrano A, Matas J, Monteserín V, Nozal F, Olive A, Ortega E, Piles E, Ramírez JI, Robador A, Roldán F, Rodríguez LR, Ruiz P, Ruiz MT, Sánchez-Carretero R, Teixell A, Oliveira JL, Pereira E, Ramalho M, País J (1995) Mapa Geológico de la Península Ibérica, Baleares y Canarias [map] (1: 1.000.000) IGME

Álvarez-Ramis C, Fernández-Marrón T, Calafat F (1995) Avance sobre la megaflora triásica, en facies germánica, de Estellencs (sector noroccidental de la Sierra de Tramontana, Mallorca). Revista Española de Paleontología, Libro Homenaje a Guillermo Collom, p 55–98

Álvarez-Ramis C, Grauvogel-Stamm L (1996) Coniferres et polen in situ du Buntsandstein de I´ile de Majorque (Baleares, Espagne). Cuad Geol Iber 20: 229–243

Anadón P, Colombo F, Esteban M, Marzo M, Robles S, Santanach P, Sugrañés L (1979) Evolución tectonoestratigráfica de los Catalánides. Acta Geológica Hispánica 14: 242–270

Angiolini L, Crippa G, Muttoni G, Pignatti J (2013) Guadalupian (Middle Permian) paleobiogeography of the Neotethys Ocean. Gondwana Research 24: 173–184

Arche A, Díez JB, López-Gómez J (2007) Identification of the Early Permian (Autunian) in the subsurface of the Ebro Basin, NE Spain, and its paleogeographic consequences. Journal Iberian Geology 33:125–133

Arche A, López-Gómez J (1992) Una nueva hipótesis sobre las primeras etapas de evolución tectonosedimentaria de la cuenca pérmico-triásica del SE de la Cordillera Ibérica. Cuadernos Geología Ibérica 16: 113–143

Arche A, López-Gómez J (1996) Origin of the Permian-Triassic Iberian Basin, central-eastern Spain. Tectonophysics 266: 443–464

Arche A, López-Gómez J (1999a) Tectonic and geomorphic control son the fluvial styles of the Eslida Formation, Middle Triassic, Eastern Spain.Tectonophysics 315: 187–207

Arche A, López-Gómez J (1999b) Subsidence rates and fluvial architecture of rift-related Permian and Triassic alluvial sediments of southeast Iberian Range, eastern Spain. Spec. Publs. Int. Ass. Sediment. 28: 283–304

Arche A, López-Gómez J (2005) Sudden changes in fluvial style across the Permian-Triassic boundary in the eastern Iberian Ranges, Spain: Analysis of possible causes. Palaeogeography, Palaeoclimatology, Palaeoecology 229(1–2): 104-106

Arche A, López-Gómez J (2006) Late Permian-Early Triassic transition in Central and NE Spain: Biotic and sedimentary characteristics. In: Lucas S, Cassinis G, Schneider J (eds): Non-Marine Permian Biostratigraphy and Biochronology. Geological Society of London, Spec Publ 265: 261–280 London

Arche A, López-Gómez J (2007) The Minas de Henarejos basin (Iberian Ranges, Central Spain): precursor of the Mesozoic rifting or a relict of the late Variscan orogeny? New sedimentological, structural and biostratigraphic data. Journal of Iberian Geology 33 (2): 237–248

Arche A, López-Gómez J (2014) The Carnian Pluvial Event in WesternEurope: new data from Iberia and correlation with the Western Neotethys and Eastern North America-NW Africa regions. Earth-Science Reviews 128: 196–231. https://doi.org/10.1016/j.earscirev.2013.10.012

Arche A, López-Gómez J, Vargas H (2002) Propuesta de correlación entre los sedimentos pérmicos y Triásicos de la Cordillera Ibérica Este y de las Islas Baleares. Geogaceta 32: 275–278

Arche A, López-Gómez J, Marzo M, Vargas H (2004) The siliciclastic Permian-Triassic deposits in Central and Northeastern Iberian Peninsula (Iberian, Ebro and Catalan Basins): A proposal for correlation. Geol. Acta 2: 305–320

Arnal I, Calvet F, Márquez L, Solé De Porta N, Trifonova E (1994) Estratigrafía y Sedimentología de la Formación Isábena (Retiense), Pirineos centrales y orientales. III Coloquio de Estratigrafía y Paleogeografía del Pérmico y Triásico de España, Cuenca, Resúmenes pp 11–12

Arribas J (1984) Sedimentología y diagénesis del Buntsandstein y Muschelkalk de la Rama Aragonesa de la Cordillera Ibérica (Provincias de Soria y Zaragoza). Unpublished PhD Thesis, Universidad Complutense, Madrid, Spain

Arribas J (1985) Base litoestratigráfica de las facies Buntsandstein y Muschelkalk en la Rama Aragonesa de la Cordillera Ibérica (zona N). Estudios Geológicos 41: 47–57

Arribas J, Gómez-Gras D, Rosell J, Tortosa A (1990) Estudio comparativo entre las areniscas paleozoicas y triásicas de la Isla de Menorca: Evidencias de procesos de reciclado. Rev. Soc. Geol. España 3 (1–2): 105-116

Arribas J, Mas R, Arribas ME, Ochoa M, González-Acebrón L (2007) Sandstone petrofacies in the northwestern sector of the Iberian Ranges. Journal of Iberian Geology 33: 191–206

Arthaud F, Matte F (1977) Late Paleozoic strike–slip faulting in Southern Europe and Northern Africa: result of a right lateral shear zone between the Appalachians and the Urals. Geological Society of America Bulletin 88: 1305–1320

Aubele K, Bachtadse V, Muttoni G, Ronchi A, Durand M (2012) A Paleomagnetic Study of Permian and Triassic rocks from the Toulon-Cuers Basin, SE France: evidence for intra-Pangea block rotations in the Permian. Tectonics 31 (3): TC3015. https://doi.org/10.1029/2011tc003026

Azambre B, Fabriès J (1989) Mesozoic evolution of the upper mantle beneath the eastern Pyrenees: Evidence from xenoliths in Triassic and Cretaceous alkaline volcanics of the eastern Corbières (France). Tectonophysics 170 (3–4): 213–230. https://doi.org/10.1016/0040-1951(89)90272-2

Azambre B, Rossy M, Lago, M (1987) Petrology of tholeiitic Triassic dolerites (ophites) from the Pyrenees. Bull Mineral 110 (4): 379–396

Barnolas A, Pujalte V (2004) La Cordillera Pirenaica: Definición, límites y división. In: Vera JA (ed) Geología de España, SGE-IGME, Madrid, p 233–241

Barón A, Fornos J J, Gelabert B, Obrador A, Pomar L, Ramos E, Sàbat F (2004) Baleares. In: J A Vera (ed) Geología de España. SGE-IGME. Madrid. p 450

Bartrina T, Hernández E (1990) Las unidades evaporíticas del Triásico del subsuelo del Maestrazgo. In: Ortí F, Salvany JM (eds) Formaciones evaporíticas de la Cuenca del Ebro y cadenas periféricas, y de la zona de Levante. ENRESA-Universitat de Barcelona, Barcelona, p 34–38

Bartrina T, Cabrera L, Jurado MJ, Guimerá J, Roca E (1992) Evolution of the central Catalan Margin of the Valencia trough, Western Mediterranean. In: Banda E, Santanach (eds) Geology and Geophysics of the Valencia Trough Western Mediterranean. Tectonophysics 203 (1–4): 219–247

Beauseigneur C, Rangheard Y (1968) Contribution a l'étude des roches éruptives de l'île d'Ibiza. Bull Soc Géol France 3 (5): 9–12

Benjamini C (1988) Triassic Foraminifera from Makhtest, central Neguev, Southern Israel. Revue de Paleobiologie, Vol Spec 2: 129–144

Benton MJ (1991) What really happened in the Late Triassic? Historical Biology 5: 263–278

Benton M J (2003) When Life Nearly Died: The Greatest Mass Extinction of All Time. London, Thames & Hudson, 336 p

Benito MI, De La Horra R, Barrenechea JF, López-Gómez J, Rodas M, Alonso-Azcárate J, Arche A, Luque J (2005) Late Permian continental sediments in the SE Iberian Ranges eastern Spain: petrological and mineralogical characteristics and palaeoenvironmental significance. Palaeogeography, Palaeoclimatology, Palaeoecology 229, 24–39

Bercovici A, Díez JB, Broutin J, Bourquin S, Linol B, Villanueva-Amadoz U, López-Gómez J, Durand M (2009) A palaeoenvironmental analysis of Permian sediments in Minorca (Balearic Islands, Spain) with new palynological and megafloral data. Review of Palaeobotany and Palynology 158: 14–28

Berra F (2012) Sea-level fall, carbonate production, rainy days: How do they relate? Insight from Triassic carbonate platforms (Western Tethys, Southern Alps, Italy). Geology 40 (3): 271–274

Besems RE (1981a) Aspects of Middle and Late Triassic palynology. 1. Palynostratigraphical data from the Chiclana de Segura Formation of the Linares-Alcaraz region (SE Spain) and correlation with palynological assemblages from the Iberian Peninsula. Rev. Paleobot. Palynol. 32: 257–273

Besems RE (1981b) Aspects of Middle and Late Triassic palynology. 2. Preliminar palynological data from the Hornos-Siles Formation of the Prebetic zone, NE province of Jaén (SE Spain). Rev Paleobot Palynol 32:389–400

Béthoux O, De la Horra R, Benito M, Barrenechea JF, Galán-Abellán B, López-Gómez J (2009) A nex triadotypomorphan insect from the Anisian (Middle Triassic) Buntsandstein facies, Spain. Jour Iber Geol 35 (2): 179–184

Béziat D, Joron JL, Monchoux P, Treuil M, Walgenwitz F (1991) Geodynamic implications of geochemical data for the Pyrenean ophites (Spain-France). Chem Geol 89(3–4):243–262. https://doi.org/10.1016/0009-2541(91)90019-n

Bialik OM, Korngreen D, Benjamini C (2013) Carnian (Triassic) aridization on the Levant margin: evidence from the M1 member, Mohilla Formation, Makhtesh Ramon, south Israel. Facies 59: 559–581

Biddle KT (1984) Triassic sea level changes and the Ladian-Carnian boundary. Nature 308: 631–633

Bixel F (1984) Le volcanisme Stephano–Permien des Pyrénées. Ph.D. Thesis, Université Paul Sabatier, Toulouse, p 342

Bixel F (1987) Le Volcanisme Stéphano-Permien des Pyrénées pétrographie, minéralogie, géochimie. Cuadernos de Geología Ibérica 11: 41–35

Bixel F, Lucas Cl (1983) Magmatisme tectonique et sedimentation dans les fosses stephano-permiens des Pyrénées occidentales. Revue de Geographie Physique et Geologie Dynamique 24 (4): 329–342

Bixel F, Lucas Cl (1987) Approche Geodynamique du Permien et du Trias des Pyrénées dans le cadre du Sudouest europeen. Cuadernos de Geología Ibérica 11: 57–81

Blumenthal M (1927) Versuch einer tektonischen gliederug der betischen cordilleren von Central, und Sud-West Andalusien. Eclogue Geologicae Helvelicac 20: 487–592

Boillot G, Dupeuble PA, Malod J (1979) Subduction and Tectonics on the continental margin of northern Spain. Marine Geology 32: 53–70

Borruel-Abadía V, Galán-Abellán AB, Kustatscher E, Diéguez C, López-Gómez J, De la Horra R, Barrenechea JF, Arche A (2014) Palaeoenvironmental reconstruction of the early Anisian from sedimentology and plant remains in the SE Iberian Range (E Spain). Palaeogeography Palaeoclimatology Palaeoecology 414: 352–369

Borruel-Abadía V, López-Gómez J, De la Horra R, Galán-Abellán B, Barrenechea JF, Arche A, Ronchi A, Gretter N, Marzo M (2015) Climate changes during the Early–Middle Triassic transition in the E. Iberian plate and their palaeogeographic significance in the western Tethys continental domain. Palaeogeography, Palaeoclimatology, Palaeoecology 440: 671–689

Borruel-Abadía V, Barrenechea JF, Galán-Abellán AB, Alonso-Azcárate J, De la Horra R, Luque FJ, López-Gómez J (2016) Quantifying aluminium phosphate-sulphate minerals as markers of acidic conditions during the Permian-Triassic transition in the Iberian Ranges, E Spain. Chemical Geology 429: 10–20

Bourquin S, Durand M, Diez JB, Broutin J, Fluteau F (2007) The Permian–Triassic boundary and Lower Triassic sedimentation in western European basins: an overview. Journal of Iberian Geology 33 (2): 221–236

Bourquin S, Bercovici A, López-Gómez J, Diez JB, Broutin J, Ronchi A, Durand M, Arche A, Linol B, Amour F (2011) The Permian–Triassic transition and the onset of Mesozoic sedimentation at the northwestern peri-Tethyan domain scale: Palaeogeographic maps and geodynamic implications. Palaeogeography, Palaeoclimatology, Palaeoecology 299: 265–280

Bourrouilh R (1973) Stratigraphie, sédimentologie et tectonique de l´lle de Minorque et du North-Est de Majorque (Baléares): La terminaison nord-orientale des cordillères Bétiques en Mediterranée occidentale. Ph.D. Thesis, Univ. Paris VI, Vol 2, p 822

Boutet C, Rangheard Y, Rosenthal P, Visscher H, Durand-Delga M (1982) Découverte d'une microflore d'age Norien dans la Sierra Norte de Majorque (Baleares, Espagne). CR Acad Sci Paris 294 (2): 1267–1270

Bouzá J (1981) Contribuciones a la paleontología de Mallorca. Boll Soc Hist Nat Balears 25: 7–20

Brandes C, Tiedt C (1991) Petrographische Bestandsaufnahme der permotriassicchen Sandsteine Menorcas (Balearen, westliches Mittelmeer). N Jb Geol Paläont Mh H4:233–242

Brandner R (1984) Meerespiegelschwankungen und tectonik in der Trias der NW-Tethys. Jahrbuch Geologische Bundesant 126: 435–475

Breda A, Preto N, Roghi G, Furin S, Meneguolo R, Ragazzi E, Fedele P, Gianolla P (2009) The Carnian Pluvial Event in the Tofane area (Cortina d´Ampezzo, Dolomites, Italy). Geo Alp 6: 80–115

Briqueu L, Innocent C (1993) Datation U/Pb sur zircon et géochimie isotopique Sr et Nd du volcanisme permien des Pyrénées occidentales (Ossau et Anayet). Comptes Rendus de l´Academie des Sciences Serie II 316 (5): 623–628

Broutin J, Gisbert J (1985) Entorno paleoclimático y ambiental de la flora stephano-autuniense del Pirineo catalán. In: Proc. 10e Congrès du Carbonifère, Madrid, 3: 53–66

Broutin J, Doubinger J, Gisbert J, Satta-Pasini S (1988) Permières datations palynologiques dans les faciès Buntsandstein des Pyrénées catalanes espagnoles. Comptes Rendus de l'Académie des Sciences de Paris 2: 159–163

Broutin J, Ferrer J, Gisbert J, Nmila A (1992) Première découverte d´ une microflore thuringienne dans le faciès saxonien de l´ile de Minorque (Baléares, Espagne). Comptes Rendus de l'Académie des Sciences de Paris 315: 117–122

Broutin J, Cabanis B, Châteauneuf JJ, Deroin JP (1994) Évolution biostratigraphique magmatique et tectonique du domaine paléotéthysien occidental (SW de l'Europe): implications paléogéographiques au Permien inférieur. Bulletin Société Géologique de France 2: 163–179

Broutin J, Chateauneuf JJ, Galtier J, Ronchi A (1999) The Autunian of Autun: Will it remain a reference for the Early Permian continental deposits in Europe? Géologie de la France 2: 17–31

Bruguier O, Becq-Giraudon JF, Champenois M, Deloule E, Ludden J, Mangin D (2003) Application of in situ geochronology and accessory phase chemistry to constraining basin development during post-collisional extension: a case study from the French Massif Central. Chemical Geology 201: 319–336

Burg JP, Brun JP, Van Den Driessche J (1990) Le sillon houiller du Massif Central Français: faille de transfert pendant l'amincissement crustal de la chaine varisque? Comptes Rendus de l'Académie des Sciences de Paris 311: 147–152

Busnardo R (1975) Prébétique et subbétique de Jaén á Lucena (Andalousie). Introduction et Trias. Doc. Lab. Geol. Fac. Sci. Lyon, 66, 183 pp.

Cadenas P, Fernández-Viejo G (2017) The Asturian Basin within the North Iberian margin (Bay of Biscay): Seismic characterization of its geometry and its Mesozoic and Cenozoic cover. Basin Research: 29: 521–541

Cadenas P, Fernandez-Viejo G, Pulgar J A, Tugend J, Manatschal G, Minshull T A (2018) Constraints imposed by rift inheritance on the compressional reactivation of a hyperextended margin: mapping rift domains in the North Iberian margin and in the Cantabrian Mountains. Tectonics 37 (3): 758–785

Calafat F (1988) Estratigrafía y sedimentología de la litofacies Buntsandstein de Mallorca. Ph.D. Thesis, Barcelona University, Barcelona, p 126

Calafat F, Fornós JJ, Marzo M, Ramos-Guerrero E, Rodríguez-Perea A (1986) Icnología de vertebrados de la facies Buntsandstein de Mallorca. Acta Geológica Hispánica, 21–22: 515–520

Calvet F, Anglada E (1987) El Triásico del Pirineo. Análisis estratigráfico, cronoestratigráfico y sedimentológico. Informe Proyecto Síntesis del Pirineo. Instituto Tecnológico y Geominero de España. p 95. Unpublished

Calvet F, Marzo M (1994) El Triásico de las Cordilleras Costero Catalanas: Estratigrafía, Sedimentología, y Análisis Secuencial. III Col Estrat Paleontol Pérmico y Triásico de España. Cuenca, Spain. Field Trip, 53 p

Calvet F, Ramón X (1987) Estratigrafía, sedimentología y diagénesis del Muschelkalk inferior en los Catalanides. Cuad Geol Iber 11: 141–169

Calvet F, Tucker, M (1988) Outer ramp cycles in the upper Muschelkalk of the Catalan Basin, northeast Spain. Sedimentary Geology 57: 185–198

Calvet F, Tucker ME (1995) Mud-mound with reefal caps in the upper Muschelkalk (Triassic), eastern Spain. Spec Publs Int Assoc Sediment 23: 311–333

Calvet F, Tucker M, Henton J M (1990) Middle Triassic carbonate ramp systems in the Catalan Basin, northern Spain: facies, system tracts, sequences and controls. IAS Special Publication 9: 79–108

Calvet F, Solé de Porta N, Salvany JM (1993) Cronoestratigrafía (Palinología) del Triásico sudpirenaico y del Pirineo Vasco-Cantábrico. Acta Geológica Hispánica 28: 33–48

Calvet C, Anglada E, Salvany JM (2004) El Triásico de los Pirineos. In: Vera JA (ed) Geología de España, SGE-IGME, Madrid, p 272–274

Capote R, Muñoz JA, Simon JL, Liesa CL, Arlegui LE (2002) Alpine Tectonics 1: The Alpine system north of the Betic Cordillera. In: Gibbons W, Moreno MT (eds) Geology of Spain, Geol Soc London, London, p 367–400

Carreras FJ, Portero JM, Del Olmo P (1979) Reinosa [map] (1:50 000) MAGNA Hoja 83, Segunda serie. IGME Report and Map, p 38

Carreras J, Druguet E (2014) Framing the tectonic regime of the NE Iberian Variscan segment. In: Schulmann K, Martínez Catalán JR, Lardeau JM, Janousek V, Oggiano G (eds) The Variscan Orogeny: Extent, Time Scale and the Formation of the European Crust. Geol Soc Lond Spec Publ 405: 249–264

Cassinis G, Toutin-Morin N, Virgili C, (1995) A general outline of the Permian continental basins in southwestern Europe. In: Scholle PA, Peryt TM, Ulmer-Scholle DS (eds) The Permian of Northern Pangea, vol 2. Springer, Heilderberg, pp 135–157

Cassinis G, Di Stefano P, Massari F, Neri C, Venturini C (2000) Permian of south Europe and its regional correlation. In: Yin H, Shi GR, Tong J (eds) Permian-Triassic Evolution of Tethys and Western Circum-Pacific. Developments in Palaeontology and Stratigraphy 18: 37–70

Cassinis G, Durand M, Ronchi A (2003) Permian-Triassic continental sequences of Northwest Sardinia and South Provence: Stratigraphic correlations and palaeogeographical implications. Bollettino della Società Geologica Italiana, Volume Speciale 2: 119–129

Cassinis G, Ronchi A, Gretter N, Durand M (2008) The Val Daone Conglomerate: a Middle Permian key unit from the central Southern Alps (western Trentino, Italy), and regional strati- graphic implications. In: Cassinis G (ed) Stratigraphy and palaeogeography of late- and post-Hercynian basins in the Southern Alps, Tuscany and Sardinia (Italy), Vol 127(3). Boll Soc Geol It (Ital J Geosci), pp 519–532

Cassinis G, Perotti CR, Ronchi A (2012) Permian continental basins in the Southern Alps (Italy) and peri-mediterranean correlations. International Journal of Earth Sciences (Geologische Rundschau) 101: 129–157

Castillo F (1974) Le Trias évaporitique des basins de la Vallée de l'Èbre et de Cuenca. Bulletin Société Géològique France 16(6): 666–675

Cebriá JM, López-Ruiz J, Doblas M, Oyarzun R, Hertogen J, Benito R (2000) Geochemistry of the Quaternary alkali basalts of Garrotxa (NE Volcanic Province, Spain): a case of double enrichment of the mantle lithosphere. J Volcanol Geotherm Res 102: 217–235. https://doi.org/10.1016/s0377-0273(00)00189-x

Colodrón I, Cabañas I, Martínez C (1979) Flix [map] (1:50 000) MAGNA Hoja 444, Segunda serie. IGME Report and Map, p 24

Colom G (1975) Geología de Mallorca. Vol 1. Instituto de Estudios Baleáricos, Palma de Mallorca: 40–84

Conte JC, Carls P, Lago M, Gascón F (1987) Materiales stephano-pérmicos en la fosa de Fombuena (provincia de Zaragoza). Boletín geológico y minero 98 (4): 14–24

Cortesogno L, Cassinis G, Dallagiovanna G, Gaggero L, Oggiano G, Ronchi A, Seno S, Vanossi M (1998) The Variscan post-collisional volcanism in Late Carboniferous–Permian sequences of Ligurian Alps, Southern Alps and Sardinia Italy: a synthesis. Lithos 45: 305–328

Dal Corso J, Mietto P, Newton R, Pancost R D, Preto N, Roghi G, Wignall PB (2012) Discovery of a major negative 13C spike in the Carnian (late Triassic) linked to the eruption of Wrangelia flood basalts. Geology 40: 79–82

Dallagiovanna G, Gaggero L, Maino M, Seno S, Tiepolo M (2009) U-Pb zircon ages for post-Variscan volcanism in the Ligurian Alps (Northern Italy). Journal of Geological Society of London 166: 101–114

Dalloni M (1930) Etude géologique des Pyrénées de Catalogne. Annales de la Faculté des Sciences de Marseille 26: 1–373

Darder B (1914) El Triásico de Mallorca. Trabajos del Museo Nacional de Ciencias Naturales de Madrid, Ser Geol 6

De la Horra R, Benito MI, López-Gómez J, Arche A, Barrenechea JF, Luque FJ (2008) Palaeoenvironmental significance of Late Permian paleosols in the SE Iberian Ranges, Spain. Sedimentology 55 (6): 1849–1873. https://doi.org/10.1111/j.1365-3091.2008.00969.x

De la Horra R, Galán-Abellán AB, López-Gómez J, Barrenechea JF, Arche A (2011) Sedimentary analysis of the earliest Mesozoic continental record in the SE Iberian Basin, Spain: Paleogeographical and paleoclimatic significance. In: Bádenas B, Aurell M, Alonso-Zarza AM (eds) Abstracts 28th IAS Meeting of Sedimentology, University of Zaragoza, Zaragoza, p 87

De la Horra R, Galán-Abellán AB, López-Gómez J, Sheldon ND, Barrenechea JF, Luque FJ, Arche A, Benito MI (2012) Paleoecological and paleoenvironmental changes during the continental Middle–Late Permian transition at the SE Iberian Ranges, Spain. Global and Planetary Change 94–95: 46-61. https://doi.org/10.1016/j.gloplacha.2012.06.008

De Torres T, Sánchez A (1990) Espesores de las facies Keuper en la Rama Castellana de la Cordillera Ibérica y en el dominio Prebético. In: Ortí F, Salvany J (eds) Formaciones evaporíticas de la cuenca del Ebro y cadenas periféricas y de las cuencas de Levante. ENRESA 212–232

De Vicente G, Giner JL, Muñoz-Martín A, González-Casado JM, Lindo R (1996) Determination of present-day stress tensor and neotectonic interval in the Spanish Central System and Madrid Basin, central Spain. Tectonophysics 266: 405–424

De Vicente G, Vegas R, Muñoz Martín A, Van Wees JD, Casas Sáinz A, Sopeña A, Sánchez Moya Y, Arche A, López-Gómez J, Olaiz A, Fernández-Lozano J (2009) Oblique strain partitioning and transpression on an inverted rift: The Castilian Branch of the Iberian Chain. Tectonophysics 470: 224–242

Debon F, Enrique P, Autran A (1995) Magmatisme Hercynien. In: Barnolas A, Chiron JC (eds) Synthèse géologique et géophysique des Pyrénées. vol 1. Edition Bureau de Recherches Géologiques et Minières (France)—Instituto Tecnológico y Geominero de España (BRGM-ITGE), pp 361–499

Decarlis A, Dallagiovanna G, Lualdi A, Maino M, Seno S (2013) Stratigraphic evolution in the Ligurian Alps between Variscan heritages and the Alpine Tethys opening: A review. Earth-Science Reviews 125: 43–68

Decourt J, Ricou L E, Vrielynck B (1993) Atlas Tethys Palaeoenvironmental Maps. Gauthier-Villars, Paris

Delgado F, Estévez F, Martín JM, Martín-Algarra A (1981) Observaciones sobre la estratigrafía de la formación carbonatada de los mantos alpujárrides (Cordilleras Béticas). Estudios Geológicos 37: 45–57

Delgado F, López-Garrido AC, Martín-Algarra A, Alonso-Chaves FM, Andreo B, Estévez A, Orozco M, Sanz de Galdeano C (2004) Sucesiones carbonatadas triásicas. In: Vera J A (ed.) Geología de España. SGE-IGME, Madrid pp. 413–414

Denèle Y, Paquette J-L, Olivier P, Barbey P (2012) Permian granites in the Pyrenees: the Aya pluton (Basque Country). Terra Nova 24: 105–113

Deroin JP, Bonin B (2003) Late Variscan tectonomagmatic activity in Western Europe and surrounding areas: The mid-Permian episode. In: Decandia FA, Cassinis G, Spina A (eds) Special Proceedings International on Late Palaeozoic to Early Mesozoic events of Mediter- ranean Europe, and additional regional reports, Siena (Italy), April–May 2001. vol spec. 2. Bolletino della Società Geologica Italiana, Siena, pp 169–184

Dewey JF, Burke CA (1973) Tibetan, Variscan and Precambrian reactivation, products of a continental collision. Journal Geology 81: 683–692

Dibblee TW (1977) Strike-slip tectonics of the San Andreas fault and its role in Cenozoic basin developement. In: Late Mesozoic and Cenozoic Sedimentation and Tectonics in California, San Joaquin Geological Society Short Course, p 26–38

Dickinson WR (1985) Provenance relations from detrital modes of sandstones. In: Zuffa GG (ed) Provenance of arenites. NATO ASI Series C-148, Springer Netherlands, Dordrecht, pp 333–361

Diez JB (2000) Geología y Paleobotánica de la Facies Buntsandstein en la Rama Aragonesa de la Cordillera Ibérica. Implicaciones bioestratigráficas en el Peritethys Occidental. Ph.D. Thesis, Univ. Zaragoza and Univ. Paris, Paris

Diez J -B, Grauvogel-Stamm L, Broutin J, Ferrer J, Gisbert J, Liñán E (1996) Prèmiere dècouverte d´une paléoflore anisienne dans le faciés Buntsandstein de la Branche Aragonaise de la Cordillère Ibérique (Espagne). Comptes Rendus de l´Academie des Sciences. Série 2. Sciences de la terre et des planètes 323: 341–347

Diez JB, Broutin J, Ferrer J (2005) Difficulties encountered in defining the Permian– Triassic boundary in Buntsandstein facies of the western Peritethyan domain based on palynological data. Palaeogeography Palaeoclimatology Palaeoecology 229: 40–53

Díez JB, Bourquin S, Broutin J, Ferrer J (2007) The Iberian Permian-Triassic "Buntsandstein" of the Aragonian Branch of the Iberian Ranges (Spain) in the West-European sequence stratigraphical framework. Bulletin Societé géologique France 178: 179–195

Díez JB, Escudero-Mozo MJ, Galán-Abellán B, López-Gómez J, Barrenechea JF, Marzo M, Martín-Chivelet J (2012) Nuevos registros palinológicos en facies Röt de la Rama Aragonesa de la Cordillera Ibérica y Cadenas Costero Catalanas (NE Península Ibérica). In: Abstract of Agora Paleobotanica Congress, Lyon, 21–22 June 2012, p 11

Dill HG (2001) The geology of aluminium phosphates and sulphates of the alunite group minerals: a review. Earth-Science Reviews 53: 35–93

Dinarès-Turell J, Bíez JB, Rey D, Arnal I (2005) Buntsandstein magnetostratigraphy and biostratigraphy reappraisal from eastern Iberia: Early and Middle Triassic stage boundary definitions through correlation to Tethyan sections. Palaeogeography Palaeoclimatology Palaeoecology 229: 137–158

Doblas M, Oyarzun R, Sopeña A, López-Ruiz J, Capote R, Hérnandez JL, Hoyos M, Lunar C, Sánchez-Moya Y (1994) Variscan-Late Variscan-Early Alpine progressive extensional collapse of Central Spain. Geodinámica Acta 7: 1–14

Domeier M, Van der Voo R, Torsvik TH (2012) Paleomagnetism and Pangea: the road to reconciliation. Tectonophysics 514–517: 14–43

Doubinger J, López-Gómez J, Arche A (1990) Pollen and spores from the Permian and Triassic sediments of the southeastern Iberian Ranges, Cueva de Hierro (Cuenca) to Chelva–Manzanera (Valencia–Teruel) region, Spain. Rev Palaeobot Palynol 66: 25–45

Druguet E, Castro A, Chichorro M, Pereira MF, Fernández C (2014) Zircon geochronology of intrusive rocks from Cap de Creus, Eastern Pyrenees. Geological Magazine 151: 1095–1114. https://doi.org/10.1017/s0016756814000041

Durand M (2008) Permian to Triassic continental successions in southern Provence (France): an overview. In: Cassinis G (ed) Special Section: Stratigraphy and Palaeogeography of Late- and Post-Hercynian Basins in the Southern Alps, Tuscany and Sardinia (Italy), vol 127. Bollettino della Società Geologica Italiana (Ital. J. Geosci), p 697–716

Durand-Delga M, Esteras M, Olivier P (2007) Los «Taríquides» (Arco de Gibraltar): Problemas estructurales, paleogeográficos y consideración histórica. Revista de la Sociedad Geológica de España 20 (3-4): 119–134

Ebinger C (1989) Tectonic development of the western branch of the East African rift system. Geological Society of America Bulletin 101: 201–207

Edel JB, Casini L, Oggiano G, Rossi P, Schulmann K (2014) Early Permian 90º clockwise rotation of the Maures-Esterel-Corsica-Sardinia block confirmed by new palaeomagnetic data and followed by a Triassic 60º clockwise rotation. In: Schulmann K, Martínez-Catalán JR, Lardeaux JM, Janousec V, Oggiano G (eds) The Variscan Orogeny: Extent, Timescale and the Formation of the European Crust. Geological Society, London, Spec Publ 405: 333–361

England P (1982) Some thermal and tectonic models for crustal melting in continental collision zones. Geological Society London Special Publication 19: 88–94

Enrique P (2012) Rocas teschenítica en el Norte de Mallorca: aproximación a su clasificación. Geogaceta 51: 11–14.

Erwin DH (1993) The Great Paleozoic crisis: Life and death in the Permian. Columbia University Press. New York, p 327

Erwin DH (2006) Extinction: How Life on Earth Nearly Ended 250 Million Years Ago. Princenton, Princenton University Press, 296 p

Escudero-Mozo M J, Martín-Chivelet J, Goy A, López-Gómez J (2014) Middle-Upper carbonate platforms in Minorca (Balearic Islands): Implications for western Tethys correlations. Sedimentary Geology 310: 41–58

Escudero-Mozo MJ, Márquez-Aliaga A, Goy A, Martín-Chivelet Z, López-Gómez J, Márquez L, Arche A, Plasencia P, Pla C, Marzo M, Sánchez-Fernández D (2015) Middle Triassic carbonate platforms in eastern Iberia: evolution of their fauna and palaeogeographic significance in the western Tethys. Palaeogeography. Palaeoclimatology Palaeoecology 417: 236–260

Espina RG (1994) Extensión mesozoica y acortamiento alpino en el borde occidental de la cuenca Vasco Cantábrica. Cuad Lab Xeol Laxe 19: 137–150

Espina RG (1997) La estructura y evolución tectonoestratigráfica del borde occidental de la Cuenca Vasco-Cantábrica (Cordillera Cantábrica, NO de España). Ph.D. Thesis (unpublished), Universidad de Oviedo, Oviedo, p 230

Espina RG, Alonso JL, Pulgar JA (2004) Extensión Triásica en la Cuenca Vasco-Cantábrica. In: Vera JA (ed) Geología de España, SGE-IGME, Madrid, p 338–339

Fallot P (1948) Les Cordillères Bètiques. Estudios Geológicos 4: 259–279

Faure M, Pons J (1991) Crustal thinning recorded by the shape of the Namurian-Wesphalian leucogranite in the Variscan Belt of the northwest Massif Central, France. Geology 19: 730–733

Faure M, Monié P, Pin C, Maluski H, Leloix C (2002) Late Visean thermal event in the northern part of the French Massif Central: new $^{40}Ar/^{39}Ar$ and Rb–Sr isotopic constraints on the Hercynian syn-orogenic extension. International Journal of Earth Sciences 91: 53–75

Faure M, Lardeaux JM, Ledru P (2009) A review of the pre-Permian geology of the Variscan French Massif Central. Compt Rendus Geosci 341: 202–213

Fernández J (1977) Sedimentación triásica en el borde sureste de la Meseta. Publicaciones Universidad Granada 161: 1–173

Fernández J, Dabrio C J (1978) Análisis sedimentológico de una capa de areniscas (Triásico del borde SE de la Meseta Ibérica). Estudios Geológicos 34: 475–482

Fernández J, Dabrio, JC, Pérez-López A (1994) El Triásico de la región de Siles Alcaraz (Cordillera Bética). In: Arche, A. (ed) III Coloquio Estratigrafía Paleogeografía del Pérmico y Triásico de España. Field Guide, Cuenca, Spain

Fernández J, Viseras C, Dabrio, C (2005) Triassic fluvial sandstones (Central South Spain): An exellent analogue for the TAGI reservoir of Algeria. 7th EAGE Conference & Exhibition, Madrid, Spain. Field Guide F1

Fernández J, Viseras C, Soria JM, García F (2005) Dinámica sedimentaria en el relleno de un paleovalle durante el Triásico Medio y Superior en la región de Almedina-Alcaraz, España. Geo-Temas 8: 151–154

Fernández-Suárez J, Dunning GR, Jenner GA, Gutiérrez-Alonso G (2000) Variscan collisional magmatism and deformation in NW Iberia: constraints from U–Pb geochronology of granitoids. Journal of the Geological Society of London 157: 565–576

Fernández-Viejo G, Gallart J, Pulgar JA, Gallastegui J, Dañobeitia JJ, Córdoba D (1998) Crustal transition between continental and oceanic domains along the North Iberian margin from wide angle seismic and gravity data. Geophysical Research Letters 25(23): 4249–4252

Fernández-Viejo G, López-Fernández C, Dominguez-Cuesta M J, Cadenas P (2014) How much confidence can be conferred on tectonic maps of continental shelves? The Cantabrian-Fault case. Scientific Reports 4: 1–7

Fontboté JM, Guimerà J, Roca E, Sàbat F, Santanach P, Fernández-Ortigosa F (1990) The Cenozoic evolution of the Valencia trough (western Mediterranean). Rev Soc Geol Esp 3: 249–259

Franke W (2000) The mid-European segment of the Variscides: tectonostratigraphic units, terrane boundaries and plate tectonic evolution. In: Dallmeyer MD (ed) Terrane in the Circum-Atlantic Paleozoic Orogens. Geol Soc Am Spec Papers 230: 67–90

Franke W (2006) The Variscan orogen in Central Europe: construction and collapse. Geological Society London Memoirs 32 (1): 333–343

Fréchengues M, Peybernès B (1991) Associations de Foraminifèrs benthoniques dans le Trias cabonaté (Anisien, Ladinien-Carnien et Rhétien) des Pyrénées espagnoles. Acta Geol Hisp 26: 67–74

Fréchengues M, Peybernès B, Zaninetti N (1990) Mise en évidence d´ associations de Foraminifères benthiques dans la séquence de dépot ladino-carnienne du "Muschelkalk" des Pyrénées catalanes (France, Espagne). C R Acad Sci Paris 310(2): 667–673

Gaboreau S, Beaufort D, Vieillard P, Patrier P, Bruneton P (2005) Aluminum phosphate-sulfate minerals associated with Proterozoic unconformity-type uranium deposits in the East Alligator River Uranium Field, Northern Territories, Australia. The Canadian Mineralogist 43: 813–827

Galán-Abellán AB, Barrenechea JF, Benito MI, De la Horra R, Luque FJ, Alonso-Azcárate J, Arche A, López-Gómez J, Lago M (2013) Palaeoenvironmental implications of aluminium phosphate–sulphate minerals in Early–Middle Triassic continental sediments, SE Iberian Range (Spain). Sedimentary Geology 289: 169–181

Galé C (2005) Evolución geoquímica, petrogenética y de condiciones geodinámicas de los magamatismos pérmicos en los sectores central y occidental del Pirineo. Ph.D Thesis. Universidad de Zaragoza, Zaragoza, p 457

Galfetti T, Hochuli P A, Brayard A, Bucher H, Weissert H, Vigran J O (2007) Smithian-Spathian boundary event: Evidence for global climatic change in the wake of the end-Permian biotic crisis. Geology 35(4): 291–294

Gand G, Kerp H, Parsons C, Martínez-García E (1997) Palaeoenvironmental and stratigraphic aspects of animal traces and plant remains in Spanish Permian red beds (Peña Sagra, Cantabrian Mountains, Spain). Geobios 30(2): 295–318

Gand G, De La Horra R, Galán-Abellán B, López-Gómez J, Barrenechea JF, Arche A, Benito MI (2010) New ichnites from the Middle Triassic of the Iberian Ranges (Spain): paleoenvironmental and paleogeographical implications. Historical Biology 22 (1–3): 40-56. https://doi.org/10.1080/08912961003644096

Gallastegui G, Suárez O, Cuesta A (2004) Zona Cantábrica: Magmatismo. In: Vera, J.A. (ed) Geologia de España, SGE-IGME: 47–49

García-Gil S (1990) Estudio sedimentológico y paleogeográfico del Triásico en el tercio noroccidental de la Cordillera Ibérica (Províncias de Guadalajara y Soria). PhD Thesis. Universidad Complutense de Madrid, Spain. Colección Tesis Doctorales 176.

García-Gil S (1991) Las unidades litoestratigráficas del Muschelkalk en el NW de la Cordillera Ibérica (España). Bol Real Soc Hist Nat 86 (1–4): 21-51.

García-Lasanta C, Oliva-Urcia B, Román-Berdiel T, Casas AM, Gil-Peña I, Sánchez-Moya Y, Sopeña A, Hirt AM, Mattei M (2015) Evidence for the Permo-Triassic transtensional rifting in the Iberian Range (NE Spain) according to magnetic fabrics results. Tectonophysics 651–652: 16–231

García-Mondéjar J (1989) Strike-slip Subsidence of the Basque-Cantabrian Basin of Northern Spain and its Relationship to Aptian-Albian Opening of Bay of Biscay. In: Tankard AJ, Balkwill HR (eds) Extensional Tectonics and Stratigraphy of the North Atlantic Margins, American Association of Petroleum Geologist, Memoir 46, p 395–409

García-Mondejar J, Pujalte V, Robles S, Castro J, Vallés J, (1989) Sistemas deposicionales, facies y evolución tectonoestratigráfica de la cubeta pérmica de Peña Labra-Peña Sagra (borde occidental de la cuenca Vasco-Cantábrica. Cantabria y Palencia). In: Libro Homenaje a Rafael Soler, Asociación de Geólogos y Geofísicos Españoles del Petróleo, p 53–65

García Senz J, Ramirez Merino JI (2009) Pont de Suert [map] (1:50.000) MAGNA Hoja 213 Segunda serie. IGME. Report and Map, p 64

Gaspar-Escribano JM, Van Wees JD, Ter Voorde M, Cloetingh S, Roca E, Cabrera L, Muñoz J, Ziegler P, García-Castellanos D (2001) Three-dimensional flexural modelling of the Ebro Basin, NE Iberia. Geophysical Journal 145: 1–26

Gaspar-Escribano J, García-Castellanos C, Roca E, Cloetingh S (2004) Cenozoic vertical motios of the Catalan Coastal Ranges (NE Spain): the role of tectonics, isostasy, and surface transport. Tectonics 23: 1–18

Gelabert B, Sabat F, Rodríguez Perea A (1992) A structural online of the Serra de Tramuntana of Mallorca (Balearic Islands). Tectonophysics 203: 167–183

Gervilla M, Beroiz C, Barón A, Ramirez del Pozo J (1978) Oviedo [map] (1:50.000) MAGNA Hoja 29, Segunda serie. IGME. Report and Map, p 64

Gianolla P, Jacquin T (1998) Triassic sequences stratigraphic framework of western European basins. In: De Graciansky P-C, Hardenbol J, Jacquin T, Vail P (eds) Mesozoic and Cenozoic sequences stratigraphy of European basins. Society for Sedimentary Geology, Special Publication 60: 643–650

Gibbs AD (1984) Structural evolution of extensional basin margins. Journal Geological Society London 141: 609–620

Gisbert J (1981) Estudio geológico–petrológico del Estefaniense-Pérmico de la Sierra del Cadí (Pirineo de Lérida): Diagénesis y sedimentología. Ph.D. Thesis, University of Zaragoza, Zaragoza, p 314

Gisbert J (1983) El Pérmico de los Pirineos españoles. In: Martínez-García, E (ed) Carbonífero y Pérmico de España. Ministerio de Industria y Energía, Madrid, p 405–420

Gisbert J (1984) Las molasas tardihercínicas del Pirineo. In: Comba JA (ed) Libro Jubilar de J M Ríos, vol 2. Instituto Geológico y Minero de España, Madrid, pp 168–186

Gisbert J, Martí J, Gascón F (1985) Guía de la excursión al Stephaniense, Pérmico Inferior catalán. In: II Col. de Estratigrafía y Paleogeografía del Pérmico y Triásico de España, Institut d'Estudis Ilerdencs, La Seu d´Urgell, 23–25 septiembre 1985, p 79

Gómez JJ (1979) El Jurásico en facies carbonatadas del sector levantino de la Cordillera Ibérica. Ph.D Thesis. Universidad Complutense. Seminarios de Estratigrafía, Serie Monografías 4: 683 p

Gómez JJ, Goy A, Barrón E (2007) Events around the Triassic-Jurassic boundary in northern and Eastern Spain: A review. Palaeogeography Palaeoclimatology Palaeoecology 244: 89–110

Gómez-Gras D (1993) El Permo-Trias de las Baleares y de la vertiente mediterránea de la Cordillera Ibérica: facies y petrología sedimentaria (Parte II). Bol Geol Min 104–105: 467–515

Gómez-Gras D, Alonso-Zarza A (2003) Reworked calcretes: their significance in the reconstruction of the alluvial sequences (Permian and Triassic, Minorca, Balearic Islands, Spain). Sedimentary Geology 158: 299–319

Goy A (1995) Ammonoideos del Triásico Medio de España: Biostratigrafía y correlaciones Cuad Geol Iber 19: 21–60

Grauvogel-Stamm L, Álvarez-Ramis C (1995) Coniféres et pollen in situ du Buntsandstein du l´ile de Majorque. Cuadernos de Geología Ibérica 20: 209–243

Gretter N, Ronchi A, Langone A, Perotti CR (2013) The transition between the two major Permian tectono- stratigraphic cycles in the central Southern Alps: results from facies analysis and U/Pb geochronology. Int J Earth Sci (Geol Rundsch) 102: 1181–1202

Gretter N, Ronchi A, López-Gómez J, Arche A, De la Horra R, Barrenechea J, Lago M (2015) The Late Palaeozoic-Early Mesozoic from the Catalan Pyrenees (Spain): 60 Myr of environmental evolution in the frame of the western peri-Tethyan palaeogeography. Earth Sciences Reviews 150: 679–708

Guimerà J (1984) Paleogene evolution of deformation of northeastern Iberian Peninsula. Geological Magazine 121: 413–420

Guimerà J (1988) Estudi estyructural de l´enllac la Serralada Ibérica y la Serralada Costanera Catalana. PhD Thesis (Unpublished). University of Barcelona, Barcelona, p 600

Gutiérrez-Alonso G, Murphy JB, Fernández-Suárez J, Hamilton MA (2008) Rifting along the northern Gondwana margin and the evolution of the Rheic Ocean: A Devonian age for the El Castillo volcanic rocks (Salamanca, Central Iberian Zone). Tectonophysics 461: 157–165

Gutiérrez-Alonso G, Fernández-Suárez J, Weil AB, Murphy JB, Nance RD, Corfu F, Johnston ST (2008) Self-subduction of the Pangaean global plate, Nat Geosci 1(8): 549–553. https://doi.org/10.1038/ngeo250

Gutiérrez-Alonso G, Fernández-Suárez J, Jeffries TE, Johnston ST, Pastor-Galán D, Murphy JB, Franco MP, Gonzalo JC (2011) Diachronous post-orogenic magmatism within a developing orocline in Iberia, European Variscides. Tectonics 30(5). doi: 10.1029/2010TC002845

Haq B U, Al-Qahtani A M (2005) Phanerozoic cycles of sea-level change on the Arabian platform. GeoArabia 10: 127–160

Hartevelt JJA (1970) Geology of the upper Segre and Valira valleys, central Pyrenees, Andorra/Spain. Leidse Geologische Mededelingen 45: 349–354

Henares S, Caracciolo L, Cultrone G, Fernández J, Viseras C (2014) The role of diagenesis and depositional facies on pore system evolution in a Triassic outcrop analogue (SE Spain). Marine and Petroleum Geology 51: 136–151

Henares S, Caracciolo L, Viseras C, Fernández J, Yeste LM (2016) Diagenetic constraints on heterogeneous reservoir quality assessment: a Triassic outcrop analogue

Hernando S (1977) Pérmico y Triásico de la región Ayllón-Atienza. Ph. D Thesis. Seminarios de Estratigrafía. Series Monográfica Vol 2. Dpt. Estratigrafía, Universidad Complutense de Madrid, Madrid, p 408

Hernando S, Schott JJ, Thuizat R, Montigny R (1980) Age des andesites et des sediments interstratifiés de la region d'Atienza (Espagne): étude stratigraphique, géochronologique et paléomagnetique. Sciences Géologiques, bulletins et mémoires 33(2): 119–128

Hirsch F (1972) Middle Triassic Conodonts from Israel, Southern France and Spain. Mitt. Ges. Geol. Bergbaustud 21: 811–828.

Hirsch F (1975) Lower Triassic Conodonts from Israel. Bull Geol Surv Israel 66: 39–48.

Hirsch F (1977) Essai de correlation biostratigraphique des niveaux Maso et Neotriasiques de facies Muschelkalk du domaine sepharade. Cuad Geol Iber 4: 511–518

Hirsch F, Márquez-Aliaga A (1988) Triassic circummediterranean bivalve facies, cycles and global sea level changes. II Congreso Geológico de España, Granada, 1: 342–344.

Hochuli P A, Frank, S K (2000) Palynology (Dinoflagelate cysts and spore-pollen) andstratigraphy of the Lower Carnian Raibl Group in Eastern Swiss Alps. Eclogae Geologicae Helvetiae 93: 429–443

Houseman GA, McKenzie DP, Molnar P (1981) Convective instability of a thickened boundary layer and its relevance for the thermal evolution of continental convergent belts. Journal Geophysical Research 86: 6115–6132

Jost A B, Mundil R, He B, Brown ST, Altiner D, Sun Y, De Paolo DJ, Payne JL (2014) Constraining the cause of the end-Guadalupian extinction with coupled records of carbon and calcium isotopes. Earth and Planetary Science Letters 396: 201–212.

Juarez-Ruiz J, Wachtler M (2015) Early-Middle Triassic (Anisian) fossil flora from Majorca (Spain). Dolomythos, Innichen, p 1–49

Julivert M (1960) Estudio geológico de la Cuenca de Beleño (Valles altos del Sella, Ponga, Nalón y Esla). Boletín del Instituto Geológico y Minero de España 71:1–346

Juncal M, Díez B, Broutin J, Martínez-García E (2016a) Palynoflora from the Permian Sotres Formation (Picos de Europa, Asturias, Northern Spain). Spanish Journal of Palaeontology 31(1): 85–94

Juncal M, Diez JB, De la Horra R, Galán-Abellán B, Borruel-Abadía V, López-Gómez J, Arche A (2016b) Anisian palynological assemblage of Eslida Formation (SE Iberian Ranges). Paper presented at the Colloque Agora Paleobotanica, Brusels, 7–10 July 2016

Juncal MA, Lloret J, Diez JB, López-Gómez J, Ronchi A, De la Horra R, Barrenechea JF, Arche A (2019) New Upper Carboniferous palynofloras from Southern Pyrenees (NE Spain): Implications for palynological zonation of Western Europe. Palaeogeography, Palaeoclimatology, Palaeoecology 516: 307–321.

Jurado MJ (1988) El Triásico de la subcuenca del Ebro. Ph.D. Thesis, Universitat Barcelona, Barcelona, p 327

Jurado M J (1989) El Triásico del subsuelo de la Cuenca del Ebro. PhD Thesis. Departamento de Geología Dinámica, Geofísica y Paleontología, Universidad de Barcelona. 259 p. Unpublished.

Jurado M J (1990) El Triásico y Liásico basal evaporíticos del subsuelo de la cuenca del Ebro. In: Ortí F, Salvany J M (eds) Formaciones evaporíticas de la Cuenca del Ebro y cadenas periféricas y de la zona de Levante. Enresa, pp 21–28.

Klimowitz J, Torrescusa S (1990) Notas sobre la estratigrafía y facies de la serie triásica en el Alóctono Surpirenaico. In: Ortí F, Salvany JM (eds) Formaciones evaporíticas de la Cuenca del Ebro y cadenas periféricas, y de la zona de Levante. ENRESA-Universitat de Barcelona, Barcelona, p 29–33

Kolar-Jurkovsek T, Jurkovsek B (2010) New paleontological evidence of the Carnian strata in the Mežica area (Karavanke Mts, Slovenia): conodont data for the Carnian pluvial event. Palaeogeography, Palaeoclimatology, Palaeoecology 290: 81–88.

Kozur H W, Bachmann G H (2010). The middle Carnian wet intermezzo of the Stuttgart formation (Schilfsandstein), Germanic Basin. Palaeogeography, Palaeoclimatology, Palaeoecology 290: 107–119.

Lago M (1980) Estudio geológico, petrológico, geoquímico y de aprovechamiento industrial de rocas ofíticas en el Norte de España. Ph.D. Thesis, Universidad de Zaragoza, Zaragoza, p 444

Lago M, Zachmann D, Vaquer R, Pocovi A (1988) Geochemical behaviour of spilitization in alkaline magmatism, Trias-Lias, of the Iberian chain and Mallorca (Spain). Chemical Geology 70 (1–2): 141–156

Lago M, Pocovi A, Zachmann D, Arranz E, Carls P, Torres JA, Vaquer R (1991) Comparación preliminar de las manifestaciones magmáticas, calcoalcalinas y stephaniense-pérmicas de la Cadena Ibérica. Cuadernos do Laboratorio Xeolóxico de Laxe 16: 95-107.

Lago M, Pocoví A, Bastida J, Arranz E, Vaquer R, Dumitrescu R, Gil-Imaz A, Lapuente MP (1996) El magmatismo alcalino, hettangiense, en el dominio nor-oriental de la placa ibérica. Cuad Geol Iber 20: 109–138

Lago M, Galé C, Arranz E, Gil-Imaz A, Pocovi A, Vaquer R (2000) The triassic alkaline dolerites of the Valacloche-Camarena area (SE-Iberian Chain, Teruel): geodynamic implications. Estudios Geológicos 56(5-6): 211–228.

Lago M, Arranz E, Galé C (2002) Stephanian-Permian volcanism in the Pyrenees. In: Gibbons W, Moreno T (eds) The Geology of Spain, Geol. Soc. London, London, p 126–128

Lago M, Arranz E, Pocoví A, Galé C, Gil-Imaz A (2004a) Permian magmatism and basin dynamics in the Southern Pyrenees: a record of transition from late Variscan transtension to early Alpine extension. In: Wilson M, Neumann ER, Davies GR, Timmerman MJ, Heeremans M, Larsen BT (eds) Permo-Carboniferous magmatism and rifting in Europe. Geological Society, London, Special Publications 223: 439–464. https://doi.org/10.1144/gsl.sp.2004.223.01.19

Lago M, Arranz Yagüe E, Pocoví A, Galé Bornao C, Gil-Imaz A (2004b) Lower Permian magmatism of the Iberian Chain and its relationship to extensional tectonics. In: Wilson M, Neumann ER, Davies G, Timmermann M, Heeremans M, Larsen BT (eds) Permo-Carboniferous magmatism and rifting in Europe. Geological Society of London Special Publication 223: 465–491

Lago M, De la Horra R, Ubide T, Galé C, Galán-Abellán AB, Barrenechea JF, López-Gómez J, Benito MI, Arche A, Alonso-Azcárate J, Luque FJ, Timmerman MJ (2012) First report of a Middle-Upper Permian magmatism in the SE Iberian Ranges: characterization and comparison with coeval magmatisms in the western Tethys. Journal of Iberian Geology 38 (2): 331–348. https://doi.org/10.5209/rev_jige.2012.v38.n2.40462

Lago M, Gil A, Arranz E, Galé C, Pocoví A (2005) Magmatism in the intracratonic Central Iberian basins during the Permian: Palaeoenvironmental consequences, Palaeogeography Palaeoclimatology Palaeoecology 229(1–2): 83–103. https://doi.org/10.1016/j.palaeo.2005.06.032

Lanaja, JM (1987) Contribución de la exploración petrolífera al conocimiento de la geología de España. IGME, Madrid, p 465

Larrasoaña JC, Parés JM, Millán H, Del Valle J, Pueyo EL (2003) Palepomagnetic, structural and stratigraphic constrains on transverse fault kinematics during basin inversion: the Pamplona fault (Pyrenees, N Spain). Tectonics 22 (6): 1071. https://doi.org/10.1029/2002tc001446

Lasheras E, Lago M, García J, Arranz E (1999) Geoquímica del magmatismo Pérmico Superior del Macizo de Cinco Villas (Pirineo Navarro). Geogaceta 25: 119–122

Lepvrier C, Martínez-García E (1990) Fault development and stress evolution of the post Hercynian Asturian Basin. Tectonophysics 184: 345–3

Linol B, Bercovici A, Bourquin S, Díez JF, López-Gómez J, Broutín J, Durand M, Villanueva-Amadoz U (2009) Late Permian to Middle Triassic correlations and palaeogeographical reconstructions in south-western European basins: New sedimentological data from Minorca (Balearic Islands, Spain). Sedimentary Geology 220: 77–99

Llompart C, Rosell J, Márquez-Aliaga A, Goy A (1987) El Muschelkalk de la Isla de Menorca. Cuadernos de Geología Ibérica 11: 323–335

Lloret J, Ronchi A, López-Gómez J, De la Horra R, Barrenechea J, Arche A (2016) Stratigraphic and sedimentary evolution of the Upper Carboniferous–Middle Triassic Malpàs-Sort Basin (Central Pyrenees): A facies analysis approach to the palaeogeographic reconstruction. In: Abstracts of the 88° Congresso della Societá Geologica Italiana, Vol. 40, Societá Geologica Italiana, Napoli, 24 Nov 2016

Lloret J, Ronchi A, López-Gómez J, Gretter N, De la Horra R, Barrenechea JF, Arche A (2018) Syn-tectonic sedimentary evolution of the continental Late Palaeozoic-Early Mesozoic Erill Castell-Estac Basin and its significance in the development of the central Pyrenees Basin. Sedimentary Geology 374: 134–157

López-Blanco MM, Marzo M, Burbank, DW, Vergès J, Anadón P, Piña J (2000) Tectonic and climatic controls on the development of foreland fan deltas: Montserrat and Sant Llorenc del Müns system (Middle Eocene, Ebro Basin, NE Spain). Sedimentary Geology 138: 17–39

López-Gómez J, Arche A (1992) Palaeogeographical significance of the Röt (Anisian, Triassic) Facies (Marines clays, muds and marls Fm.) in the Iberian Ranges, easternSpain. Palaeogeography, Palaeoclimatology, Palaeoecology 91: 347–361.

López-Gómez J, Arche A (1993) Sequence stratigraphic analysis and paleogeographic interpretation of the Buntsandstein and Muschelkalk facies (Permian-Triassic) in the SE Iberian Ranges, E Spain. Paleogeography Paleoclimatology Paleoecology 103: 176–201

López-Gómez J, Más R, Arche, A (1993) The evolution of the Middle Triassic(Muschelkalk) carbonate ramp in the SE Iberian Ranges, eastern Spain: sequence stratigraphy, dolomitization processes and dynamic controls. Sedimentary Geology 87: 165–193

López-Gómez J, Arche, A, Calvet F, Goy A (1998) Epicontinental marine carbonate sedimentsof the Middle and Upper Triassic in the westernmost part of the Tethys Sea, Iberian Península. Zentralblatt für Geologie und Paläontologie 9–10: 1033–1084.

López-Gómez J, Arche A, Pérez-López A (2002) Permian and Triassic. In: Gibbons W, Moreno T (eds) The Geology of Spain. Geological Society of London, London, p 185–212

López-Gómez J, Arche A, Marzo M, Durand M (2005) Stratigraphical and palaeogeographical significance of the continental sedimentary transition across the Permian-Triassic boundary in Spain. Palaeogeography Palaeoclimatology Palaeoecololy 229: 3–23

López-Gómez J, Arche A, Vargas H, Marzo M (2010) Fluvial architecture as a response to two-layer lithospheric subsidence during the Permian and the Triassic in the Iberian Basin, Eastern Spain. Sedimentary Geology 223: 320–333

López-Gómez J, Galán-Abellán A B, De la Horra R, Barrenechea J F, Arche A, Bourquin S, Marzo M, Durand M (2012) Sedimentary evolution of the continental Early–Middle Cañizar Formation (Central Spain): implications for life recovery after the Permian–Triassic crisis. Sedimentary Geology 249–250: 26–44

López-Gómez J, Escudero-Mozo M J, Martín-Chivelet J, Arche A, Lago M, Galé C (2017) Western Tethys continental–marine responses to the Carnian Humid Episode: Palaeoclimatic and-palaeogeographic implications. Global and Planetary Change 148: 79–95

López-Gómez J, Martin-Gonzalez F, Heredia N, De la Horra R, Barrenecheaa J F, Cadenas P, Junca M, Diez J B, Borruel-Abadia V, Pedreira D, Garcia-Sansegundo J, Farias P, Gale C, Lago M, Ubide T, Fernandez-Viejo G, Gand G (2019) New lithostratigraphy for the Cantabrian Mountains: A common tectonostratigraphic evolution for the onset of the Alpine cycle in the W Pyrenean realm, N Spain. Earth-Science Reviews 188: 249–271

Lucas Cl (1985) Le grès rouge du versant nord des Pyrénées. Essai sur la Geodynamique de depots continentaux du Permien et du Trias. Ph.D Thesis, Toulouse III, p 269

Lucas Cl (1989) Le Permien des Pyrenées. In: Synthese géologique des bassins permiens francais. Edition Bureau Recherche Geologique et Miniere, Mem 128: 139–150

Lucas Cl, Gisbert-Aguilar J, Bixel F, Cazetien R, Valero-Garcés BL (1996) Carbonifere Superieur–Permien. In: Barnolas A, Chiron, JC (eds) Synthese geologique et geophysique des Pyrenees, vol 1. Edition BRGM-*ITGE*, Orleáns, Madrid, pp 339–359

Maas K (1974) The geology of Liébana, Cantabrian Mountains, Spain; flysh area. Leidse Geologische Mededelingen 49: 379–465

Maillard A, Mauffred A, Watts AB, Torné M, Pascal G, Buhl P, Pinet B (1992) Tertiary sedimentary history and structure of the Valencia trough (western Mediterranean). Tectonophysics 203: 57–75

Maino M, Dallagiovanna G, Gaggero L, Seno S, Tiepolo M (2012) U-Pb zircon geo-chronological and petrographic constraints on late to post-collisional Variscan magmatism and metamorphism in the Ligurian Alps, Italy. Geological Journal 47: 632–652

Maino M, Decarlis A, Felletti F, Seno S (2013) Tectono-sedimentary evolution of the Tertiary Piedmont Basin (NW Italy) within the Oligo-Miocene central Mediterranean geodynamics. Tectonics 32: 593–619

Majarena U, Gil-Imaz A, Lago M, Galé C (2015) El magmatismo pérmico del sector de Atienza (extremo W de la Cordillera Ibérica): nuevos datos petro-estructurales para su interpretación genética. Geogaceta 58: 39–42

Majarena U, Lago M, Galé C, Esteban J J, García de Madinabeitia S (2017) El magmatismo Pérmico Inferior de la Sierra de Pardos (Rama Aragonesa de la Cordillera Ibérica, Zaragoza): petrología y geoquímica. Geogaceta 61: 111–114

Malavielle J, Guihot P, Costa S, Lardeaux JM, Gardien V (1990) Collapse of the thickened variscan crust in the French Massif Central: Mont Pilat extensional zone and the Saint Etienne Late Carboniferous basin. Tectonophysics 177: 139–149

Mamet B, Martínez-García E (1995) Permian microcodiaceans (algae, incertae sedis) Sotres Limestone, Asturias. Revista Española de Micropaleontologia XXVII 3:107–116.

Manjón M, Gutiérrez-Claverol M, Martínez-García E (1992) La sucesión posthercínica preliásica del área de Villabona (Asturias, N de España). In: Proccedings of III Congreso de Geología de España, vol 2. Universidad de Salamanca, Salamanca, pp 107–111

March M (1991) Los conodontos del Triásico Medio (facies Muschelkalk) del noroeste de la Península Ibérica y de Menorca. PhD Thesis. Universidad de Valencia. 394p

Marin Ph (1974) Stratigraphie et évolution paléogégraphique post-hercynienne de la Chaîne Celtibérique orientale aux confines de l'Aragon et le Maestrazgo (Provinces de Teruel et Castellón, Espagne). Ph. D. Thesis, Université Claude Bernard, Lyon, p 231

Márquez L (2005) Foraminiferal fauna recovered after the Late Permian extinctions in Iberian and the westernmost Tethys area. Palaeogeography, Palaeoclimatology, Palaeoecology 229: 137–157

Márquez L, Trifonova E, Calvet F, Tucker, M (1990) Los foráminíferos del complejo arrecifal del Triásico (Ladiniense superior) de la Sierra de Prades (Tarragona). VI Jornadas de Paleontología, España. p 40

Márquez-Aliaga A, Ros S (2003) Associations of bivalves of Iberian Peninsula (Spain): Ladinian. Albertiana 28: 85–89.

Martí J, Barrachina A (1986–87) Las ignimbritas de Castellar de N´Hug (Pirineo Catalán). Acta Geológica Hispánica 21-22: 561–568

Martín-Algarra A, Vera JA (2004) La Cordillera Bética y las Baleares en el contexto del Mediterráneo Occidental. In: Vera J A (ed.), Geología de España. SGE-IGME, Madrid, 352–354

Martínez Catalán JR, Arenas R, García FD, Cuadra PG, Gómez-Barreiro J, Abati J, Castiñeiras P, Fernández-Suárez J, Martínez SS, Andonaegui P (2007) Space and time in the tectonic evolution of the northwestern Iberian Massif: Implications for the Variscan belt. Geological Society of America Memoirs 200: 403–423

Martínez-García E (1981) Tectónica y mineralizaciones pérmicas en la Cordillera Cantábrica (Noroeste de España). Cuad Lab Xeol Laxe 2: 263–270

Martínez-García E (1991) Hercynian syn-orogenic and post-orogenic successions in the Cantabrian and the Palentian zones (NW Spain). Comparison with other western European occurrences. Giornale di Geologia 53: 209–228

Martínez García E (1999) Orogénesis y sedimentación a finales del Paleozoico en el NW del Macizo Ibérico (Asturias, Cantábria y Palencia). In: Libro Homenaje a José Ramírez del Pozo. AGGEP, Madrid, p 167–174

Martínez-García E, Tejerina L (1985) Fluorspar deposits associated with Carboniferous and Permian rocks in Asturias and León (Northwest Spain). In: C.R. IX Inter. Congr. Stratigraphy and Geology of the Carboniferous, Washington-Urbana/Champaing, 1985, vol 5, pp 467–478

Martínez García E, Luque C, Burkhardt R, Gutiérrez-Claverol, M (1991) Hozarco: un ejemplo de mineralización de Pb-Zn-Hg de edad Pérmica (Cordillera Cantábrica, NW de España). Boletín de la Sociedad Española de Mineralogía 14: 107–106

Martínez García E, Roquel R, Gutiérrez Claverol M, Quiroga J (1998) Edad del "Tramos de Transición" entre el Pérmico y el Jurásico en el área de Gijón (Asturias, NW de España). Geogaceta 24: 215–218

Martínez-Álvarez JA (1968) Consideraciones respecto a la zona de fractura ("Falla Cantábrica") que se desarrolla desde Avilés (Asturias) hasta Cervera de Pisuerga (Palencia). Acta Geológica Hispánica 3(5): 142–144

Martín-Algarra A (1987) Evolución geológica alpina del contactoentre las Zonas Internas y las Zonas Externas de la Cordillera Bética. PhD Thesis, University of Granada, Granada, Spain

Martín-Algarra A, Márquez-Aliaga A, Solé de Porta N, Valenzuela JM (1993) La serie triásica de Los Pastores (Algeciras). Estudios geológicos 49: 21–39

Martín-Algarra A, Solé de Porta N, Márquez-Aliaga A (1995) Nuevos datos sobre la estratigrafía y procedencia paleogeográfica del Triásico de las escamas del Corredor del Boyar (Cordillera Bética Occidental). Cuadernos de Geología Ibérica 19: 279–307

Márquez-Aliaga A, Hirsch F (1988) Migration of Middle Triassic Bivalves in the Sephardic Province. II Congreso Geológico de España, Granada 1: 301–304

Martínez González RM, Vaquer R, Lago M (1998) El volcanismo jurásico de la Sierra de Javalambre (Cadena Ibérica, Teruel). Teruel 86 (1): 43–61

Martín-González F, Heredia N (2011) Geometry, structures and evolution of the western termination of the Alpine-Pyrenean Orogen reliefs (NW Iberian Peninsula). Journal of Iberian Geology: 37 (2): 103–120

Marzo M (1980) El Buntsandstein de los Catalánides: Estratigrafía y procesos de sedimentación. PhD Thesis (Unpublished). Barcelona University, Barcelona, p 317

Marzo M (1986) Secuencias fluvio-eólicas en el Buntsandstein del Macizo de Garraf (provincia de Barcelona). Cuad Geol Iber 10: 207–233

Marzo M, Anadón P (1977) Evolución y características sedimentológicas de las facies fluviales basales del Buntsandstein de Olesa de Montserrat (provincia de Barcelona). Cuad Geol Iber 4: 211–222
Marzo M, Calvet F (1985) Guía al Triásico de los Catalánides. Institut d'Estudis Ilerdencs. Field Guide. 175 p
Matte P (1988) Tectonics and plate tectonics model for the Variscan Belt of Eutrope. Tectonophysics 126: 329–364
Matte P (1991) Accretionary history and crustal evolution of the Variscan belt in Western Europe. In: Hatcher RD Jr, Zoneshain L (eds) Accretionary Tectonics and Composite Continents. Tectonophysics 196: 309–337
Matte P (2001) The Variscan collage and orogeny (480–290 Ma) and the tectonic definition of the Armorica microplate: a review. Terra Nova 13: 122–128
McCann T, Pascal C, Timmerman MJ, Krzywiec P, López-Gómez J, Wetzel A, Krawczyk CM, Rieke H, Lamarche J (2006) Post-Variscan (end Carboniferous–Early Permian) basin evolution in Western and Central Europe. In: Gee DG, Stephenson RA (eds) European Lithosphere Dynamics. Geological Society of London Memoirs 32: 355–388
Menard G, Molnar P (1988) Collapse of a Hercynian Tibetan Plateau into a Late Paleozoic Basin and Range province. Nature 334: 235–237
Mercedes-Martín R, Salas R, Arenas C (2013) Facies heterogeneity and depositional models of a Ladinian (Middle Triassic) microbial-dominated carbonate ramp system (Catalan Coastal Ranges, NE Spain). Marine and Petroleum Geology 46: 107–128
Mercedes-Martín R, Arenas C, Salas R (2014a) Diversity and factors controlling widespread occurrence of syn-rift Ladinian microbialites in the western Tethys (Triassic Catalan Basin, NE Spain). Sedimentary Geology 313: 68–90
Mercedes-Martín R, Salas R, Arenas C (2014b) Microbial-dominated carbonate platforms during the Ladinian rifting: sequence stratigraphy and evolution of accommodation in a fault-controlled setting (Catalan Coastal Ranges, NE Spain). Basin Research 26(2): 269–296
Merino-Tome O, Bahamonde J R, Colmenero J, Heredia N, Villa E, Farias P (2009) Emplacement of the Cuera and Picos de Europa imbricate system at the core of the Ibero-Armorican arc (Cantabrian Zone, N Spain): new precisions concerning the timing of arc closure. Geological Society America Bulletin 121: 729–751
Mey PHW (1968) Geology of the Upper Ribagorzana and Tor valleys, Central Pyrenees, Spain. [map] Sheet 8 (1:50.000). Leidse Geologische Mededelingen 41: 229–292
Mey PHW, Nagtegaal PJC, Roberti KJ, Hartevelt JJA (1968) Lithostratigraphic subdivision of post-Hercynian deposits in the South-Central Pyrenees, Spain. Leidse Geologische Mededelingen 41: 221–228
Mitjavila J, Martí J (1986) El vulcanismo triásico del sur de Catalunya. Revista d'investigacions geologiques 42–43: 89–130
Montigny R, Azambre B, Rossy M, Thuizat R (1982) Etude K/Ar du magmatisme basique lié au Trias supérieur des Pyrénées. Conséquences méthodologiques et paléogéographiques. Bull Mineral 105: 673–680
Morad S, Al-Asam I, Longstaff F, Marfil R, Johansen H, Marzo M (1995) Diagenesis of a mixed siliciclastic/evaporitic sequence of the Middle Muschelkalk (Middle Triassic), the Catalan Coastal Range, NE Spain. Sedimentology 42: 749–768
Morata D (1990) Estructuras fluidales de las «ofitas» de la zona Subbética. Boletín de la Sociedad Española de Mineralogía 13–1: 160 p
Morata D, Puga E, Demant A, Aguirre L (1997) Geochemistry and tectonic setting of the «ophites» from the external zones of the Betic Cordilleras (S. Spain). Estudios Geológicos 53 (3-4): 107–120.
Mueller S, Krystyn L, Krüschner M (2016) Climate variability during the Carnian pluvial phase-a quantitative palynological study of the Carnian sedimentary succession at Lunz am see, northern calcareous alps, Austria. Palaeogeography, Palaeoclimatology, Palaeoecology 441: 189–211
Mujal E, Gretter N, Ronchi A, López-Gómez J, Falconnet J, Diez JB, De la Horra R, Bolet A, Oms O, Arche A, Barrenechea J, Steyer JS, Fortuny J (2016a) Constraining the Permian/Triassic transition in continental environments: Stratigraphic and paleontological record from the Catalan Pyrenees (NE Iberian Peninsula). Palaeogeography Palaeoclimatology Palaeoecology 445: 18–37
Mujal E, Fortuny J, Oms O, Bolet A, Galobart A, Anadón P (2016b) Palaeoenvironmental reconstruction and Early Permian ichnoassemblage from the NE Iberian Peninsula (Pyrenean Basin). Geol Mag 153: 578–600
Mujal E, Gretter N, Ronchi A, López-Gómez J, Falconnet J, Diez J B, De la Horra R, Bolet A, Oms O, Arche A, Barrenechea J F, Steyer J-S, Fortuny J (2016c) Insights on the Permian/Triassic transition in Western Tethys: new stratigraphic and paleontological data from the Catalan Pyrenees (NE Iberian Peninsula). Permophiles 63: 21–27
Müller D (1969) Perm und Trias im Valle del Baztán (Spanische westpyrenäen). Ph.D Thesis. Technische Universität Clausthal, Clausthal-Zellerfeld, p 128
Müller D (1973) Perm und Trias in Valle del Batzán, Spanische West-Pyrenees. Neues Jahrbuch für Geologie und Paläontologie. Abhandlungen 142: 30–43
Muñoz A, Ramos, A, Sopeña A, Sánchez-Moya Y (1995) Caracterización de las Unidades Litoestratigráficas del Triásico en el subsuelo del tercio noroccidental de la Cordillera Ibérica y áreas adyacentes. Cuadernos de Geología Ibérica 19: 129–171
Muñoz JA (2002) Alpine tectonic I: The Alpine system north of the Betic Cordillera. Tectonic setting; the Pyrenees. In: Gibbons W, Moreno T (eds) The Geology of Spain. Geol Soc London, London, p 370–385
Muñoz JA, Puigdefábregas C, Fontboté JM (1983) El Pirineo. In: Comba JA (ed) Libro Jubilar JM Ríos, vol 2. IGME, Madrid, pp 161–205
Murphy JB, Nance RD, Cawood PA (2009) Contrasting modes of supercontinent formation and the conundrum of Pangea. Gondwana Research 15: 408–420
Murphy JB, Keppie JD, Nance RD, Dostal J (2010) Comparative evolution of the Iapetus and Rheic Oceans: A North America perspective. Gondwana Research 17: 482–499. https://doi.org/10.1016/j.gr.2009.08.009
Mutti M, Weissert H (1995) Triassic monsoonal climate and its signature in Ladinian–Carnian carbonate platforms (Southern Alps, Italy). Journal of Sedimentary Research 65B: 357–367
Muttoni G, Kent DV, Garzanti E, Brack P, Abrahamsen N, Gaetani M (2003) Early Permian Pangea "B" to Late Permian Pangea "A". Earth and Planetary Science Letters 215(3): 379–394
Muttoni G, Gaetani M, Kent DV, Sciunnach D, Angiolini L, Berra F, Garzanti E, Mattei M, Zanchi A (2009) Opening of the Neo-Tethys Ocean and the Pangea B to Pangea A transformation during the Permian. GeoArabia 14(4): 17–48
Nagtegaal PJG (1969) Sedimentology, Palaeoclimatology and diagenesis of post-hercynian deposits in Southern-Central Pyrenees (Spain). Leidse Geologische Mededelingen 42: 143–238
Nakada R, Ogawa K, Suzuki N, Takahashi S, Takahashi Y (2014) Late Triassic compositional changes of aeolian dusts in the pelagic Panthalassa: response to the continental climatic change. Palaeogeography, Palaeoclimatology, Palaeoecology 393: 61–75
Navidad M, Álvaro M (1985) El vulcanismo alcalino del triásico superior de Mallorca (Mediterráneo occidental). Boletín Geológico y Minero 96: 10–22
Nicholson C, Seeber L, Williams P, Sykes IR (1986) Seismic evidence for conjugate slip and block rotation within the San Andreas fault system, Southern California. Tectonics 5: 629–648

Ochoa M, Arribas J, Mas R, Goldstein R H (2007) Destruction of a fluvial reservoir by hydrothermal activity. Sedimentary Geology 202: 158–173

Oliva-Urcia B, Pueyo EL, Larrasoaña JC, Casas AM, Román-Berdiel T, Van Der Voo R, Scholger R (2012) New and revisited paleomagnetic data from Permian Triassic red beds: two kinematic domains in the west-central Pyrenees. Tectonophysics 522: 158–175

Ortí F (1974) El Keuper del Levante español. Estudios Geológicos 30: 7–46

Ortí F (1982–83) Sur les conditions de dépôt, la diagnèse et la structure des évaporites triasiques dans l'Est de l'Espagne. Sciences de la Terre 25 (2): 179–199

Ortí F, García-Veigas J, Rosell L, Jurado MJ, Utrilla R (1996) Formaciones salinas de las cuencas triásicas en la Península Ibérica: caracterización petrológica y geoquímica. Cuadernos de Geología Ibérica 20: 13–35

Ortí F, Pérez-López A, García-Veigas J, Rosell, Cendón DI, Pérez-Valera F (2014) Sulfate isotope compositions ($\delta^{34}S$, $\delta^{18}O$) and strontium isotopic ratios ($^{87}Sr/^{86}Sr$) of Triassic evaporites in the Betic Cordillera (SE Spain). Revista Sociedad Geológica España 27 (1): 79–89

Ortí F, Pérez-López A, Salvany J A (2017) Triassic evaporitic of Iberia: Sedimentological and palaeogeographical implications for the western Neotethys evolution during the Middle Triassic-Earliest Jurassic. Palaeogeography, Palaeoclimatology, Palaeoecology 471: 157–180

Ortí F, Salvany JM, Rosell L, Castelltort X, Inglès M, Playà E (2018) Middle Triassic evaporite sedimentation in the Catalan basin: Implications for the paleogeographic evolution in the NE Iberian platform. Sedimentary Geology 347: 158–178

Pastor-Galán D, Groenewegen T, Brouwer D, Krijgsman W, Dekkers MJ (2015) One or two oroclines in the Variscan orogen of Iberia? Implications for Pangea amalgamation. Geology 43: 527–530. https://doi.org/10.1130/g36701.1

Payne JL, Kump LR (2007) Evidence for recurrent Early Triassic massive volcanism from quantitative interpretation of carbon isotope fluctuations. Earth and Planetary Science Letters 256: 264–277

Pereira MF, Castro A, Chichorro M, Fernández C, Díaz-Alvarado J, Martí J, Rodríguez C (2014) Chronological link between deep-seated processes in magma chambers and eruptions: Permo-Carboniferous magmatism in the core of Pangaea (Southern Pyrenees). Gondwana Research 25: 290–308

Pérez-Arlucea M (1991) Características de los sedimentos carbonáticos de la segunda trangresion del Triásico Medio (Ladiniense) en la zona central de la Cordillera Ibérica. Rev. Soc Geol España 4: 143–164.

Pérez-Arlucea M (1992) Características de los sedimentos de la segunda transgresión del Triásico Medio (Ladiniense) en la zona central de la Cordillera. Revista de la Sociedad Geológica de España 4: 143–164

Pérez-Arlucea M, Sopeña A (1985) Estratigrafía y sedimentología del sector central de la Rama Castellana de la Cordillera Ibérica. Estudios Geológicos 41: 207–222

Pérez-López A (1991) El Trías de facies germánica del sector central de la Cordillera Bética. Ph.D. Thesis, University of Granada, Granada, p 400

Pérez-López A (1996) Sequence model for coastal-plain depositional systems of the Upper Triassic (Betic Cordillera, southern Spain). Sedimentary Geology 101: 99–117

Pérez-López A, Pérez-Valera F (2007) Palaeogeography, facies and nomenclature of the Triassic units in the different domains of the Betic Cordillera (S Spain). Palaeogeography, Palaeoclimatology, Palaeoecology 254: 606–626

Pérez-López A, Pérez-Valera F (2012) Tempestite facies model for the epicontinental Triassic carbonates of the Betic Cordillera (southern Spain). Sedimentology 59: 646–678

Pérez-Valera F, Pérez-López A (2008) Stratigraphy and sedimentology of Muschelkalk carbonates of the Southern Iberian Continental Palaeomargin (Siles and Cehegín Formations, Southern Spain). Facies 54: 61–8

Pérez-López A (2000) Epicontinental Triassic of the Southern Iberian Continental Margin (Betic Cordillera, Spain). In: Bachmann GH, Lerche I (eds) Epicontinental Triassic vol 2. E. Schweizerbart'sche Verlagsbuchhandlung, Stuttgart, p 1009–1031

Pérez-López A, Pérez-Valera F, Pérez-Valera J A (2011) Complex Palaeogeography of the Epicontinental Carbonate Platform in Southern Spain during the Ladinian. Abstract, 28 th IAS Meeting of Sedimenology, Zaragoza, Spain. p 242

Pérez-López A, Márquez L, Pérez-Valera F (2005) A foraminiferal assemblage as a bioevent marker of the main Ladinian transgressive stage in the Betic Cordillera, southern Spain. Palaeogeography, Palaeoclimatology, Palaeoecology 224: 217–231

Pérez-López A, López Garrido AC, Márquez-Aliaga A, Sanz de Galdeano C, García Tortosa FJ (2003) Ladinian Carbonates of the Cabo Cope Unit (Betic Cordillera, SE Spain): a Tethys-Maláguide Palaeogeographic Gateway. Facies 48: 1–8

Pérez-Valera F (2005) Estratigrafía y tectónica del Triásico Sudibérico en el sector oriental de la Cordillera Bética. Ph.D. Thesis, University of Granada, Granada, p 303

Pérez-Valera JA (2015) Ammomoideos y bioestratigrafía del Triásico Medio (Ladiniense) del sector oriental de la Cordillera Bética. PhD thesis, University of Complutense Madrid 489 p

Pérez-Valera J A, Barroso-Barcenilla F, Goy A, Pérez-Valera F (2016) Nautiloids from the Muschelkalk facies of the Southiberian Triassic (Betic Cordillera, southern Spain). Journal of Systematic Palaeontology 1–21

Pérez-Valera F, Solé de Porta N, Pérez-López A (2000) Presencia de facies Buntsandstein (Anisiense–Ladiniense?) en el Triásico de Calasparra (Murcia). Geotemas 1: 209–211

Pereira MF, Castro A, Fernández C (2015) The inception of a Paleotethyan magmatic arc in Iberia. Geoscience Frontiers 6 (2): 297–306

Perini G, Timmerman, M J (2008) Permian 40Ar/39Ar ages for post-Variscan minor intrusions in the Iberian Range and Spanish Central System. Geologica Acta 6 (4): 335–344

Perri F, Critelli, S, Martín-Algarra, A, Martín-Martín M, Perrone V, Mongelli G, Zattin M (2013) Triassic redbeds in the Malaguide complex (Betic Cordillea-Spain): petrography, geochemistry and geodinamic implications. Earth-Science Review 117: 1–28

Pettijohn FJ, Potter PE, Siever R (1972) Sand and Sandstones. Springer-Verlag, Berlin, Heidelberg, p 618

Pettijohn F P, Potter P E, Siever R (1973) Sand and Sandstones. Springer-Verlag, New York. 618 p

Pieren A, Areces J, Toraño J, Martínez-García E (1995) Estratigrafía y estructura de los materiales permotriásicos del sector Gijón-La Camocha (Asturias). Cuad Geol Ibér 19: 309–335

Poblet J (1991) Estructura de les unitats del vessant sud de la zona axial del Pirineu central. Ph.D Thesis, Universitat de Barcelona, Barcelona, p 604

Pomar L (1979) La evolución tectosedimentaria de las Baleares: Análisis crítico. Acta Geol Hisp 14: 293–310

Portugal-Ferreira M, Morata D, Puga E, Demant A, Aguirre L (1995) Evolución geoquímica y temporal del magmatismo básico mesozoico en las Zonas Externas de las Cordilleras Béticas. Estudios Geológicos 51: 109–118

Preto N, Kustatscher E, Wignall P B (2010) Triassic climates - state of the art and perspectives. Palaeogeography, Palaeoclimatology, Palaeoecology 290: 1–10

Puga E, Beccaluva L, Bianchini G, Díaz de Federico A, Díaz Puga MA, Álvarez-Valero AM, Galindo-Zaldívar J, Wijbrans JR (2010) First evidence of lamprophyric magmatism within the Subbetic Zone (Southern Spain). Geologica Acta 8 (2): 111–130

Pulgar JA, Alonso JL, Espina RG, Marín JA (1999) La deformación alpina en el basamento Varisco de la Zona Cantábrica. Trabajos de Geología 21: 283–294

Ramon X, Calvet F (1987) Estratigrafía y desimentología del Muschelkalk inferior del dominio Montseny-Llobregat (Catalánides). Estudios Geológicos 43 (5-6): 471–487

Ramos A (1979) Estratigrafía y paleogeografía del Pérmico y Triásico al oeste de Molina de Aragón. Ph.D Thesis. Seminarios de Estratigrafía. Series Monográfica Vol 6. Dpt. Estratigrafía, Universidad Complutense de Madrid, Madrid, p 313

Ramos A (1995) Transition from alluvial to coastal deposits (Permian-Triassic) on the Island of Mallorca, western Mediterranean. Geol Mag 132: 435–447

Ramos A, Doubinger J (1989) Premières datations palynologiques dans le facies Buntsandstein de l´ille de Majorque (Baleares). C R Acad Paris 309: 1089–1094

Rangheard Y (1972) Étude géologique des iles d´Ibiza et da Formentera (Baleares). Mem. Int. Geol. Min. España, 82: 340 p, Madrid.

Ríos JM, Galera JM, Barettino D, Lanaja JM (1987) Sallent [map] (1:50.000) MAGNA Hoja 145, Segunda serie. IGME Report and Map, p 61

Rigo M, Mazza M, Karádi V, Nicora A (2017) New Upper Triassic conodont biozonation in the Tethyan realm. In: Tanner L H (ed) The Late Triassic World: Earth in a Time of Transition. Springer. Berlin

Robles S, Pujalte V (2004) El Triásico de la Cordillera Cantábrica. In: J.A. Vera (ed) Geología de España. SGE-IGME, Madrid, p 274–276

Robles S, Llompart C (1987) Análisis paleogeográfico y consideraciones paleoicnológicas del Pérmico Superior y Triásico Inferior en la transversal del río Segre (Alt Urgell, Pirineo de Lérida). Cuadernos de Geología Ibérica 11: 115–130

Robles S, García-Mondejar J, Pujalte V (1987) Sistemas aluviales pérmicos del área de Peña Labra-Peña Sagra (Cantabria y Palencia). Cuadernos de Geología Ibérica 11: 5–21

Roca E (1992) L´estructura de la conca Catalano-Balear: paper de la compressió i de la distensió en la seva génesi. PhD Thesis (Unpublished). Barcelona University, Barcelona, p 330

Roca E, Guimerà J (1992) The Neogene structure of the eastern Iberian margin: structural constrains on the crustal evolution of the Valencia trough (western Mediterranean). Tectonophysics 203: 203–218

Roca E, Sans M, Cabrera Ll, Marzo M (1999) Modelo tectonosedimentario del sector central y septentrional del smargen catalán sumergido (cubetas de Barcelona, San Feliú, Begur y Riumors-Roses). Libro Homenaje a José Ramírez del Pozo. AGGEP, Madrid p 99–217

Rodríguez-Méndez L, Cuevas J, Esteban JJ, Tubía JM, Sergeev S, Larionov A (2014) Age of the magmatism related to the inverted Stephanian–Permian basin of the Sallent area (Pyrenees). The Geological Society of London 394: 101–111

Rodríguez-Méndez L, Cuevas J, Tubía JM (2016) Post-Variscan basin evolution in the central Pyrenees: Insights from the Stephanian–Permian Anayet Basin. J Comptes Rendus Geoscience 348 (3–4): 333–341. doi: http://dx.doi.org/10.1016/j.crte.2015.11.006

Rodríguez-Perea A, Ramos-Guerrero E, Pomar L, Paniello X, Obrador A, Martí J (1987) El Triásico de las Baleares. Cuadernos de Geologia Iberica 11: 295–321

Roep TB (1972) Stratigraphy of the "Permo-Triassic" Saladilla formation and its tectonic setting in the Betic of Malaga (Vélez Rubio region, SE Spain). Proc. K. Ned. Akad. Wet., Ser. B Phys. Sci. 75: 223–247

Roger P (1965) Étude stratigraphique et structural de la zone des Nogueras entre l'Esera et l'Isabena (Huesca, Espagne). Actes de la Société linnéenne de Bordeaux 102B: 1–23

Roghi G, Gianolla P, Minarelli L, Pilati C, Preto N (2010) Palynological correlation of Carnian humid pulses throughout western Tethys. Palaeogeography, Palaeoclimatology, Palaeoecology 290: 89–106

Romano C, Goudemand N, Vennenmann TW, Ware D, Scheneebeli-Hermann E, Hochuli PA, Brüwiler T, Brinkmann W, Bucher H (2013) Climatic and biotic upheavals following the end-Permian mass extinction. Nature Geoscience 6, 57–60.

Ronchi A, Sarria E, Broutin J (2008) The "Autuniano Sardo": basic features for a correlation through the Western Mediterranean and Paleoeurope. Bollettino Società Geologica Italiana (Italian Journal of Geosciences) 127: 655–681

Rosell J, Elízaga E (1989): Evolución tectosedimentaria del Paleozoico de la isla de Menorca. Bol Geol Min 100: 193–204

Rosell J, Arribas J, Elízaga E, Gómez-Grass D (1988) Caracterización sedimentológica y petrográfica de la serie roja permo-triásica de la isla de Menorca. Boletín Geológico y Minero 99: 71–82

Rosell J, Gómez-Gras D, Elízaga E (1989). Mapa geológico de España, 1:25.000. Hojas 618 (Cap Menorca y Ciutadella), 619 (Ses Coves Noves), 646 (Cala en Brut i Alaior), 647 (Maó). ITGE, Madrid.

Rosenbaum G, Lister GS, Duboz C (2002) Relative motions of Africa, Iberia and Europe during Alpine orogeny. Tectonophysics 359: 117–129

Rossi P, Cocherie A, Fanning CM, Ternet Y (2003) Datation U–Pb sur zircons des dolérites tholéiitiques pyrénéennes (ophites) à la limite Trias–Jurassique et relations avec les tufs volcaniques dits «infra-liasiques» nord-pyrénéens. C R Geosci 335: 1071–1080. https://doi.org/10.1016/j.crte.2003.09.01

Ruffell A, Simms M J, Wignall P B (2016) The Carnian Humid Episode of the Late Triassic: a review. Geological Magazine 153: 271–284

Ruiz M (2007) Caracterització structural I sismotectònica de la litosfera en el domini Pirenaico-Cantàbric a partir de mètodes de sísmica active I passive. Ph.D Thesis, Universidad de Barcelona, Barcelona, p 354

Sabat F, Muñoz JA, Santanach P (1988) Transversal and oblique structures at the serres de Llevant thrust belt (Mallorca Island). Geologische Rundchau 77: 529–538

Salas R, Guimerà J, Mas R, Martín-Closas C, Meléndez A, Alonso A (2001) Evolution of the Mesozoic Central Iberian Rift System and its Cainozoic inversion (Iberian Chain). In: Ziegler P A, Cavazza W, Robertson A H F, Crasquin-Soleau S (eds) Peri-Tethys Memoir 6: Peri-Tethys Rift/Wrench basins and Passive Margins. Mèm Mus Nat Hist Nat, Paris 186: 145–185.

Salvany JM (1990) El Keuper del diapiro de Poza de La sal. In: Ortí F, Salvany JM (eds) Formaciones evaporíticas de la Cuenca del Ebro y cadenas periféricas, y de la zona de Levante. ENRESA-Universitat de Barcelona, Barcelona, p 54–58

Salvany JM, Ortí F (1987) El Keuper de los Catalánides. Cuadernos Geología Ibérica 11: 215–236

Salvany JM, Bastida J (2004) Análisis litoestratigráfico del Keuper surpirenaico central. Rev Soc Geol España 17: 3–26

Sanz T, Lago M, Gil-Imaz A, Galé C, Ubide T, Larrea P, Ramajo J, Tierz P, Pocoví A (2012) Stratigraphy and petrology of the Baix Ebre volcanic region (Tarragona, Spain): magmatic stages and age. Geogaceta 52: 33–36

Sánchez-Martínez S, De La Horra R, Arenas R, Gerdes A, Galán-Abellán AB, Lopez-Gómez J, Barrenechea JF, Arche A (2012) U-Pb Ages of Detrital Zircons from the Permo-Triassic Series of the Iberian Ranges: A Record of Variable Provenance during Rift Propagation. Journal of Geology 120, 135–154.

Sánchez Moya Y, Sopeña A (2004) El rift Mesozoico Ibérico. In: J.A. Vera (ed) Geología de España. SGE-IGME, Madrid, p 484–522
Sánchez Moya Y, Sopeña A, Ramos A (1996) Infill architecture of a non-marine halfgraben Triassic basin (central Spain). J Sediment Res 66: 1122–1136
Sanz T, Lago M, Gil A, Galé C, Ramajo J, Ubide T, Pocovi A, Tierz P, Larrea P. (2013). *Journal of Iberian Geology* 39(1): 331–352
Saura E (2004) Anàlisi estructural de la zona de les Nogueres Pirineus Centrals. Ph.D Thesis, Universitat Autònoma de Barcelona, Barcelona, p 92
Saura E, Teixell A (2006) Inversion of small basins: effects on structural variations at the leading edge of the Axial Zone antiformal stack (Southern Pyrenees, Spain). Journal of Structural Geology 28: 1909–1920
Schmidt M (1935) Fossilien der spanischen Trias. Abh Heidelb Akad Wiss Math Naturwiss Kl 22: 1–140
Scotese CR (1984) Paleozoic paleomagnetism and the assembly of Pangea. In: Van der Voo R, Scotese CR, Bonhommet N (eds) Plate reconstruction from Paleozoic paleomagnetism. American Geophysical Union 12: 1–10
Scotese CR (2003) PALEOMAP Project. http://www.scotese.com/newpage9.htm
Seguret M (1972) Étude tectonique des nappes et séries décollées de la partie centrale du versant sud des Pyrénées. Caractère synsédimentaire, rôle de la compression et de la gravité. Ph.D Thesis, Presses Univ. Sci. Tech, Languedoc, Montpellier, p 155
Seranne M (1992) Devonian extension tectonics versus Carboniferous inversion in the Northern Orcadian Basin. Journal Geological Society London 149: 27–37
Sibuet JC, Srivastava SP, Spakman W (2004) Pyrenean orogeny and plate kinematics. Journal of Geophysical Research 109, B08104. https://doi.org/10.1029/2003jb002514
Simms M J, Ruffell A H (1989) Synchronicity of climatic change and extinctions in the Late Triassic. Geology 17: 265–268
Simms M J, Ruffell A H (1990) Climate and biologic change in the LateTriassic. Journal of the Geological Society London 147: 321–327
Simon O J, Kozur H (1977) New data on the (Permo-) Triassic of the Betic Zone (Southern Spain). Cuad Geol Iber 4: 307–321
Solé de Porta N, Ortí F (1982) Primeros datos cronoestratigráficos de las series evaporíticas del Triásico superior de Valencia. Acta Geol. Hispánica 17: 185–191
Solé de Porta N, Calvet F, Torrentò L (1987) Análisis palinológico del Triásico de los Catalánides (NE de España). Cuad Geol Geol 11: 237–254
Sopeña A (1979) Estratigrafía del Pérmico y Triásico del NW de la provincia de Guadalajara. Ph.D Thesis. Seminarios de Estratigrafía. Series Monográfica Vol 5. Dpt. Estratigrafía, Universidad Complutense de Madrid, Madrid, p 329
Sopeña A, Doubinger J, Ramos A, Pérez-Arlucea M (1995) Palynologie du Permien et du Trias dans le centre de la Péninsule Ibérique. Sciences Géologiques Bulletin 48: 119–157
Sopeña A, Feys R, Ramos A, Virgili C (1977) Estheria tenella en el Pérmico de Pálmaces de Jadraque, provincia de Guadalajara. Cuadernos de Geología Ibérica 4: 135–144
Sopeña A, Sánchez-Moya Y (1997) Tectonic systems tract and depositional architecture of the western border of the Triassic Iberian Trough (central Spain). Sediment Geol 113: 245–267
Sopeña A, Sánchez-Moya Y (2004) Las cuencas continentales del fin de la orogenia varisca. In: Vera JA (ed) Geología de España, SGE-IGME, Madrid, p 479–481
Sopeña A, Virgili C, Arche A, Ramos A, Hernando S (1983) El Triásico. In: Comba J A (ed.) Geología de España: Libro Jubilar J. M. Ríos. Instituto Geológico y Minero Español. Madrid: 47–62
Sopeña A, López-Gómez J, Arche A, Pérez-Arlucea M, Ramos A, Virgili C, Hernando S(1988) Permian and Triassic rift basins of the Iberian Peninsula. In: Manspeizer W (ed.) Triassic–Jurassic Rifting—Continental Breakup and the Origin of the Atlantic Ocean and Passive Margins, Developments in Geotectonics 22B. Elsevier, Amsterdam, pp. 757–786
Sopeña A, Ramos A, Villar MV (1990) El Triásico del sector Alpera-Montealegre del Castillo (Prov. de Albacete). In: Ortí F, Salvany JM (eds) Formaciones evaporíticas de la cuenca del Ebro y Cadenas periféricas y de la zona de Levante. ENRESA-Universitat de Barcelona, Barcelona, p 224–231
Sopeña A, Sanchez-Moya Y, Barrón E (2009) New Palynological and Isotopic Data on Triassic of Western Cantabrian Ranges. Journal of Iberian Geology 32(1): 35–45
Soria A R, Liesa C, Rodríguez-López J P, Meléndez, N, De Boer P, Meléndez A (2011) An Early Triassic evolving erg system (Iberian Chain, NE Spain): paleoclimate implications. Terra Nova 23: 76–84.
Stampfli GM (1991) Tethyan Ocean. In: Bozkurt E, Winchister JA, Piper JDA (eds) Tectonics and Magmatism in Turkey and the Surrounding Area. Geological Society London Special Publications 173: 1–23
Stampfli GM, Borel GD (2002) A plate tectonic model for the Paleozoic and Mesozoic constrained by dynamic plate boundaries and restored synthetic oceanic isochrones. Earth and Planetary Science Letters 196: 17–33
Stampfli GM, Mosar J, Favre P, Pillevuit A, Vannay JC (2001) Permo-Mesozoic evolution of the western Tethyan realm: the Neotethys/East-Mediterranean connection. In: Cavazza W, Robertson AHFR, Ziegler PA (eds) Peri-Tethys Memoir 6, Peritethyan Rift/Wrench Basins and Passive Margins, Vol 186, Bull. Museum Nat Hist Nat, Paris, pp 51–108
Stampfli GM, Hochard C, Vérard C, Wilhem C, von Raumer J (2013) The formation of Pangea. Tectonophysics 593: 1–19. doi.org/10.1016/j.tecto.2013.02.037
Stefani M, Furin S, Gianolla P (2010) The changing climate framework and depositional dynamics of Triassic carbonate platforms from the dolomites. Palaeogeography, Palaeoclimatology, Palaeoecology 290: 43–57
Stoffregen RE, Alpers ChN (1987) Woodhouseite and svanbergite in hydrothermal ore deposits: products of apatite destruction during advanced argillic alteration. The Canadian Mineralogist 25: 201–211.
Suárez J (2007) La Mancha Triassic and Lower Lias Stratigraphy, a well log interpretation. Journal Iberian Geology 33(1): 55–78
Suárez-Rodríguez A (1988) Estructura del área de Villaviciosa-Libardon (Asturias, Cordillera Cantábrica). Trabajos de Geología 17: 87–98
Sun Y D, Joachimski M M, Wignall P B, Chunbo Ch, Haishui J, Lina W, Xulo L (2012) Lethally hot temperatures during the Early Triassic greenhouse. Science 338: 366–370
Sun Y, Wignall P, Joachimski M, Bond D, Grabs S, Sun S, Yan CB, Wang LN, Chen YL, Lai XL (2015) High amplitude redox changes in the Late Early Triassic of South China and the Smithian/Spathian extinction. Palaeogeography, Palaeoclimatology, Palaeoecology 427: 62–78.
Teixell A (1992) Estructura alpina de la transversal de la terminación occidental de la Zona Axial Pirenaica. Ph.D Thesis, Universitat de Barcelona, Barcelona
Teixell A (1998) Crustal structure and orogenic material budget in the west-central Pyrenees. Tectonics 17: 395–406
Teixell A, García-Sansegundo J (1994) Zuriza [map] (1:50.000) MAGNA Hoja 118, Segunda serie. IGME
Teixell A, García-Sansegundo J, Zamorano M (1994) Ansó [map] (1:50.000) MAGNA Hoja 144, Segunda serie. IGME Report and Map, p 62

Tucker ME, Calvet F, Hunt D (1993) Sequence stratigraphy of carbonate ramps: systems tracts, models and application to the Muschelkalk carbonate platforms of eastern Spain. Spec. Publs. Int. Assoc. Sediment. 18: 397–415

Tugend J, Manatschal G, Kusznir NJ, Masini E, Mohn G, Thinon I (2014) Formation and deformation of hyperextended rift systems: Insights from rift domain mapping in the Bay of Biscay-Pyrenees. J Tectonics 33: 1239–1276. doi: 10.1002/ 2014TC003529

Ubide T (2013) The Cretaceous Alkaline Magmatism in Northeast Iberia. Igneous Processes and Geodynamic Implications. Ph.D. Thesis. Universidad de Zaragoza, Zaragoza

Ubide T, Wijbrans JR, Galé C, Arranz E, Lago M, Larrea P (2014) Age of the Cretaceous alkaline magmatism in northeast Iberia: Implications for the Alpine cycle in the Pyrenees. Tectonics 33: 1444–1460. https://doi.org/10.1002/2013tc003511

Utrilla R, Pierre C, Ortí F, Pueyo JJ (1992) Oxygen and sulfur isotope composition as indicators of the origin of Mesozoic and Cenozoic evaporites from Spain. Chemical Geology 102: 229–244

Valero Garcés BL (1991) Los sistemas lacustres carbonatados del Stephaniense y Pérmico en el Pireneo Central y Occidental. Ph.D Thesis, Universidad de Zaragoza, p 413

Valero Garcés BL (1993) Lacustrine deposition and related volcanism in a transtensional tectonic setting: upper Stephanian lower Autunian in the Aragón-Béarn Basin, Western Pyrenees (Spain-France). Sedimentary Geology 83: 133–160

Valero Garcés BL (1994) Carbonate lacustrine episodes in the continental Permian Aragón–Béarn Basin (Western Pyrenees). In: Gierlowski-Kordesch E, Kelts K (eds) Global Geological Record of lake Basins, Vol 1. Cambridge University Press, Cambridge, p 107–119

Valero Garcés BL (1994) The Permian lacustrine basque basin (Western Pyrenees): an example of high environmental variability in small and shallow carbonate lakes developed in closed systems. In: Gierlowski-Kordesh E, Kelts K (eds) Global Geological Record of Lake Basins, Vol 1. Cambridge University Press, Cambridge, p 101–106

Valero Garcés BL, Gisbert Aguilar J (1992) Shallow carbonate lacustrine facies models in the Permian of the Aragón–Béarn basin (Western Spanish-French Pyrenees). Carbonates and Evaporites 7: 112–130

Valero Garcés BL, Gisbert Aguilar J (1994) Permian saline lakes in the Aragón–Béarn Basin (Western Pyrenees). In: Last W, Renaut R (eds) Sedimentology and geochemistry of modern and ancient saline lakes SEPM 50: 265–290

Valero Garcés BL, Gisbert Aguilar J (2004) El Estephaniense y Pérmico de los Pirineos. In: Vera JA (ed) Geología de España. SGE-IGME, Madrid, p 266–268

Valero-Garcés BL, Gisbert–Aguilar J (2004) El Stephaniense y Pérmico de los Pirineos. In: Vera JA (ed) Geología de España, SGE-IGME, Madrid, p 266–268

Valero J (1974) Géologie structurale du Paléozoïque de la région de Panticosa de Huesca (Espagne). Ph.D Thesis, Bourdeaux Université, Bordeaux, p 78

Valle Aguado B, Azevedo MR, Schaltegger U, Martínez Catalán JR, Nolan J (2005) U–Pb zircon and monazite geochronology of Variscan magmatism related to syn-convergence extension in Central Northern Portugal. Lithos 82: 169–184

Valverde-Vaquero P (1992) Permo-Carboniferous magmatic activity in the Cantabrian Zone (NE Iberian Massif, Asturias, NW Spain). MSc Thesis. Boston College, USA 198 p

Van Den Driessche J, Brun JP (1989) Un modèle de l'extension paléozoïque supérieur dans le Sud du Massif Central. Comptes Rendus de l'Académie des Sciences de Paris 309: 1607–1613

Van Wees J D, Arche A, Beijdorff C G, López-Gómez J, Cloetingh SAPL (1998) Temporal and spatial variations in tectonic subsidence in the Iberian Basin (eastern Spain): inferences from automated forward modelling of high-resolution stratigraphy (Permian–Mesozoic). Tectonophysics 300: 285–310

Vargas, H. (2002). Análisis y comparación de la subsidencia entre las cuencas Ibérica y Ebro Central durante el Pérmico y Triásico y su relación con el relleno sedimentario. Ph.D Thesis (Unpublished). Universidad Complutense de Madrid, Madrid, p 310

Vargas H, Gaspar-Escribano J, López-Gómez J, van Wees JD, Cloetingh S, De la Horra R, Arche A (2009) A comparison of the Iberian and Ebro Basins during the Permian and Triassic, eastern Spain: a quantitative subsidence modelling approach. Tectonophysics 474: 160–183

Vera JA (2001) Evolution of the South Iberian Continental Margin. In: Ziegler P A, Cavazza W, Robertson AHF Crasquin-Soleau S (eds) Peri-Tethys Memoir 6: Peri-Tethys Rift/Wrench Basins and Passive Margins. Mém Mus Nat Hist Nat Paris 186: 109–143

Vegas R, Banda E (1982) Tectonic framework and Alpine evolution of the Iberian Peninsula. Earth Evolution Sciences 4: 320–343

Vergés J (2003) Evolución de los sistemas de rampas oblicuas de los Pirineos meridionales: fallas del Segre y Pamplona. Boletín Geológico y Minero 114: 87–101

Vieillard P, Tardy Y, Nahon D (1979) Stability fields of clays and aluminum phosphates: parageneses in lateritic weathering of argillaceous phosphatic sediments. American Mineralogist 64: 626–634

Virgili C (1952) Hallazgo de nuevos ceratites en el Triásico de Mallorquín. Memortias del Instituto Geológico Provincial de Barcelona 9: 19–38

Virgili C (1958) El Triásico de los Catalanides. Boletín del Instituto Geológico de España 69: 1–856

Virgili C, Cassinis G, Broutin J (2006) Permian to Triassic sequences from selected continental areas of southwestern Europe. In: Lucas S, Cassinis G, Schneider JW (eds) Non-Marine Permian Biostratigraphy and Biochronology. Geological Society, Special Publication 265: 231–260

Visscher H, Krystyn L (1978) Aspects of Late Triassic Palynology, 4: A palynological assemblage from amonoid controlled Late Karnian (Tuvalian) sediments of Sicily. Rev Paleobot Palyn 26: 93–112

Vissers RLM, Meijer PT (2012) Mesozoic rotation of Iberia: Subduction in the Pyrenees? J Earth-Science Reviews 110:93–110. https://doi.org/10.1016/j.earscirev.2011.11.001

Viseras C, Fernández J, Henares S, Cuéllar N (2011) Facies architecture in outcrop analogues for the TAGI reservoir. Exploratory interest. AAPG Search and Discovery Article, AAPG International Conference and Exhibition, Milan, Italy, #90135

Voigt S, Haubold H (2015) Permian tetrapod footprints from the Spanish Pyrenees. Palaeogeography Palaeoclimatology Palaeoecology 417: 112–120

Von Raumer J, Bussy F, Schaltegger U, Schulz B, Stampfli, GM (2013) Pre Mesozoic Alpine basements—their place in the European Paleozoic framework. GSA Bulletin 125(1/2): 89–108

Wagner RH, Álvarez C (2010) The Carboniferous floras of the Iberian Peninsula: A synthesis with geological connotations. Review of Palaeobotany and Palynology 162: 239–324

Wagner RH, Talens J, Meléndez B (1985) Upper Stephanian Stratigraphy and Megaflora of Henarejos (Province of Cuenca) in the Cordillera Ibérica, Central Spain. In: Lemos de Sousa MJ, Wagner RH (eds) Papers on the Carboniferous of the Iberian Peninsula (Sedimentology, Stratigraphy, Palaeontology, Tectonics and Geochronology. Anais da Faculdade de Ciências, Supplement to Vol 64. Universidade do Porto, (1983), pp 445–480, pls 1–8

Warren JK (2006) Evaporites: Sediments, Resources, Hydrocarbons. Springer, New York, p 1035

Weil AB, Van der Voo R, Van der Pluijm BA (2001) Oroclinal bending and evidence against the Pangea megashear: the Cantabria–Asturias Arc (northern Spain). Geology 29(11): 991–994

Wernicke B (1981) Low angle normal faults in the Basin and Range province: nappe tectonics in an extending orogeny. Nature 291: 645–698

Wernicke B, Burchfield BC (1982) Modes of extensional tectonics. Journal Structural Geology 4: 105–115

Wignall P B (2015) The Worst of Times. How Life on Earth Survived Eighty Million Years of Extinctions. Princenton 199 p

Xu G, Hannah J L, Stein H, Mork A, Vigran J O, Bingen B, Schutt D, Lundschien B A (2014) Cause of Upper Triassic climate crisis revealed by Re–Os geochemistry of Boreal black shales. Palaeogeography,Palaeoclimatology, Palaeoecology 395: 222–232

Zhou M-F, Malpas J, Song X-Y, Robinson PT, Sun M, Kennedy AK, Lesher CM, Keays RR (2002) A temporal link between the Emeishan large igneous province (SW China) and the end-Guadalupian mass extinction. Earth and Planetary Science Letters 196: 113–122.

Ziegler PA (1982) Triassic rifts and facies patterns in Western and Central Europe. Geolog Runds 71: 747–772

Ziegler PA (1988a) Evolution of the Artic-North Atlantic and the Western Tethys. In: AAPG Memoir, vol 43, AAPG, p 198

Ziegler PA (1988b) Post-Hercynian plate reorganization in the Tethys and Artic-North Atlantic domains. In: Manspeizer W (ed) Triassic-Jurassic rifting. Continental Breakup and the Origin of the Atlantic Ocean and Passive Margins. Developments in Geotectonics 22B. Elsevier, Amsterdam, p 711–755

Ziegler PA (1990) Geological Atlas of Western and Central Europe. Shell Internationale Petroleum Maatschappij BV and Geological Society Publishing House, London, p 239

Ziegler PA, Stampfli G M (2001) Late Paleozoic-Early Mesozoic plate boundary reorganization: collapse of the Variscan Orogen and opening on the Neotethys. Mus. Civ Sc Nat Bresc Ann 25: 17–34